Evaluating Microglia Dynamics in Blast and Impact-Induced Neurotrauma and Assessing the Role of Hemostatic Nanoparticles in Microglia Activation

Michelle Renee White

Dissertation submitted to the faculty of the Virginia Polytechnic Institute and State University in partial fulfillment of the requirements for the degree of

Doctor in Philosophy

In

Biomedical Engineering

Pamela J. VandeVord, Chair

Erin B. Lavik

Yong Woo Lee

Jennifer M. Munson

Abby R. Whittington

August 23, 2022

Blacksburg, Virginia

Keywords: microglia, NLRP3, activation, inflammation, blast exposure, controlled cortical impact

Evaluating Microglia Dynamics in Blast and Impact-Induced Neurotrauma and Assessing the Role of Hemostatic Nanoparticles in Microglia Activation

Michelle Renee White

ABSTRACT

Traumatic brain injury (TBI) is a major medical concern that has demonstrated to be particularly challenging to treat because of the disparity amongst injury modes and severities. Increased use of explosive devices during combat has caused blast TBI (bTBI) to become a widespread consequence in military and Veteran populations, and impact-related trauma from contact-related sports or motor vehicle accidents has made mild impact-induced TBIs (concussion) a major health problem. There is a high risk for those who have sustained a TBI to develop behavioral and cognitive disorders following injury, and these symptoms can present as delayed onset, causing diagnosis to be a major feat when planning for treatment and long-term healthcare. Both preclinical and clinical studies report the neuropathological changes following TBI, yet investigating the distinct mechanistic changes in blast and impact trauma that contribute to pathological disparities has yet to be elucidated.

Microglia dynamics play a key role in initiating the inflammatory response after injury, as microglia become activated by undergoing morphological changes that influence their function in the injured brain, and unique signaling pathways influence their functional inflammatory states. While previous literature report on the unique responses of microglia, their mediated-inflammatory responses are still not well defined. This work aimed to investigate the acute and subacute responses of microglia to injury through their diverse activation states following blast and impact trauma. The work herein employed rodent models to investigate these changes, finding that microglia activation was spatially and temporally heterogeneous within and across injury paradigms. Three days following bTBI, activated microglia in the cortex displayed morphologies similar to microglia that are known to increase their interactions with dysfunctional synapses, while dystrophic microglia were prevalent in the hippocampus seven days following injury. Moreover, transhemispheric changes in microglia activation were noted following impact TBI, with

stressed/primed microglia responding to immune challenges of the cortex at three days, whereas a unique morphological state that was markedly different from those traditionally reported in CNS injury and disease was present within the hippocampus three- and seven-days following injury. State-of-the-art cell sorting techniques were used for *in vivo* analysis of microglia, which also exhibited that functional changes of microglia vary between injury paradigms, providing insight into how differences in primary insult may elicit distinct signaling pathways involved in microglia-mediated inflammatory responses. These *in vivo* studies were then crucial in understanding the malleable responses of microglia to complex injuries such as “blast plus impact” TBI, indicating that phenotypic changes in microglia following this injury are also unique and spatially heterogeneous. To date, therapeutic efforts for TBI are limited due to the lack of understanding the underlying mechanisms that influence TBI pathology. This work also investigated novel therapeutic targets, noting that administration of polyester nanoparticles restored microglia to baseline levels following impact. The fundamental research presented in this study is innovative and advantageous as it can provide essential data into targeted and personalized treatments that can improve long-term healthcare and ultimately, the quality of life for those suffering from a TBI.

Evaluating Microglia Dynamics in Blast and Impact-Induced Neurotrauma and Assessing the Role of Hemostatic Nanoparticles in Microglia Activation

Michelle Renee White

GENERAL AUDIENCE ABSTRACT

Traumatic brain injury (TBI) is a major medical concern that has demonstrated to be particularly challenging to treat because of the differences in injury modes and severities. Increased use of explosive devices during combat has caused blast TBI (bTBI) to become a widespread result in military and Veteran populations, and impact-related trauma from contact sports or motor vehicle accidents has made mild impact-induced TBIs (concussion) a major health problem. There is a high risk for those who have sustained a TBI to develop behavioral and cognitive disorders following injury, and these symptoms can present later on, causing diagnosis to be a major feat when planning for treatment and long-term healthcare.

Microglia play a key role in inducing the inflammatory response after injury, as they change shape and size, which then influences their function in the injured brain. Although prior research reports on the unique responses of microglia, their effects on inflammation following TBI are still not well defined. This work aimed to investigate the early responses of microglia to injury through their diverse activation states following blast and impact trauma. The experiments in this study used animal models, finding that microglia activation can be distinct across time and brain regions, which may be injury-type-specific. To date, therapeutic efforts of TBI are limited due to the lack of understanding the underlying mechanisms that influence TBI pathology. This work also investigated beneficial treatments for TBI, noting that administration of nanoparticles helped restore microglia to levels similar to the control group. The fundamental research presented in this study is innovative and important as it can provide essential data into targeted and personalized treatments that can improve long-term healthcare and ultimately the quality of life for those suffering from a TBI.

"The Lord is my light and my salvation; whom shall I fear? The Lord is the strength of my life; of whom shall I be afraid?" Psalm 27:1. To God be all the glory for bringing me this far. I am forever grateful. To my beautiful sister in heaven, Tiffany Marie Alicee' (1983-2018), I dedicate this to you. You have been with me every day as I walked this journey, pushing me to be the best I could be. I love and miss you always.

Acknowledgments

To my mother, if it were not for your constant advocacy and support for me throughout high school, I would not be where I am today. You have always had my best interest at heart, moving mountains to make sure I had the opportunity to go to college, which then motivated me to pursue my Ph.D. Because of your gracious support for me always, I owe this degree and achievements throughout my undergraduate and graduate career to you.

To my father, through every exam, project, and low point throughout this journey, your voice telling me to "keep my eye on the prize" is what kept me uplifted. Your encouragement, even when things seemed grim, was the motivation I needed to keep moving forward. I cannot even begin to express how grateful I am.

To my beautiful sisters Gabrielle and Rochelle, thank you for all the pep talks, late-night phone calls, and visits to Blacksburg just to keep me company. I cherish all of our memories together and the amazing support system that we have. I love you both so much and I am so blessed to call you, my sisters. Tiffany would be so proud of us all.

To my lifelong friends and family who were always checking in and offering their love, support, and encouragement, I thank you all as you were instrumental in my success.

I would like to thank my advisor Dr. VandeVord for seeing something in me that I did not originally see in myself. I started this journey feeling inadequate and discouraged, and you granted me the opportunity to grow as a researcher under your leadership, which is an experience I will always cherish. I am extremely appreciative of the time you have dedicated to me, as your infinite wisdom, patience, and guidance throughout this process have been crucial to my success. You have granted me experiences and knowledge that will last a lifetime, and because of that, I cannot thank you enough.

I would also like to thank each of my committee members, Dr. Munson, Dr. Lavik, Dr. Whittington, and Dr. Lee. Your input and feedback have been essential to the progression of my work, and the mentorship offered by you all has allowed me to grow into a well-rounded scientist.

To the TNT lab, thank you for all your support and willingness to help with my projects. Your contributions to ideas and help with animal testing are the reason I was even able to finish my dissertation. You are all amazing.

Thank you to my undergraduate advisor Dr. Wilsaan Joiner at George Mason University. If it was not for your mentorship, opportunities, and resources that you gave me, pursuing a Ph.D. would not have been possible, and for that, I am extremely grateful.

To my friends and family at Virginia Tech and the greater Blacksburg area, the spontaneous coffee runs, craft nights, home-cooked meals, Bible studies, zoom productivity hours, long walks, movie nights, and frequent Zaxby's lunches have made this an experience I will never forget. Thank you for keeping me sane, allowing me to debrief after long, hard days, and being the support system I needed to push through. I am grateful for the life-long friendships I have built.

To my Mentor/Sister-in-Christ Monet, thank you for your mentorship that has allowed me to pursue avenues in advocacy, service, and leadership within the Virginia Tech community. Because of your mentorship paving the way for me, I can pay it forward to other students, lifting as I climb within the academy. Through the toughest moments, you have always been there for me, keeping me on track, and I cannot thank you enough for your friendship.

Finally, my deepest level of gratitude goes to my husband Imai. You have always been there for me, even when I was far away from home. You have carried me through all the trials and tribulations of this crazy journey, always making sure I had what I needed to get through the most stressful of days. Thank you for always being my shoulder to cry on, the calm in the middle of the storm, and my partner through all that life has to offer. Your unconditional love has been my constant strength, and I look forward to our next adventure together.

Table of Contents

List of Figures

List of Tables

List of Abbreviations

ABS	Advanced Blast Simulator
ANOVA	Analysis of Variance
ATP	Adenosine 5'-triphosphate
BBB	Blood Brain Barrier
BSA	Bovine Serum Albumin
bTBI	Blast Induced Traumatic Brain Injury
cCCI	Closed-Head Controlled Cortical Impact
CD11b	Cluster of Differentiation 11b
CD40	Cluster of Differentiation 40
CD206	Cluster of Differentiation 206
cDNA	Complementary DNA
CNPs	Control Nanoparticles
CNS	Central Nervous System
COX-2	Cyclooxygenase-2
CTE	Chronic Traumatic Encephalopathy
DAMPs	Danger Associated Molecular Patterns
DAPI	4',6-diamidino-2-phenylindole
DCM	Dichloromethane
DG	Dentate Gyrus
DAI	Diffuse Axonal Injury
DMSO	Dimethyl Sulfoxide
DNA	Deoxyribose Nucleic Acid
EBSS	Earl's Balanced Salt Solution
EDC	N-hydroxysuccinimide
EWE	End Wave Eliminator
FPI	Fluid Percussion Injury
GAPDH	Glyceraldehyde-3 Phosphate Dehydrogenase
GFAP	Glial Fibrillary Acidic Protein
GRGDS	Glycine-arginine-glycine-aspartic acid-serine
HNPs	Hemostatic Nanoparticles
IACUC	Institutional Animal Care and Use Committee
IBA-1	Ionized calcium-binding adaptor molecule
ICP	Intracranial Pressure
IFN-γ	Interferon Gamma
IGF-1	Insulin-Like Growth Factor
IgG	Immunoglobulin G
IHC	Immunohistochemistry
IL-1β	Interleukin 1 Beta

IL-6	Interleukin 6
IL-16	Interleukin 16
ITGAM	Integrin Subunit Alpha M
MACS	Magnetic Activated Cell Sorting
MBP	Myelin Basic Protein
MC	Motor Cortex
mg	Milligrams
mM	Micro Molar
MMP-9	Matrix Metallopeptidase 9
ms	Milliseconds
mTBI	Mild TBI
NHS	1-ethyl-3-(3-dimethylaminopropyl) carbodiimide
NLRP3	Nucleotide-Binding Domain (NOD)-Like Receptor Protein 3
NMR	Nuclear Magnetic Resonance
OCT	Optimal Cutting Temperature
OPA	o-phthalaldehyde
PAMPs	Pathogen Associated Molecular Patterns
PBS	Phosphate Buffered Saline
PBX	Phosphate Buffered Saline with 0.3% Triton-X
PDLA	Poly(D-lactic acid)-b-poly(ethylene glycol)
PEG	Poly(ethylene glycol)
PLA	Poly(lactic acid)
PLLA	Poly(L-lactic acid)
PSI	Pounds per Square Inch
qPCR	Quantitative Polymerase Chain Reaction
RANTES	Regulated on Activation, Normal T expressed and Secreted
RBFOX3	RNA Binding Fox-1 Homolog 3
RNA	Ribonucleic Acid
RT	Reverse Transcription
SC	Somatosensory Cortex
SEM	Standard Error of Mean
TBI	Traumatic Brain Injury
THF	Tetrahydrofuran
TLRs	Toll-Like Receptors
TMEM-119	Transmembrane Protein 119
TNF-α	Tumor Necrosis Factor-Alpha
TREM2	Triggering Receptor Expressed on Myeloid Cells 2
µl	Microliters
µm	Micrometers

Chapter 1: Background

1.1 Significance

Traumatic brain injury (TBI) is prevalent among civilian and military populations, with high morbidity, mortality, and economic costs.[1–3] Mild TBIs (mTBI) are the most common type of brain injury where there is usually an absence of external signs of damage; however, clinical symptoms of mTBI are frequently reported.[4–8] For example, mild blast-induced TBIs (bTBI) account for 25% of all injuries among military personnel and Veterans. Despite the apparent functional recovery of military personnel who have sustained a bTBI, they are susceptible to a subsequent TBI. Repetitive bTBI can lead to detrimental effects such as late-onset neurodegenerative disease development and long-term cognitive and behavioral deficits.[9,10] Moreover, those who have suffered from mTBI caused by an impact, such as concussions sustained in a motor vehicle accident or contact sports, are also susceptible to further damage that can lead to similar short- and long-term sequelae.[11,12] While clinical symptoms that accompany blast and impact TBI are reported, their injury mechanisms are poorly understood, which might result in distinctions in their pathology and clinical symptoms.

Clinical symptoms of TBI are driven by secondary injury mechanisms such as acute and chronic inflammation, which can be induced by the resident immune cells within the brain known as microglia. Reports of microglia undergoing diverse morphological changes, exhibiting specific functions in response to the injured brain, have come to the forefront, making it imperative to study the spatiotemporal response of microglia phenotypes in blast and impact TBI. Furthermore, the discovery of the Nucleotide-Binding (NOD)-Like Receptor Protein 3 (NLRP3) inflammasome, a pivotal contributor to pro-inflammatory cytokine release which is located in microglia, plays a major role in neuroinflammation.[13] While the microglia-induced inflammatory response is prevalent following injury, the longitudinal response of microglia activation, there is still a lack of knowledge on the transient functional changes of microglia and whether they are injury-type-specific. Thus, characterizing microglia activation following TBI through their diverse activation states and NLRP3-mediated pathways may aid in developing targeted treatment options for those suffering from a TBI.

As there are limited therapeutic strategies to treat neuroinflammation, *it is imperative to advance the understanding of microglia dynamics between injury paradigms, observing morphological and pathological differences that may result between in blast and impact TBI.* Hemostatic nanoparticles (HNPs) have been studied as a novel therapeutic strategy to alleviate

both behavioral and pathological outcomes following bTBI. *Expanding this work to investigate how the administration of HNPs will specifically influence the microglia response in the injured brain* will be imperative in improving healthcare and the quality of life for TBI patients.

1.2 Hypothesis and Specific Aims

This work hypothesizes that blast and impact TBI induces distinct acute and subacute microglia-induced inflammatory profiles through mechanically derived signals, which impart unique pathological changes within microglia. Treating these injuries with HNPs will limit microglia activation, restoring microglia to sham levels. This hypothesis was tested using the following specific aims.

Specific Aim 1: Define spatial and temporal changes in the pathological characteristics of microglia as it relates to the inflammatory response following traumatic brain injury. It is crucial to clarify the spatial and temporal heterogeneity of microglia activation through its unique morphological phenotypes following TBI. Moreover, minimal studies utilize closed-head pre-clinical models to assess pathological changes following impact-induced TBI. Therefore, this specific aim is delineated into two sub-aims.

Sub-aim 1.1: Determine changes in microglia activation as it relates to the acute and subacute stages of the microglia-induced inflammatory response following blast-induced neurotrauma

Sub-aim 1.2: Characterize a pre-clinical model of closed-head controlled cortical impact to study the acute and subacute microglia response related to impact-related TBI.

Specific Aim 2: Investigate acute and subacute microglia-specific gene expression patterns by assessing the NLRP3-mediated pro-inflammatory response following repeated blast exposure and impact trauma. This aim seeks to provide a rigorous analysis of the non-autonomous microglia-specific responses following TBI by evaluating gene expression patterns within microglia that contribute to neuroinflammation.

Specific Aim 3: Identify microglia pathological changes in a novel injury model and evaluate the ability of hemostatic nanoparticles to modulate the sub-acute inflammatory response following TBI. Studies have indicated that specific clinical manifestations of bTBI can be hypervigilance and risk-taking behaviors that can lead to further injuries such as a subsequent impact TBI. Therefore, it is essential to characterize a blast plus impact TBI model, evaluating the microglia-induced inflammatory response that can lead to future diagnostic tools. Moreover, this

aim seeks to investigate mechanisms that may influence microglia-mediated pathological responses, improving TBI outcomes.

Sub-aim 3.1: Characterize a novel injury model that utilizes repeated blast exposure and closed head controlled cortical impact to study microglia dynamics in a complex injury model.

Sub-aim 3.2: Evaluate the use of hemostatic nanoparticles as a strategy to delineate the mechanisms of microglia-mediated pathology in impact-induced neurotrauma allowing for a better understanding of the secondary injury mechanisms.

Chapter 2: Literature Review

2.1. Traumatic Brain Injury – Epidemiology

Traumatic Brain Injury (TBI) is one of the leading causes of mortality and morbidity, with high incidence in both military and civilian populations.[14–16] About 1.7 million people in the United States are afflicted by TBI annually, contributing to 30% of all injury-related deaths.[17,18] TBIs are challenging to treat because they are heterogeneous and often induce complex pathogenesis.[19] For example, TBIs are clinically grouped by severity: mild, moderate, and severe, contributing to the heterogeneity in patients with this injury.[20] Moreover, different TBIs are caused by penetrating objects, acceleration or deceleration forces (impact), and blast waves.[21] The mechanical response from each of these types of injuries and severities of the brain varies, further complicating treatment. This chapter will focus on summarizing the mechanisms and secondary injury responses of TBIs that result from closed head impacts and blast exposures.

TBIs are classified into two types of injury states: Diffuse and Focal.[22–25] Diffuse injury refers to the bulk mechanical effects associated with pathological changes in both neurons and glial cells, and changes in vascularization that can lead to diffuse brain swelling.[26] This type of injury is also known for causing damage to the axonal structure, which is commonly known as diffuse axonal injury (DAI). Focal brain injury results from localized brain responses to loading,[27] and can occur when there is a tangential motion of the brain surface relative to the cranium's interior surface. This motion can even cause contusions or rupture blood vessels leading to a hematoma and is more commonly seen in patients with moderate to severe TBIs.[28] When identifying these two classes of injuries and their distinctions from one another, it is essential to note which types of TBIs fall within these categories. Studies show that impact TBI can be classified as diffuse and focal, with more injuries falling in the focal injury category, with blast TBI (bTBI) falling within the diffuse injury category.[27,28] As the primary insult imparted on the brain following blast exposure or impact trauma are unique, it is important to delineate the secondary injury mechanism between the two injury modes, as neuropathology could vary between blast and impact TBI.

2.2. Impact Induced Traumatic Brain Injury

Impact TBI is typically caused by blunt non-penetrating trauma through forceful impacts to the head.[29–36] Impact TBI is commonly seen in contact sports such as football and soccer, motor vehicle accidents, or physical attacks from a dull or sharp object.

2.2.1 Impact TBI Biomechanics

Impact TBI is due to a direct impact to the head, which results in sudden acceleration/deceleration or rotational forces.[37] Quantitative data on the macroscopic and microscopic interactions of the head-brain complex is essential in the mechanical assessment of these injury mechanisms.[38] To date, the current steps taken to understand and predict the incidence of TBI in humans are as follows: 1) defining the external mechanical loads on the head in injury-causing situations, 2) using brain models (physical, analytical, and/or computational), estimating how the external mechanical loads translate to mechanical conditions in the brain at the tissue and cellular level, and 3) using tissue and cellular tolerance criteria to identify the areas in the brain that will be injured as a result of external applied loading.[26] The sudden change in linear acceleration/deceleration forces imparted to the brain is known to be a mechanism for closed head injury, and as a result, focal lesions to some brain regions (i.e., ipsilateral and contralateral sides of impact) can develop.[38] In addition, the rotational or angular movement of the head that takes place as a consequence of the impact can cause shear stress and strain on the tissue, triggering signaling pathways involved in the secondary injury response.[39–41]

2.2.2 Impact TBI Preclinical Models

Using animal models for impact TBI research has become crucial in understanding the injury mechanisms. Models that try to replicate the unique features of impact TBI, such as the biomechanical forces that occur because of the impact, have been developed.[42] Researchers have used preclinical TBI models such as fluid percussion injury (FPI), piston-driven devices: controlled cortical impact (CCI), and the weight drop model to study the mechanical and pathophysiological changes.[43–45] FPI has been widely used in animal models of impact TBI making it advantageous to compare research and outcomes across laboratories.[46] One limitation is that this model includes a craniotomy, exposing the brain before inducing injury, which may lack clinical

relevance, as humans do not have an exposed brain when an injury occurs. Even though this model is widely used, the mechanical variation between parameters can cause a difference in outcomes.[47]

The weight drop model has become advantageous, as it was one of the first TBI models that do not require a craniotomy.[48–51] The weight drop model consists of dropping a projectile of specific characteristics through a tube at a specified height onto the head of the animal. Even though this model is commonly used, review data has reported considerable variation in the projectile's reported weight and drop height between studies, causing increased variability in the severity of the injury. This increased variability between studies has proven to be a significant disadvantage of this model.[42,52] Piston-driven models are also a standard method used to induce injury (Fig. 1).[53] This model is particularly advantageous as it delivers an injury at a specific depth, velocity, and impact force.[53,54] Piston-driven models provide valuable data in determining the parameters that guide the mechanical changes following impact TBI. One type of piston device that has been used to replicate impact TBIs is the CCI model. Many studies have used CCI models, which included a craniotomy before inducing injury.[55–61] but research is starting to focus on using this device for closed head injuries.[62–66] This device has either a pneumatically driven or electromagnetic driver that is used to impact the animal.[42,53] Applications of this study have helped model sports-related concussions, motor vehicle crash injuries, and injuries due to military conflicts. Manipulating the parameters of this model can be utilized to control clinically relevant variables, studying pathological outcomes that resemble aspects of human TBI.[67]

Figure 1. Schematic of an electromagnetic controlled cortical impact device. The impactor is mounted onto a stereotaxic frame allowing for adjustability of the impact angle. The impactor is connected to a control box that allows various parameters to be set.

2.3. Blast Induced Traumatic Brain Injury

Blast-induced traumatic brain injury (bTBI) results from direct or indirect exposure to an explosive event.[68] These injuries are common in conflicts where explosive devices such as improvised explosive devices are commonly used.[16,69,70] Per the Defense and Veterans Brain Injury Center (DVBIC), 414,000 military individuals sustained a TBI from 2000-2019, and one-third were exposed to a blast event.[16]

2.3.1 Blast TBI Biomechanics

The blast wave travels faster than the speed of sound from the center of the explosion and displaces and subsequently compresses an equal volume of surrounding air at a high velocity.[71] This phenomenon is the blast wave's overpressure phase, followed by an exponential decrease that passes through zero and begins a negative pressure phase.[72,73] The components of the blast wave can be described and represented by the Friedlander waveform (Fig. 2).[74] This wave describes an ideal blast from a spherical source in an open environment.[71,75]

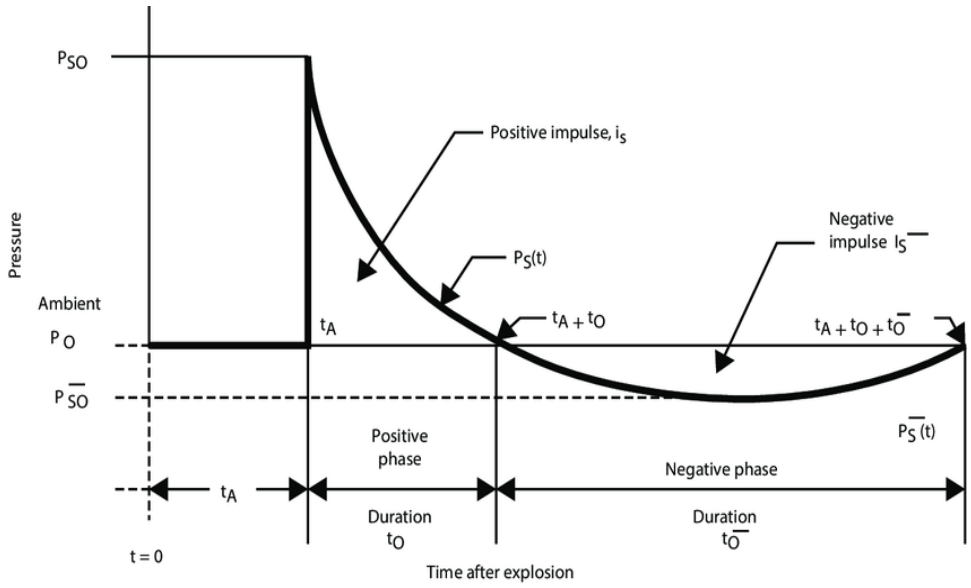

Figure 2. Friedlander Waveform represents the free field pressure-time profile of a blast wave. The blast wave is characterized by a positive phase that is followed by a negative phase. The blast wave is also defined by several parameters: peak overpressure, rise time, positive and negative impulses, and positive and negative durations.

Five parameters have been identified that may contribute to damage to the head and brain caused by blast waves. These include (1) the peak of the initial positive-pressure wave, (2) the duration of overpressure, (3) the medium of the explosion, (4) the distance from the epicenter of the blast wave, and (5) the degree of focusing because of a confined area or walls.

Blast injuries can be divided into four categories (Fig. 3).[74] The primary blast injury is due to blast wave propagation through tissue, also called barotrauma. Secondary injuries are caused when objects thrown by the blast wave hit a person. Tertiary injuries are caused by the blast wind, including the deceleration during impact with structures in the environment. Lastly, quaternary injuries are caused by thermal and chemical exposures from the explosion itself. For this review, the mechanism and neuropathological mechanism associated with blast injury will be focused on the consequences of primary blast injury.

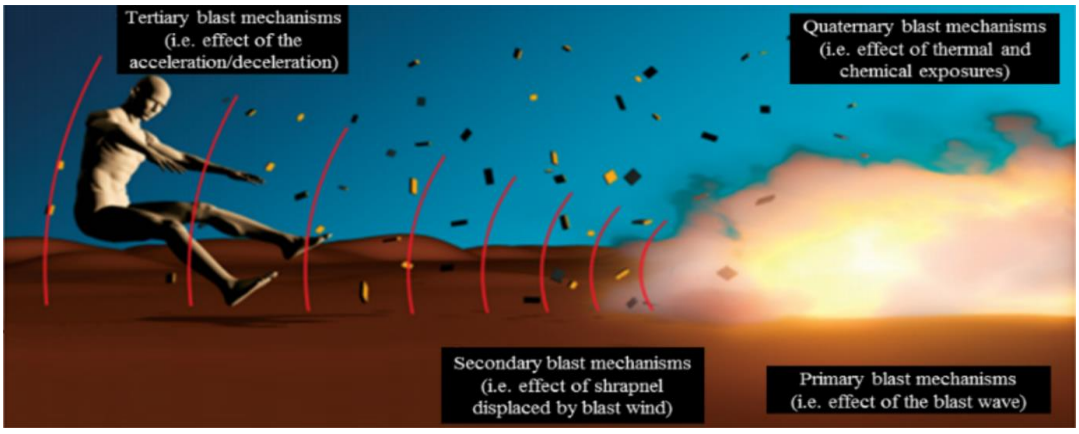

Figure 3. The four injury modes following blast exposure. The primary blast injury occurs from the static overpressure created by the blast wave. The second blast mechanism is a result from the effect of shrapnel and objects thrown by the blast wave. The tertiary blast mechanism is the displacement of people as a result of the dynamic overpressure effect. Finally, the quaternary blast mechanisms are the effect of thermal and chemical injuries sustained because of the blast overpressure.

The underlying blast mechanisms of primary bTBI have been challenging to define, and studies are ongoing to increase the knowledge of blast wave characteristics that complicate prevention and treatment efforts. The current theories of blast injury include blast wave transmission through the skull orifices, direct cranial transmission, skull flexure dynamics, and thoracic surge.[72,76] CJ Clemedson postulated from his experimental work that the impulse of the

pressure wave and/or the pressure variations alongside the wave's propagation throughout the body generates tissue-specific responses. He also suggests that the pressure-wave interactions suggested that inertia, implosion, and cavitation as the primary mechanisms.[77] More specifically, it was identified that the pressure wave causes an interface between two media of different densities, and inertial effects at this interface can cause stress and strain at tissue interfaces leading to displacement, deformation, or rupture of tissues and organs.[74] Understanding the responses to injury that causes neuropathological changes is still difficult as these theories are still currently being tested. Additional studies testing the theory of inertial loading on the brain following blast have addressed Clemedson's postulates, indicating that brain tissue at the interfaces with fluid, such as tissue surrounding the cerebrospinal fluid-filled ventricles, are thought to be particularly susceptible to primary blast injury. This is due to the reflection of blast waves at the border of these areas due to their differing densities.[38,78,79] The stress on tissue interfaces is likely contributing to the cellular response triggered by blast overpressure. Another injury mechanism that is reported is the skull deformation theory. This theory indicates that pressure oscillations from blast waves are associated with skull deformation, directing the intracranial pressure response (ICP).[72,80–82] As direct or indirect mechanisms of blast injury propose potential pathways on how the overpressure causes TBI, it is important to note that variable pathologies can exist due to sustaining either a single or repeated bTBI.[83]

2.3.2 Blast TBI Preclinical Models

There have been several experimental models used to study blast injury, which has led to the exploration of neuropathology, such as glia reactivity and oxidative stress, as well as other sequelae such as cognitive and behavioral impairment.[84–89] Historical models used in the 1940s by Krohn, Whitteridge, and Zuckerman involved detonating seventy pounds of explosives in paper containers placed on the ground, with animals raised above it or mounted on a scaffold above the explosive device.[90,91] Even though these experimental studies aimed at identifying the most critical mechanisms of blast-body interactions, there were still aspects of the study that needed to be refined. These aspects include limiting blast-body interactions to the primary injury, not secondary blast effects such as thermal exposure or body displacement.[71,74] Recent models have utilized shock tubes that produce a shock wave that the specimen experiences while suspended in the tube. The tube consists of three primary components: an expansion chamber, a frangible diaphragm, and

a compression chamber. To simulate the blast, the pressure within the compression chamber causes the sudden rupture of the diaphragm, creating a high-velocity pressure shock wave in the expansion chamber (Fig. 4).[92] These models have been advantageous but still prove complicated as the direction of the shock wave is not parallel to the wall of the tube, which can cause a series of reflective shock waves.[92]

While a shock tube is a common experimental model used, and has improved reproducibility, the disadvantages, such as the complexity of reflective shock waves, make it difficult to define and study primary blast injury and its secondary mechanisms.[92–95] Furthermore, animals placed in the mouth of the shock tube are at a more considerable risk of exposure to reflective and refraction shock waves that cause injuries that are more severe and complex than what is commonly reported in blast victims.[96,97]

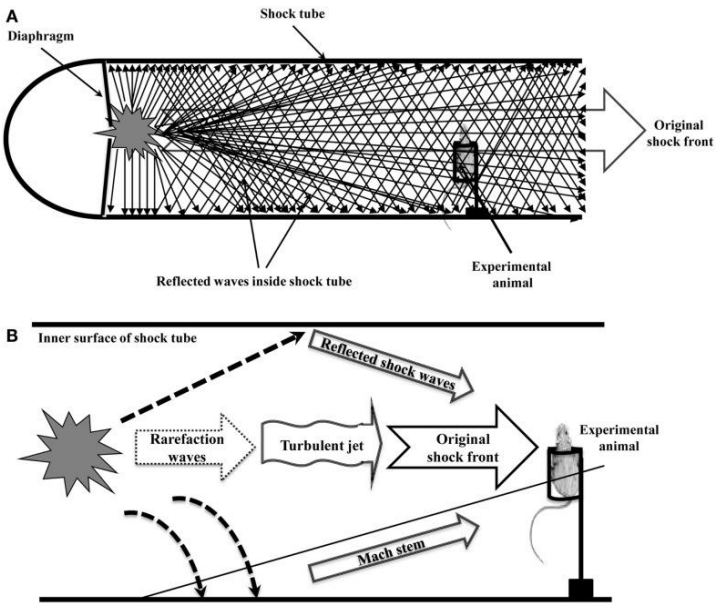

Figure 4. Reflective shock waves that can be generated from the use of a shock tube.

The VandeVord lab and others have utilized a custom-made Advanced Blast Simulator (ABS) that improves upon the commonly used shock tube.[89,98] The ABS system has three distinct sections to create, develop, and dissipate the blast wave. The first section, the driver, develops the blast wave when acetate membrane sheets are passively ruptured following pressurization using helium gas. The second section is the transition section, where the animal is located and is exposed to a single peak overpressure. Lastly, downstream of the transition section, a passive end-wave eliminator (EWE) is located to facilitate the dissipation of the blast wave through a series of baffles. As a result, the animal is exposed to an overpressure representing a free-field blast exposure, eliminating the chance for exposure to reflective blast waves. Compared to a shock tube system, the advantage of this system is that it produces an actual blast wave and not a shock wave, which is more representative of what military personnel experience in the field. This means that the ABS produce a Friedlander waveform that consists of the positive duration, peak overpressure, and

negative duration phase. In contrast, shock waves do not consistently produce the negative duration phase (Fig. 5). As it is still undefined which component of the blast waveform causes injury or the pathological changes following injury, it is advantageous to use the ABS to continue to examine the mechanisms of injury as advances to this system encompasses more characteristics of the blast wave than shock tubes.

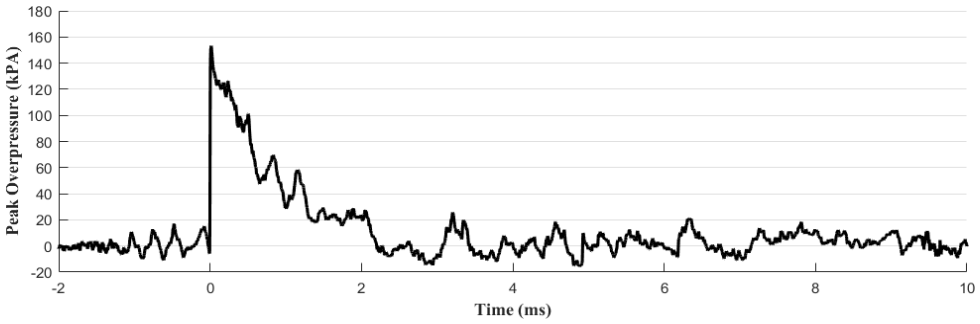

Figure 5. Representative profile of the blast wave that the ABS generates. Characteristics of the Friedlander Waveform such as rise time, peak overpressure, and positive and negative durations are maintained within the pressure profile produced in the ABS.

2.4. Secondary Injury Mechanisms Following Blast and Impact TBI

The physiological effects of blast and impact TBI have been studied, showing evidence associated with neurological disorders and long-term physical, cognitive, behavioral, and emotional changes. Morbidities such as increased ICP, mitochondrial dysfunction, oxidative stress, inflammation, and blood-brain barrier (BBB) disruption have been reported.[24,88,99–109] Key players in the secondary response include glial cells such as microglia, astrocytes, and oligodendrocytes.[60,110–114] Neuronal dysfunction in response to injury can elicit responses from glial cells, contributing to secondary injury mechanisms of TBI.[115–118] Even though secondary responses such as inflammation and BBB disruption are well-defined responses following TBI, the underlying mechanisms that contribute to these pathologies and how they may differ across injury paradigms are still poorly understood. Secondary injury caused by activation of multiple molecular pathways has been associated with both impact and blast injuries, and may be able to provide insight into pathological changes that may be specific to blast or impact TBI.[19,102,106,117,119] This review will focus on the role of microglia in the secondary injury response, specifically their functional role in the inflammatory response.

2.5. Microglia: Function in the Healthy Brain

Microglia represent the major cellular component of the innate immune system in the brain. Until now, microglia were considered the "macrophages of the central nervous system (CNS)," though recent findings have established that microglia have a distinct lineage and molecular signature that differs from circulating/infiltrating monocytes that differentiate into tissue macrophages.[120] Microglia have distinct functions in brain development as they promote neurogenesis, axon fasciculation, myelination/oligodendrogenesis, cell death or survival, and synaptic development and maturation by releasing diffusible substances.[121–125] For example, microglia secrete factors such as insulin-like growth factor 1 (IGF-1) and a variety of cytokines such as interferon-gamma (IFN-γ) to support cell genesis and cell health, with the release of cytokines and other microglial factors stimulating dendritic spine and synapse formation.[126–129] Microglia phenotypes in the developing brain include an amoeboid morphology that facilitates phagocytosis, aligning along axon tracts where oligodendrocytes are also located.[128,130] Microglia in the healthy adult brain display a highly ramified morphology and constitute up to 20% of the glia content in the CNS.[131] Highly ramified microglia were assumed to be resting and inactive in the healthy brain, but *in vivo* studies have indicated that microglia are still highly active in the healthy brain, with their highly ramified morphology indicative of their long cellular processes undergoing continuous cycles of extension to scan their environment for disruptions in homeostasis.[110,114,132]

Microglia possess an abundance of sensors that allow them to survey their environment through cell surface receptors and ion channels.[133,134] It is estimated that resident microglia scan the entire brain volume over a few hours, providing even more evidence to support their role in maintaining homeostatic environments in a healthy brain. [135] These observations again, are seen through the morphological state that microglia take on when in a "non-activated state," as the fine processes of microglia continuously contact neurons, axons, and dendritic spines.[132] Microglia distribution in the healthy adult brain is also influenced by local cytoarchitecture.[136] Research has indicated that microglia functions go beyond its immune function, playing a crucial role in shaping homeostasis in the brain through its cross-talk with other brain cell types. For example, white matter microglia show elongated somas and processes oriented along fiber tracts, while microglia in the circumventricular, a region characterized by a leaky BBB, exhibit compact morphology with short processes.[137,138] In contrast, gray matter microglia exhibit many elaborate radially oriented

arbors determining that there is anatomical diversity seen in microglia, independent of activation state that is still largely unknown, contributing to the heterogeneity of microglial cells.[139] Either way, it is indicated that the cell process movement generally occurs in a way that maintains the overall size and symmetry of individual microglia territory, and direct contact with microglia processes and their high degree of motility facilitates immune surveillance, contributing to the health of the brain.[120]

2.6. Microglia Activation in Response to the Injured Brain

Microglia play a crucial role in maintaining the integrity of the healthy brain and responding to injury and disease of the brain, which can be both beneficial and detrimental. Concerning activation, microglia are traditionally known to polarize into two major subtypes that are categorized as "M1" and "M2" (Fig. 6).[132,140] The classical M1 subtype secretes pro-inflammatory cytokines such as the production of high levels of interferon-gamma (IFN-γ), tumor necrosis factor (TNF-α), interleukin 1 (IL-1), and promotes cell-mediated immunity. The alternatively activated M2 phenotype is then subdivided into three polarization phenotypes: M2a, M2b, and M2c, each with a specific function and pattern of phenotype marker expression. M2-a polarized cells upregulate several markers, such as CD206, and increase the production of scavenger receptors for phagocytosis. M2b has either pro- or anti-inflammatory function and is associated with immunological memory, while M2c undergoes a "deactivated" phenotype in response to markers such as IL-10. This phenotype is involved in tissue remodeling and matrix deposition after inflammation has been downregulated.[141–144]

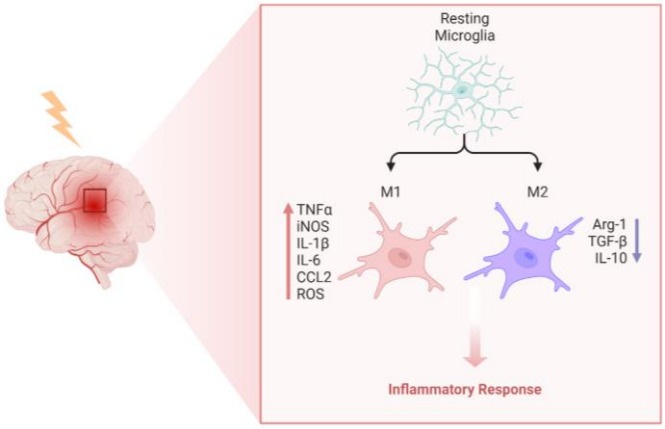

Figure 6. Microglia dynamics are traditionally known to polarize into two states: M1 and M2. M1 microglia function in a pro-inflammatory state while M2 microglia function in an anti-inflammatory state. Created with BioRender.com.

While the M1 and M2 phenotypes are still widely used to understand microglia activation, exploring the morphological phenotypes of microglia in response to injury is essential. Following injury, it has been hypothesized that both pro- and anti-inflammatory microglia located around traumatic lesions take on morphological changes in response to these lesions.[143–146] For example, microglia can convert from a "healthy" ramified shape to a "rod-like" shape in response to neuronal dysfunction or can display amoeboid morphologies that aid in phagocytosis that either can lead to further neuronal loss or can promote neuroplasticity (Fig. 7).[147–149] Moreover, studies are conveying that microglia phenotypes are indicative of their function in the injured brain, providing a more comprehensive analysis of microglia activation state that goes beyond the "M1" and "M2" phenomena.

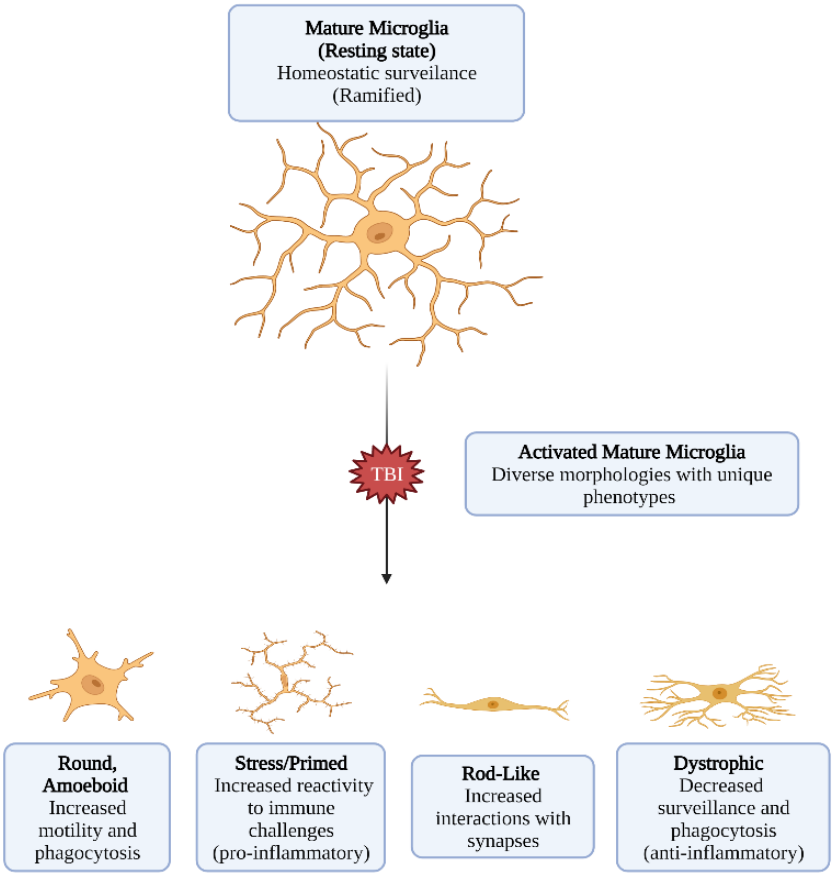

Figure 7. Microglia undergo unique morphological changes in response to TBI. Microglia display diverse morphologies when activated which are indicative of their functions in the injured brain.

A porcine model of closed-head, non-impact, rotational acceleration TBI was used to test for neuronal permeability and how this affects the microglial response.[150] Overall, the study showed that neuronal permeability is one of the drivers of reactive microglia. More specifically, previous literature has indicated that microglia around the permeabilized neurons exhibited shorter process lengths and larger body diameters but did not exhibit a rod shape that other rodent studies of diffuse TBI have alluded to.[151] In regions of the brain that did not show neuronal permeability, microglia were not significantly different in density or morphology compared to sham animals. These results suggest that neuronal membrane perturbation could drive the microglial response following injury. Even though this is an essential step in understanding the reactivity of microglia in response to the injured brain, more studies still need to be done, especially as microglia phenotypes and reactivity have shown to vary across species and changes in injury paradigms (blast vs. impact) could indicate morphological heterogeneity across regions.

2.7. Acute Drivers of Neuroinflammation

Initially, the prevalent inflammatory reaction to TBI was viewed to occur through the peripheral immune mediators entering through the disturbed BBB.[152] More recent studies have recognized that the inflammatory response is a more robust and complex interaction between central and peripheral cellular components that are influenced by the mechanism of injury and the degree of injury (mild, moderate, and severe).[117] In particular, in response to injury, the expression of pathogen recognition receptors such as toll-like receptors (TLRs) and nod-like receptors (NLRs), that respond to pathogen-associated molecular patterns (PAMPs) and endogenously produced danger-associated molecular patterns (DAMPs) can influence the microglia-mediated inflammatory responses.[153–158] DAMPs and PAMPs as acute cues are released passively or actively following injury to initiate immune cell activation. Transient membrane permeabilization can release DAMPs, which can be proteins, nucleic acids, or other molecules present in the cells before the injury and then are passively released by damaged cells following trauma which results in cell activation.[159,160] One of the most established DAMPs is extracellular adenosine 5'-triphosphate (ATP).[161,162] ATP, a storage modulus of chemical energy, can be passively released when neurons are transiently permeabilized or actively released by reactive astrocytes.[163] When released from astrocytes, ATP may act to amplify extracellular signals and function as a chemoattractant signal

for peripheral immune cells. Laser injury studies have shown this chemo-attraction signal to induce microglial proliferation, chemotaxis, and inflammatory protein synthesis.[114] In addition to passive molecules, active upregulation of synthesis and release of various molecules can also drive immune cell reactivity. It is well established that molecules such as TNF-α, IL-1β, IL-6, IL-10, and IL-16 become upregulated, driving neuroinflammation.[153] In pre-clinical rodent models, these cytokines were detectable at acute and sub-acute time points.[164–167]

Proteases are another source of active inflammation because they can process enzymes and cytokines into their bioactive form. The most common activation of this type is matrix metalloproteinase (MMP) activation.[153] In a closed head weight drop murine model, MMP-2 and MMP-9 were detectable as early as ten minutes of injury and peaked within one hour of injury in the cortex. The formation of inflammasomes in microglia and neurons can also amplify the production of inflammatory signaling molecules. Inflammasomes are intracellular complexes that assemble in response to DAMPs and stimulate the production of pro-inflammatory factors.[168] The signals that stimulate the formation of inflammasome complexes can be ROS, signals of dysfunctional mitochondria that release ATP, and/or crystalline substances such as amyloid-β.[169] The inflammasome complex that has emerged, contributing to the production and secretion of IL-1β in microglia is known as NLRP3.[170] Following a weight drop model of TBI, NLRP3 mRNA expression increased incrementally over the first week.[170] There have also been studies of impact injury showing that interfering with the formation of NLRP3 can reduce inflammation and contusion volume, and in turn, modulation of the inflammasome formation can reduce microglial activation, decreasing pro-inflammatory cytokine production.[171] Even though this has been shown in impact models, understanding this mechanism of inflammation in blast injury has yet to be elucidated.

As cytokine production and secretion are primary drivers of inflammation following injury, exploring the hallmark characteristics of inflammasome activation in microglia is critical. In the presence of immune activators such as PAMP, DAMPs, or other invaders or environmental stress, NLRP3 opens and allows for interactions between the pyrin domains (PYDs) in NLRP3 and ASC. Following this, ASC's caspase recruitment domain (CARD) binds to the CARD domain on procaspase-1, forming the NLPR3 inflammasome complex. Once this inflammasome complex is formed, it triggers procaspase-1 self-cleavage, generating the active caspase-1 p/10/p20 tetramer, inducing the conversion of pro-inflammatory cytokines from their immature "pro" forms to active

forms that are secreted outside of the cell.[172] When this inflammasome is activated, it takes place in two steps. The first step involves a priming signal in which PAMPs or DAMPs are recognized by TLRs, leading to the activation of nuclear kappa B (NF-κB) mediated signaling, which upregulates transcription of inflammasome regulated components such as inactive NLRP3, and the immature "pro" forms of IL-1β and IL-18. This priming step has been studied and shown *in vivo* using the stimulation of microglia with lipopolysaccharide (LPS).[171] The second step of activation is the oligomerization of procaspase-1 to caspase-1, as well as the production and secretion of mature IL-1β (Fig. 8).[173] Munoz-Planillo et al. reported that LPS priming can also activate the second step of the NLRP3 complex in addition to ATP, enhancing K+ efflux caused by particulate activators.[174]

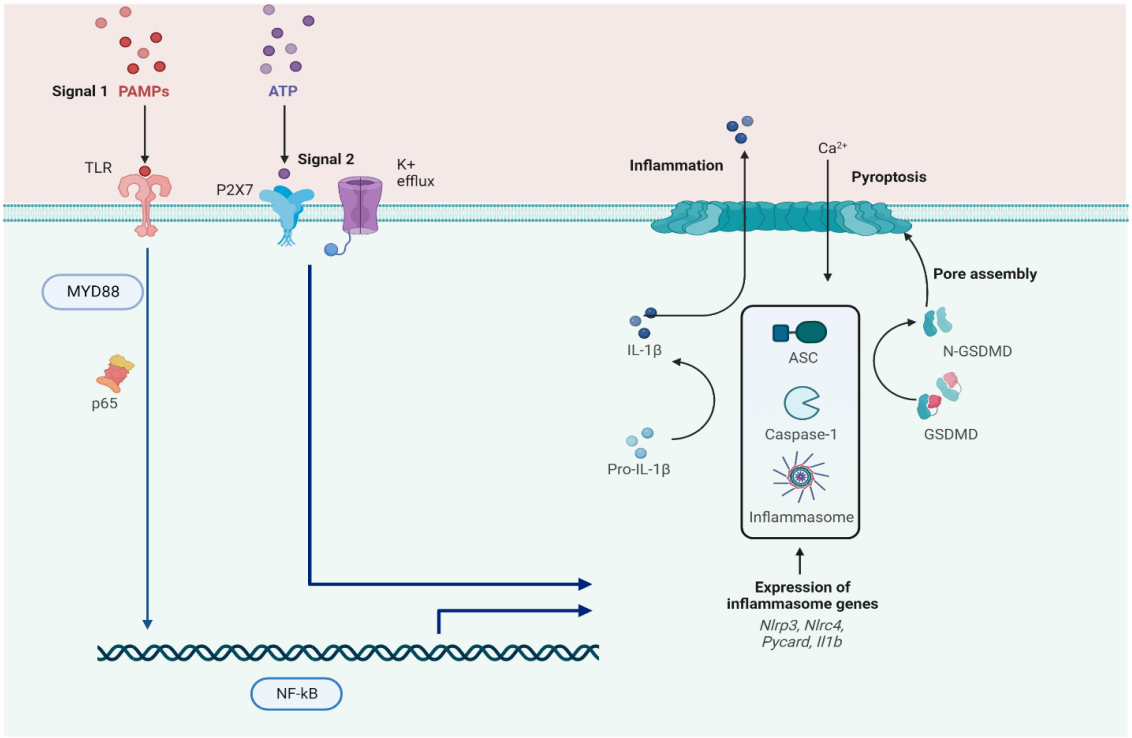

Figure 8. Activation of the NLRP3 inflammasome. A pathway that activates in two steps: PAMPs are recognized by TLRs activating NF-kB, upregulating inflammasome genes. The second step involves ATP acting as an NLRP3 antagonist, inducing K+ efflux, which oligomerizes the NLRP3 complex (inflammasome, caspase-1, and ASC), increasing production and secretion of IL-1β. Created with Biorender.com

2.8. Therapeutic Methods

The current approaches to treatment for TBI include acute interventions that suppress the response to primary insult and minimize the secondary complications caused by injury. If TBI in a patient is diagnosed early, treatment methods include early rehabilitation to improve residual function, quality of life, and independence.[54] Numerous preclinical studies have tested the therapeutic efficacy of drugs in animal models of TBI that target secondary injury mechanisms such as calcium channel blockers, antagonists, and free radical scavengers, but there are still no treatments that have made it past Phase III clinical trials.[175] One therapeutic method studied is using the endogenous inhibitor of IL-1, "Interleukin-1 receptor antagonist" (IL-1RA). This inhibitor is widely used to treat autoimmune and inflammatory diseases such as rheumatoid arthritis and inflammatory bowel disease. An active trial in Phase II has been utilizing IL-1RA through subcutaneous administration or intravenous delivery to treat patients with severe TBI, but the mechanistic benefits are still undetermined.[175] The use of cognitive behavioral therapy to reduce depression and memory deficits following TBI has been a helpful intervention, but unfortunately, this only treats the symptoms and not the secondary injury mechanisms that may cause depressive symptoms.[176–178]

In addition to the lack of treatments for TBI, additional complications make it challenging to deliver drugs to the brain. Complications may be due to the BBB, the vasculature of the CNS that acts as a physical barrier. The BBB inhibits the delivery of therapeutic agents to the CNS, such as the obstruction of a large number of drugs, including antibiotics and neuropeptides that cannot pass through the endothelial capillaries in the brain.[179,180] Some studies have utilized therapeutic methods and strategies to treat the injured or diseased brain, completely bypassing the BBB through direct administration to the brain parenchyma, yet they may not be clinically relevant as they are highly invasive.[181,182] Current routes of delivery such as topical, inhalation, intraventricular, oral, and intravenous administration of free-circulating drugs lack success in effectively delivering the optimal amount of drug to the brain to treat injury or disease. This is due to decreased uptake in the area of interest because of non-specific binding or poor retention within the body.[183] As the disadvantages of current treatment options continue to delay medical interventions to patients suffering from TBIs, critical technological advances to deliver drugs to the brain are being sought out.

Nanoparticles break the biological barriers seen with other drug delivery methods because they improve site-specific delivery, bioavailability, shelf life and circumvent any potential adverse effects of the therapeutic.[184] Nanoparticles also offer reduced size, longer suspension in the body and the brain, and can be engineered to target specific cells that drugs or biological agents need for optimal release.[185] In TBI specifically, where there is a compromise and dysfunction of the BBB, the nanoparticles can be transported passively into the brain, and their small size can also allow for multiple dosing even if BBB integrity has been restored.[186] Once in the brain, research has suggested that nanoparticles remain stable once they penetrate through the brain parenchyma due to their physicochemical properties. As efforts have increased to understand the influence of size, concentration, and stability of nanoparticles in the brain microenvironment, studying the use of nanoparticles to suppress the secondary mechanisms of injury following TBI has been applicable. Research has utilized antioxidant nanoparticles such as iron oxide and cerium oxide, which contain functional groups that inactivate reactive oxygen species (ROS), and gold nanoparticles that can suppress the inflammatory response following injury.[187,188] Additionally, the use of gold nanoparticles have been completed as their rigid core can be easily modified, and they are easy to visualize when studying their retention and biodistribution in the body.[189] Further studies understanding the use of antioxidant and gold nanoparticles as a treatment option for brain injury and disease are warranted, as they also cause adverse effects such as accumulation and aggregation at the BBB and to other brain cells.[190,191]

The use of a specific type nanoparticle otherwise known as polyester nanoparticles that encompass either a poly(lactic-co-glycolic) acid (PLGA) or poly(lactic) acid PLA core has also been introduced to repair brain function following TBI, as their core and architecture provide synthetic versatility and stability (Fig. 9). Their efficacy can also be enhanced by surface Poly(ethylene glycol) (PEGylation) which can increase their stealth properties, otherwise known as their ability to evade immune recognition, enhancing their circulation time and the chances of reaching their target.[192,193] Furthermore, their ability to degrade, and clear from the body, is also essential for their use. These nanoparticles may also include 800CW, a cyanide dye that binds to necrotic areas, increasing the targeting of injured areas.[194,195] The size of polyester nanoparticles can also be easily manipulated, supporting studies that focus on the impact of nanoparticle size on targeting and accumulating in injured areas of the brain.[190,195] In addition to their size, core, and PEGylation, which is imperative to their efficacy in targeting and delivery, studies have also

indicated that polyester nanoparticles may be able to target and accumulate in endothelial cells and microglia, improving injury outcomes.[196–198]

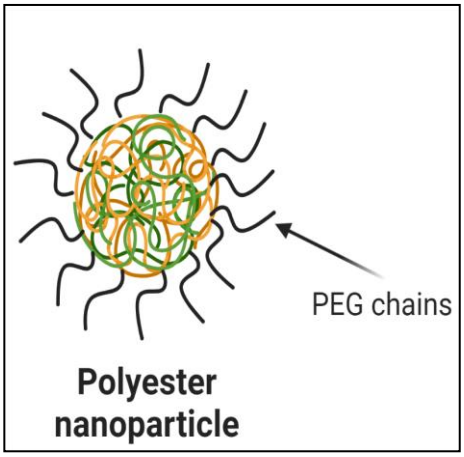

Figure 9. Representative image of a polyester nanoparticle. Polyester nanoparticles can have either a PLGA or PLA core with or without PEGylated chains. Polyester nanoparticles can vary in size which aid in penetrating the BBB, effective targeted delivery, and accumulation of nanoparticles at the injury site. Created with BioRender.com

While many strategies are currently being tested and researched to treat TBI, technological advances such as nanoparticle delivery are promising avenues that can assist in targeting the secondary injury mechanisms that contribute to TBI outcomes. Polyester nanoparticles have stood out as advantageous due to their permeability and accumulation rates, and their simplistic design process can support a range of molecules for targeted drug delivery. Thus, it is vital to continue to study their efficacy in treating TBI, especially in microglia-mediated inflammation.

2.9. Brain Regions of Interest

The VandeVord lab has taken a comprehensive approach to studying the pathological changes that are taking place following blast injury within the brain. However, characterizing the microglial response to the injury is lacking. The hippocampus, a complex structure embedded deep into the temporal part of the cerebral cortex, will be a region of interest when investigating microglia dynamics following TBI. The hippocampus plays a significant role in learning and memory, so damage to this region can lead to memory deficits, a frequently reported symptom of

TBI.[199] A study by Caplan et al. demonstrated the importance of investigating microglia activation in the hippocampus, as its interactions with neuronal synapses determined that microglia play a crucial role in the formation and processing of spatial learning, thus the hippocampus is quite vulnerable to microglia activation following injury or disease.[200]

Another study by Madathil et al. demonstrated that at early time points (three days), there was a dominant M1 microglia response in the hippocampus following closed head concussive injury.[201] While microglia polarization states have supported that microglia activation in the hippocampus is present, exploring morphologically driven functional changes in microglia following TBI will contribute to understanding the underlying mechanisms that drive neuropathology. The motor cortex (MC) is also a region of interest when identifying the problematic nature of TBI and its symptoms. Neuronal dysfunction has been studied extensively in the MC following TBI, with limited research investigating microglia activation, which may be in response to neuronal perturbations in this region.[202–204]

Additionally, studies following impact TBI have indicated changes in microglia activation in the injured brain's contralateral and ipsilateral sides, with temporal heterogeneity driving this response.[205] Understanding the functional changes within this region in a closed-head model of impact TBI can aid in understanding acute and subacute microglia changes and if differences in the contralateral and ipsilateral sides of the MC are still observed. Injury to the MC also contributes to disruption in sensorimotor networks, deficits in motor function, and studies have indicated injury-induced plasticity occurring in this region; thus, how microglia-mediated responses contribute to these outcomes in TBI is imperative. Dickerson et al. also indicated that dysfunction within the MC and the hippocampus persist chronically following TBI, contributing to behavioral deficits such as anxiety-and depressive-like behaviors.[206] Thus, wading into the details of the functional states of activated microglia in these regions following TBI is important to consider. Finally, the somatosensory cortex (SC) within the parietal lobe has been the location of impact in CCI models.[207–209] As characterization and repeatability of a closed-head CCI model for this work are achieved, the ipsilateral and contralateral sides of the SC will also be a primary region of interest.

Chapter 3: Investigating the Characteristics of Microglia Activation Following Blast Induced Neurotrauma

The materials and methods section within Chapter 3 are adapted, in part, from: Dickerson, M., Bailey Z., Murphy, S., Urban, M., White, Z., VandeVord, P.J, "Glial Activation in the Thalamus Contributes to Vestibulomotor Deficits Following Blast-Induced Neurotrauma," *Front. Neurol.*, vol. 11, 2020, doi: 10.3389/fneur.2020.00618.

3.1 Introduction

Blast-induced TBI is a prevalent injury within military populations, with mild bTBI having the highest reported severity in the active military and Veteran populations.[210–212] There has been growing concern about the detrimental effects of repeated mild bTBIs due to exposure to low-level blasts during military training.[108,213,214] Additionally, mild bTBIs have an "invisible nature," meaning that there are no obvious outward signs of injury, so one can unknowingly sustain a bTBI, making them susceptible to multiple bTBIs over time. Also, there is a growing concern about the detrimental effects of multiple low-level blasts that military personnel experience during combat training.[108,215] The secondary injury mechanisms following repeated blast exposure can lead to the mechanical compromise of cells that can influence sequelae such as inflammation, changes in ICP, and BBB dysfunction, as mentioned in section 2.4. For microglia, in particular, they contribute to maintaining homeostasis within the brain, meaning the role of these cells within the injured brain can lead to phagocytosis of cell debris, maintaining the integrity of synapses, further surveying of the brain in response to compromise of other glia such as astrocytes and oligodendrocytes, and tissue plasticity.[123,216] Despite a general understanding of neuropathology following blast injury, further understanding of the underlying mechanisms that are involved in microglia-induced inflammation following repeated blast exposure is necessary.

This study aimed to establish early patterns of microglia dysfunction that contribute to the pro- and anti-inflammatory response following repeated blast exposure. Moreover, some aspects of microglia activation are poorly understood following bTBI, making it imperative to study the spatial and temporal changes that microglia undergo following blast injury. Previous studies have shown that increases in microglia cells and their expression of proteins such as ionized calcium-binding adapter molecule 1 (IBA-1) compared to controls are an indicator of activation. Pathological changes taking place in areas such as the hippocampus and the MC even persisted for days, even months, following blast injury.[103,214,215–217] Previously, it was understood that microglia were classified into two subsets following disease or injury: M1 (pro-inflammatory) and M2 (anti-inflammatory). However, emerging research indicates that microglia play a more elaborate role in the resolution of inflammatory responses, and this is due to the morphological changes that take place as a part of their activation, as illustrated in Figure 7. While the knowledge of the various morphological states of microglia is emerging, there is still a lack of understanding as to what

microglia's acute and subacute morphologically driven functions are within the brain following repeated blast exposure.

The NLRP3 inflammasome complex located within the cell is a novel molecule that is also a driving force inducing microglia activation.[221,222] Following blast injury, molecules such as PAMPs or DAMPs trigger mechanistic pathways within microglia, activating the complex and releasing pro-inflammatory cytokines such as Il-1β, contributing to the neurotoxic inflammatory response. Due to the presence of these molecules, exploring NLRP3 levels following repeated blast exposure may give insight into the complex functions of microglia in the injured brain. This study aimed to understand microglia dynamics in an *in vivo* bTBI model, investigating spatial and temporal changes in microglia proliferation, IBA-1 expression, and morphological states, which are all hallmark characteristics of microglia activation.

3.2. Methods

The Virginia Tech Institutional Animal Care and Use Committee (IACUC) approved the experimental protocols described herein. Before experimentation, male Sprague Dawley rats (Envigo, Dublin, VA, USA) weighing approximately 240-260 g were acclimated for several days (12 h light/dark cycle) with food and water provided *ab libitum*.

3.2.1. Blast Induced Traumatic Brain Injury

The blast wave was generated using a custom Advanced Blast Simulator (ABS) (200 cm x 30.48 cm x 30.48 cm) located in the Center of Injury Biomechanics at Virginia Tech University. The ABS consists of three distinct sections to create, develop, and dissipate the blast wave (Fig. 10). These sections include: 1) the driver section, which developed the blast wave following a helium-driven rupture of calibrated acetate membranes, 2) the transition section where the animal was exposed to a single peak overpressure representing a free-field blast exposure, and 3) an end-wave eliminator located downstream the test location to facilitate the dissipation of the blast wave through a series of baffles.

Figure 10. Advanced Blast Simulator (ABS). The ABS was used to re-create free field blast exposures. Acetate membranes are passively ruptured following pressurization using helium gas in the driver section (left). The blast waves reaches the animal located in the transition section (middle window) and is dissipated in the end-wave eliminator (right).

Before blast exposure, the animal was anesthetized with 5% isoflurane and then placed in the ABS. Each animal was supported in the prone position inside the ABS, facing the oncoming shock front using a mesh sling. The sling was designed to minimize flow hindrance and isolate primary blast injury by eliminating acceleration/deceleration injuries. Animals were exposed to three blasts (~17 psi) separated by one hour each (3 x 1h) (n = 8). There was also a sham group for each time point (n = 8). Sham animals received all the same procedures except the blast insult. Following the sham or blast procedures, animals were observed through the recovery stages of injury and anesthesia.

3.2.2 Immunohistochemistry

Three- or seven-days following injury, animals were euthanized by transcardial perfusion of 0.9% saline and 4% paraformaldehyde. Following perfusion, brains were collected and stored in a 4% paraformaldehyde fixative solution. After 24 hours in the fixative, whole brains were cryoprotected in a 30% sucrose solution for tissue sectioning preparation. Once whole brains were submerged entirely in sucrose solution (~48 hours), tissues were then embedded in Tissue-Tek optimal cutting temperature (OCT) embedding medium (Sakura Finetek US, Inc., Torrance CA) and frozen at -80^{o}C for cryostat processing. Brains were sectioned at 30 µm in the coronal plane. Samples were rinsed three times with phosphate-buffered saline (PBS) and were permeabilized in PBS with 0.3% Triton X (PBX) for 30 minutes at room temperature. Samples were incubated in 2% bovine serum albumin (BSA) or 5% Normal Donkey Serum in PBS for 1 hour at room

temperature. Sections were incubated for 16-18 hours at 4oC with the primary antibody ionized calcium-binding adaptor molecule 1 (IBA-1, 1:300, Biocare Medical, Concord, California) or NLRP3 (1:200, Invitrogen, Carlsbad, CA). The following day, sections were washed three times for 5 minutes in PBX and incubated for 1.5 hours at room temperature with a secondary antibody (Alexa Flour 546 anti-mouse IgG antibody (Invitrogen, Carlsbad, California)). After three more 5-minute PBX washes, samples were mounted and cover-slipped with Slow Fade Reagent with DAPI (Invitrogen, Carlsbad, CA). Sections were then imaged under a Zeiss fluorescence microscope at 20X magnification. Brain sections included the MC and the hippocampus, further delineating the hippocampus into its four sub-regions: DG, CA1, CA2, and CA3.

3.2.3 Image Acquisition and Analyses

Images were acquired in each region and then processed with background subtraction and fixed thresholding to generate masks of IBA-1+ microglia and NLRP3. Using FIJI/Image J software, a comprehensive analysis of neuropathology was provided by quantifying four specific parameters using ImageJ software (NIH, Bethesda, MD). These parameters include area fraction, count per area, fluorescence intensity, and mean area/cell. Area fraction quantifies the percentage of positive signals within the region of interest. Count per area represents the total number of positive cells divided by the area. Fluorescence intensity measures the level of fluorescence intensity in the positive signal using the gray pixel intensity. Mean area/cell provides detail to the average cell size normalized to the area, giving the average area/cell. Count per area and mean area/cell was completed using the "analyze particles" function with the “pixel area size threshold” of 25 to exclude slight pixel noise and extract objects of interest. Brain region values were averaged from four images for each animal per stain.

3.2.4 Quantifying Microglia Morphology

To provide a greater understanding of the changes of IBA-1+ microglia, we quantified microglia morphology. The skeleton analysis method developed by Young and Morrison was used for this analysis.[223] Images were converted to binary and skeletonized using ImageJ software (Fig. 11). The AnalyzeSkeleton plugin was then applied to all skeletonized images to collect data on the number of branch endpoints and branch length per frame. A cut-off branch length value of 0.45 um was used to exclude small fragments from each data set. The data from each frame was then

divided by the number of microglia in the corresponding image to give branch length/cell and branch points/cell.

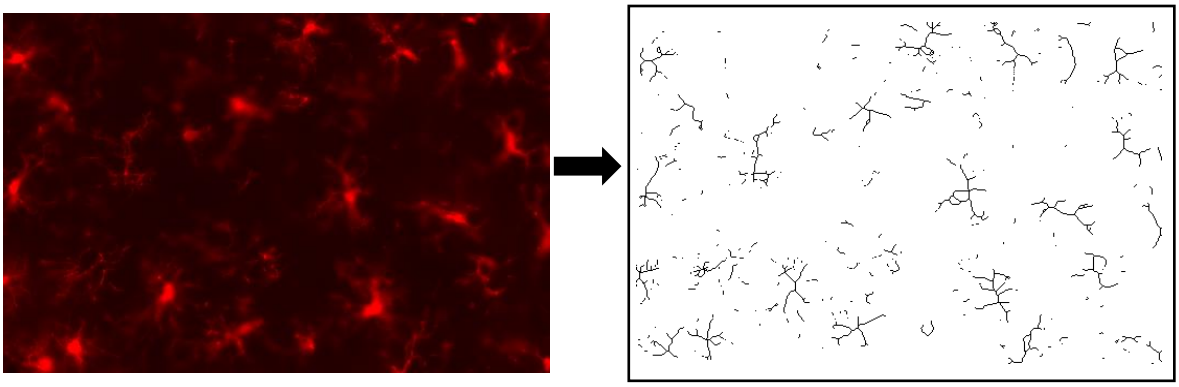

Figure 11. Using fluorescent imaging of IBA-1 for skeleton analysis. (Left) Image of IBA-1 with its corresponding illustration of skeletonized microglia (Right).

3.2.5 Statistical Analysis

GraphPad Prism Version 9 was used for all statistical analyses (GraphPad Software, La Jolla, CA). The student's t-test was used to evaluate the statistical differences between the blast and sham groups, with the assumptions of normality and equality of variances examined using the Shapiro-Wilk test and Levene's test, respectively. Welch's corrective t-test or Mann Whitney's non-parametric test was used to evaluate data that failed the normality and equal variance assumptions. At $p<0.05$ and $p<0.1$, respectively, data were considered statistically significant and trending. All histology data were normalized to respective shams, and data are represented as the mean ± standard error of the mean (SEM).

3.3 Results

Blast animals (n = 8) were exposed to three blast events one hour apart. Blast wave parameters are described in Table 1. Sham animals (n = 8) were exposed to all procedures with the exception of the blast exposures. Following exposures, no obvious external signs of injury were discernible. Over the three- and seven-day period, there was no significant difference in the weights measured in the repeated bTBI group compared to shams.

Table 1. Summary of Blast Wave Characteristics. The average peak pressure resulted in a blast wave magnitude of approximately 17 psi. Results are represented as Mean ± SEM.

Group	Peak Pressure (psi)	Duration (ms)	Impulse (psi*ms)	Rise Time (ms)
3 days	17.48 ± 0.37	2.18 ± 0.04	14.42 ± 0.32	0.05 ± 0.02
7 days	16.52 ± 2.12	2.12 ± 0.21	13.34 ± 1.69	0.02 ± 0.002

3.3.1 Examining pathological changes in microglia in the MC three days following injury

To capture the regional and longitudinal changes in microglia following repeated blast exposure, levels of IBA-1 in the MC and hippocampus were measured following injury using immunohistochemistry analysis (IHC). At the three-day time point, a significant increase in cell size (mean area/cell) was observed in the MC of blast animals compared to shams ($p=0.03$)(Fig. 12). No significant differences were found for area fraction, count per area, or fluorescent intensity within this region.

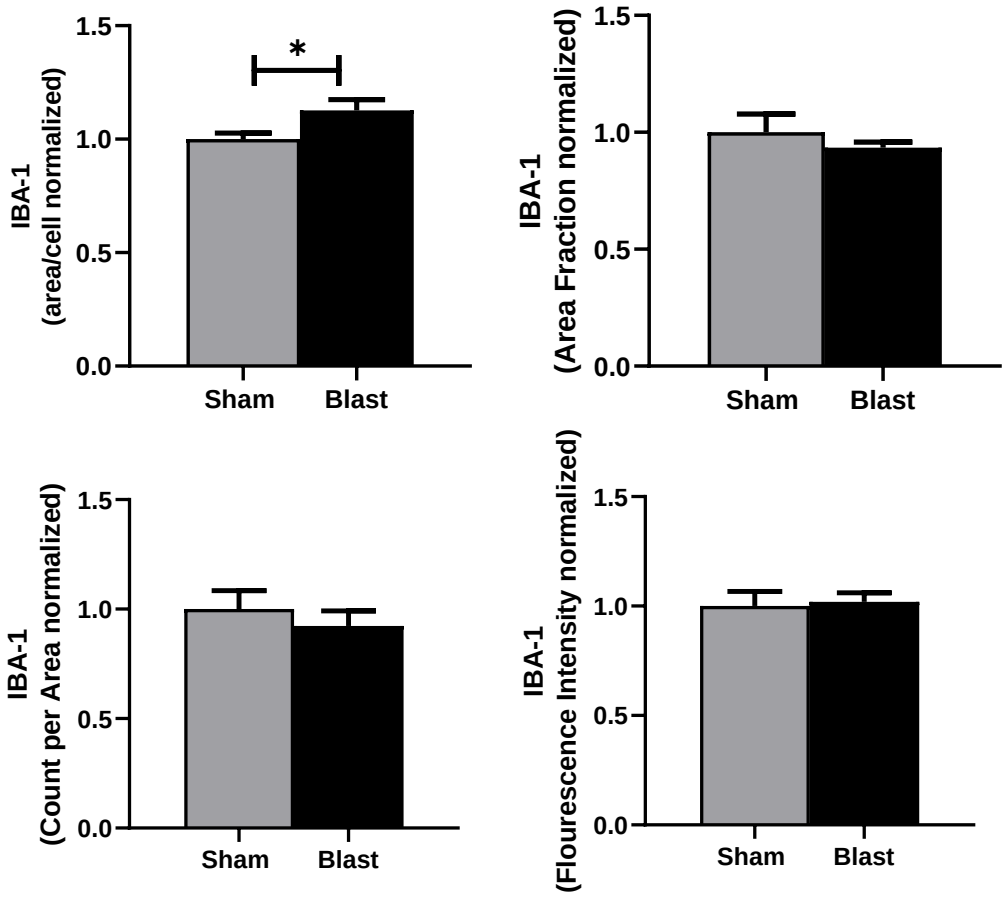

Figure 12. Changes in the size of microglia were present in the MC in response to injury. Significant decreases in area/cell were seen in the motor cortex of blast animals compared to shams three days following injury. *$p<0.05$. Data represented as Mean ± SEM.

To analyze the morphological changes of microglia, skeleton analysis allowed for the quantification of increases and/or decreases in branch length and branch points of microglia to aid in understanding what morphologies microglia may be undergoing in response to injury (Figure 13). Skeleton analysis indicated a significant decrease in branch length/cell in blast animals compared to shams ($p=0.02$), with a trending decrease in branch points/cell in blast animals compared to shams ($p=0.06$) (Fig. 14).

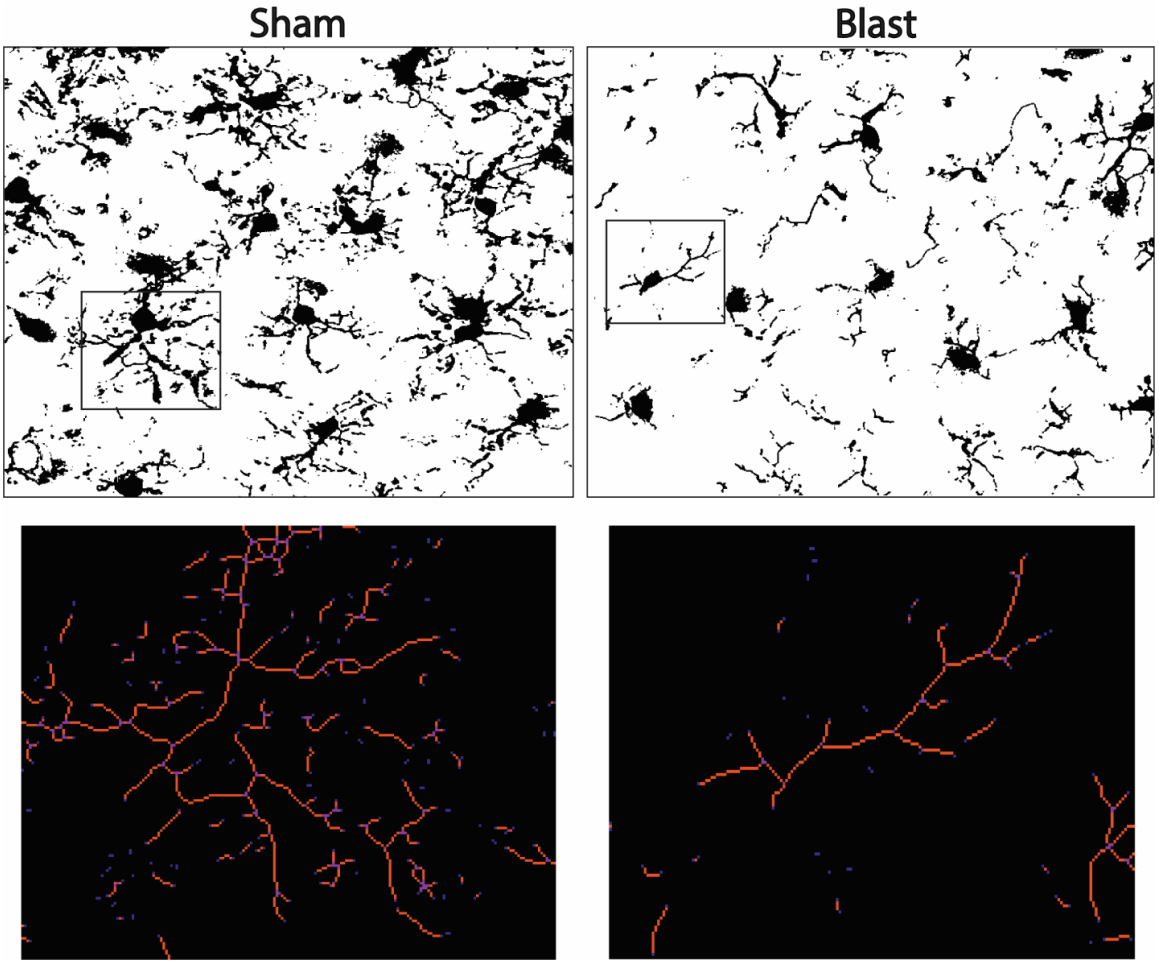

Figure 13. Representative image showing morphological changes that occurred following blast injury. (Top) Microglia in the MC of blast animals show morphologies representative of elongated cell bodies, decreases in branch length and decreases in branch points. (Bottom) Microglia were then skeletonized, extracting information needed to quantify parameters used for morphological analysis.

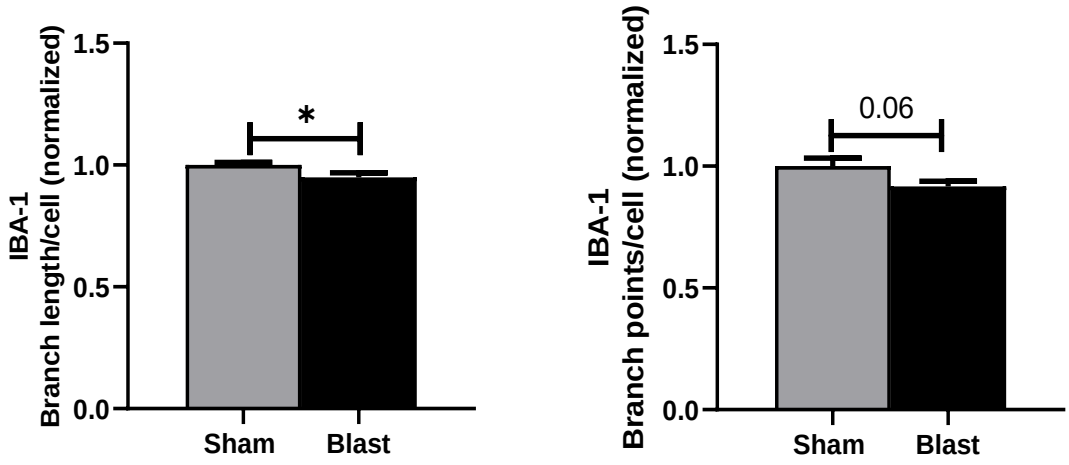

Figure 14. Changes in microglia morphology are observed in the MC three days following blast injury. A significant decrease in branch length/cell was observed in the blast group compared to shams. A trending decrease in branch points/cell was also found in the blast group. *p<0.05. Data represented as Mean ± SEM.

3.3.2 Limited changes in microglia activation are observed within the hippocampus at three days

Within the hippocampus, limited activation was observed three days following repeated blast exposure. Within the CA1 sub-region of the hippocampus, the amount of positive signal of IBA-1 was significantly increased within the blast group compared to their sham counterparts (p=0.04). No significant differences were observed in the hippocampus for area/cell, count per area, or fluorescent intensity (Fig. 15).

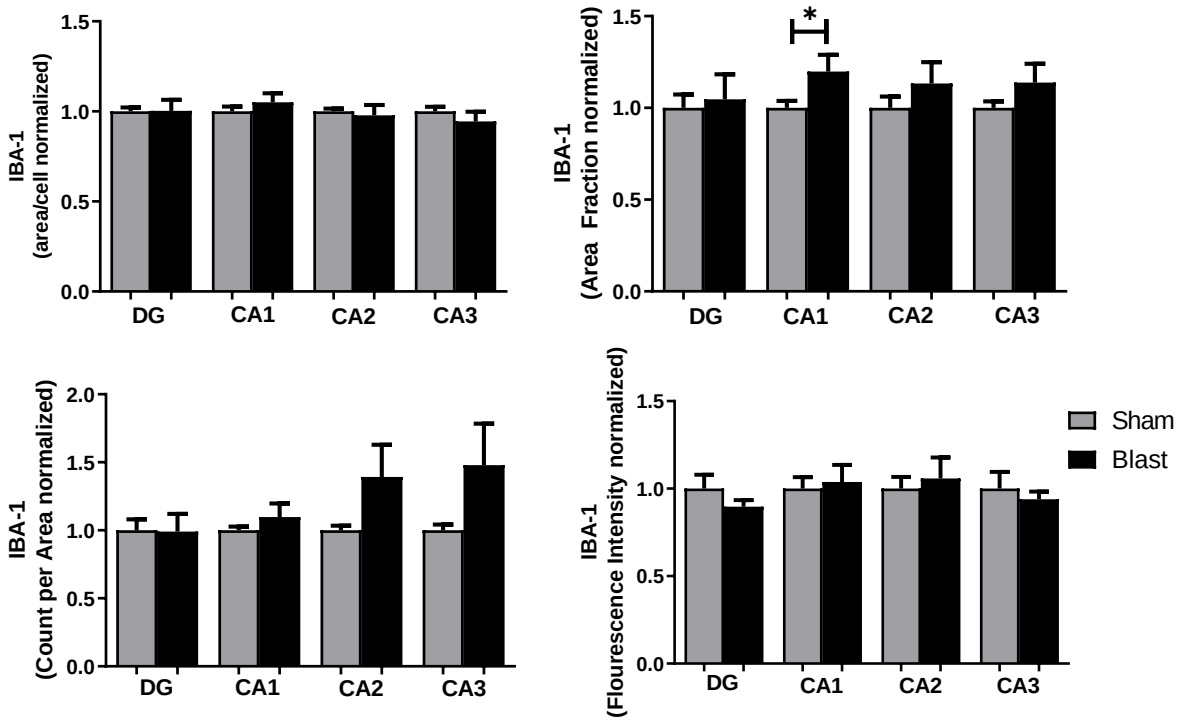

Figure 15. Increased presence of IBA-1 was found in the CA2 three days following injury. A significant increase in area fraction was detected in the CA2 sub-region of the hippocampus in blast animals compared to shams. No other significance was found in the other sub-regions. *p<0.05. Data represented as Mean ± SEM.

No significant changes in microglia morphology were observed within the hippocampus three days following repeated blast exposure. Trending decreases in branch length/cell were observed in the CA2 sub-region of blast animals compared to shams (p=0.07), with no significant or trending changes in any other sub-region for this parameter. No significant differences in branch points/cell were observed between groups in the hippocampus (Fig. 16).

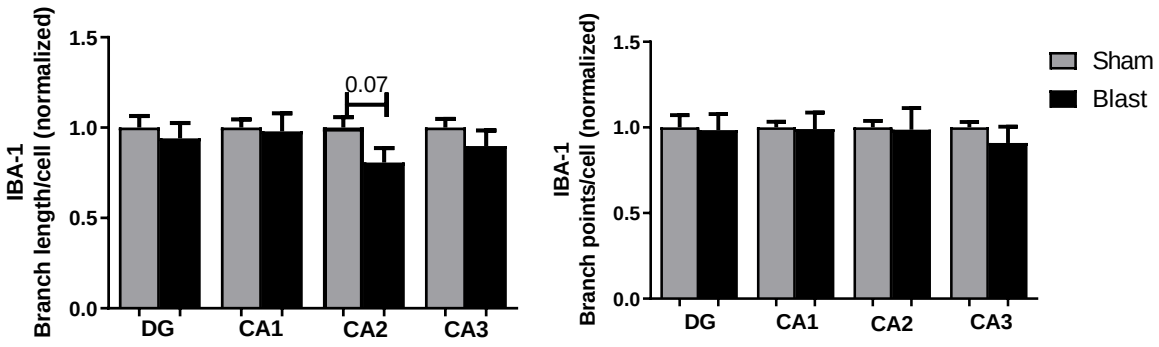

Figure 16. Limited changes in microglia morphology were seen in the hippocampus three days following injury. A trending decrease in branch length/cell was found within the CA2 sub-region of the hippocampus. Data represented as Mean ± SEM.

3.3.3 Observing microglia pathology in the MC seven days following injury

At the seven-day time point, significant differences were observed in the MC region. A significant decrease in mean area/cell was observed in the blast group compared to shams ($p=0.02$). Trending decreases in area fraction were observed in the blast group ($p=0.08$), with similar decreases in fluorescent intensity ($p=0.06$) (Fig. 17). While there was a significant decrease in the size of microglia, further morphological analysis did not show significant decreases in branch points/cell or branch length/cell for either group in the MC (Fig. 18).

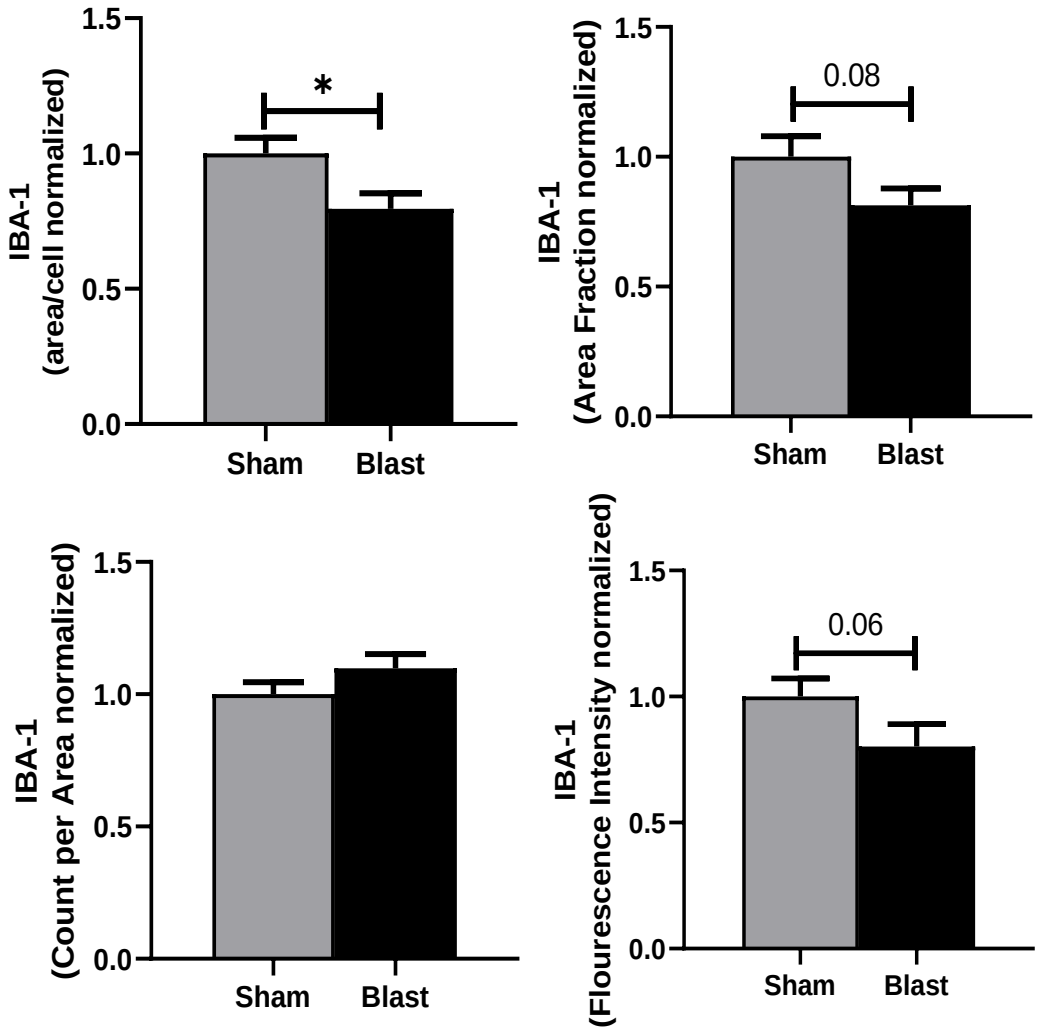

Figure 17. Changes in IBA-1+ microglia were found in the MC seven days following blast injury. Significant decreases in area/cell were seen in the motor cortex of blast animals compared to shams. Trending decreases are also depicted in area fraction and fluorescent intensity within this region of blast animals. *$p<0.05$. Data represented as Mean ± SEM.

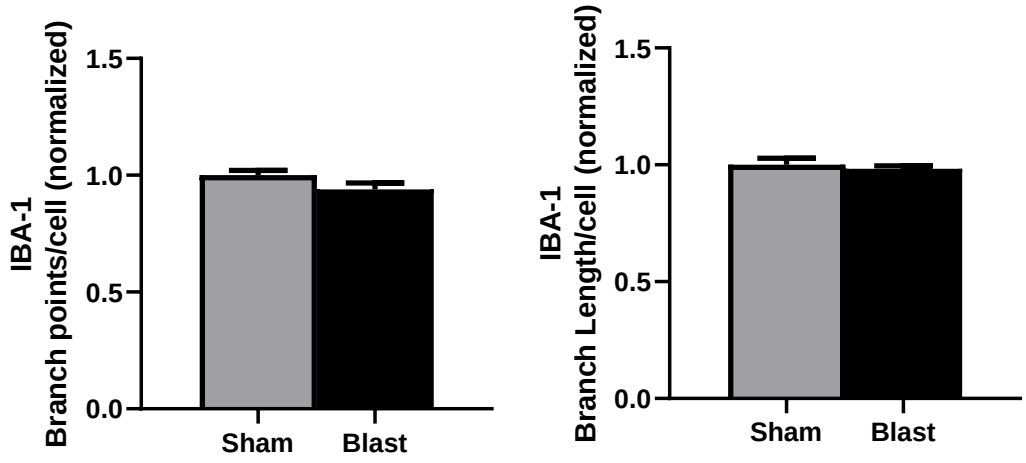

Figure 18. Quantifying microglia morphology using skeleton analysis. No significant changes in branch length/cell or branch points/cell were noted in the MC seven days following injury**.** Data represented as Mean ± SEM

3.3.4 Microglia Responses to injury are detected in the hippocampus seven days post blast

Within the hippocampus, microglia activation was observed, with Figure 19 depicting this change. A significant decrease in mean area/cell was observed within the CA1 (p=0.007), CA2 (p=0.006), and the CA3 sub-region of the hippocampus (p=0.02). Significant decreases in area fraction were found in the DG (p=0.05), CA1 (p=0.02), CA2 (p=0.007), and the CA3 sub-region (p=0.05) of the hippocampus. Decreases in IBA-1 expression (fluorescence intensity) was also observed in the DG (p=0.02), CA1 (p=0.0008), CA2 (p=0.006), and the CA3 sub-region of the hippocampus (p=0.02). No significant changes in the amount of IBA-1+ microglia (count per area), were observed in the hippocampus (Fig. 20).

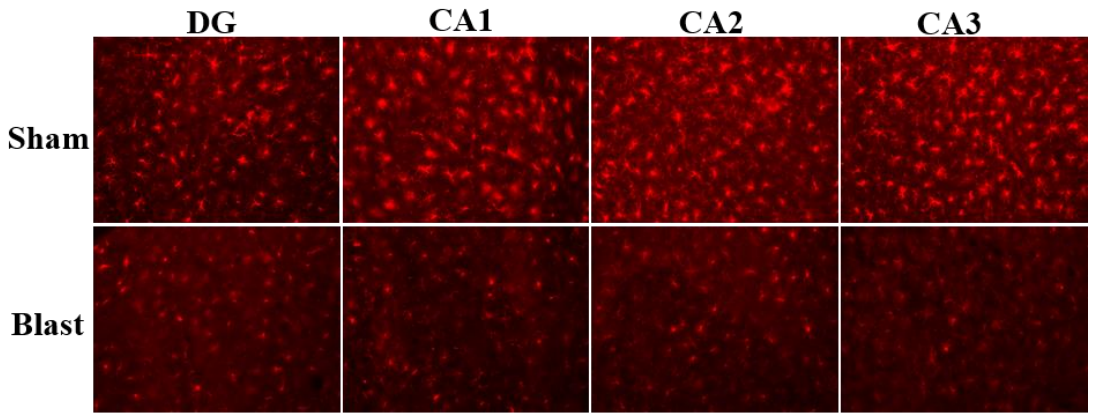

Figure 19. Representative images of IBA-1 expression in the hippocampus. Significant decreases ($p<0.05$) in IBA-1 expression were seen across all sub-regions in the blast group.

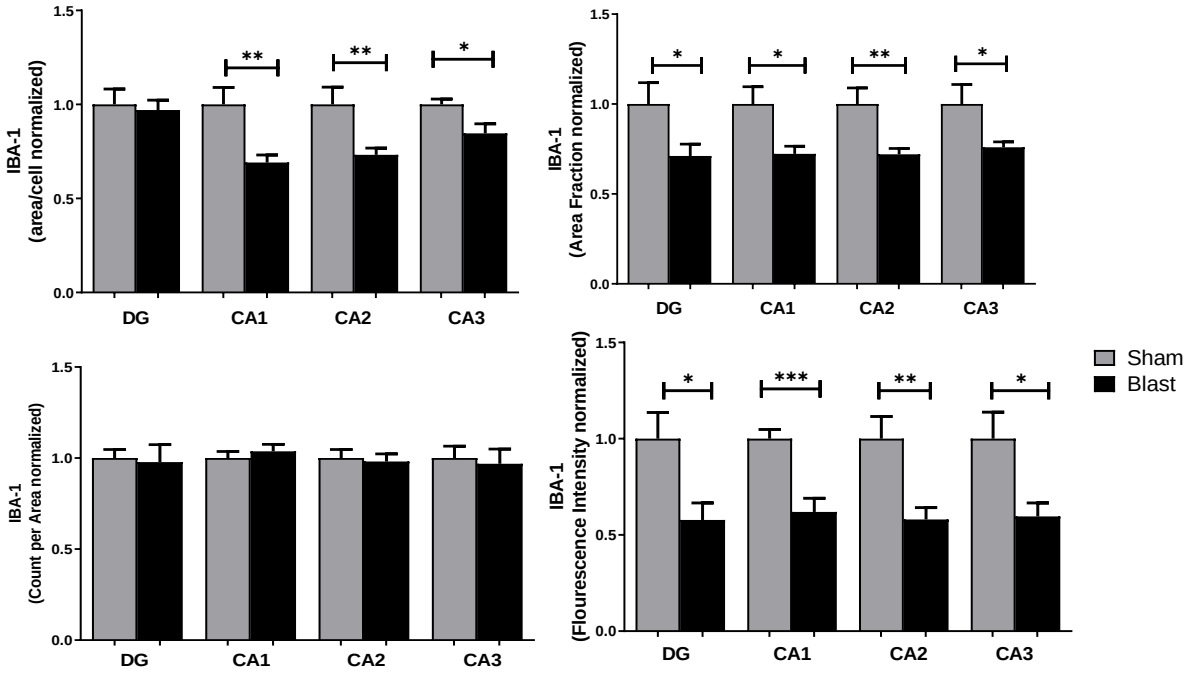

Figure 20. Microglia activation was depicted in the hippocampal sub-regions of blast animals seven days following blast exposure. Significant decreases were shown in blast animals in area/cell, integrated density of fluorescence and area fraction. *$p<0.05$, **$p<0.01$, ***$p<0.001$. Data represented as Mean ± SEM**.**

With the significant changes in IBA-1 expression and cell body size identified in the hippocampus seven days following repeated blast exposure, quantifying the morphological changes could give further insight into the subacute pathological changes of microglia (Fig. 21). Skeleton analysis indicated a significant increase in branch length/cell in the CA1 sub-region ($p=0.03$), the CA2 ($p=0.002$), and trending increase in the CA3 ($p=0.06$). Branch endpoints/cell showed similar increases with a trending increase in the CA1 ($p=0.07$), the CA2 ($p=0.01$), and the CA3 ($p=0.04$) (Fig. 22).

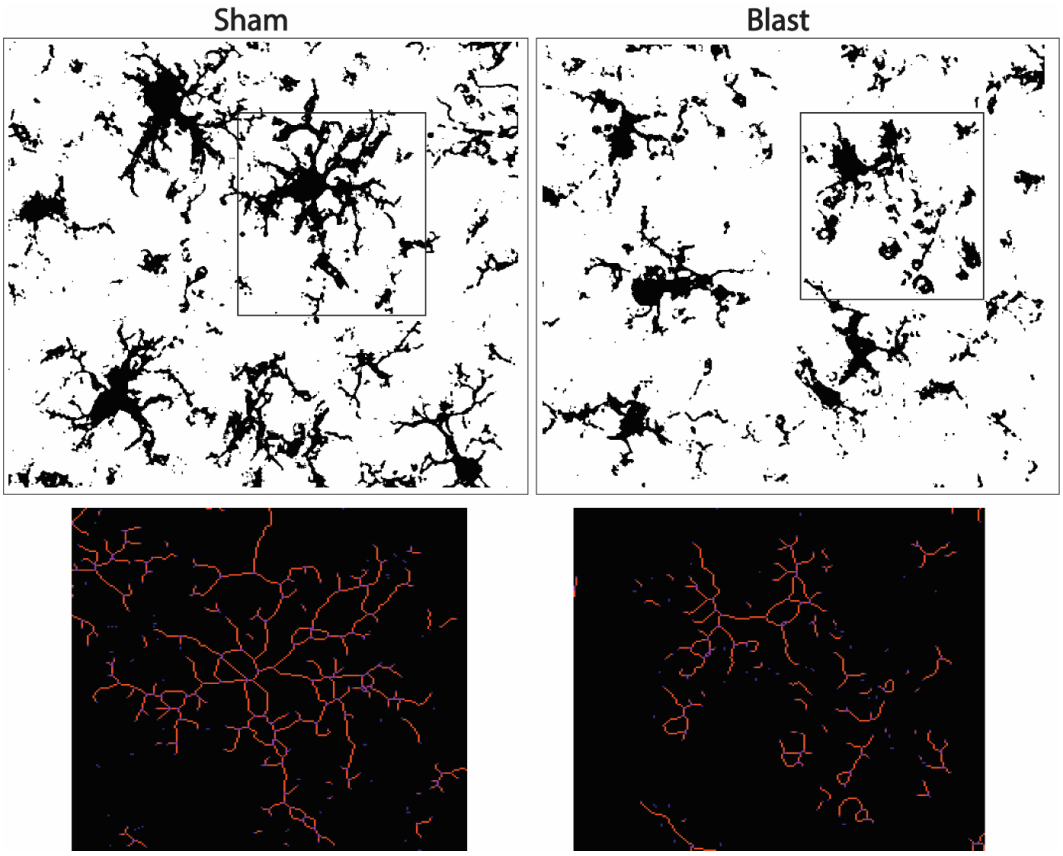

Figure 21. Representative image showing morphological changes in the CA2 that occur seven days following repeated blast exposure. (Top) Microglia in the CA2 of blast animals show morphologies that are representative of a swelled soma, fragmented branches, and increased branching. (Bottom) An example of skeletonizing microglia for morphological analysis.

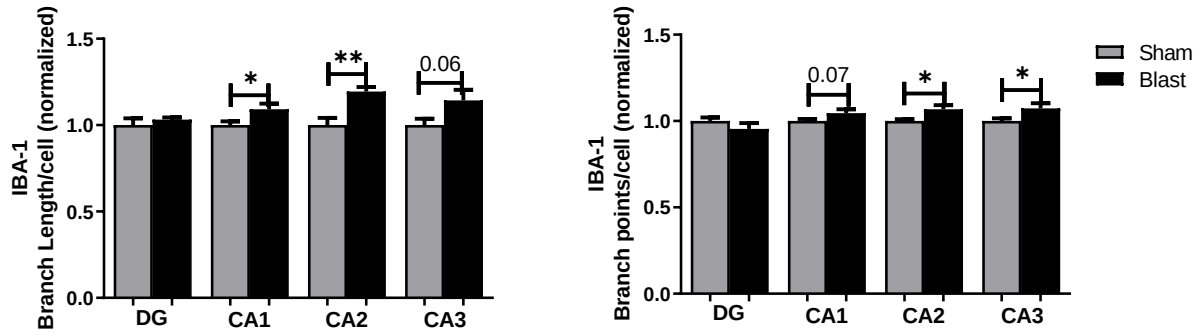

Figure 22. Sub-region morphological analysis of microglia seven days following bTBI. Significant increases in branch length/cell were observed in the CA1 and CA2 with a trending increases in the CA3, while significant increases in branch points/cell were found in the CA2 and CA3, with a trending increase in the CA1 of blast animals compared to shams. *$p<0.05$, ** $p<0.01$. Data represented as Mean ± SEM.

3.3.5 Limited changes in NLRP3 in the MC and hippocampus seven days following repeated blast exposure

With pathological changes of microglia prevalent seven days following injury, exploring the inflammatory response on a molecular level was conducted. NLRP3, an inflammasome found within microglia, aids in the secretion of pro-inflammatory cytokines such as IL-1β when activated due to injury or disease. The amount of NLRP3+ molecules (count per area) and NLRP3 expression (fluorescence intensity) was quantified to further explore whether there is a pro- or anti-inflammatory-driven response occurring seven days following repeated blast exposure. Figure 23 shows both NLRP3+ cells and intracellular NLRP3 signals within the brain.

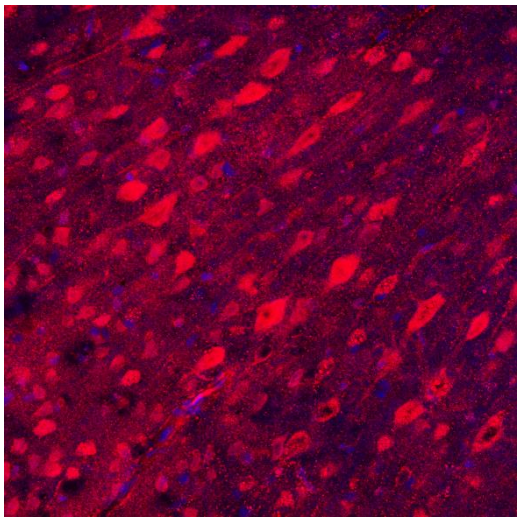

Figure 23. Representative image of NLRP3 within the brain. NLRP3 co-labeled with DAPI shows intracellular NLRP3, as well as NLRP3+ cells.

No significant changes in the amount of NLRP3+ molecules or the fluorescent intensity of NLRP3 were observed within the MC region between the blast and sham groups (Fig. 24). Within the hippocampus, trending decreases in count per area were observed in the DG (p=0.06) and the CA2 sub-region (p=0.09) of the hippocampus. When analyzing fluorescent intensity, a trending decrease was seen in the CA1 sub-region (p=0.08) (Fig. 25).

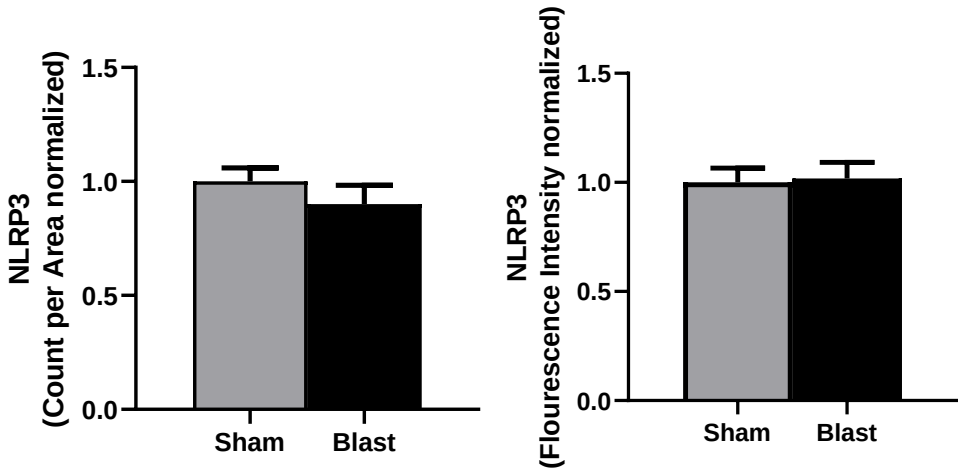

Figure 24. Limited changes in NLRP3 were seen in the MC seven days following repeated blast exposure. No significant changes in count per area of NLRP3 or fluorescent intensity of NLRP3 were observed in the MC seven days following injury. Data represented as Mean ± SEM.

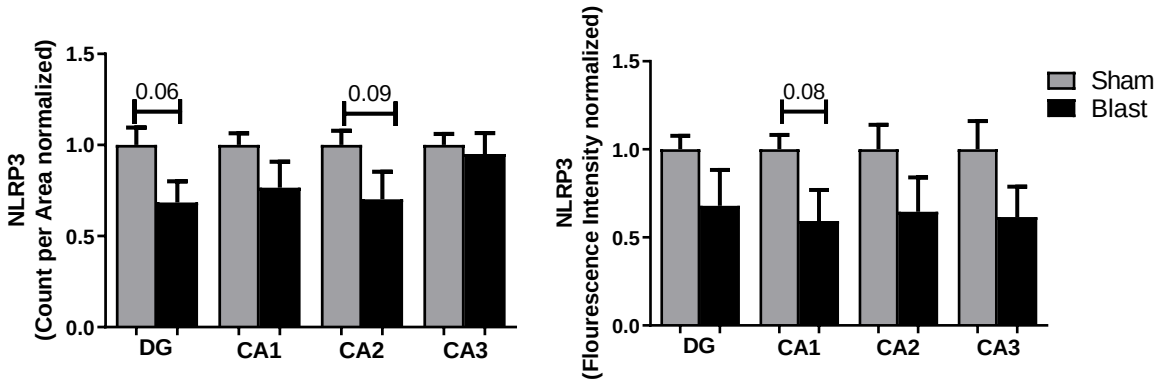

Figure 25. Decreased NLRP3 expression was detected in the hippocampus of blast-injured animals. Trending decreases ($p<0.1$) in count per area are observed in the DG and CA2 sub-regions, while trending decreases in fluorescent intensity are observed in the CA1 of blast-injured animals compared to shams. Data represented as Mean ± SEM.

3.4 Discussion

With neurological impairments reported and diagnosed in the Veteran community following bTBI,[224–226] it is vital to study the consequences caused by blast injury. While it is known that blast exposure can lead to acute and even chronic pathologies, an understanding of microglia's dynamic role in contributing to neuroinflammation following bTBI is lacking. In this study, animals were subjected to three blast insults separated by one hour each. Results from this preclinical study indicated that repeated blast exposures led to microglial changes within the brain that are both time, and region-specific.

Several studies have shown that microglia play an essential role in the secondary injury response following TBI. However, little is known about the underlying molecular details contributing to microglia's acute and sub-acute involvement within the injury response and what morphologies microglia display following bTBI. These details are critical in generating relevant information that can aid in developing strategies for therapeutic intervention in both the acute and even chronic stages of injury. In order to investigate the phenotypic changes of microglia following repeated blast injury, IHC was performed in the MC and hippocampus regions of the brain to assess pathology three- and seven-days following injury. Three days following repeated blast exposure, increases in the cell body size of IBA-1+ microglia were observed in the MC of blast

animals compared to shams. To explore the meaning of this increase in the area/cell, quantifying microglia morphology was done to determine what morphologies of microglia were present in this region following blast exposure. While an increase in cell body size was observed, a decrease in the branch length/cell and branch points/cell were identified in the MC at this three-day time point. An increase in cell size and a decrease in both branch length/cell and branch points/cell may be consistent with microglia adopting a "rod-like" morphology, meaning their cell bodies are elongated with their primary processes projected toward the two ends of the cell. A rod-like morphology has been described as having an increased cell length-to-width ratio, with a reduced number and length of side branches,[227] which is consistent with the results found in our IHC studies. "Rod-like" microglia play a neuroprotective role within the brain through reorganizing and remodeling neuronal and synaptic circuitry following CNS injuries.[228,229] Moreover, they also exert phagocytic functions as they respond to neural insults, aligning adjacent to injured dendrites and axons. Rodent studies have also indicated that rod-like microglia are more commonly found in the cerebral cortex in the acute stages of injury models such as fluid percussion-induced TBI or ischemia.[230] The results from the current study indicate that rod-like microglia are present within the cortex in the acute stages of bTBI as well.

Within the hippocampus, small changes in microglia pathology were observed (Fig. 15). The amount of positive IBA-1 signal was increased in the CA1 sub-region of blast animals compared to shams. However, other forms of microglia activation, such as a decrease or increase in IBA-1+ microglia, changes in cell shape or size, and/or IBA-1 expression, were not present. A previous study by Huber et al. observed microglia changes in the brain 4 hours following a single blast overpressure.[231] However, very few have reported on the pathological changes of microglia three days following blast injury, with no studies observing changes following repeated blast exposure. Due to this, it is difficult to speculate what time-dependent and/or region-specific role microglia is taking on at this time point. Microglia could be trying to return to pre-injury levels within the hippocampus three days following injury, or microglia cells could be constantly migrating in and out of this area at this time, which may lead to minute differences between blast and shams. More studies are needed to support these claims.

At the seven-day time point, an opposite effect seems to occur within the MC compared to the pathological changes within the MC three days following repeated blast exposure. For example, mean area/cell was significantly decreased in blast animals compared to shams seven

days following injury, whereas an increase in cell size was observed in the MC three days following repeated blast exposure. To explore microglia size and shape further, changes in branch points/cell and branch length/cell were explored, but no significant differences were found between the blast and sham groups in this region. With the size of the cell decreasing in the MC at seven days, and no changes in morphology, microglia could be trying to return to a pre-injured, ramified state at this specific time point in this region. Within the hippocampus, evidence of microglia activation was observed through a decrease in mean area/cell, area fraction, and fluorescent intensity of IBA-1 seven days following repeated blast exposure. Changes in IBA-1 expression have been observed following blast exposure of varying magnitudes with a study by Hubbard et al. demonstrating decreases in IBA-1 expression seven days following a single blast injury, whereas studies by Sajja et al. demonstrated increases in expression seven days following a single blast exposure.[88,232,233] While the results herein demonstrate that activation consistently takes place sub-acutely, varying severity, such as single versus repeated blast, or increases in pressure magnitudes may play a role in functional changes of microglia.

While microglia activation has been established in both a single and repeated blast exposure, this is the first study to speculate on functional changes of microglia based on their morphology following a repeated blast injury. Quantification of microglia morphology indicated increases in branch length/cell in the CA1 and CA2 sub-regions of blast animals and significant increases in branch points/cell in the CA2 and CA3 sub-regions. The increases in area/cell, branch length/cell, and branch points/cell could indicate that microglia are becoming more dystrophic. Dystrophic microglia are known to have a fragmented cytoplasm, spheroidal inclusions (rounded swelling), and more distal, fragmented processes and branches.[234–236] Dystrophic microglia undergo an "anti-inflammatory role" with decreased surveillance and phagocytosis and have traditionally been shown to respond to increases in TAU.[237] Studies also show its prevalence in the aging brain, especially the hippocampus, in response to neurodegenerative diseases such as Alzheimer's disease.[236,238–240] This abnormal morphology that microglia take on has also been associated with the degeneration of microglia itself, with researchers hypothesizing that degenerating microglia and the loss of their neuroprotection is what influences neuronal degeneration.[238]

Hippocampal vulnerability to CNS injury has been reported,[233,241–243] but the mechanisms contributing to its vulnerability to blast injury still need to be elucidated. The hippocampus forms

a unidirectional pathway, with pyramidal neurons located in the CA1, CA2, and CA3, that all interconnect to one another, receiving inputs from the DG.[244–246] The vasculature architecture within these areas is also distinct, with the CA1 vascularized by a large ventral artery and the CA3 surrounded by capillaries that supply blood, nutrients, and O2 to active neurons.[247,248] In response to injury, changes in the vasculature can contribute to increases in reactive oxygen species, neurotransmitters, and ions that can lead to the upregulation of cytokine and chemokine expression in microglia. Moreover, as the hippocampus is filled with neurons with high-energy demands, alterations in homeostasis can increase mitochondrial dysfunction in neurons, upregulating the secretion of molecules such as glutamate that can increase the expression of TLRs in microglia. Activation of TLRs and increases in cytokine and chemokine expression of microglia can be characterized by a dystrophic morphology, which can lead to degeneration.[155,249] The mechanistic changes that influence hippocampal vulnerability following injury could also explain the results in the current study, as microglia displayed a dystrophic morphology following bTBI at seven days. Grabert et al. also described how activated microglia in the hippocampus decrease their expression of genes related to environment sensing, a characteristic of loss of their physiological function, which can lead to neurodegeneration.[250] The results from microglia morphological analysis in the present study could support the claims of researchers that persisting neuroinflammation following bTBI could lead to the onset of neurodegenerative diseases in patients long-term, as dystrophic microglia are present in the sub-acute stages of injury.

Furthermore, if microglia are degenerating within the hippocampus, losing physiological function, it might be rational to hypothesize that dystrophic microglia are not expressing high levels of IBA-1 (fluorescent intensity). Future studies should explore RNA sequencing of microglia in the hippocampus seven days following injury. Exploring upregulated and downregulated genes in dystrophic/degenerating microglia will support results that dystrophic microglia are present not only in the aging, diseased brain but can exist following bTBI as well.[251,252]

Due to the overwhelming presence of microglia activation in the brain seven days following repeated blast exposure, IHC was performed to investigate levels of NLRP3 within the brain and their role in helping drive the inflammatory response. While the response was not significant, trending decreases in the amount of NLRP3+ molecules and NLRP3 protein expression were found within the hippocampus. Studies have indicated that increases in NLRP3 are a sign of

the activation of its complex, leading to increased secretion of pro-inflammatory cytokines such as IL-1β.[253(p3),254–256] Morphological analysis of microglia indicated that the type of microglia within the hippocampus is dystrophic, which undergoes anti-inflammatory phenotypes in response to injury. Because dystrophic microglia are present in the hippocampus seven days after injury, this may explain why low levels of NLRP3, an inflammasome that drives pro-inflammatory responses in microglia, were observed. While limited evidence of microglia activation was present in the hippocampus three days following blast injury, additional bTBI studies investigating levels of NLRP3 are warranted to understand thoroughly the temporal response of molecular changes that influence microglia-mediated inflammation.

While morphological analysis of IBA-1+ microglia give robust insights into the unique role that microglia play within the inflammatory response following blast injury, a limitation of this study is that IBA-1 also has an affinity to tissue-derived macrophages, which could be influencing results gained from quantifying microglia morphology. As microglia-specific antibodies emerge within the field, future IHC studies should utilize antibodies such as TMEM-119, TREM2, and/or P2RY12 to co-localize with IBA-1 to provide a more comprehensive look into the microglia-specific response. Additionally, NLRP3 is present in microglia but can also be found in macrophages, and fluorescent microscopy showed that NLRP3 may also have an affinity to neuronal cell bodies. While a decrease in NLRP3 within the brain seven days following injury would be reasonable to believe because of the overwhelming presence of anti-inflammatory microglia within the hippocampus, it is difficult to speculate if the affinity of NLRP3 to other brain cells may have also influenced this result. Studies exploring NLRP3-mediated pro-inflammatory responses within microglia should include the co-staining of NLRP3 with microglia-specific markers to aid in a more robust analysis.

The work presented in this study began to successfully characterize the various phenotypic changes that microglia undergo in response to repeated blast injury within the MC and hippocampus, as specified in Specific Aim 1. Time-dependent and region-specific pathological changes indicated that microglia take on a pro-inflammatory role to respond to neuronal dysfunction, such as synaptic pruning within the MC three days following injury, with an increase in the IBA-1 positive signal within the hippocampus. However, no acute changes were observed in microglia morphology in the hippocampus. Meanwhile, seven days following injury, decreases in IBA-1 positive signal and expression are observed within the hippocampus, with microglia

taking on a dystrophic, abnormal morphology with an anti-inflammatory role, while no sub-acute morphological changes in microglia were observed in the MC. These results suggest that microglia play a dynamic role in neuroinflammation following blast exposure, with heterogeneous phenotypes that are time-dependent throughout the progression of repeated bTBI. The robust analysis of the spatial and temporal changes in microglia activation provides a novel avenue for further investigation of therapeutic strategies. The work here may also present a potential therapeutic time window that may be crucial in improving the quality of life for bTBI patients, such as those in the Veteran community.

Chapter 4: Characterizing the Regional and Longitudinal Effects of Microglia Activation Following Impact-Induced Neurotrauma

4.1 Introduction

Impact TBIs occur when an object strikes the head or when the head strikes a surface.[257] A complex response makes this injury unique, with the mechanical properties encompassing contact and inertial forces. Both contact and inertial forces occur during impact loading when the head is struck, but only inertial loading (acceleration/deceleration forces) arises from the impulsive head motions from impact.[257,258] Direct contact loading can result in primary injuries in both the region of impact (ipsilateral) and the opposite side of the impact (contralateral), as well as other areas distant from the impact site. Once impact loading on the skull occurs, a reduction in its structural and mechanical properties contributes to primary injury across regions.[257]

There are acceleration/deceleration forces that are involved in this injury, and they can be classified as linear and rotational acceleration. These forces can result in tissue deformation because of shear forces on the brain, leading to increased ICP.[259–261] Similar to bTBI, impact TBIs are heterogeneous and can be delineated into three severities: mild, moderate, and severe. Mild impact-induced TBIs (mTBIs) are more commonly reported and are referred to as concussions. Concussive injury can be sustained from vehicular accidents, military conflicts, and contact sports such as football or soccer, with clinical symptoms of concussions including headaches, balance problems, dizziness, memory deficits, insomnia, anxiety, and/or depression.[262–270] While concussions (mTBIs) are the most common type of impact TBI, the exact mechanisms of concussions and what leads to the myriad of symptoms associated with this injury are still unknown.

The use of animal models in impact TBI research is crucial in understanding the injury mechanisms, with the use of closed-head impact injury systems coming to the forefront. Previous literature using this model are yet to clearly define injury severity, with its characterization focusing on neuronal dysfunction in response to injury.[64,271–273] Glial cells such as microglia also play an integral role in impact trauma. They may provide insight into the secondary injury cascades that occur because of impact loading to the head. Microglia can respond to neuronal dysfunction by initiating inflammatory responses that can clear cell debris and orchestrate neuronal restorative processes. A study that explored microglia activation in post-mortem samples of TBI patients indicated that shear forces directly impact microglia morphology,[274] making it imperative to study their responses further. With the limited studies on the robust analysis of microglia morphology following impact injury,[44,275] continuing work that characterizes impact injury through microglia-

mediated responses may lead to the generation of data that is useful in developing diagnostic tools and therapeutic interventions. Moreover, due to impact loading, the rotational and linear acceleration forces on the brain produce a disordered metabolic cascade or biochemical injury that may influence diverse microglia activation states that are unique to this type of injury.[263] Thus, advancing studies that explore the underlying mechanisms that control neuropathological changes in impact TBI are essential.

For this study, we chose to use the closed-head CCI model because of its advantages over other models, such as the open-head CCI and FPI, which require a craniotomy, lacking translational aspects; and the weight drop model, whose limitations involve difficulties in reproducibility. We hope to characterize this model to produce mTBI as commonly reported in humans through a closed-skull impact that will not produce skull fracture or other obvious signs of injury (invisible nature of mTBI). We also hypothesize that this model will induce microglia activation as a secondary injury response to impact, persisting up to seven days following injury, with changes indicated within the brain region located within the impact site and its contralateral side.

4.2. Methods

The Virginia Tech Institutional Animal Care and Use Committee (IACUC) approved the experimental protocols described herein. Before experimentation, male Sprague Dawley rats (Envigo, Dublin, VA, USA) weighing approximately 300-315g were acclimated for several days (12 h light/dark cycle) with food and water provided *ab libitum*.

4.2.1. Closed-Head Cortical Impact Model (cCCI)

An impactor device induced a mild closed head injury in rats (n = 6). Under 5% isoflurane, animals were placed in the stereotaxic frame where the head was shaven, teeth were placed in the teeth bar, and the nose was placed in the stereotaxic nose cone to maintain anesthesia. A foam pad was then situated within the stereotaxic frame, where the animal's head lay against without ear bars. An electromagnetic actuator was mounted onto the stereotaxic crossbar to allow for precise localization of the impact center (Fig. 26). A skull template was used to mark the center of impact (right somatosensory cortex, ~3.5-5 mm posterior to Bregma), and the injury tip was firmly zeroed

against the skin. The impactor (tip diameter: 5 mm) created a force at a velocity of 6 m/s at a depth of 8 mm and a dwell time of 300 ms inducing the injury (Impact One, Leica Biosystems, Buffalo Grove, IL). Animals were then placed on a heating pad at 37^{o}C, monitored, and righting time was recorded. Sham animals underwent the same procedures except for the impact (n = 6).

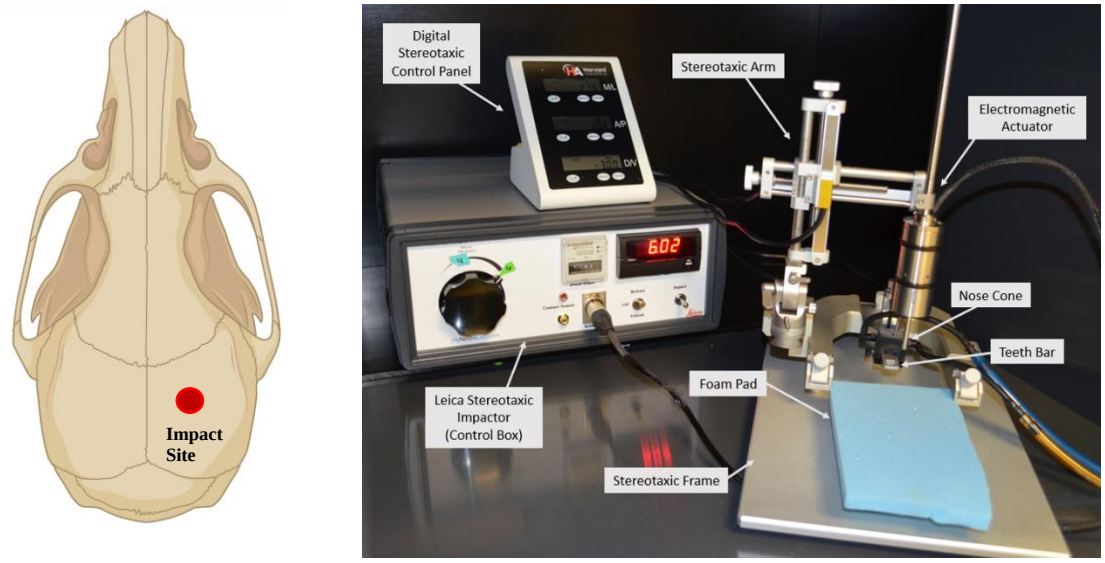

Figure 26. Closed Head Controlled Cortical Impact. (Left) The impact area was on the right side of the rat's head, specifically on the right parietal bone, where the brain's somatosensory cortex is located. Created with BioRender.com. (Right) The impactor was mounted onto the stereotaxic frame, which aligns with the right somatosensory cortex of the animal. The foam pad was placed under the animal's head, as the head was not attached to the ear bars. The impactor was connected to the control box where the dwell time and velocity were set.

4.2.2 Tissue Processing and Analysis

Three- or seven-days following injury, animals were euthanized, and brains were collected and stained for IBA-1 and NLRP3, as described previously in Section 3.2.2. The site of impact of the animals was located on the right somatosensory cortex. As the diameter of the impactor tip was 5 mm, and the depth of impact 8 mm, the motor cortex (MC), which is adjacent to the somatosensory cortex (SC), and the hippocampus, which is lateral to the cortex, were also regions of interest when identifying microglia activation (Fig. 27). Tissue sections were then imaged and

analyzed as described previously in section 3.2.3, with further understanding of changes in IBA-1+ microglia achieved through quantifying morphological changes as described in section 3.2.4.

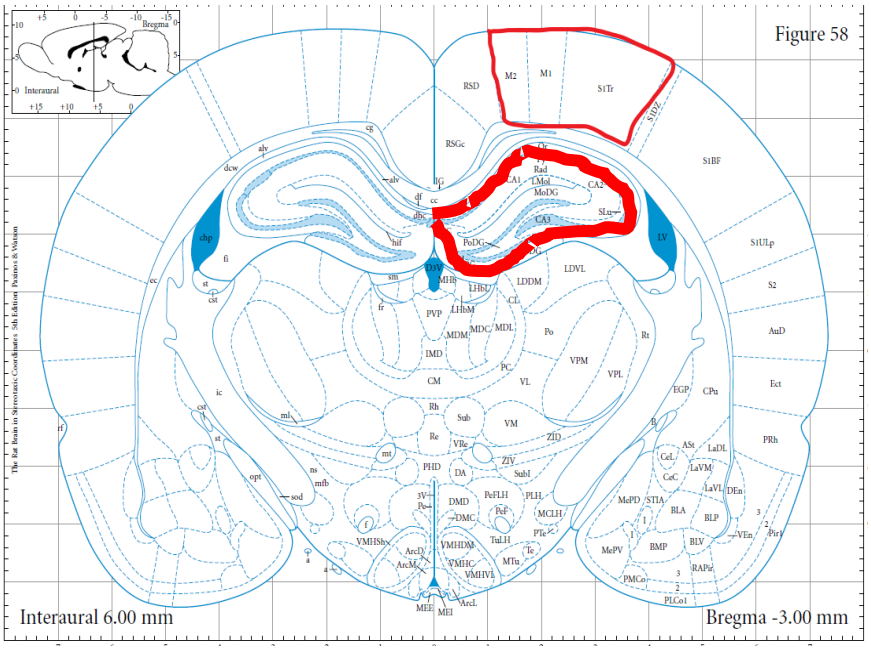

Figure 27. Representative image of the coronal section of the brain that is -3.00 mm posterior from Bregma. The SC, MC, and hippocampus are all located within this section, and these sections were collected, stained, imaged, and analyzed.

4.2.3 Statistical Analysis

All statistical analyses were performed in GraphPad Prism Version 9 (GraphPad Software, La Jolla, CA). The Kolmogorov-Smirnov test, in association with the Shapiro-Wilk Test, was performed to test for normal distribution and equal variance of the data. If the data passed the two assumptions, a one-way ANOVA and post hoc tests were performed where appropriate for sham group, the contralateral side, and the ipsilateral side of the cCCI group. Data that did not pass normality or equal variance assumptions were assessed using a one-way Kruskal Wallis test or pairwise Welch's correction test. Data were considered statistically significant with $p<0.05$ and trending at $p<0.1$. All histology data were normalized to respective shams. All data is represented as the mean ± standard error of the mean, or SEM.

4.3 Results

4.3.1 Animal Recovery and Righting Reflex for the three-day group

Following cCCI, no apparent signs of injury were discernible. Animals subjected to cCCI showed a significant delay in righting compared to the sham group (p=0.0093) (Fig. 28). Over the three days, there was no significant difference in weights observed in the cCCI animals compared to the sham group. The average weight of the cCCI group was 310 g ± 2.44, while the average weight of the sham group was 319 g ± 3.11.

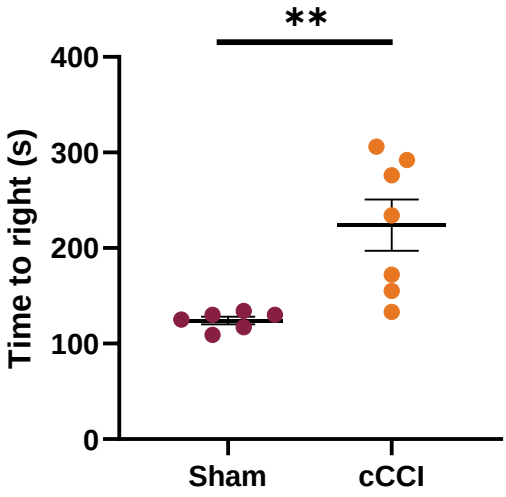

Figure 28. Physiological outcomes were quantified by measuring time to right. Compared to shams, cCCI animals showed significant delays in righting time. **p<0.01. Data represented as Mean ± SEM.

4.3.2 Identifying microglia pathology in the SC and MC three days following cCCI

Changes in IBA-1 expression were observed when comparing sham and cCCI groups, which may be indicative of microglia activation taking place three days following injury (Fig. 29). When investigating differences in overall IBA-1 positive signal (area fraction), a one-way ANOVA revealed that there was a statistically significant difference in area fraction (F (2, 14) = 4.124, p=0.03), with post hoc test indicating a substantial increase in this parameter in the contralateral side of the SC in cCCI animals compared to the SC in shams (p=0.03). The same increases were observed for count per area (F (2, 14) = 4.386. p=0.03), with the amount of IBA-1+ microglia significantly higher in the contralateral side of the SC of cCCI animals compared to

shams (p=0.02). Significant differences in fluorescent intensity were also indicated (F (2, 14) = 4.100, p=0.03), with multiple comparisons test showing a significant increase in fluorescent intensity of IBA-1 in the contralateral side of the SC compared to shams. No significant changes were found in the SC for the mean area/cell or between the ipsilateral and contralateral sides of the SC region in cCCI animals for any parameter (Fig. 30).

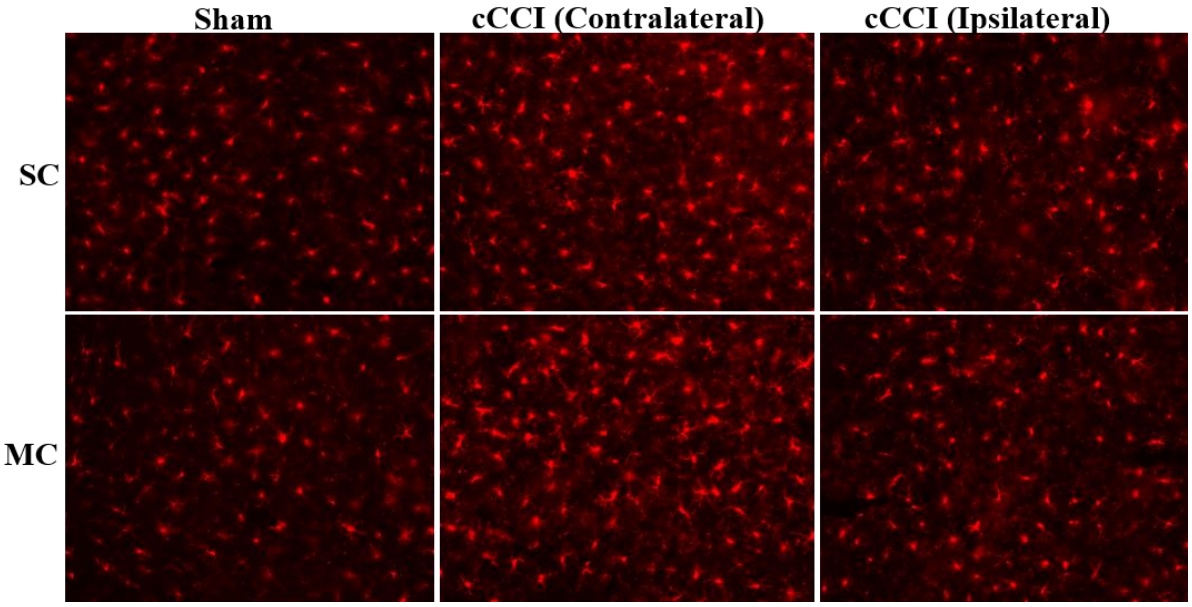

Figure 29. Representative of IBA-1 expression in the SC and MC. Significant increases in IBA-1 expression ($p<0.05$) were observed in the contralateral side of the SC and MC compared to the ipsilateral side, and the SC and MC of the sham animals.

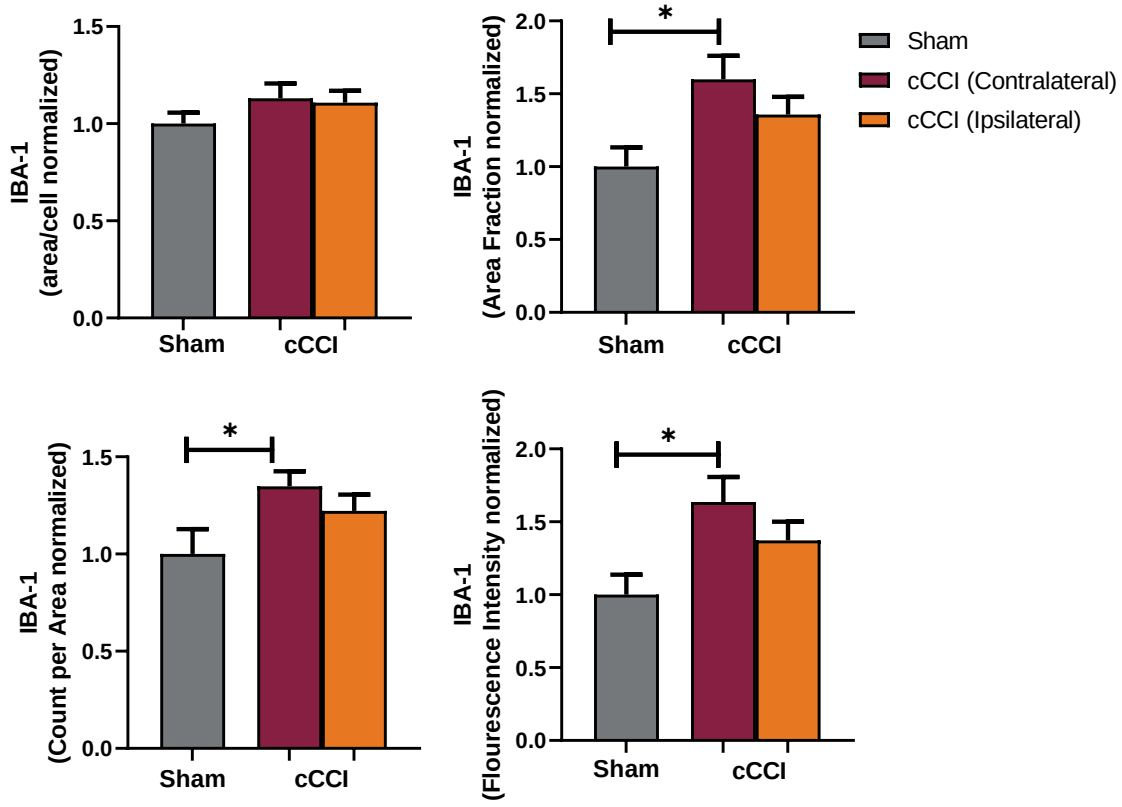

Figure 30. Microglia activation within the SC of the cCCI group. Significant increases in area fraction, count per area, and fluorescent intensity were observed in the contralateral side of the SC in the cCCI group compared to shams. *p<0.05. Data represented as Mean ± SEM.

One-way ANOVA indicated a significant difference in area fraction in the MC ($F(2, 14) = 3.514$, $p=0.05$), with area fraction within the contralateral side of the MC in cCCI animals significantly greater than the sham group ($p=0.04$). Significant differences between groups were also observed for count per area ($F(2, 14) = 4.386$, $p=0.03$), with the contralateral side of the MC in cCCI animals showing significantly more microglia compared to shams ($p=0.02$). This similar increase was also noted for fluorescent intensity ($F(2, 14) = 3.696$, $p=0.05$). Post hoc comparisons showed a significant increase in fluorescent intensity of IBA-1 in the contralateral side of the MC of cCCI animals compared to the MC in the sham group ($p=0.04$). Trending increases ($p=0.06$) were noted between the contralateral and ipsilateral sides of the MC of the cCCI group, but when compared to shams, no significant differences were observed. Additionally, no significant changes

between the ipsilateral and contralateral side of the MC in the cCCI group were seen for any parameter, nor were significant differences observed between the ipsilateral side of the MC of the cCCI group and the SC of the sham group (Fig. 31).

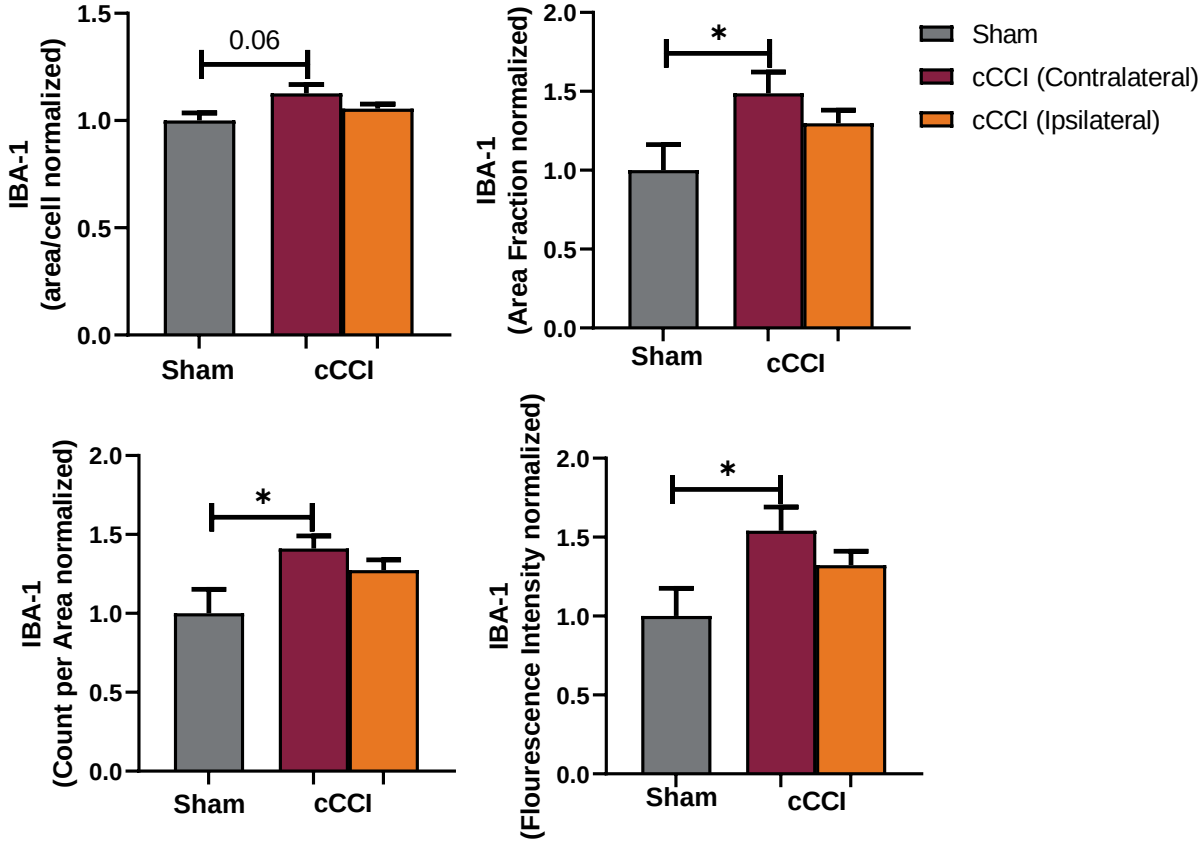

Figure 31. Microglia activation was observed within the MC of the cCCI group. Significant increases in area fraction, count per area, and fluorescent intensity was observed in the contralateral side of the SC compared to shams. *p<0.05. Data represented as Mean ± SEM.

4.3.3 Quantifying morphological changes in microglia in the SC and MC three days following injury

While no significant changes in cell size were found between the sham and cCCI groups, identifying whether microglia were still undergoing morphological changes within the SC and MC following injury was completed. A one-way ANOVA showed that there were no significant changes in either branch length/cell or branch points/cell in the SC in the ipsilateral and

contralateral sides of the SC in cCCI animals compared to the SC in shams, or between the contralateral side and ipsilateral side of the SC in the cCCI group (Fig. 32). Within the MC, a Kruskal-Wallis test indicated significant changes in branch points/cell (p=0.01), with Dunn's multiple comparison test showing a significant increase in branch points/cell on the ipsilateral side of the MC in cCCI animals compared to shams (p=0.1). No significant differences were found in this region for branch length/cell (Fig. 33).

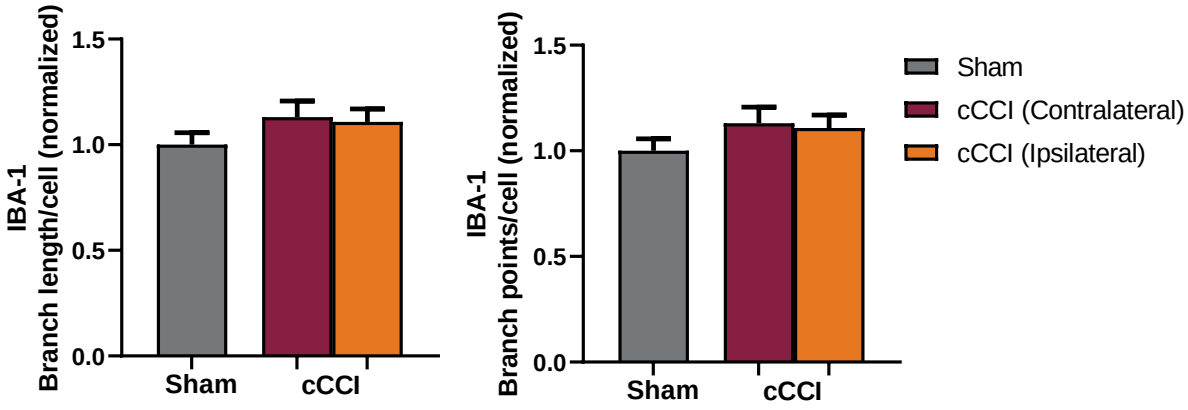

Figure 32. No notable changes in microglia morphology in the SC three days following cCCI. No significant increases or decreases in branch length/cell or branch points/cell were found in the contralateral or ipsilateral side of the SC compared to the SC in the sham group. Data represented as Mean ± SEM.

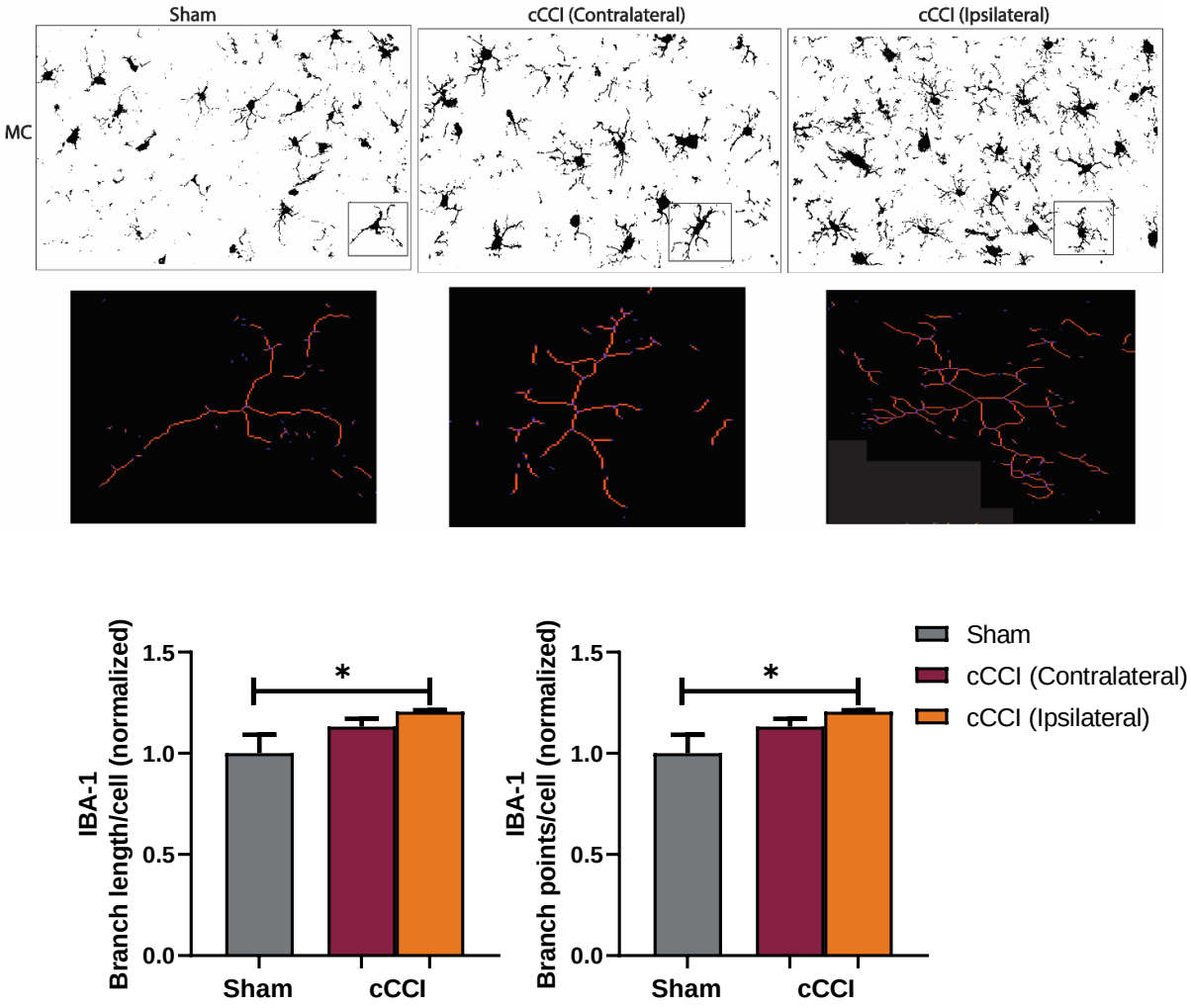

Figure 33. Morphological changes in microglia were detected in the MC three days following impact trauma. (Top) Representative images showing morphological changes within the MC of cCCI animals. (Bottom) Significant increases in branch length/cell and branch points/cell were observed in the ipsilateral side of the MC compared to the MC in the sham group. No significant changes between the contralateral side and the ipsilateral side were observed. *$p<0.05$. Data represented as Mean ± SEM.

4.3.4 Pathological changes in microglia were present in the hippocampus three days following cCCI

Evidence of microglia activation was also observed within the hippocampus three days following cCCI (Fig. 34). A one-way ANOVA indicated significant changes in the area fraction of IBA-1 in the CA2 sub-region of the hippocampus between the sham, contralateral, and ipsilateral sides of the CA2 in the cCCI group ($F(2, 15) = 6.326$, $p=0.01$). More specifically, multiple comparison tests indicated a significant increase in area fraction in the contralateral region of the CA2 in cCCI animals compared to shams ($p=0.007$). Additionally, significant changes in fluorescent intensity was also observed in the CA2 ($F(2, 15) = 6.420$, $p=0.009$). There was an increase in the fluorescent intensity of IBA-1 in the contralateral side of the CA2 in the cCCI group compared to shams ($p=0.008$). Trending changes ($p<0.1$) were observed in the hippocampus for area/cell and count per area (Fig. 35).

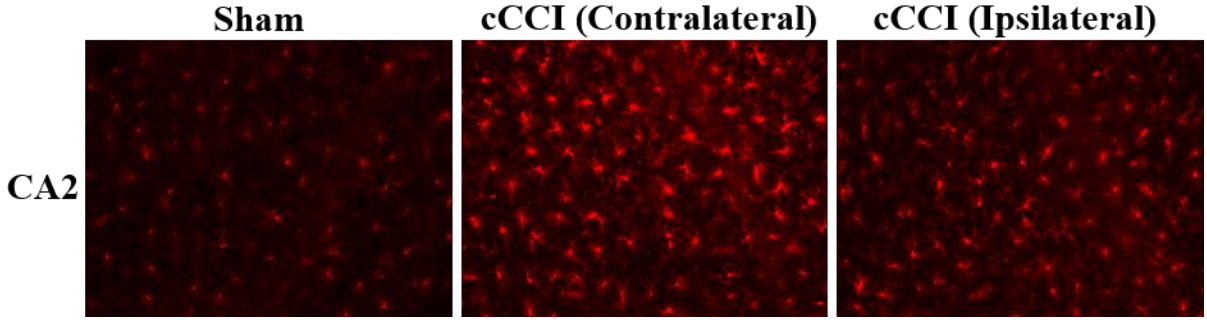

Figure 34. Increases in IBA-1 expression may be indicative of microglia activation three days following cCCI. Representative images show increases in fluorescent intensity of IBA-1 within the CA2 sub-region of the hippocampus in the cCCI group compared to their sham counterparts.

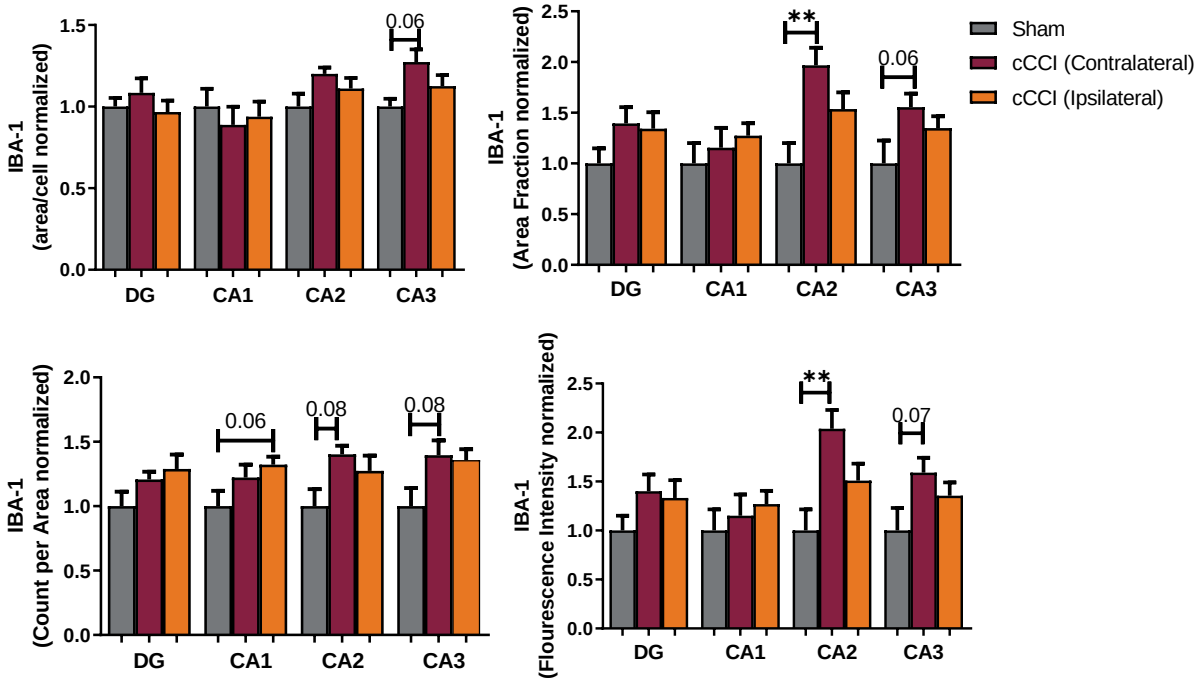

Figure 35. Microglia activation was observed within the hippocampus of the cCCI group after three days. Significant increases in area fraction and fluorescent intensity were observed in the contralateral side of the SC compared to shams in the CA2 sub-region. **p<0.01. Data represented as Mean ± SEM.

4.3.5 Changes in microglia morphology were observed in the hippocampus three days following cCCI

When quantifying morphological changes of microglia, significant differences were found for branch points/cell in the CA2 sub-region (F (2, 14) = 4.451, p=0.03) and the CA3 sub-region (F (2, 14) = 6.025, p=0.01) of the hippocampus. Post hoc tests indicated a significant increase in branch points/cell when comparing the contralateral side of the CA2 in the cCCI group to shams (p=0.05), as well as the ipsilateral side of the cCCI group to shams (p=0.03). This same significant change was found within the CA3 with a significant increase in branch points/cell within the contralateral side of the cCCI group compared to shams (p=0.04) and the ipsilateral side compared to shams (p=0.01). No significant changes were found for the DG or CA1 regions. Furthermore, between groups, no significant branch length/cell changes were found within the hippocampus (Fig. 36).

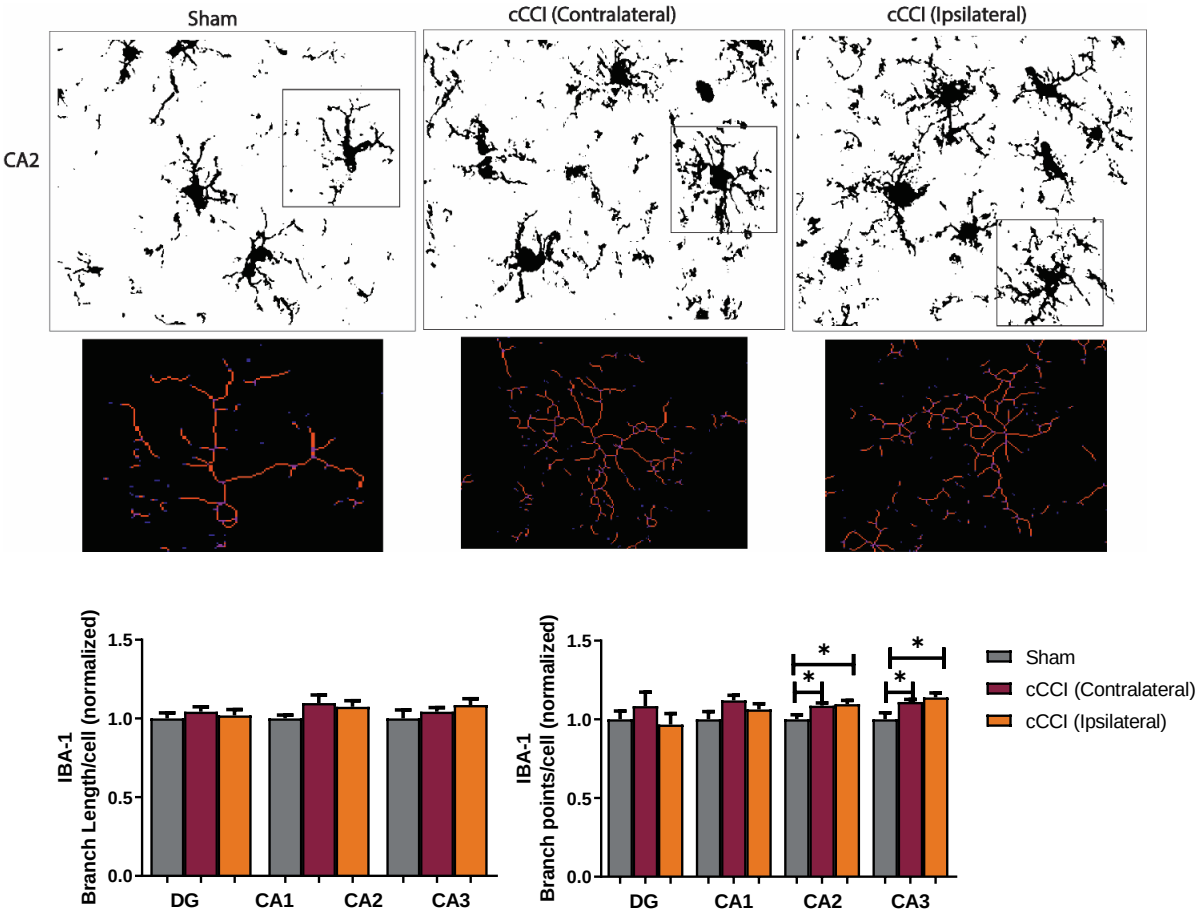

Figure 36. Changes in microglia morphology were observed within the hippocampus. (Top) Representative images show increased branching in the CA2 of the cCCI group. (Bottom) Increases in branch points/cell were found within the ipsilateral and contralateral sides of the CA2 and CA3 sub-region compared to their sham counterpoints. *p<0.05. Data represented as Mean ± SEM.

4.3.6 Animal Recovery and Righting Reflex following cCCI for the seven-day group

Animals subjected to cCCI showed significant delays in righting in comparison to the sham group, and no other apparent signs of injury were discernible (p=0.02) (Fig. 37). Over the seven days, there was no significant difference in weights observed in the cCCI group compared to the sham group. The average weight of the cCCI group was 296 g ± 22.3, while the average weight of the sham group was 337.4 g ± 7.16.

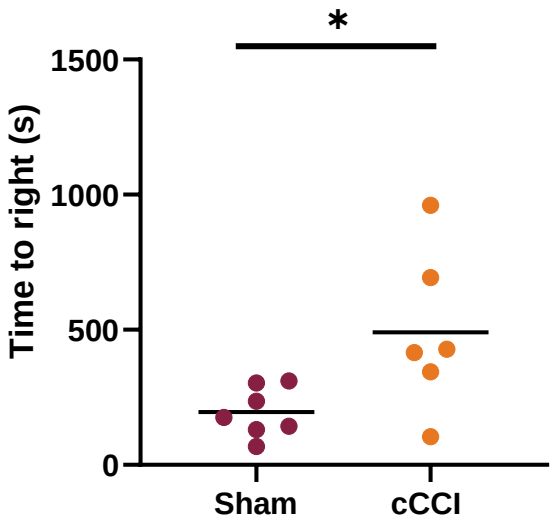

Figure 37. Delays in righting reflexes were observed in the cCCI animals compared to shams. *p<0.05. Data represented as Mean ± SEM.

4.3.7 Identifying pathological changes in microglia in the SC and the MC seven days following cCCI

Within the SC, a one-way ANOVA indicated significant differences in the number of microglia cells (count per area) between the shams and the contralateral and ipsilateral sides of the SC of cCCI animals ($F(2, 12) = 5.217$, $p=0.02$). More specifically, a significant decrease in count per area was found when comparing the sham group and the contralateral side of the SC in the cCCI group ($p=0.02$). A trending reduction was found when comparing the sham group to the ipsilateral side of the SC ($p=0.06$). For area fraction and fluorescent intensity, trending increases were observed when comparing the ipsilateral side of the SC to the contralateral side in the cCCI group (Fig. 38).

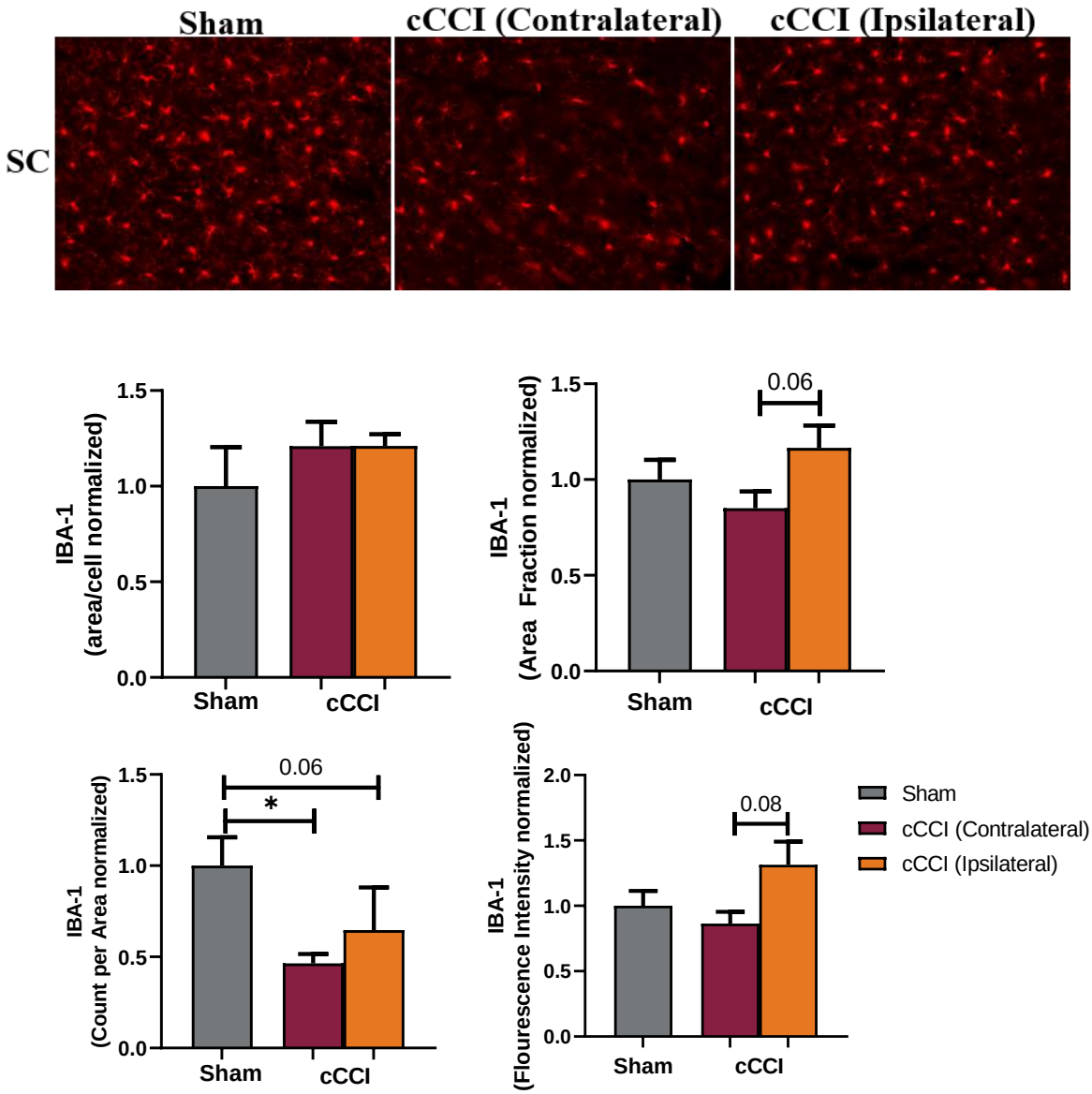

Figure 38. Changes in the number of microglia within the SC seven days after cCCI. (Top) Representative images show decreases in IBA1+ microglia in the contralateral side of the SC in the cCCI group. (Bottom) Significant decreases in count per area were observed in the contralateral side of the SC compared to the SC in the sham group. *p<0.05. Data represented as Mean ± SEM.

Changes in levels of IBA-1 were observed in the MC following cCCI, indicating that microglia activation may be taking place (Fig. 39). Increases in cell body size of IBA-1+ microglia (area/cell) were indicative of microglia activation ($F(2, 11) = 22.32$, $p=0.0001$). More specifically, significant increases in area/cell were observed in the ipsilateral side of the MC compared to the contralateral side in cCCI animals ($p=0.0005$), and the ipsilateral side of the cCCI group compared to the MC in the sham group ($p=0.0001$). A one-way ANOVA indicated that the area fraction of IBA-1 was significantly increased in the MC seven days following injury ($F(2, 12) = 7.370$, $p=0.009$). More specifically, post hoc tests showed increases in the ipsilateral side of the MC compared to the contralateral side in cCCI animals ($p=0.007$), with this increase found to be trending when comparing the ipsilateral side of the MC of the cCCI groups to shams ($p=0.09$). Significant decreases in the number of IBA-1+ microglia (count per area) were observed in the MC as well ($F(2, 10) = 4.866$, $p=0.03$). Post hoc multiple comparison tests indicated a significant decrease in count per area in the contralateral side of the MC of cCCI animals compared to the MC of the sham group ($p=0.03$). No significant changes in count per area were found between the contralateral and ipsilateral sides of the MC in cCCI animals or between the ipsilateral side of the MC in the cCCI group and the MC of the shams. Significant increases in fluorescent intensity were also observed ($F(2, 11) = 6.104$, $p=0.01$). These significant increases were found when comparing the ipsilateral side of the MC to the contralateral side in cCCI animals ($p=0.01$), and a significant increase was indicated when comparing the ipsilateral side of the MC of the cCCI group to shams ($p=0.05$) (Fig. 40).

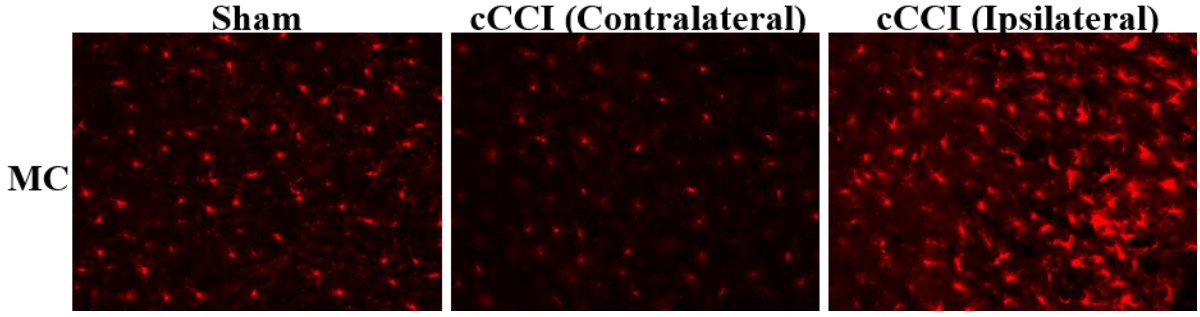

Figure 39. Changes in IBA-1 levels are observed in the MC following cCCI. Representative images show an increase in fluorescent intensity in the ipsilateral side of the MC following injury, and a decrease in the amount of IBA-1+ microglia in the contralateral side of the MC.

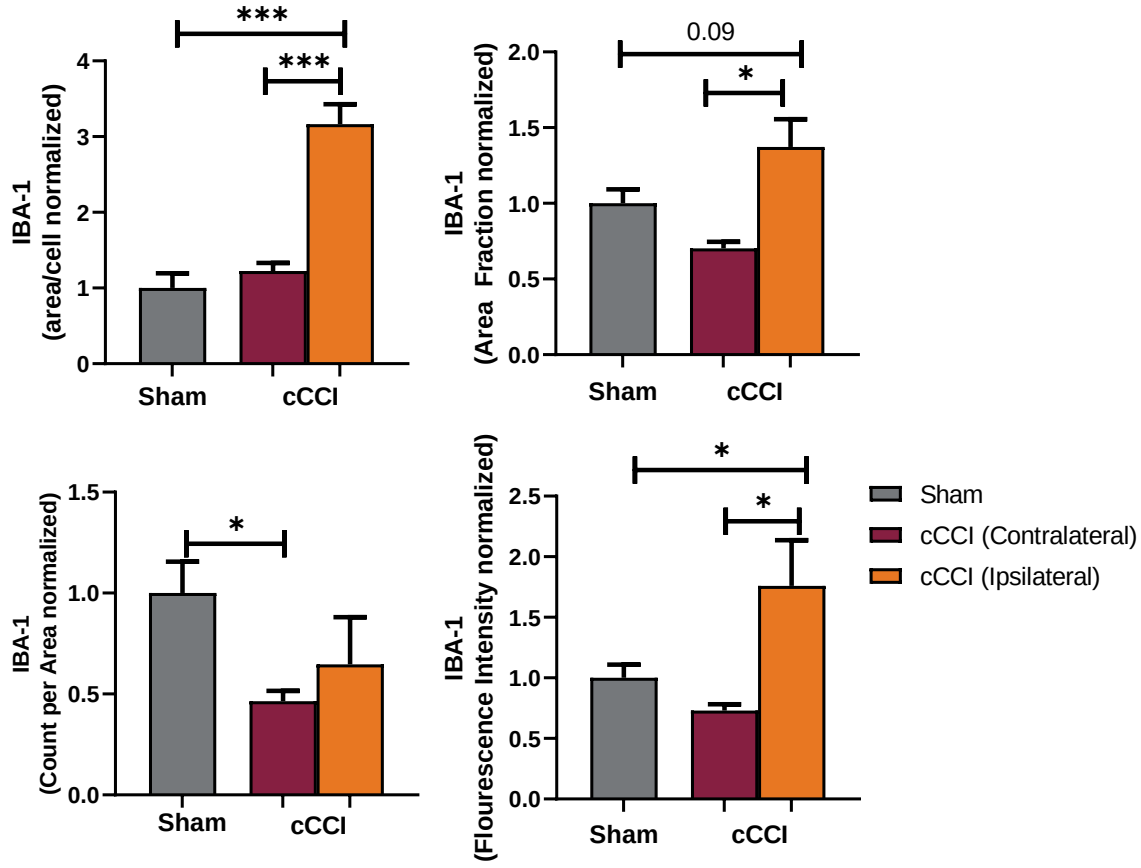

Figure 40. Microglia activation was observed within the MC of the cCCI group. Significant increases in area/cell, area fraction, and fluorescent intensity was observed in the ipsilateral side of the MC compared to shams. A significant decrease in count per area was observed in the contralateral side of the MC compared to shams seven days following injury. *p<0.05, ***p<0.001. Data represented as Mean ± SEM.

4.3.8 Changes in microglia morphology are noticeable within the SC and MC seven days following impact trauma

Within the SC, a one-way ANOVA indicated significant differences in branch points/cell ($F(2, 13) = 3.583$, $p=0.05$). More specifically, an increase in branch points/cell was observed in the ipsilateral side of the SC in the cCCI group compared to the contralateral side ($p=0.04$). No significant changes were observed in the SC between any groups when quantifying branch length/cell (Fig. 41). Within the MC, significant differences in branch length/cell were found ($F(2,12) = 4.957$, $p=0.02$), with post hoc tests showing a significant increase in branch length/cell in

the contralateral side of the MC in the cCCI group compared to the MC of the sham group (p=0.03). An increase in branch length/cell in the contralateral side was trending compared to the ipsilateral side of the MC in the cCCI group (p=0.06). A significant increase in branch points/cell was found (Kruskal-Wallis test, p=0.01), with Dunn's multiple comparison test indicating this significant increase when comparing the contralateral side of the MC to the MC in the sham group (p=0.03) (Fig. 42).

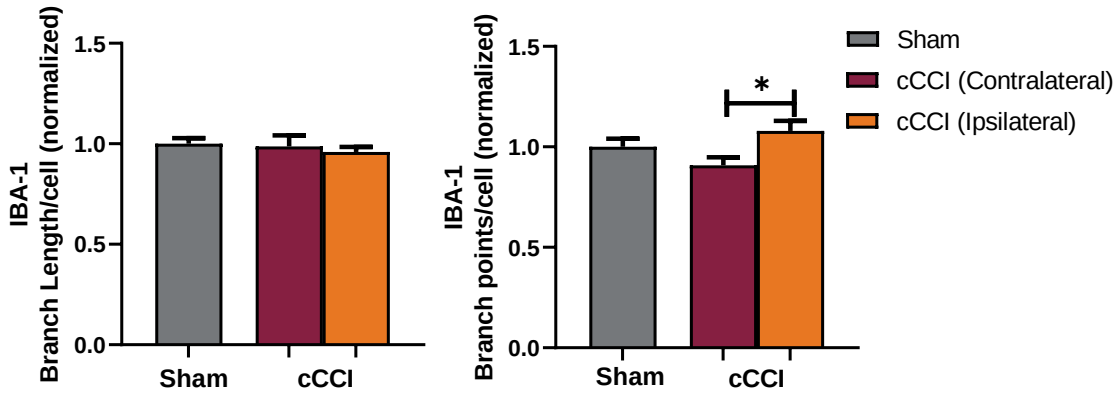

Figure 41. Increases in branching were seen in the SC seven days following cCCI. Significant increases in branch points/cell were found within the contralateral side of the SC compared to the ipsilateral side. *p<0.05. Data represented as Mean ± SEM.

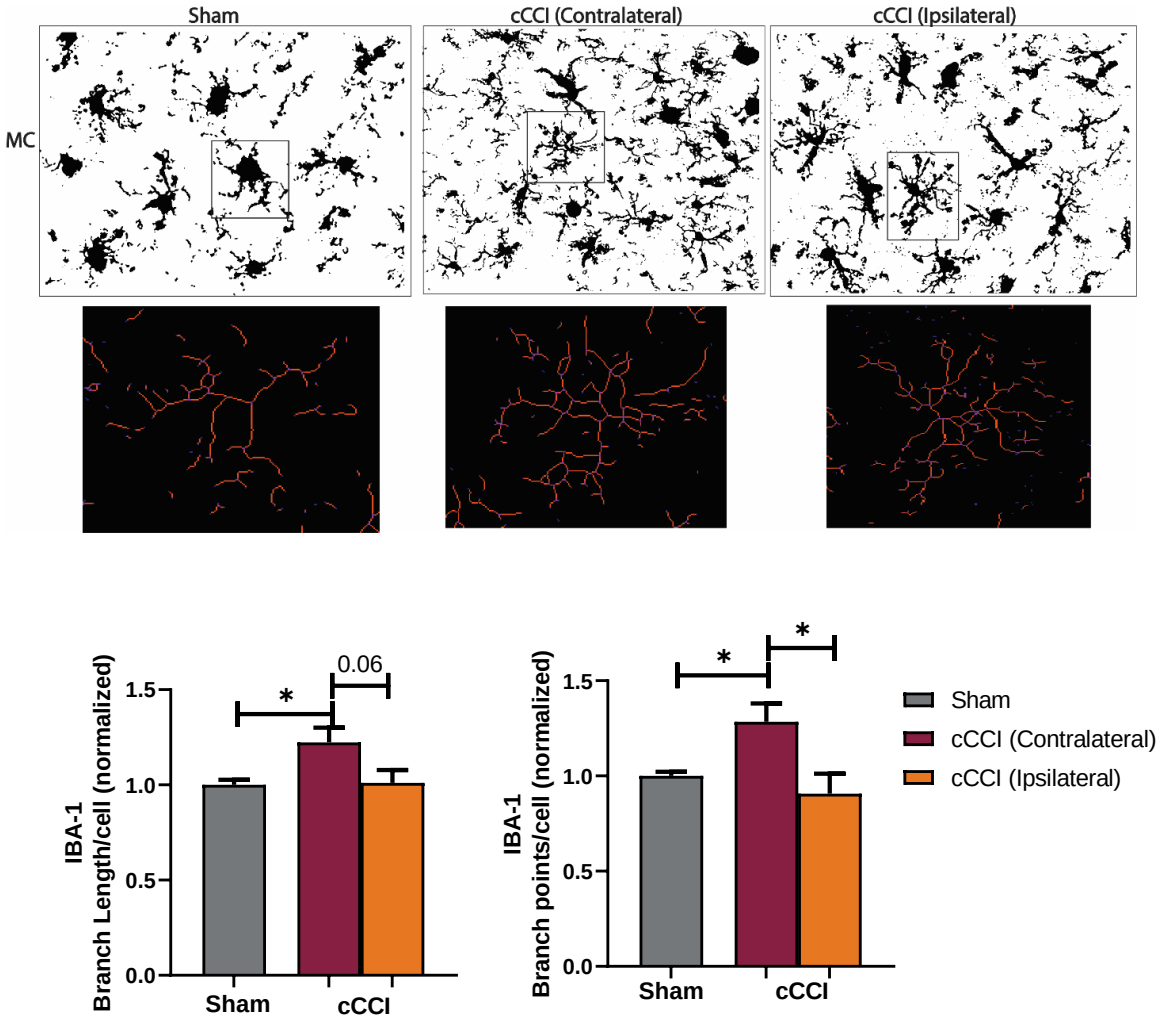

Figure 42. Changes in microglia processes were present following impact trauma. (Top) Representative images show increases in branch length in the contralateral and ipsilateral sides of the MC following injury, with increased branching within the ipsilateral MC. (Bottom) Compared to shams, significant increases in branch length/cell and branch points/cell were observed in the ipsilateral side of the MC. *p<0.05. Data represented as Mean ± SEM.

4.3.9 Changes in IBA-1 expression were notable in the hippocampus seven days following cCCI

Within the hippocampus, decreases in microglia and IBA-1 expression were notable (Fig. 43). A one-way ANOVA indicated a significant decrease in area fraction of IBA-1 in both the contralateral and ipsilateral sides of the CA2 in the cCCI group compared to shams ($F(2, 11) = 22.68$, $p=0.001$). This was also observed in the CA3 sub-region, with area fraction significantly

decreasing in the contralateral and ipsilateral sides of the cCCI group compared to their sham counterparts ($F(2, 11) = 6.799$, $p=0.01$). Decreased IBA-1 expression (fluorescent intensity) was observed in both the contralateral and ipsilateral sides of the CA2 sub-region in cCCI animals compared to the sham group ($F(2, 12) = 11.09$, $p=0.001$). Decreases in IBA-1+ microglia were observed in the contralateral side of the DG in cCCI animals compared to shams ($F(2, 12) = 5.130$, $p=0.02$). In the CA2 sub-region, count per area was significantly decreased in the contralateral and ipsilateral sides of the cCCI group compared to shams ($F(2, 12) = 9.015$, $p=0.004$). This same trend was observed in the CA3, with the count per area in the contralateral and ipsilateral sides of the injured sub-region in cCCI animals significantly decreased compared to shams ($F(2, 12) = 17.55$, $p=0.0003$) (Fig. 44).

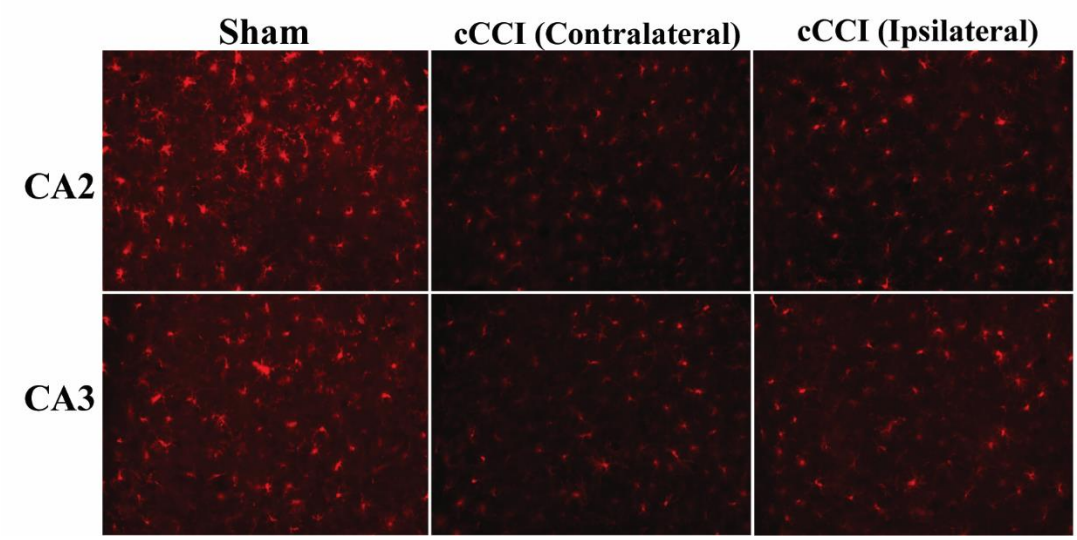

Figure 43. Microglia activation in the CA2 and CA3 is presented as a decrease in IBA-1 expression seven days following cCCI. Images taken at 20x magnification in the CA2 and CA3 sub-regions of the hippocampus show decreased fluorescent intensity of IBA-1**.**

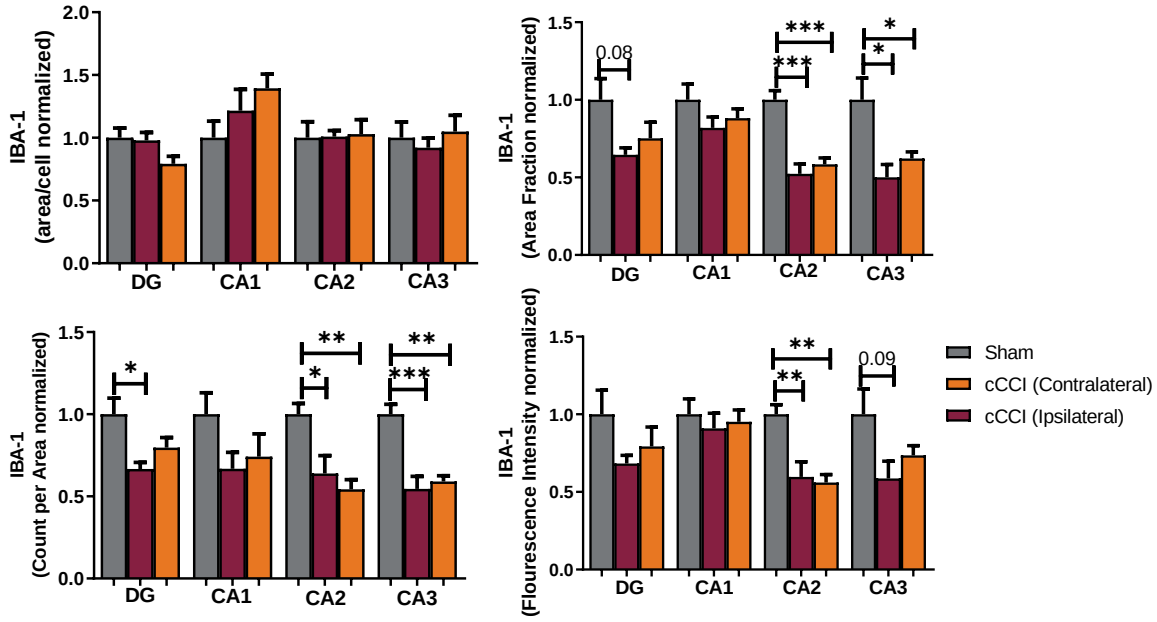

Figure 44. Significant decreases in IBA-1+ microglia and their expression of IBA-1 were found in the hippocampus seven days following injury. Compared to shams, a significant decrease in area fraction was notable in the contralateral and ipsilateral sides of the CA2 and CA3 in the cCCI group. A significant decrease in count per area was discovered in the contralateral side of the DG compared to shams, and both the contralateral and ipsilateral sides of the CA2 and CA3 in cCCI animals compared to their sham counterparts. *p<0.05. **p<0.01. ***p<0.001. Data represented as Mean ± SEM.

4.3.1.0 Limited changes in microglia morphology were found in the hippocampus seven days following injury

When observing branch points/cell, a significant difference was found within the CA2 (Welch's ANOVA test p=0.007), with post hoc tests indicating a significant increase in branch points/cell on the contralateral side of the CA2 compared to the CA2 of the sham group (p=0.007), with a significant increase also observed within the ipsilateral side of the CA2 compared to the CA2 of the sham group (p=0.02). No significant changes were observed in any other sub-region for branch points/cell, and no significant differences were found within the hippocampus for branch length/cell (Fig. 45).

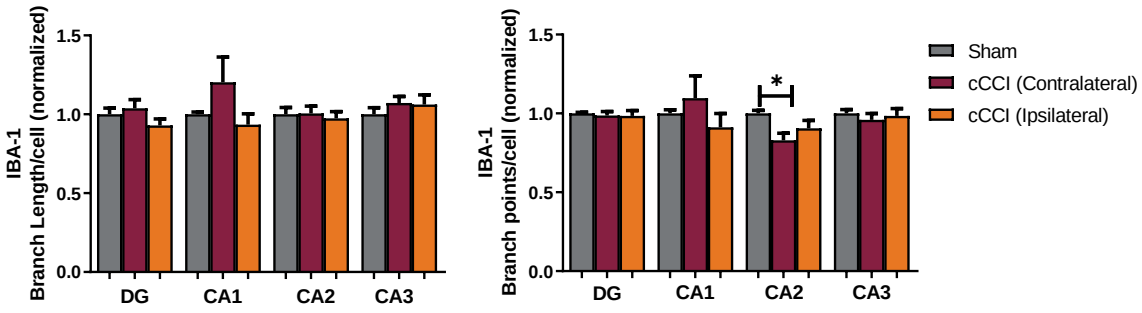

Figure 45. Limited changes in microglia morphology were observed in the hippocampus seven days following injury. Compared to the sham group, significant decreases in branch points/cell were observed in the contralateral CA2. No significant changes in branch length/cell were observed in the hippocampus. *p<0.05. Data represented as Mean ± SEM.

4.3.1.1 Decreases in the levels of NLRP3 were notable in the cortex of animals following injury

Increased NLRP3 production has been associated with activation following injury, contributing to the pro-inflammatory response. With the overwhelming evidence of microglia activation within the MC, SC, and hippocampus seven days following injury, further exploration into the microglia-induced molecular changes that contribute to neuroinflammation were examined. A one-way ANOVA indicated significant differences in the number of NLRP3+ molecules (count per area) in the SC ($F(2, 12) = 12.48$, $p=0.001$). Furthermore, there was a significant decrease in NLRP3 count per area in the contralateral side of the SC compared to the SC of the sham group ($p=0.0004$) and a significant decrease in the ipsilateral side compared to shams ($p=0.005$). No significant difference in the fluorescent intensity of NLRP3 was observed within the SC (Fig. 46).

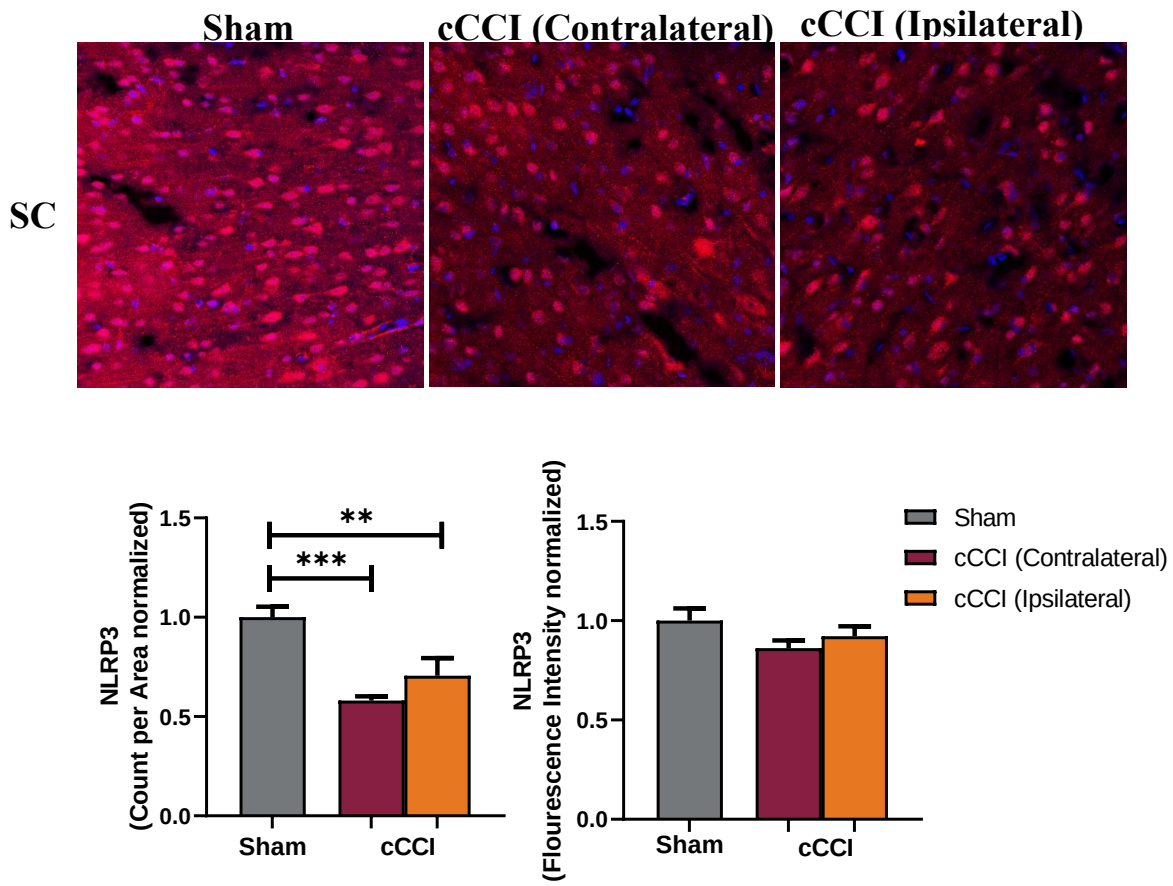

Figure 46. Decreases in NLRP3 levels were seen in the SC seven days following cCCI. (Top) Representative images taken at 20x magnification show notable decreases in NLRP3 in cCCI animals compared to shams. (Bottom). Significant decreases in count per area were observed in the contralateral and ipsilateral sides of the SC compared to the SC in the sham group. **p<0.01 ***p<0.001. Data represented as Mean ± SEM.

In the MC, a one-way ANOVA indicated significant changes in NLRP3 production ($F(2, 11) = 7.393$, $p=0.009$), with post hoc multiple comparison tests showing a significant decrease in count per area in the contralateral side of the MC compared to the MC of the shams ($p=0.009$). A significant decrease in count per area on the contralateral side of the MC in the cCCI group compared to the ipsilateral side ($p=0.02$) was also observed. Changes in NLRP3 expression (fluorescent intensity) were also found to be significant in the MC ($F(2, 12) = 5.229$, $p=0.02$). More specifically, a significant decrease in the fluorescent intensity of NLRP3 was found within

the contralateral side of the MC in the cCCI group compared to the MC of shams (p=0.02) (Fig. 47).

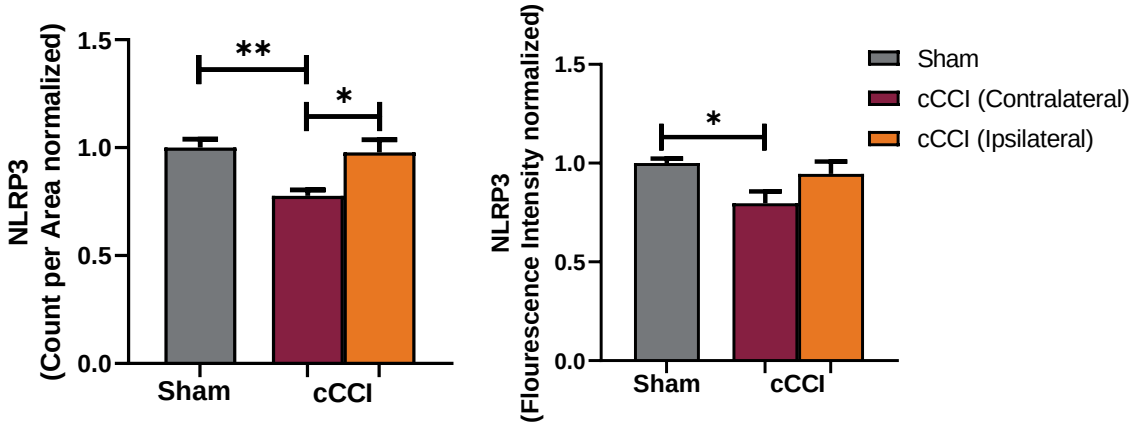

Figure 47. Decreased expression of NLRP3 was found within the MC seven days following impact. Significant decreases in count per area of NLRP3 were observed in the contralateral side of the MC compared to the ipsilateral side. This decrease in the contralateral side of the MC was also observed compared to shams. A decrease in fluorescent intensity of NLRP3 was also observed in the contralateral side of the MC compared to shams. *p<0.05, **p<0.01. Data represented as Mean ± SEM.

4.3.1.2 NLRP3 expression was decreased in the hippocampus seven days following cCCI

Significant changes in fluorescent intensity were observed in the DG ($F(2, 12) = 4.463$, $p=0.03$). More specifically, a significant decrease in fluorescent intensity of NLRP3 was found in the contralateral side of the DG compared to the DG of the sham group ($p=0.02$). Within the CA3, significant changes were also found ($F(2, 11) = 19.89$, $p=0.002$), with multiple comparisons indicating a substantial decrease in fluorescent intensity on the contralateral side of the CA3 compared to the sham group ($p=0.001$), as well as the ipsilateral side compared to the sham group ($p=0.0003$) (Fig 48).

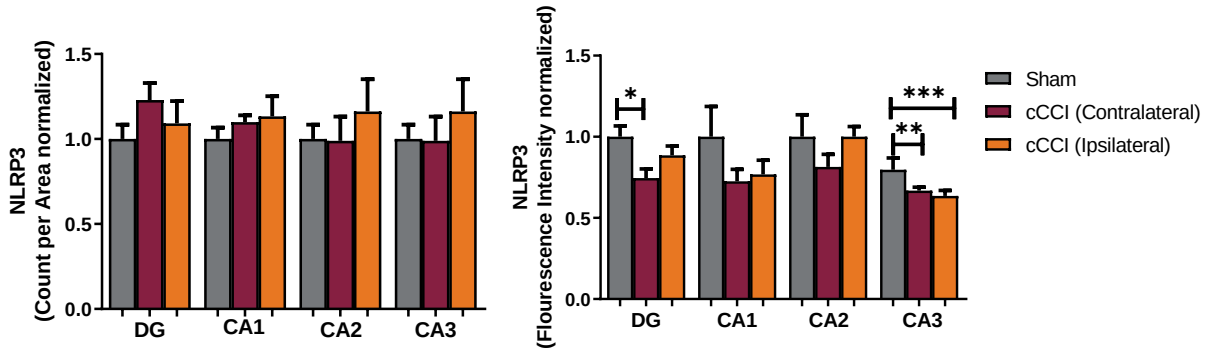

Figure 48. Decreases in NLRP3 expression were observed in the hippocampus following cCCI. A significant decrease in fluorescent intensity is observed in the contralateral side of the DG compared to the DG of shams. Additionally, a significant decrease in fluorescent intensity is observed in the contralateral and ipsilateral sides of the CA3 compared to the CA3 of the sham animals. *p<0.05. **p<0.01. ***p<0.001. Data represented as Mean ± SEM.

4.4 Discussion

This study utilizes a closed-head, closed-skull model of concussion in the adult rat using a CCI device (cCCI), consistent with "mild" injury manifestations, as it does not produce skull fracture. Still, it does create delays in righting time.[271,276] Understanding the spatial and temporal response of microglia following this injury mechanism was made by comparing the microglia response three- and seven-days following cCCI in both the ipsilateral (side of injury) and the contralateral (opposite side of injury) regions.

The right primary somatosensory cortex was where the injury was sustained, with other regions of interest including the MC and the hippocampus. Our results observed a transient profile in microglia activation in these regions. Previous research has shown microglia playing an active role in the neuroinflammatory response following CCI, with an increase in microglia found within the injured brain within the acute stages.[277–279] While these have been crucial to advancing TBI research, our innovative use of the closed-head model is distinct from other preclinical models that utilize an "open-head" model involving a craniotomy. The traditional uses of CCI differ from the clinical condition where the injury occurs in a closed system. When observing the IHC results of the present study three days following injury, our results indicated an increase in IBA-1 expression

and an increase in the amount of IBA-1+ microglia within the contralateral side of the SC compared to the SC of the sham group. These results are consistent with changes in the cortex of open-head CCI models within the acute stages, which may lead to conclusions on repeatability, and consistency in parameters for severity, yet spatial heterogeneity may vary in open-head vs. closed-head models, which is why advancing these studies are warranted.

While no significant changes were indicated in the mean area/cell within the SC and MC three days post-impact, quantifying the morphological changes of microglia following cCCI to advance the understanding of the phenotypic changes that are taking place within the injured brain was completed. No significant changes in microglia morphology were found within the SC. Still, an increase in branch length/cell and branch points/cell on the ipsilateral side of the MC was observed when compared to the MC of the sham group. This is interesting as significant changes in overall IBA-1 expression (area fraction, count per area, and fluorescent intensity) were observed within the contralateral side of the SC compared to shams, with no significance found within the ipsilateral side. This indicates unique transhemispheric changes taking place following impact. In what is also known as diaschisis,[280,281] anatomical and functional alterations develop in initially undamaged regions. In a study by Le Prieult et al., following an open-head model of CCI, up to four days following injury, impairments in Gamma-aminobutyric acid (GABA)ergic transmission and neuronal hyperactivity were observed in the contralateral somatosensory cortex, and microglia in response to cellular debris were restricted to the area of injury.[282] The researchers of this study attributed neuronal activity in the contralateral side to an adapting mechanism to compensate for the functional loss of neuronal activity within the ipsilateral side of the brain. In the present study, increases in IBA-1 expression and IBA-1+ microglia within the contralateral side of the brain could be linked to a transient response to microglia interacting with neurons to compensate and stabilize the disrupted brain functions. While the experimental design of Le Prieult and colleagues' study varied from ours, their results and theories may explain why microglia alterations in distant regions of the brain of the current study are present. As the intrinsic and extrinsic properties of microglia and neurons are interconnected to respond to injury, future studies that explore changes in neuronal dysfunction following cCCI and how microglia functional states are altered as neural activity changes, can aid in supporting studies of the contralateral side of the brain compensating for disrupted brain functions following injury.

With microglia showing an increase in branch points/cell and branch length/cell, microglia within the ipsilateral MC could be undergoing a stress/primed morphology, meaning they are hyper-ramified with longer processes.[283–285] Stress/primed microglia are known to function in a pro-inflammatory state, with increased reactivity to immune challenges such as an excess release of pro-inflammatory cytokines like IL-1β, IL-6, and TNF-α from neighboring cells.[284,285] Studies have indicated that microglia undergo this "primed" phenotypic change acutely following TBI. Still, the studies researching this morphology have focused on severe TBIs caused by a penetrating injury or within the aging brain, showing the importance and innovation of the present study in finding changes following a concussive-like injury.

Within the hippocampus, similar shifts in levels of IBA-1 expression were also observed three days following injury. There was an increase in area fraction and fluorescence intensity within the contralateral side of the CA2 sub-region compared to the sham group. No significant differences were found for any parameter when comparing the ipsilateral side of the hippocampus to the sham group. Again, this may be due to microglia becoming activated in response to neuronal activity, with microglia compensating in this region to stabilize altered brain function due to injury.

Furthermore, closed-head injury studies have indicated changes in IBA-1 expression as early as four hours, returning to baseline three days following injury.[286] This shows the unique transient and heterogeneous response of microglia following impact TBI as microglia may be trying to return to baseline within the ipsilateral side, with a delayed response shown on the contralateral side as dysfunction persists. While levels of IBA-1 expression were found to be increased on the contralateral side of the hippocampus, changes in branch points/cell were increased on both the ipsilateral and contralateral side of the CA2 and CA3 sub-regions compared to these same sub-regions in the sham group. While branch points/cell was significantly increased, no changes in branch length/cell or alterations in cell body size were found within any hippocampus sub-region. A study by Hinwood et al. observed changes in microglia morphology following stress within the prefrontal cortex, revealing that stress increased the internal complexity of microglia. They saw enhanced ramification (increased branching) without altering the overall area occupied by the cell (cell body perimeter) or the length of the branches. Their results indicated that this specific morphology was not associated with increased pro-inflammatory cytokines, instead, this phenotypic change was markedly different from those traditionally observed following injury. The unique morphology they observed was associated with an upregulation in

β1-integrin (CD29), a protein involved in the ramification of microglia, most often upregulated in neurodegenerative diseases.[287,288] Similarities in morphology were notable in the present study, meaning that microglia display a unique type of "hyper-ramification in the hippocampus at the acute stages. A study by Kim et al. indicated that cultured microglia activated by LPS showed proliferation and morphological changes dependent on β1-integrin signaling in response to neuron-released α-synuclein,[289] with evidence showing that α-synuclein regulates neurotransmitter release and the interaction and assembly of synaptic vesicles.[290,291]

Moreover, a study by Luna et al. indicated that differential α-synuclein expression within CA2 and CA3 neuron subpopulations contributes to hippocampal vulnerability to injury.[292] The evidence from these studies may show a unique and specific microglia-mediated inflammatory cascade dependent on β1-integrin signaling. With microglia morphologies displaying functional changes like microglia that increase their β1-integrin signaling, this remarkable secondary injury cascade may be present in the hippocampus in the acute stages of impact injury. Future studies that explore α-synuclein in neurons and its relationship to up- or downregulation of β1-integrin expression in microglia following cCCI are needed to advance the understanding of this specific pathway.

An opposite shift in the levels of IBA-1 expression and the amount of microglia within the cortex was observed seven days following injury. Increases in IBA-1 expression were observed in the SC and MC of the cCCI animals compared to shams. Still, an overall decrease in the number of microglia cells was present within these regions. Results from Jamnia et al., who've utilized the closed-head CCI model to study neuropathology of impact TBI, observed changes in microglia distribution and morphology and found no significant differences four or eight days following a single cCCI in the cortex, contrasting with the presence of microglia activation observed in the present study. This could be due to variation in experimental design, such as differing injury parameters that may increase or decrease injury severity, or the fact that the contralateral and ipsilateral sides of the cortex were not delineated in the comparative study, which may dilute changes present in subacute microglia responses. Furthermore, significant changes in microglia morphology as quantified through skeleton analysis were found within the cortex seven days following injury, which was found to be negligible in the compared study.[64] In the SC, an increase in branch points/cell was observed within the ipsilateral side compared to the contralateral side, yet no significant differences were found for branch length/cell. Whereas in the MC, a substantial

increase in branch length/cell and branch points/cell was found in the ipsilateral side of the MC compared to the MC of the sham group. With significant increases in area/cell, branch length/cell, and branch points/cell in the ipsilateral MC of the cCCI animals, microglia could be undergoing a dystrophic "bushy" morphology associated with microglia degeneration, with decreased surveillance and phagocytosis (anti-inflammatory).

Within the hippocampus, significant decreases in the number of microglia cells and IBA-1 expression were present in the DG, CA2, and CA3 sub-regions of the hippocampus. The hippocampus is quite susceptible to injury, as explained in section 3.4, with previous literature even demonstrating that the DG, CA2 and CA3 regions are particularly vulnerable to impact TBI because of increased neuronal loss, driving microglia activation.[59,293–295] Likewise, microglia depletion has also been linked to attenuating dendritic spine loss and neuronal apoptosis[296] which could explain why microglia depletion was observed in the DG, CA2, and CA3 of the present study. Moreover, other explanations for decreases in microglia and IBA-1 expression within the hippocampus could be attributed to apoptosis, or microglia proliferating in other areas to maintain homeostatic function in response to impact. Future studies investigating neuronal dysfunction through dendritic and synapse loss that can drive microglia pathology are warranted to further explore hippocampal vulnerability in cCCI. Investigating specific markers such as Caspase-3 and TUNNEL, and actin-related proteins such as coronins, will also contribute to discovering whether microglia are dying in response to injury and insight into their subacute motility and migration patterns.

When quantifying morphological changes within the hippocampus, a significant decrease in the number of branch points was found within the contralateral side of the CA2 compared to the sham group. Still, no other changes were noted, such as an increase or decrease in cell body size or branch length/cell. While a unique morphological change was present within the hippocampus three days following injury, more studies are needed to understand what functional changes, if any, are taking place in the hippocampus at seven days as decreases in branching were the only changes observed.

Levels of NLRP3 are a way to understand microglia activation on a molecular level by acknowledging whether there is a dominant presence of pro or anti-inflammatory microglia within regions of interest. Within the SC and MC, a significant decrease in NLRP3 protein levels was found in the contralateral and ipsilateral regions compared to the cortices of the sham group. It is

logical that a reduction of NLRP3 would be present in the cortex as morphological analysis indicated a dominant presence of dystrophic microglia, which are known to exhibit anti-inflammatory functions.

Within the hippocampus, no significant changes were found when quantifying the amount of NLRP3+ molecules, but significant decreases in fluorescent intensity were observed. As a unique microglia-mediated inflammatory pathway may be present, driven by α-synuclein and β1-integrin signaling, NLRP3 activation may not be a driving factor within this injury cascade. This could explain decreases in its expression and negligible changes in the number of NLRP3 in the hippocampus. Furthermore, if microglia apoptosis occurs, this may also explain decreases in NLRP3 expression.

This study successfully provided insight into acute and sub-acute microglia-induced inflammation in a closed head model of CCI. Responses in the ipsilateral and contralateral sides of the regions of interest exhibited unique transhemispheric changes following impact trauma that needs to be studied further. In this case, the results revealed that while one side of the head is subjected to impact, dysfunction occurs in various brain regions regardless of distance to the area of impact. This could be due to impact loading subjecting forces onto the skull and brain that lead to a more diffuse injury, evidence that has been supported in mild impact injuries.[297] Likewise, damage to neuronal projections that span across regions in the brain could influence microglia responses. Biomechanical studies investigating stress and strain on the skull and brain tissue are necessary to understand their relationship to inducing specific injury cascades and signaling pathways.

One limitation of this study is that, because the injury model is a closed head one, there is no exposure of the skull to locate the bregma and pinpoint the impact area. While most CCI injuries are open head, or even in Jamnia et al., where the skull is exposed first, the researcher can locate the skull's sutures, injuring the animal in the specified stereotaxic coordinates. Unfortunately, in a properly closed head injury model, it is more challenging to locate bregma, which could introduce variability in the study's outcomes. A skull template was used to mark the injury site in the specified coordinates. This template was a skull previously extracted from one of the test rats, and a hole was drilled into the parietal bone (somatosensory cortex region of the brain), allowing for a mark on the top of the head of each animal. This approach concerns ensuring that the skull template is placed precisely over bregma each time. While this limitation is present, three- and seven-day

studies have indicated consistent changes taking place in the regions of impact, adding confidence that the results are reproducible.

For the first time, this work has demonstrated the specific, unique roles that microglia display within a closed-head model of CCI within adult rats, with increasing evidence of specific biochemical responses and pathways that are mediated by microglia in response to impact trauma. The results from this study are imperative in understanding the underlying mechanisms that contribute to adverse TBI outcomes and generating relevant data that can aid in improving diagnostic tools, rehabilitation, and therapeutic interventions for TBI patients.

Chapter 5: Isolated Microglia Exhibit Unique Transcriptional Changes Following Traumatic Brain Injury

Images and text from the introduction and materials/methods sections are adapted, in part, from: Dickerson, M., Guilhaume-Corrêa, F., Strickler, J., VandeVord, P.J., 2022. Age-relevant in vitro models may lead to improved translational research for traumatic brain injury. Current Opinion in Biomedical Engineering 22, 100391. https://doi.org/10.1016/j.cobme.2022.100391

5.1 Introduction

Microglia play an essential role in neuropathology following TBI. Through their activation following the primary insult, they are crucial in repairing and remodeling the injured brain but also undergo functional changes that lead to neurotoxicity. Thus, highlighting the specific contributions of microglia following TBI is imperative. Traditionally, to study microglia-specific activation following TBI, *in vitro* models involving either primary microglia isolated from neonatal rodents or microglial cell lines have been utilized.[149,298–302] While *in vitro* work is crucial in elucidating the role of microglia activation through its molecular pathways, many single-cell microglia models lack the cell-to-cell interactions seen within the CNS microenvironment that may influence microglia activation following injury or disease. Furthermore, there are no *in vitro* methods available that recapitulate all the characteristics of adult homeostatic microglia following TBI. *In vivo* analysis allows for the non-autonomous responses of microglia to be investigated, but it has proven difficult to study microglia-specific contributions to injury due to the inability to distinguish microglial genetic patterns from other CNS populations.[303] Magnetic activated cell sorting (MACS) has come to the forefront as a technique that can isolate individual cellular populations within the CNS, enabling an enrichment of single cell populations across development, into late adulthood.[304,305] Isolating microglia populations using MACS also builds upon *in vitro* work, allowing for microglia-specific responses that mediate neuroinflammation to be studied *in vivo*, encompassing the homeostatic functions or lack thereof of adult microglia following TBI.

Studying microglia's intrinsic and extrinsic factors has led to comprehending the immunophenotypic changes and functions that microglia sustain (pro vs. anti-inflammatory) that occur in response to injury. These changes include the release of cytokines (such as IL-1β), activation states that lead to phagocytosis, and their ability to activate and recruit other cells to injured areas of the brain.[19,306–308] As mentioned in Chapter 3, studies have discovered that one of the critical drivers of the microglia-mediated pro-inflammatory response following injury is the NLRP3 inflammasome. In brain injury, DAMPs and PAMPs such as ATP and high amounts of extracellular potassium are released from dysfunctional or dying cells, which are recognized by the NOD or Toll-like receptor. The trigger response from DAMPs or PAMPs then activates the complex that involves NLRP3, ASC, and caspase 1, cleaving IL-1β into its active form and rapidly releasing it from the cell (Fig. 8). Additionally, markers such as cyclooxygenase-2 (COX-2) and

CD206 have been traditionally used to indicate microglia activation, as expression has shown to peak three days following injury, persisting into the sub-acute stages.[309–311] Increased expression of COX-2 from microglia has been linked to unique inflammatory pathways, as they interact with neuronal synapses.[312] As phenotypic changes in microglia following both blast and impact-induced TBI have indicated that microglia displaying a "rod-like" phenotype interact with dysfunctional neurons, especially in the cortex within the acute stages of injury, it is imperative to understand if microglia-specific COX-2 expression may accompany these phenotypic changes. Finally, CD206 plays a critical role in the injury response as CD206 is the first step to recognizing pathogens, influencing phagocytosis within microglia.[313] Microglia who display amoeboid and rod-like morphologies also function in highly phagocytic states,[129,227,314] thus, it is important to understand the relationship between morphological states of microglia and their expression patterns of markers related to their activation.

While research has supported NLRP3 in microglia pro-inflammatory responses, and COX-2 and CD206 as markers of activation, understanding microglia patterns in response to TBI still prove challenging. Historically, studying these expression patterns utilizes *in vitro* models that have presented with its disadvantages,[315–319] and traditional methods of *in vivo* analysis utilize tissue homogenates that capture all cell types, which can complicate investigating microglia-specific contributions. This is because other CNS subpopulations such as neurons and astrocytes also express NLRP3, COX-2, and even CD206 under specific physiological conditions following TBI.[320–325] Utilizing MACS to combat these challenges, will allow for robust *in vivo* analysis of microglia-specific patterns, and their temporal changes, leading to increases in understanding the underlying mechanisms that influence neuropathology following TBI.

To date, no studies have used MACS to extract pure microglia from the adult rodent brain for various downstream applications following blast or impact TBI. Understanding this response will provide critical information on microglia-specific changes of markers involved in diverse activations states of microglia such as NLRP3 and its effect on IL-1β production, COX2, and CD206 following TBI.

5.2. Methods

5.2.1. Animal Procedures and Blast Injury

The Virginia Tech Institutional Animal Care and Use Committee (IACUC) approved the experimental protocols described herein. Before any experimentation, 8-week-old male Sprague Dawley rats (Envigo, Dublin, VA, USA) (250-300g) were acclimated for several days (12 h light/dark cycle) with food and water provided *ad libitum.*

The blast wave was generated using a custom ABS (Fig, 10) as described previously in section 3.2.1. Before blast exposure, animals were anesthetized with 5% isoflurane and placed in the ABS where each animal was supported in the prone position facing the oncoming shock front using a mesh sling. Animals were exposed to three static overpressure insults separated by one hour each (3x1h; n = 6). A sham group (n = 6) received the same procedures except for the blast insults. All animals were observed through the recovery stages of injury and anesthesia.

5.2.2 Closed-Head Injury Model

An impactor device was used to induce a mild closed head injury in rats (n = 6) with the right somatosensory cortex as the impact site, as described previously in section 4.2.1. Righting reflex was recorded, and animals were observed through injury and anesthesia recovery stages. Sham animals received the same procedures except for the impact (n=6).

5.2.3. Isolating Microglia through Magnetic Bead Cell Separation (Fig 49).

The following protocol was adapted from Holt et al.[304] Three- or seven-days following repeated blast exposure or cCCI, animals were euthanized using CO_2 and decapitated. The right cerebral cortex was micro-dissected, and meninges were removed in dissociation media (200 nM glucose, 500 µL of anti-anti, Earl's Minimal Essential Media) bubbled with 95% oxygen: 5% Carbon Dioxide. Following cortical isolation, the tissue was minced into 1 mm^3 pieces and was dissociated using Worthington's Papain Dissociation Kit (Worthington Biochemical, Lakewood, NJ). This included releasing the settled mince tissue into the Papain/DNase solution, which was then incubated in a hot water bath at 37^oC for fifteen minutes. Tissue was subsequently titrated into a single cell suspension and then centrifuged at 300xg for three minutes at room temperature. The supernatant was discarded, and the cell pellet was carefully suspended in resuspension media,

which included Earle's Balanced Salt Solution (EBSS, Worthington Biochemical, Lakewood, NJ) and albumin-ovomucoid (Worthington Biochemical, Lakewood, NJ). Once resuspended, the homogenous solution was carefully layered onto the albumin density gradient and centrifuged. The supernatant was discarded, and the pelleted cells were resuspended in 10 mL of 0.5% BSA. The solution was then filtered using a 70 um BD falcon filter to remove any non-dissociated tissue.

Once dissociated, 500uL of the filtered solution was taken out as "whole tissue fraction" to be used for qPCR to check for cell purity. This solution was then centrifuged at 300xg for three minutes at 4^{o}C. The supernatant was discarded, and the cell pellet was stored at -80^{o}C for future use. The remaining solution to isolate microglia were centrifuged at 300xg for three minutes at 4^{o}C. The supernatant was discarded, and the pellet was immediately resuspended in 250 µL of 0.5% BSA. 30 µL of Myelin microbeads were added to the resuspended solution, and cells were incubated for 10 minutes at 4^{o}C, gently mixing the solution every two minutes. Cells were washed with 1 mL of 0.5% BSA and centrifuged at 300xg for 3 minutes to remove unbound beads from the pellet. The pellet was resuspended in 500 uL of BSA and applied directly onto a prepped LS column fitted into a MACS Midi magnetic cell separator (Mitenyi Biotec, Gaithersburg, MD). The column was washed twice with 3 mL of BSA, and the flow-through was collected in a 15 mL conical tube. The flow-through containing the microglia, astrocyte, and neuron populations was centrifuged at 300g for 3 minutes, and the supernatant was discarded. 30 µL of Anti-CD11b+ microbeads were then added to the resuspended solution, and cells were incubated for 15 minutes at 4^{o}C, gently mixing the solution every 2 minutes. After 15 minutes, cells were washed with 1 mL of 0.5% BSA and centrifuged at 300xg for 3 minutes to remove unbound beads from the pellet. The pellet was resuspended in 500 uL of BSA and applied directly onto a prepped LS column fitted into the MACS Midi magnetic cell separator. The column was again washed two times with 3 mL to allow unlabeled cells to be discarded with the flow-through. The column was removed from the magnetic field and placed in a collection tube (15 mL tube). The target population (Cd11b+ microglia) was collected by adding 5 mL of BSA to the plunger and pushing the supplied plunger to allow the cells within the column (microglia fraction) to be collected into the tube. The solution was centrifuged for 3 min at 300g, and the supernatant was discarded. The remaining pellet, including the microglia fraction, was stored at -80C until further use.

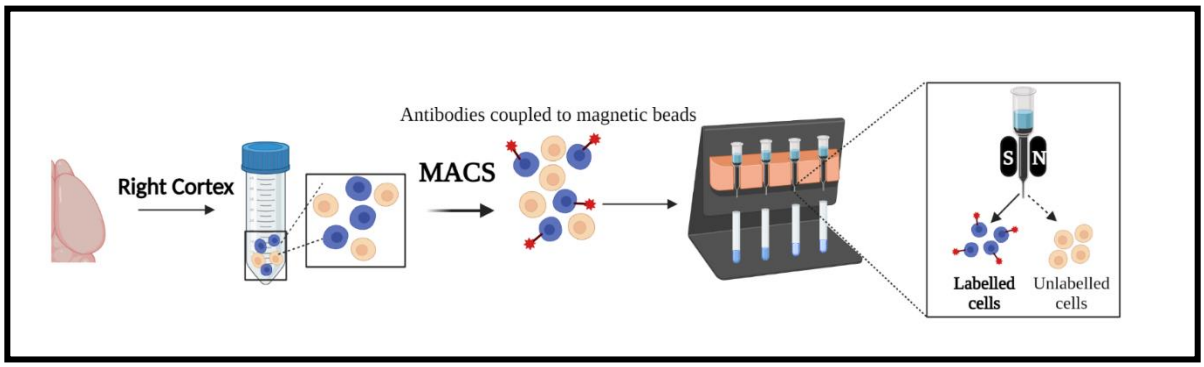

Figure 49. Magnetic-activated cell sorting for isolating brain cells from the adult rodent brain. First, the rodent brain is extracted and undergoes tissue dissociation. Cell-specific antibodies are tagged to allow for the separation and collection of targeted cells through a column placed on a powerful magnetic field, retaining the labeled cells.

5.2.4. RNA Isolation and Quantitative Reverse-Transcriptase Polymerase Chain Reaction (qPCR)

Quantitative PCR was used to optimize and measure gene expression from the isolated microglia populations. Total RNA was extracted using Trizol (Invitrogen, Carlsbad, CA) and the Purelink RNA MiniLink Kit (Invitrogen, Carlsbad, CA) following the manufacturer's protocol. RNA concentration and purity were determined using the Nanodrop (Thermofisher Scientific, Waltham, MA), which gave ultraviolet measurements at 260 nm and 280 nm. Reverse transcriptase was used to convert mRNA to a cDNA template using the iScript Reverse Transcription Supermix Kit (Biorad, Hercules, CA). The reaction mixture was then placed in the thermocycler to incubate and complete the reaction (Table 2).

A purity check using qPCR was performed to confirm that the isolated cells were pure microglia. The process includes normalizing a mixed cellular population (whole tissue fraction) to examine the enrichment or depletion of microglia. The following specific cell type markers were used to check for this enrichment: *ITGAM* (microglia), *GFAP* (astrocytes), *RBFOX3* (neurons), and *MBP* (oligodendrocytes). Glyceraldehyde-3 phosphate dehydrogenase (GAPDH) was used as an endogenous control for the normalization of RNA quantity. The PCR reaction was performed with an Applied Biosystems QuantStudio 3 Real-Time PCR System (Thermofisher Scientific, Waltham, MA) with fold changes in gene expression relative to the whole tissue fraction assessed using the $\Delta\Delta C_T$ method. Following the purity check, qPCR was again used to measure pure microglia gene expression patterns of NLRP3, IL-1β, COX-2, and CD206. Fold changes in gene

expression relative to GAPDH were analyzed using the $\Delta\Delta C_T$ method, with and then normalized to respective shams. All primers used are listed in Table 3.

Table 2. Iscript Reverse Transcription Supermix Thermocycler Reaction Protocol. The protocol converts the RNA to DNA, amplifying the DNA.

Priming	5 min at 25°C
Reverse Transcription	20 min at 46°C
RT inactivation	1 min at 95°C

Table 3. Name and Gene ID of all Taqman Primers Used for qPCR. All primers were purchased through Thermofisher Scientific.

Primer	Gene ID
ITGAM	Rn0070342_m1
GFAP	Rn0056603_m1
RBFOX3	Rn01464214_m1
MBP	Rn01399619_m1
NLRP3	Rn04244620_m1
IL-1β	Rn00580432_m1
COX-2	Rn01483828_m1
CD206 (MRC-1)	Rn01487342_m1

5.2.5. Statistical Analysis

All statistical analyses were performed in GraphPad Prism version 9 (GraphPad Software, La Jolla, CA) as previously described in section 3.2.5. All gene expression data were then normalized to respective shams. All data is represented as the mean ± standard error of the mean, or SEM.

5.3 Results

5.3.1 Blast Event and Animal Recovery

Blast animals (n = 6) were exposed to three blast events separated by one hour each, with blast wave characteristics described in Table 4. Following exposures, no apparent signs of injury were discernable. Over the three- and seven-day period, there was no significant difference in weights observed in the blast group compared to the sham group.

Table 4. Blast Wave Characteristics. Male Sprague Dawley rats were subjected to three blast insults separated by 1 hour each. The average peak pressure was ~17 psi, with sham animals receiving the same procedures except for the blast insult.

Time Point	Peak Pressure (psi)	Duration (ms)	Impulse (psi*ms)	Rise time (ms)
3 days	17.48 ± 0.37	2.18 ± 0.04	14.42 ± 0.32	0.05 ± 0.02
7 days	16.52 ± 2.12	2.12 ± 0.21	13.34 ± 1.69	0.02 ± 0.002

5.3.2 Animal Recovery following cCCI

Following cCCI, no apparent signs of injury were discernable. Animals subjected to cCCI showed significant delays in righting time compared to the sham groups (Fig. 50). Over the three- and seven-day periods, no significant differences in weights were observed when comparing the cCCI groups to their respective sham groups.

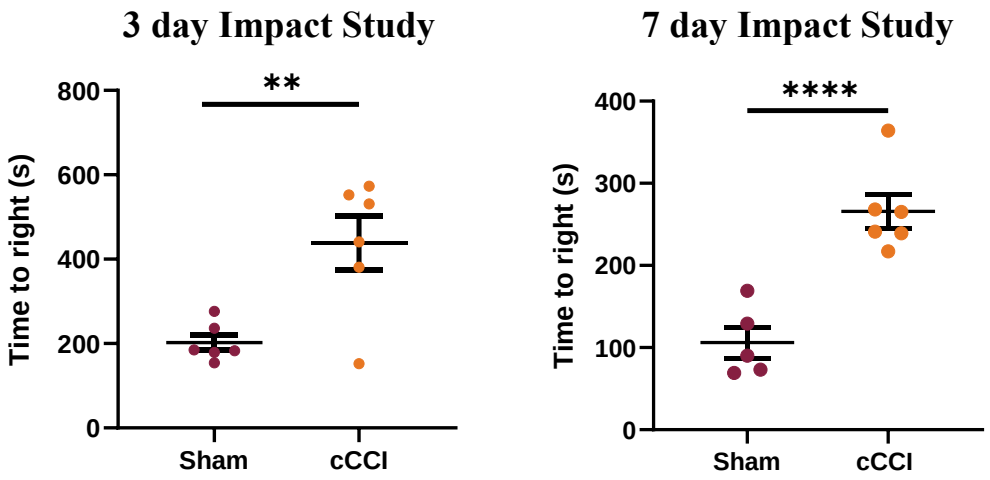

Figure 50. Observing injury recovery through righting reflex. In both the three and seven day impact groups, animals that received a cCCI showed significant delays in righting time compared to the sham group. **p<0.01, ****p<0.0001. Data represented as Mean ± SEM.

5.3.3 Isolation of microglia populations following MACS shows enrichment

Cell purity was confirmed via qPCR by evaluating cell-type-specific gene expression. In both the blast and impact groups, an enrichment of CD11b+ microglia were observed. When normalized to the whole tissue fraction, low levels of expression of the astrocytic gene GFAP, oligodendrocyte gene MBP, and neuronal gene RBFOX3 were found post-magnetic sorting (Fig. 51). A small amount of myelin contamination (6%) is present in the isolated microglia of the impact group.

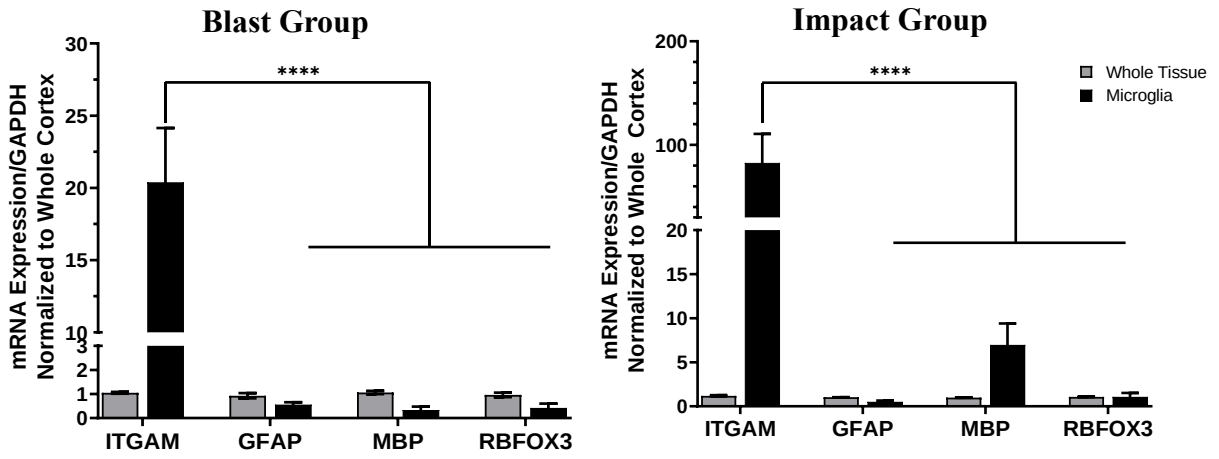

Figure 51. Microglia purity was achieved following MACS cell isolation. Quantitative PCR of isolated microglia from adult rats indicates a significant enrichment in the expression of ITGAM, a microglia-specific marker, and low levels of astrocytes, oligodendrocytes, and neurons when normalized to whole tissue from the cortex. ****$p<0.0001$. Data represented as Mean ± SEM.

5.3.4 Limited changes in gene expression patterns of microglia were observed three days following repeated blast exposure

Understanding microglia-specific gene expression patterns may further interpret the transient inflammatory response following repeated blast exposure. To investigate this role, mRNA expression levels of NLRP3, IL-1β, COX2, and CD206 were measured using qPCR, with all genes normalized to the reference gene GAPDH to explore fold expression. A significant increase in gene expression of COX2, a marker commonly upregulated in activated microglia in injury and diseased conditions, was observed in blast animals compared to shams ($p=0.03$). No significant changes in gene expression were found for NLRP3, IL-1β, and CD206 (Fig. 52).

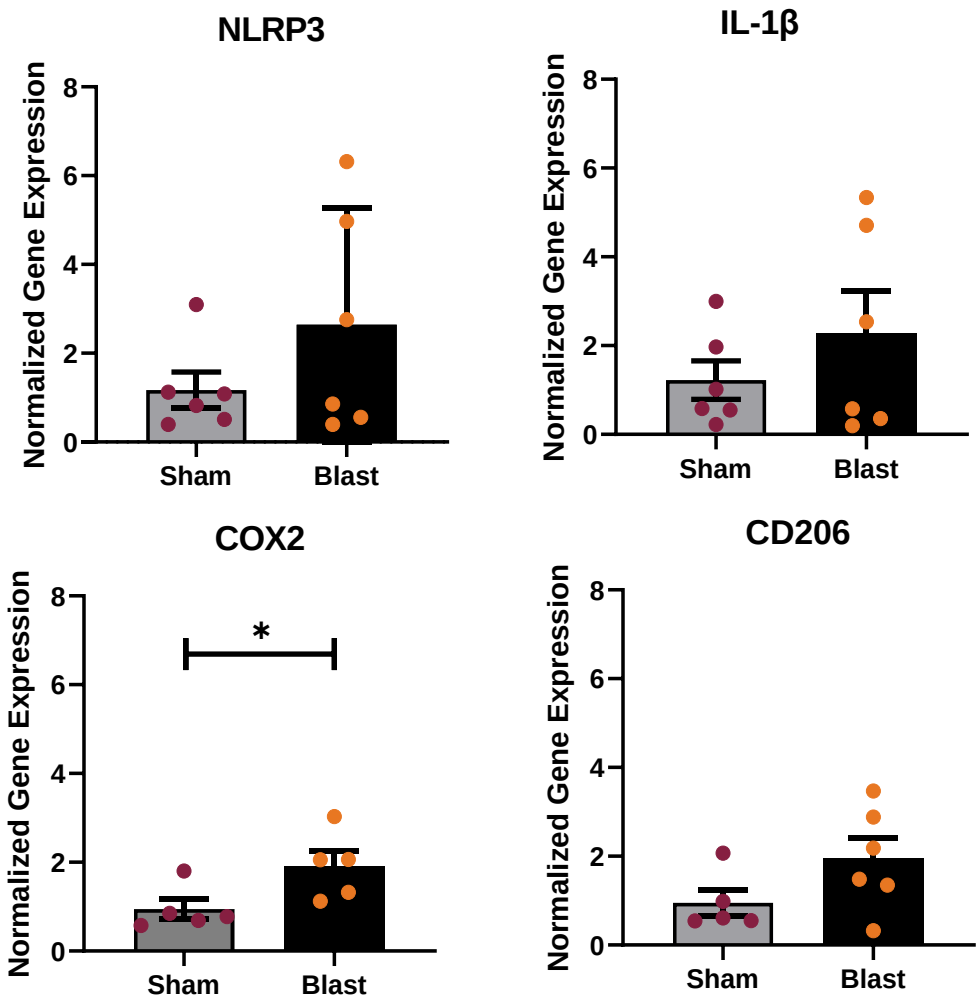

Figure 52. Molecular changes in genes involved in microglial activation between the sham and blast groups were determined by qPCR analysis. A significant increase in the genetic expression of COX2 was observed in cortical microglia three days following repeated blast exposure. No significant changes were found for any other gene. *p<0.05. Data represented as Mean ± SEM.

5.3.5 Altered gene expression within microglia was observed seven days following blast injury

Seven days following injury, all genes presented an increase greater than two-fold in blast animals compared to shams. The increase in fold expression of CD206, a cell-surface marker expressed on microglia undergoing an anti-inflammatory phenotype, was found to be significant when comparing the blast group to shams (p=0.02). Trending increases in fold expression were

observed in the blast group for IL-1β (p=0.07) and COX2 (p=0.06). No significant changes in gene expression of NLRP3 were observed (Fig. 53).

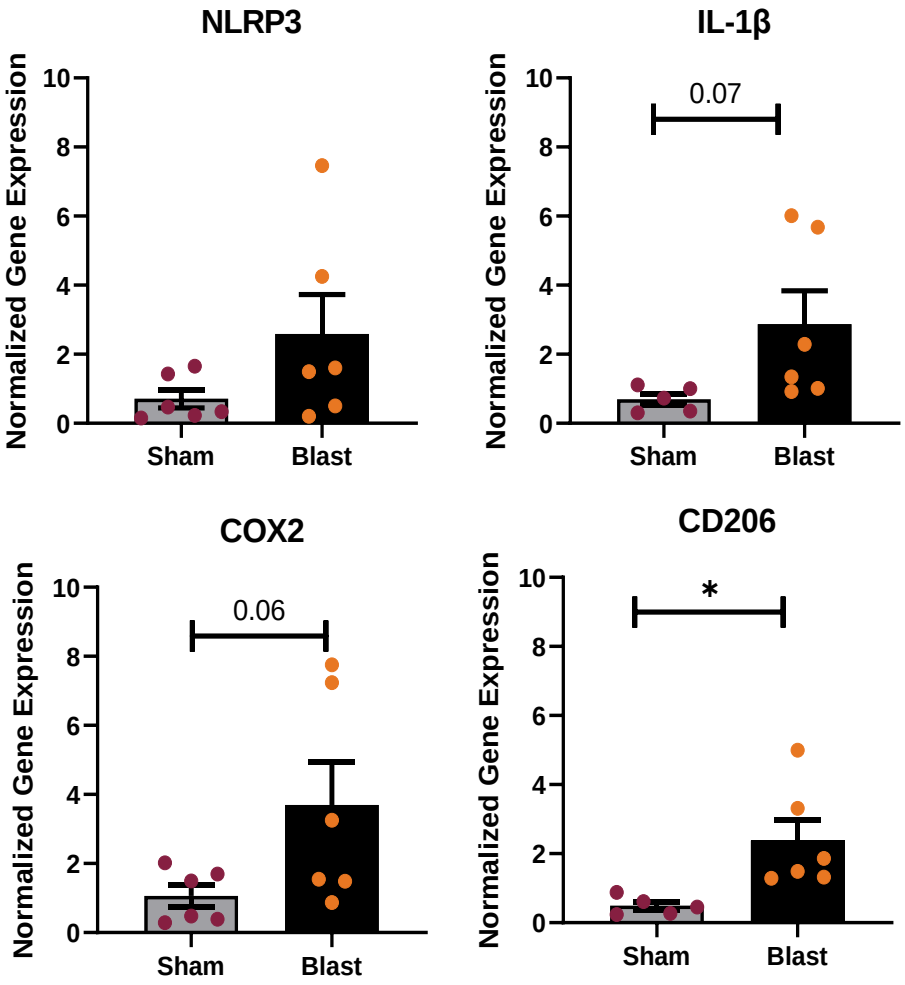

Figure 53. Increases in microglia-specific gene expression were observed seven days following blast injury. A significant increase in mRNA expression of CD206 was observed in the blast animals compared to shams. A trending increase in gene expression of IL-1β and COX2 was indicated in blast animals compared to the sham group. *p<0.05. Data represented as Mean ± SEM.

5.3.6 Transcriptional changes in isolated microglia showed activation three days following cCCI

Microglia from the right cortex (side of impact) were isolated using MACS to investigate whether there were transcriptional changes within microglia, which may indicate acute activation following cCCI. A significant increase in mRNA expression of NLRP3 (p=0.04), COX2

(p=0.004), and CD206 was observed within cortical microglia in the cCCI group three days following injury. Trending increases in mRNA expression of IL-1β (p=0.08) in microglia were also observed in the cCCI animals compared to shams (Fig. 54).

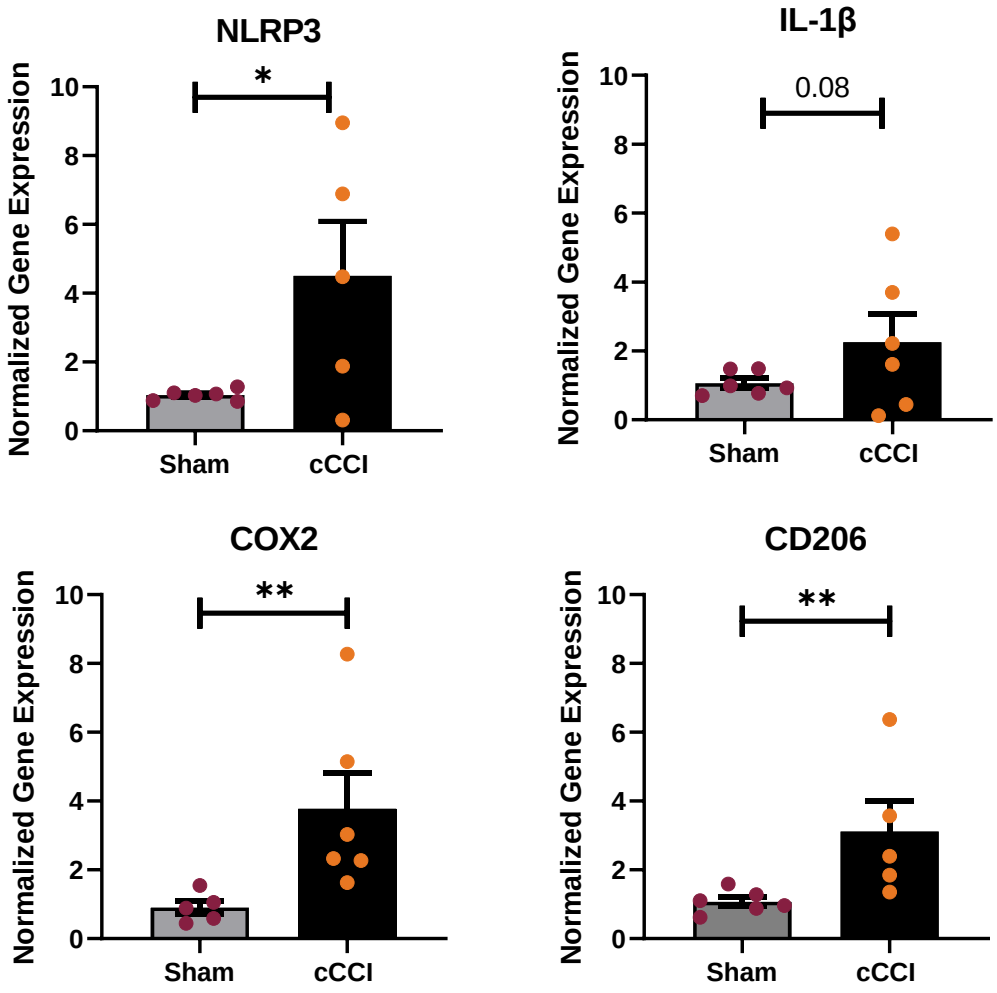

Figure 54. Increases in microglia-specific gene expression were observed three days following cCCI. A significant increase in mRNA expression of NLRP3, COX2, and CD206 was observed in isolated cortical microglia in the cCCI animals compared to shams. A trending increase in gene expression of IL-1β was found in the cCCI group compared to shams. *p<0.05, **p<0.01. Data represented as Mean ± SEM.

5.3.7 Transcriptional changes showed diverse activation states in isolated microglia seven days following cCCI

Quantitative PCR analysis showed a significant increase in gene expression of NLRP3 ($p=0.002$) and IL-1β ($p=0.008$) in isolated cortical microglia from cCCI animals compared to their sham counterparts. Significant increases in gene expression of COX2 ($p=0.04$) and CD206 ($p=0.01$) were also observed in cortical microglia in cCCI animals compared to shams seven days following cCCI (Fig. 55).

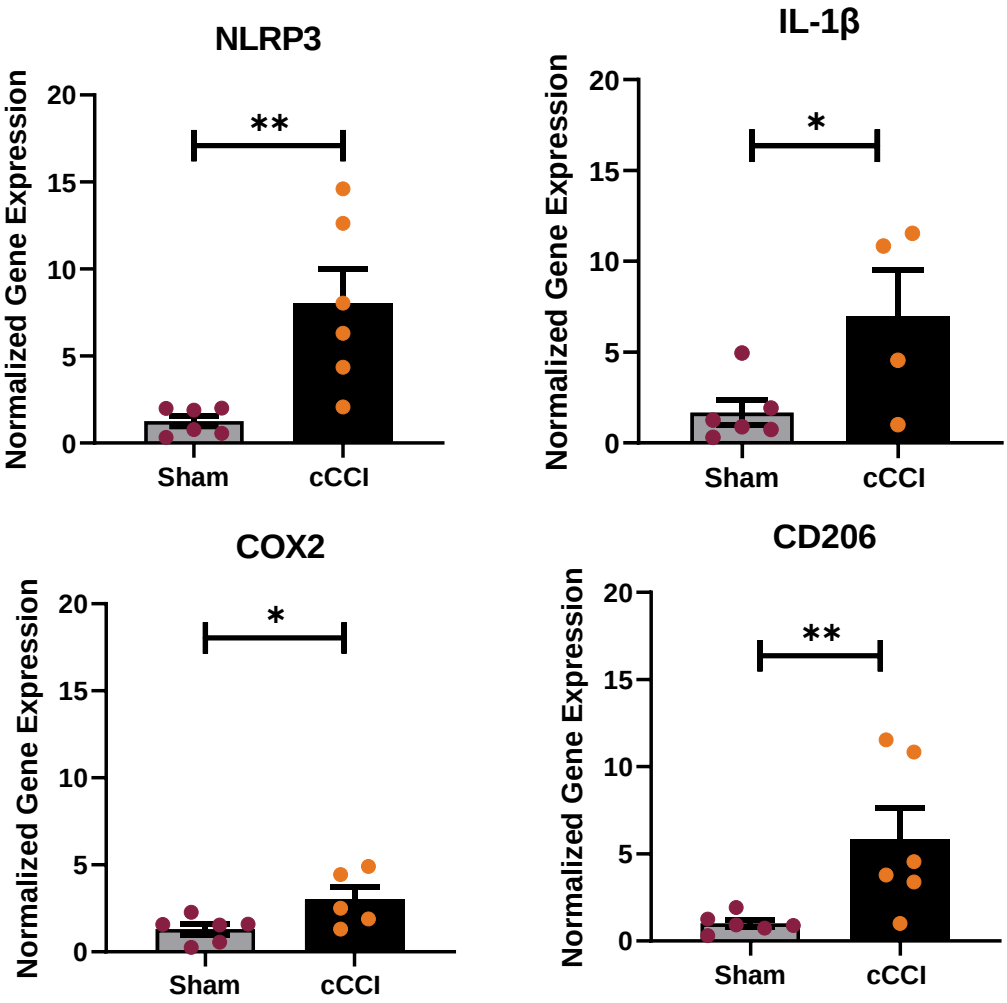

Figure 55. Diverse transcriptional changes in cortical microglia were found seven days following cCCI. A significant increase in mRNA expression of NLRP3, Il-1β, COX2, and CD206 was observed in isolated cortical microglia in the cCCI animals compared to shams. *$p<0.05$, **$p<0.01$. Data represented as Mean ± SEM.

5.4 Discussion

The microglia-mediated inflammatory response following TBI is a vital secondary injury mechanism that can drive tissue plasticity or trauma-induced neurodegeneration.[326–329] However, little is known about the diverse phenotypic changes that microglia undergo following injury and the molecular mechanisms that drive these changes. Investigating *in vivo* microglia-contributions to neuropathology through MACS can give substantial insights into injury progression. In the present study, microglia were isolated from the adult rat brain following both blast- and impact-induced TBI, leading to a high enrichment of the cell populations (Fig. 51). This method is advantageous as it allowed data to be generated on microglia-specific patterns, without the influence of other CNS subpopulations that may also express the same markers in the injured microenvironment. This novel approach could be an innovative area for intervention design as understanding the transient response of microglia activation can lead to targeted-therapies to limit persisting inflammation.

Genetic changes in NLRP3 activation triggered by physiological changes due to injury were analyzed to understand what drives microglia-mediated inflammation. NLRP3 is activated by extracellular signals that then activate the NF-κB pathway, and transcriptional changes in NLRP3 influence the oligomerization of the complex that includes NLRP3, ASC, and Caspase-1. Once the inflammasome complex is activated, IL-1β is primed and released from the cell, influencing pro-inflammatory responses triggered by microglia. Thus, identifying the temporal changes within microglia following TBI is an ideal way to understand microglia-specific activation on a molecular level. While increased, no significant transcriptional changes in mRNA levels of NLRP3 or IL-1β were present in isolated microglia from blast animals three days following repeated blast exposure. In contrast, a significant increase in genetic expression of NLRP3 was observed in isolated cortical microglia in the cCCI group compared to their shams counterparts three days following injury, with no significant increases in IL-1β observed. Seven days following repeated blast exposure, no significant increases in gene expression of NLRP3 and IL-1β were found within cortical microglia in the blast group compared to their shams. In contrast, a substantial increase in NLRP3 and IL-1β was observed in the cCCI group compared to the sham group. The results herein suggest that downstream signaling cascades that influence NLRP3-mediated microglia activation are present following cCCI, which might be influenced by the specific primary insult, such as the rotational acceleration forces on the tissue that can influence

signaling pathways, as discussed in Chapter 4. Further studies are needed to provide evidence to support this claim, especially to understand injury-type-specific induction of secondary inflammatory pathways, as changes in NLRP3 were not observed in blast animals at three days. In regards to limited changes observed in IL-1β, reports have indicated that closed head injuries show a transient cytokine profile, with pro-inflammatory mediators upregulated early following TBI, returning to baseline at three days, and peaking again at seven days.[167] With no significant transcriptional changes in IL-1β occurring in either injury modality three days post-injury, the results in the present study may also indicate cytokine levels returning to baseline, or there are other mediators and signaling pathways in part from NLRP3 that are influencing IL-1β expression at three days. Additionally, the results at seven days were in agreement with reports that cytokine levels peak at seven days, but within microglia specifically, this transient response may be specific to cCCI and not repeated blast exposure. Sustained release of cytokines and chemokines, as well as changes in other cells such as astrocyte reactivity, could contribute to IL-1β cytokine levels observed at these specific stages in other studies. Continuing to study the microglia-specific molecular changes that influence this pro-inflammatory response can include investigating ASC and Caspase-1 expression, which can provide additional evidence into the oligomerization needed to activate the inflammasome complex across injury modalities, producing IL-1β. Moreover, studying other cytokines that are produced and secreted through NLRP3 activation such as IL-18 should be investigated for a more comprehensive analysis of NLRP3 signaling pathways within cortical microglia.

A significant increase in the genetic expression of COX-2 was found within isolated cortical microglia in both the blast and cCCI animals compared to their sham counterparts three days following injury. Seven days following injury, upregulation of COX-2 continued to persist in the cCCI group. At the same time, a non-significant increase ($p=0.06$) was observed in blast animals compared to their sham counterparts. A two-day *in viv*o study by Shojo et al. assessed genetic and histological alterations in COX-2 following an open-head impact injury (FPI). They marked an increase in genetic expression of COX-2 that increased 3h and 12h following injury, with immunostaining indicating COX-2 expression co-localized with IBA-1 peaks at two days.[330] Data presented in the current study indicated that COX-2 expression within microglia continues up to seven days following impact injury, building upon their hypothesis of the dynamic temporal expression of COX-2. While their results are meaningful, their genetic alterations of COX-2

encompasses all cell types and not just microglia, which may influence observing the sensitive changes in COX-2 expression, which may have contributed to the negligible changes in mRNA levels of COX-2 after 12 hours. Isolating microglia for *in vivo* analysis indicated microglia-specific COX-2 expression continues to persist through the sub-acute stages, which is a crucial observation in elucidating secondary injury responses to neurotrauma. Other research models used traditional *in vitro* models to study microglia-specific changes in CNS injury, examining transcriptional changes in COX-2 expression as a form of microglia activation with these models using traditional *in vitro* methods to study microglia-specific changes.[331–333] Results herein were able to build upon this work, showing transient changes in microglia-specific responses *in vivo*, which encompasses all factors within the CNS microenvironment that influence the malleability of the microglia response to injury.

CD206 is expressed on tissue-derived macrophages and activated microglia, functioning to phagocytose cellular debris, which is vital for immune homeostasis. A study by Greenlagh and David suggested that the phagocytic response of microglia differs from peripheral macrophages, with microglia playing a significant role in the early response of CNS injury, with higher efficacy to process CNS debris than peripheral macrophages.[334] This increased efficacy is vital in the neuroprotection of the injured brain, making it imperative to understand the temporal response of CD206 within microglia. The present study showed a significant increase in genetic expression of CD206 in cortical microglia of cCCI animals compared to shams both three and seven days following injury. In contrast, increases in CD206 expression were only observed in blast animals seven days following injury. This may suggest that CD206 expression within microglia can persist past 24 hours, but this may depend on the injury modality and the secondary cascades associated with them. A study by Sabirzhanov et al. indicated that upregulation of microRNAs following CCI enhanced neuronal cell death.[335] Increased cell death can influence microglia that function in a phagocytic state, which could explain why upregulation of CD206 is present up to seven days in this closed-head CCI study. In addition, other studies have noted increases in phagocytic activity of microglia in relation to neuronal death and synaptic loss following CCI early on in the injury response that has persisted in the subacute stages.[336–338] In contrast, neuronal dysfunction that influences myelin and dendritic debris following mild bTBI, have been commonly found starting up to five days following blast exposure,[233,339] which may explain the delayed onset of phagocytic microglia in the cortex in the present study. This may also provide insight on the diverse role of

rod-like microglia, as observations discussed in Chapter 3 indicated rod-like microglia, who are known to have phagocytic properties, were present in the cortex at three days, yet up-regulation of CD206 was not present at three days. Future studies are necessary to continue to understand the functional roles of microglia who take on diverse activation states following blast injury. Overall, data from the present study, utilizing microglia-specific *in vivo* analysis, showed that transient responses of microglia may be specific to TBI-type.

The work presented in this study provided an initial understanding of microglia-specific pathological responses within the cortex following TBI. MACS isolation techniques allow for *in vivo* analysis of microglia-specific transcriptional changes to CNS injury, a novel approach that to our knowledge, has not been studied following blast injury or cCCI. Isolation of cortical microglia suggests that diverse activation states of microglia are present within the cortex following TBI, which may be time-dependent and injury-type-specific. Future directions are needed to further explore this claim by analyzing transcriptional changes earlier on following both repeated blast exposure and cCCI (4h, 24h, 48h), as well as in the early chronic stages (< 7 days). Furthermore, identifying gene expression patterns within microglia in other brain regions, such as the hippocampus, amygdala, thalamus, etc., is also important and may provide more insight into the spatial heterogeneity of microglia following TBI. Future work should also explore other surface, intracellular, and released molecules within microglia such as TREM2, CCR2, and MMP-9 to expand on understanding the diverse subsets of microglia and their specific functions in neuroinflammation following TBI. Exploring transcriptional changes within microglia should also include proteomics to understand the differences in protein expression and how this expression varies in accordance with gene expression. Proteomics will also prove beneficial in contributing to a representative profile of the functional changes that are taking place within microglia following TBI. Overall, the presented study has provided an understanding of the diverse changes within microglia across time following TBI and the feasibility of MACS to evaluate microglia pathology within the adult rodent brain. Understanding the susceptibility of microglia in response to TBI is imperative in generating meaningful data that can contribute to developing to personalized treatments to mitigate inflammation following TBI.

Chapter 6: Evaluating Phenotypic Changes in Microglia Following Blast Plus Impact Traumatic Brain Injury

6.1 Introduction

Chronic clinical symptoms of bTBI are frequently reported, with increased records of disinhibition in Veterans returning home from active duty.[340] Previous studies have linked blast-induced changes in the dopaminergic system with novelty-seeking behaviors, which is a behavior closely resembling traits associated with disinhibition such as risk-taking behaviors, aggression, and impulsivity, which can also lead to maladaptive behaviors such as substance abuse.[341–343] Reports have also linked military personnel who have sustained a bTBI with "premature mortality" from what was known as "thrill-seeking behaviors", with clinical research indicating a positive relationship between these behaviors and motor vehicle accidents, falls, and assault.[343,344] A review by Bernstein et al. supports evidence of risk and thrill-seeking behaviors with subsequent accidents as twenty-two studies linked co-morbidities from TBI and post-traumatic stress disorder (PTSD) with increases in objective driving behaviors that led to hospitalization due to accidents.[345] Decreased life expectancy for Veterans experiencing disinhibition can be linked to a plethora of issues such as diabetes, cardiovascular problems, or substance abuse related deaths, in addition to accidents, but reports of an "injury frequent effect," can explain poor outcomes following thrill seeking behaviors. More specifically, people who experience recurrent TBI's such as repeated blast exposure in combat, and then a subsequent TBI as a result from an accident or assault, may experience increased frequency and severity of clinical symptoms associated with TBI.[346] While population based-samples have provided support to this theory, there is still a lack of research in understanding how the injury frequency effect works, especially in complex injuries sustained by Veterans such as the "blast plus" complex injuries.[347] Moreover, to our knowledge, only one study has explored preclinical models to understand whether blast exposure increases susceptibility to a subsequent TBI, or if bTBI predisposes the brain to increased pathological outcomes following concussion (mild impact TBI).[348] Overall, it is imperative to answer the fundamental questions regarding "blast plus impact" TBIs, such as neuropathology associated with these complex injuries.

Evidence suggests that clinical manifestations of blast- or impact-induced TBI are similar, but biological outcomes that influence clinical symptoms may differ.[349] Specific aim 1 explored the spatial and temporal response of microglia following both blast and impact TBI; showing that IBA-1 expression was significantly increased in the acute stages of injury (three days) but were decreased compared to sham animals at the subacute stages (seven days) in both blast and impact-

related injuries. Furthermore, morphological changes and microglia-specific genomics indicated that pro-inflammatory and phagocytic cortical microglia are present in the acute and subacute stages following impact injury, with dystrophic, degenerating, and phagocytic microglia persisting in the subacute stages of blast-injured animals. With complex inflammatory cascades occurring that may be injury-type-specific, in-depth analysis of microglia responses to blast plus impact injuries are needed to understand functional changes when these two injury modes are combined.

Injury frequency, such as repeated head impacts have been defined in sports-related environments, with repeated mild TBIs over an extended period leading to chronic traumatic encephalopathy (CTE).[11,96] Neuropathology following repeated blast exposure has also been found to persist, in the chronic phases, yet studying blast plus impact TBIs have rarely been considered, despite increased reports of poor outcomes in Veterans who have sustained these injuries. As mentioned, there is only one preclinical study that has explored neurological and cognitive deficits following blast plus impact TBI. Because of this, further in-depth analysis of neuroinflammation following this injury still needs to be considered. Exploring whether microglia activation states are more severe, or present differently in comparison to blast-only or impact-only injuries (Chapters 3 and 4) can provide insight to this complex injury as it relates to poor outcomes after the fact. This study aimed to develop a pre-clinical model to understand microglia contributions to pathological outcomes following blast plus impact trauma and whether repeated blast exposure predisposes the brain to more severe microglia-mediated outcomes once a subsequent impact TBI occurs.

6.2 Materials and Methods

6.2.1 Animal Procedures and Experimental Groups

The study described was carried out in accordance with all experimental protocols approved by Virginia Tech's University Institutional Animal Care and Use Committee. Prior to experimentation, male Sprague Dawley rats weighing approximately 250-275 g (Envigo, Dublin, VA, USA) were acclimated for several days (12 h light/dark cycle) with food and water provided *ad libitum.* All animals were randomly assigned to one of four groups: Sham only (n=10), blast only (n=7), impact only (n=10), blast+impact (n=11).

6.2.2 Blast + Impact Model (Fig. 56)

The blast wave was generated using the custom ABS as previously described in section 3.2.1. Prior to blast exposure, animals were anesthetized with 5% isoflurane and then placed in the ABS. Animals were exposed to three blasts (17.27 psi ± 0.19) separated by one hour each (3x1h). Fourteen days following repeated blast exposure, the animals assigned to the "blast plus impact" group were placed under anesthesia again and were subjected to a single closed-head controlled cortical impact, as previously described in section 4.2.1. Following impact, animals were placed on a heating pad at 37C, monitored, and righting time was recorded.

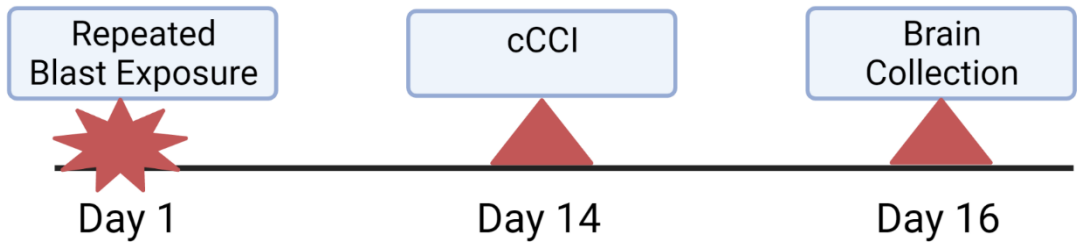

Figure 56. Timeline representing Blast+Impact Model. On Day 1, animals were exposed to three blast insults separated by one hour each. On Day 14, animals were subjected to a single cCCI, with brains collected on Day 16.

6.2.3 Physiological Measures

Physiological measures such as weight loss and/or percent weight gain and righting reflex were measured for all groups of animals. Sham, blast+impact, and impact-only animals were immediately placed on a heating pad at 37ºC in the supine position, and the time for the animal to right was recorded. Animals were weighed before the blast and/or impact injury to evaluate the percentage of weight gained or lost post-injury.

6.2.4 Immunohistochemistry

Two days following cCCI (16 days post-blast), animals were transcardially perfused with 0.9% saline and 4% PFA. Brains were then collected, cryopreserved, and sectioned into 30 µm coronal sections to be used for immunohistochemical analysis. Sections containing the motor

cortex, somatosensory cortex, and hippocampus (-3.00 mm posterior to Bregma) were stained for IBA-1, a microglia marker, as described previously in section 3.2.2. Tissues were imaged on a Zeiss Fluorescent Microscope, and quantification for overall pathological changes included analyzing levels of IBA-1 (area fraction and fluorescent intensity) the number and size of cells within each region (area/cell and count per area), and morphological changes of microglia (Branch length/cell and Branch points/cell) were completed as described in section 3.2.3 and 3.2.4.

6.2.5 Statistical Analysis

All statistical analyses were performed in GraphPad Prism Version 9 (GraphPad Software, La Jolla). The Kolmogorov-Smirnov test, in association with the Shapiro-Wilk test, was performed to test for normal distribution and equal variance. If the data passed the two assumptions, a one-way ANOVA and post hoc tests were performed where appropriate for sham, blast+impact, blast-only, and impact-only groups. Data that did not pass normality or equal variance assumptions were assessed using a one-way Kruskal Wallis test or the Brown-Forsythe test. Data were considered statistically significant with $p<0.05$ and trending at $p<0.1$. All histology data was normalized to respective shams. All data is represented as the mean ± standard error of the mean, or SEM.

6.3 Results

6.3.1 Physiological Outcomes

Righting reflexes in the sham, blast+impact, and impact-only groups were not found to be significantly different from one another (Fig. 57). Sixteen days post blast; the blast-only group had a 12% weight increase. The blast+impact group had an 11% increase at the time of impact (Day 14), with a 0.6% decrease in weight loss two days following impact (Day 16). A 4% loss in weight was observed in the impact-only group at the time of euthanasia.

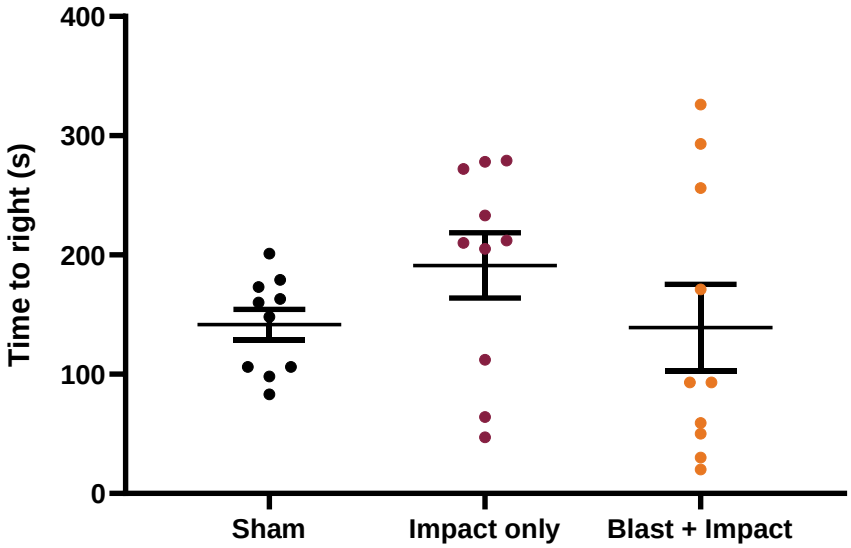

Figure 57. Righting reflex across experimental groups. No significant differences in righting time were observed across groups. Data represented as Mean ± SEM.

6.3.2 Changes in microglia size are prevalent in the SC following Blast+Impact Injury

A Brown-Forsythe ANOVA test indicated significant changes in area/cell in the SC between groups. A significant increase in area/cell was observed in the blast+impact group compared to shams ($p=0.02$) and the blast-only group ($p =0.005$). A significant increase in area/cell was also observed between the impact-only groups compared to shams ($p<0.005$). A significant increase in area fraction was also found between the blast plus impact group compared to the blast only group ($p<0.05$) ($F (3, 33) = 2.816$, $p=0.05$). No significant differences were found between any groups for count per area or fluorescent intensity (Fig. 58).

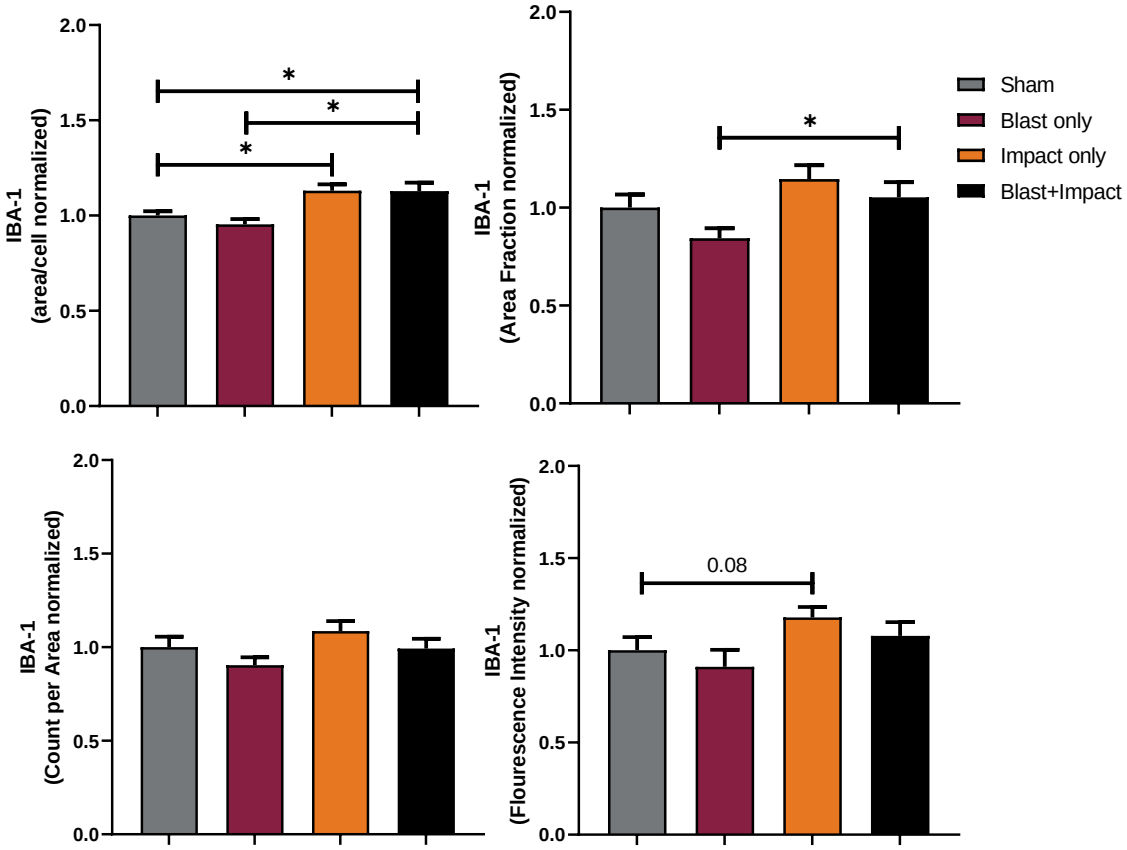

Figure 58. Changes in microglial responses were observed in the SC following blast+impact injury. Significant increases in area/cell were found in the blast+impact group compared to shams and the blast-only group. A significant increase in area/cell was also found in the impact-only group compared to shams. An increase in area fraction was observed in the blast+impact group compared to the blast-only group. *p<0.05. Data represented as Mean ± SEM.

6.3.3 Morphological changes in the SC were prevalent following impact

Microglia morphology was quantified through skeleton analysis for a robust understanding of microglia activation following blast+impact injury. A one-way ANOVA indicated significant differences in branch length/cell across groups ($F(3, 32) = 8.435$, $p=0.0003$). Furthermore, a significant increase in branch length/cell was observed in the blast+impact group compared to the sham group ($p=0.03$). This significant increase was also found between the blast+impact and impact-only groups ($p=0.03$). A significant decrease in branch length/cell was found when comparing the impact-only group to shams ($p<0.0001$). When analyzing branch points/cell, the

only significance found was between the blast+impact and the impact-only group (p=0.04) (Fig. 59).

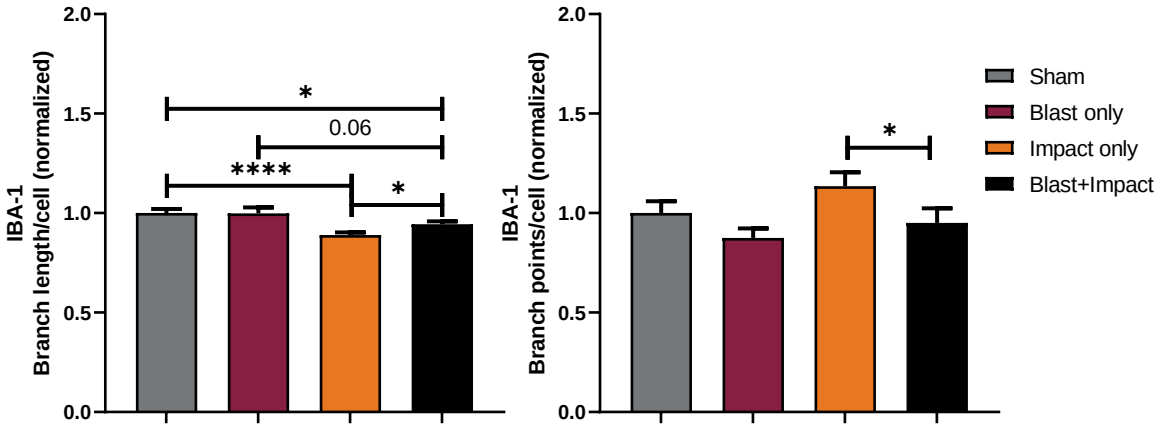

Figure 59. Changes in microglial morphology were prevalent in the SC following impact. A significant decrease in branch length/cell was observed in the impact-only group compared to shams and the blast+impact groups. A significant increase in branch length/cell was also observed in the blast+impact group compared to shams. A significant increase in branch points/cell was found in the impact-only group compared to the blast+impact group. *p<0.05, ****p< 0.0001. Data represented as Mean ± SEM.

6.3.4 Evidence of microglia activation in the MC varied across experimental groups

Significant changes in area/cell of microglia were observed in the MC following blast+impact injury (F (3, 33) = 4.187, p=0.01). More specifically, post hoc tests indicated a significant increase in area/cell in the blast+impact group compared to shams (p=0.05), and the impact-only group compared to shams (p=0.003). A trending decrease in area/cell was observed between the blast+impact group and the impact-only group (p=0.09). A significant reduction in the number IBA-1+ microglia (count per area) was found when comparing the blast-only group to shams (p=0.04). This decrease was also found to be trending between the blast only and blast+impact group (p=0.06). Increases in IBA-1 expression (fluorescent intensity) were observed within the MC of the impact-only group compared to shams (p=0.03). A trending increase in fluorescent intensity was observed between the blast+impact group and the blast-only group

(p=0.08). No other significant differences among groups were found for this parameter. Moreover, no significant differences between groups for area fraction were observed (Fig. 60).

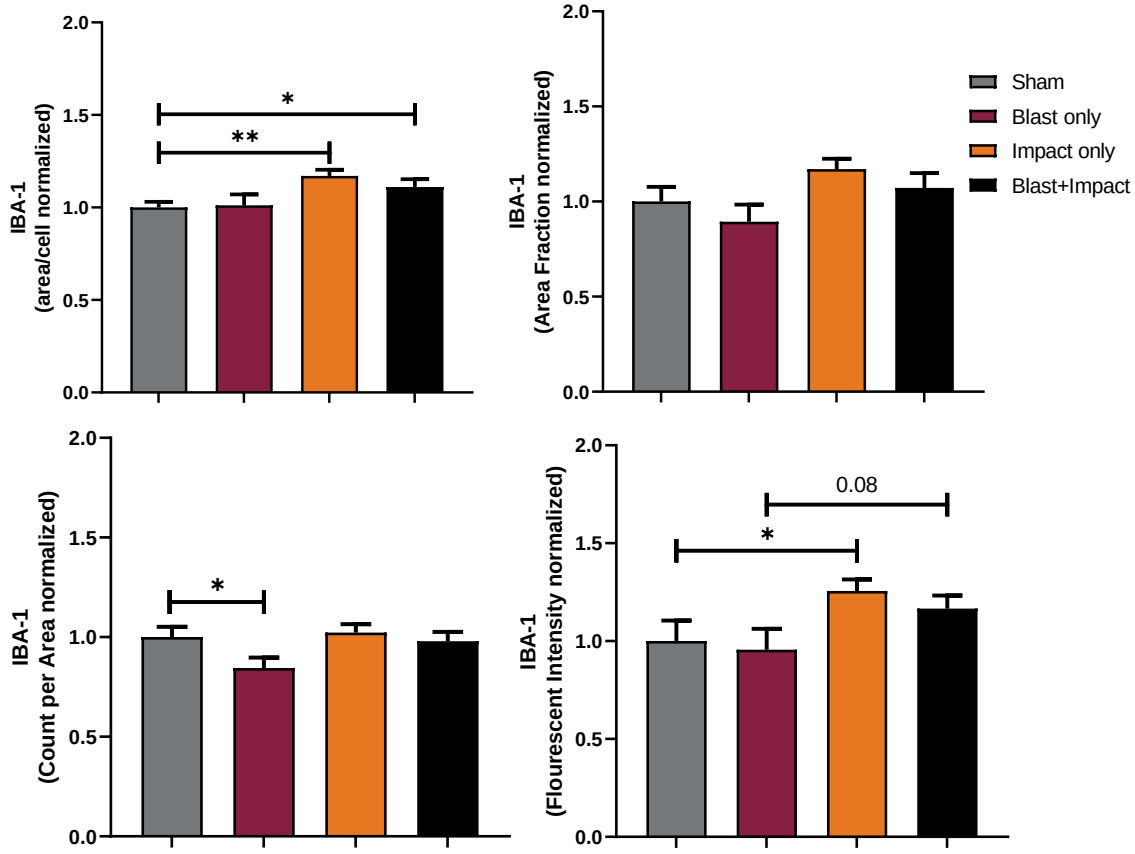

Figure 60. Microglia activation were observed in the MC across injury groups. A significant increase in area/cell was observed in the blast+impact group compared to shams, as well as the impact-only group compared to shams. A significant decrease in count per area was observed in the blast-only group compared to shams. For fluorescent intensity, a significant increase was observed in the impact-only group compared to shams, with this increase found to be trending in the blast+impact group. *p<0.05, **p<0.01. Data represented as Mean ± SEM.

6.3.5 Changes in microglia morphology within the MC were detected across all groups

Skeleton analysis indicated changes in microglia morphology within the MC following injury (F (3, 32) = 3.209, p=0.03) (Fig. 61). More specifically, significant decreases in branch length/cell were observed when comparing the blast+impact group to shams (p=0.01), the blast-only group to shams (p=0.02), as well as the impact-only group to shams (p=0.02). No significant

differences were found between the blast+impact, blast-only, and impact-only groups. A trending decrease in branch points/cell was found within the blast+impact group compared to shams, but no other significant or trending differences were observed between any other group (Fig. 62).

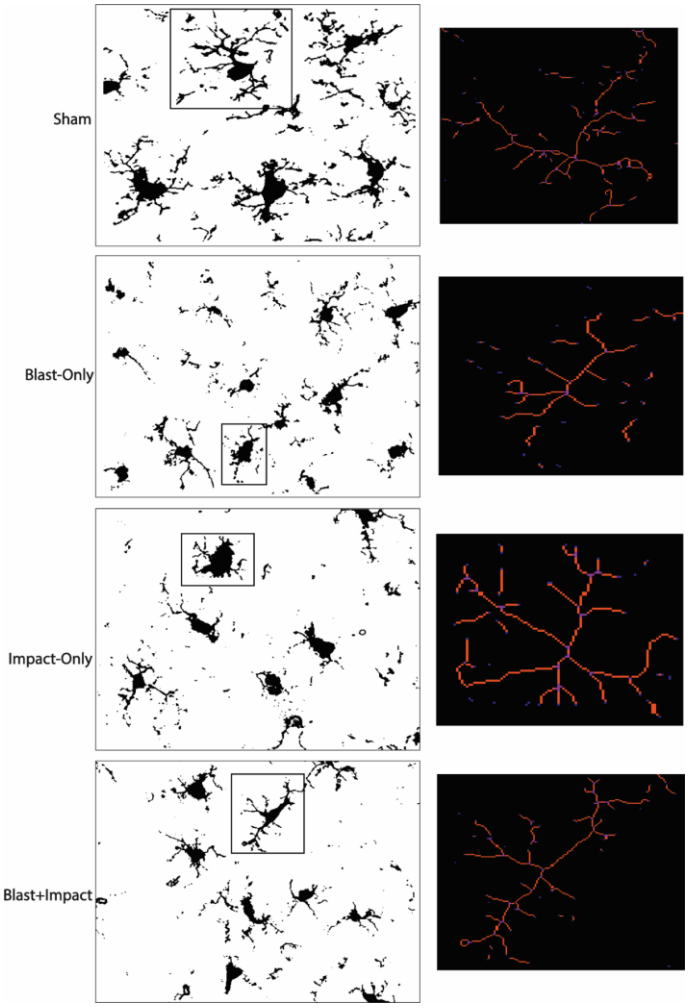

Figure 61. Representative images showing changes in microglia morphology across groups. Fluorescent images were skeletonized, with analysis indicating decreases in branch length of microglia in the blast-only, impact-only, and blast+impact groups' compared to shams.

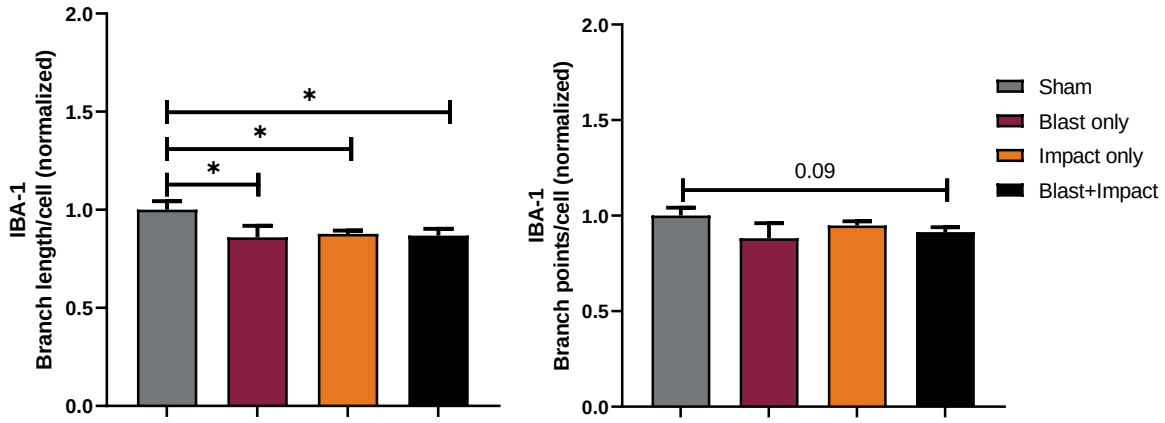

Figure 62. Changes in microglial morphology were found in the MC following blast+impact injury. A significant decrease in branch length/cell was observed in the blast+impact group, blast-only, and impact-only group compared to sham. A trending increase in branch points/cell was found in the blast+impact group compared to the sham group. *p<0.05. Data represented as Mean ± SEM.

6.3.6 Changes in microglia size were notable in the hippocampus following blast+impact injury

Within the DG, significant changes in area/cell was observed ($F(3, 32) = 3.507$, $p=0.02$). Post hoc tests indicated a significant increase in area/cell when comparing the blast+impact group to shams ($p=0.003$), with a significant increase also observed in the blast-only animals compared to shams ($p=0.04$), and the impact-only group compared to shams ($p=0.05$). These significant differences were also observed within the CA1 ($F(3, 32) = 4.518$, $p=0.0094$). More specifically, a significant increase in area/cell of microglia was found when comparing the blast+impact group to shams ($p=0.005$). A significant increase in area/cell was also observed in the blast-only group compared to shams ($p=0.009$) and the impact-only group compared to shams ($p=0.003$). Within the CA2, significant changes were found ($F(3, 30) = 3.336$, $p=0.03$), with significant increases in area/cell between the blast+impact group and shams ($p=0.004$). The CA3 sub-region also indicated differences, with a significant increase in area/cell found in the blast+impact group compared to shams. No significant differences in area/cell were found between blast+impact, blast only, and/or impact only groups in the hippocampus (Fig. 63).

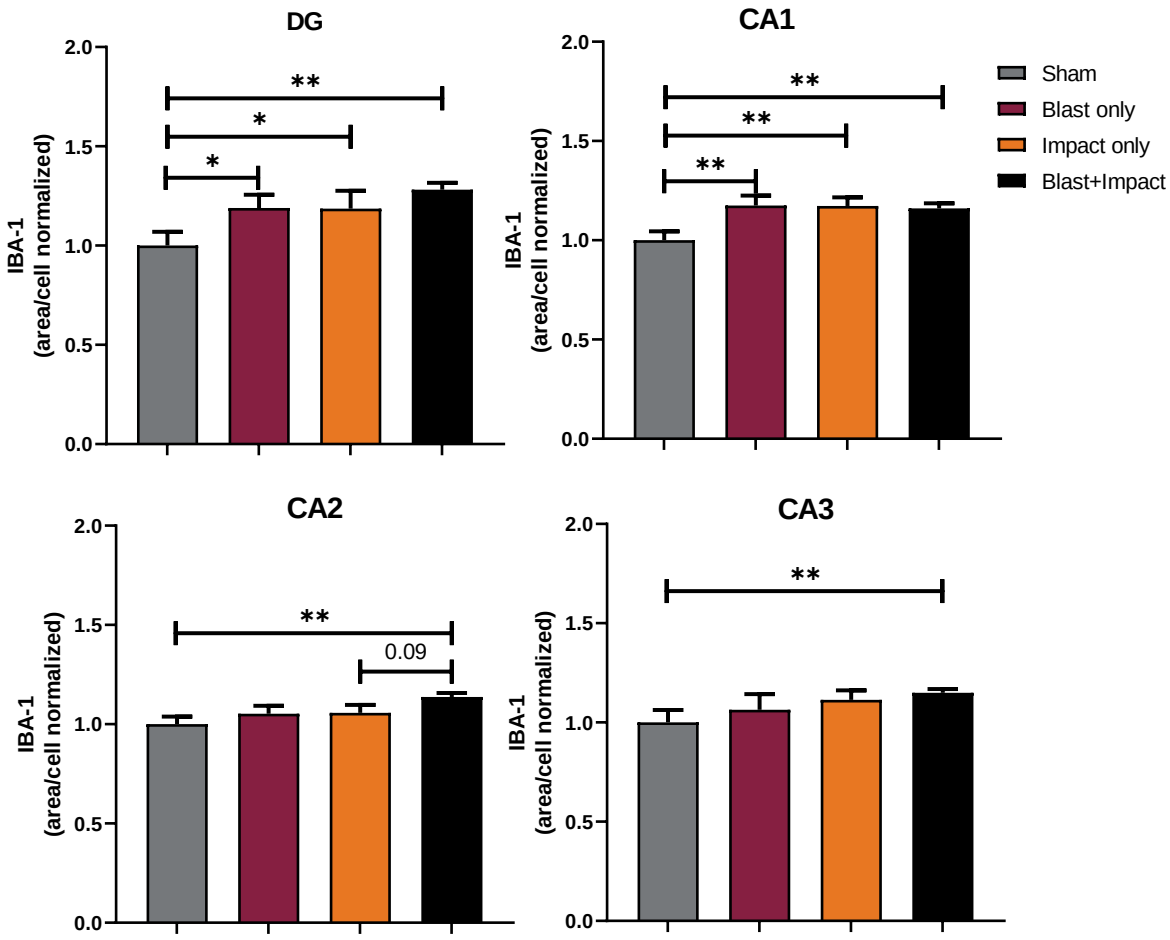

Figure 63. Blast and Impact injury led to microglia activation within the hippocampus. In the DG and CA1, a significant increase in area/cell was observed in the blast+impact, blast-only, and impact-only groups compared to shams. In the CA2 and CA3, a significant increase was observed in the blast+impact group compared to shams. *p<0.05, **p<0.01. Data represented as Mean ± SEM.

6.3.7 Limited changes in IBA-1 positive signal was observed in the hippocampus

A one-way ANOVA indicated significant changes in the CA3 sub-region of the hippocampus ($F(3, 31) = 3.877$, $p=0.0183$), with a significant increase in area faction observed in the CA3 of the blast+impact group compared to shams ($p=0.003$). While no significant changes in area fraction were observed in any of the other sub-regions, trending increases in area fraction

were observed in the CA1 in the blast-only group compared to shams (p=0.07), and a trending increase in the CA2 of the blast+impact group compared to the blast-only group (Fig. 64).

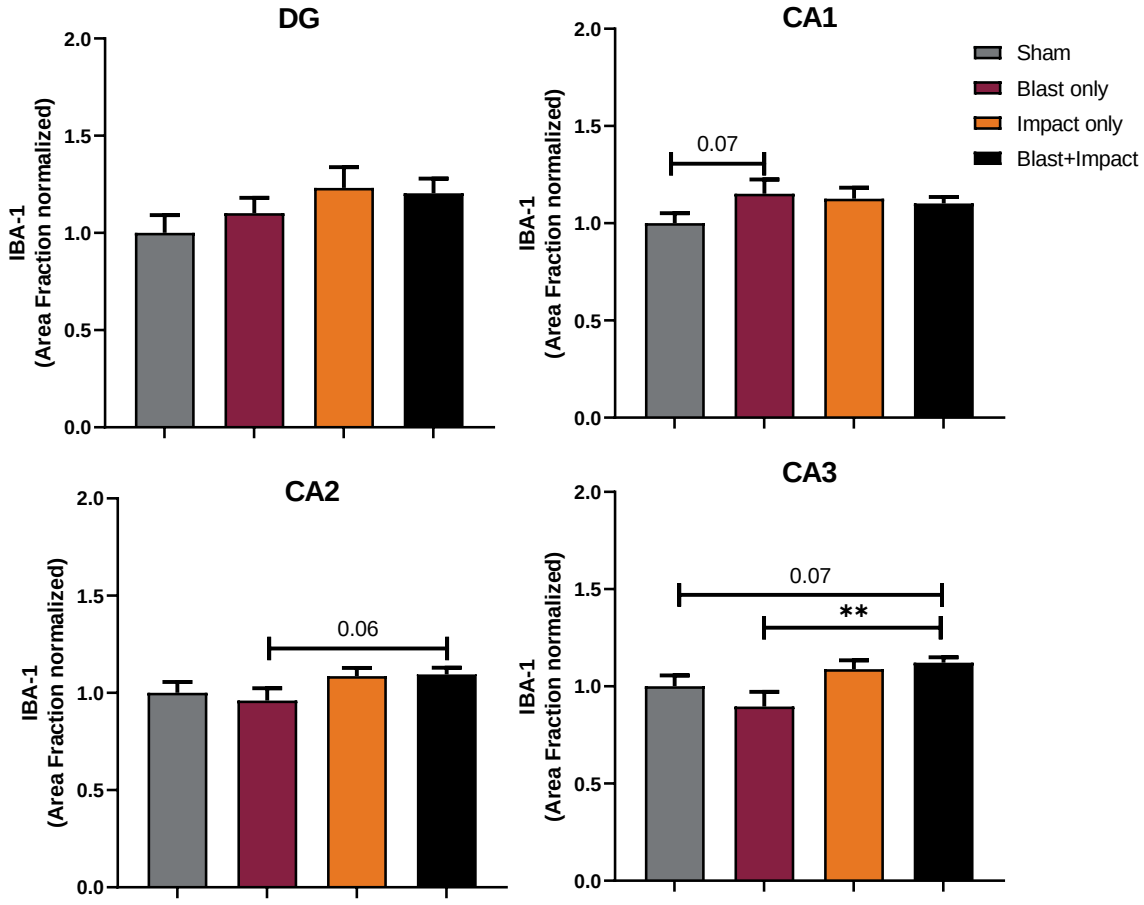

Figure 64. Limited changes in the amount of IBA-1 positive signal were observed in the hippocampus following blast+impact injury. In the CA3, a significant increase in area fraction was observed in the blast+impact group compared to the blast-only group. No significant differences were found amongst the injury groups for any other sub-region. **p<0.01. Data represented as Mean ± SEM.

6.3.8 Blast+Impact injury did not lead to changes in the number of microglia in the hippocampus

Limited changes in the number of IBA-1+ microglia (count per area) were found amongst injury groups. More specifically, no significant differences were observed in any of the sub-regions of the hippocampus (Fig. 65).

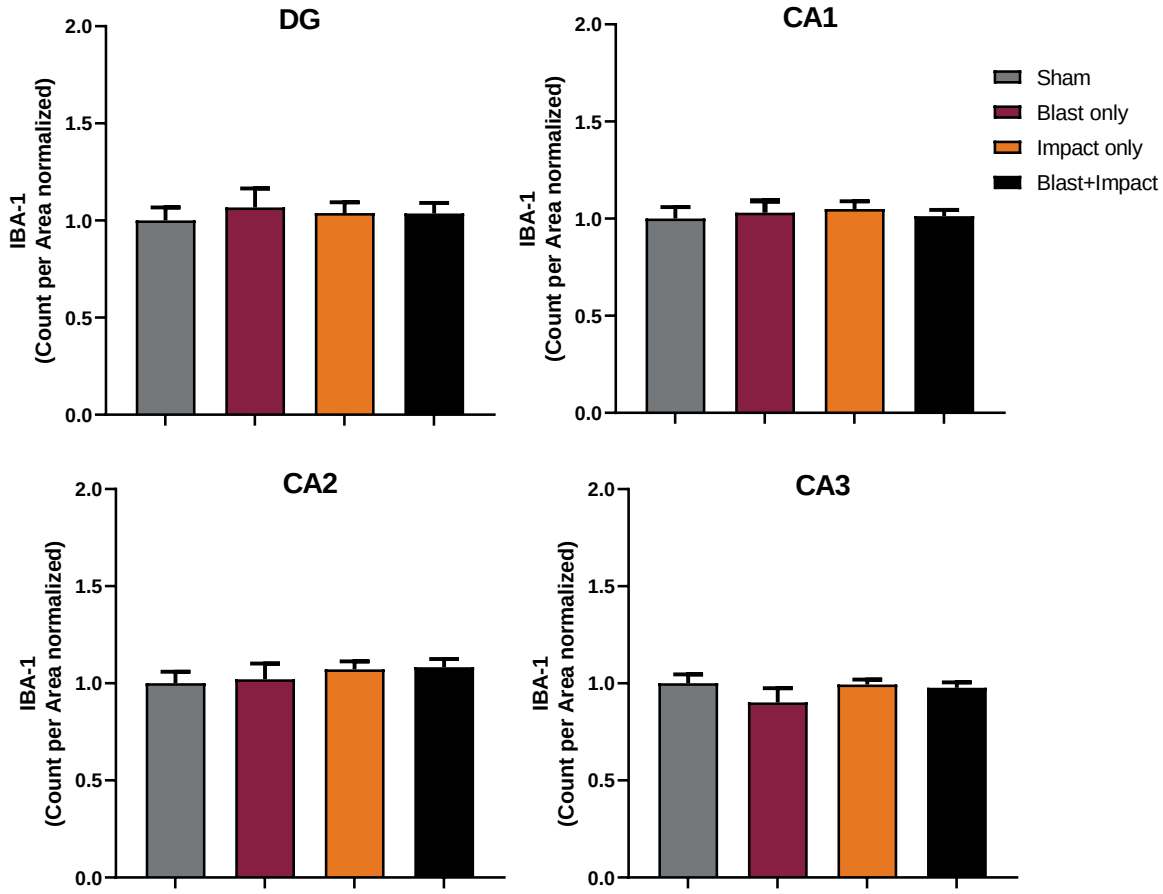

Figure 65. Blast+impact injury did not lead to changes in microglia populations. No significant differences in count per area were observed in any of the injury groups in the hippocampus. Data represented as Mean ± SEM.

6.3.9 Changes in IBA-1 expression within the hippocampus are limited across injury groups

A one-way ANOVA exhibited significant differences within the CA3 sub-region of the hippocampus ($F(3, 30) = 4.008$, $p=0.01$). Moreover, a significant increase in fluorescent intensity was found in the CA3 of the blast+impact group compared to the blast-only group ($p=0.0023$). A trending decrease in fluorescent intensity was observed when comparing the blast-only group to shams ($p=0.06$). No significant differences were observed between other groups or sub-regions (Fig. 66).

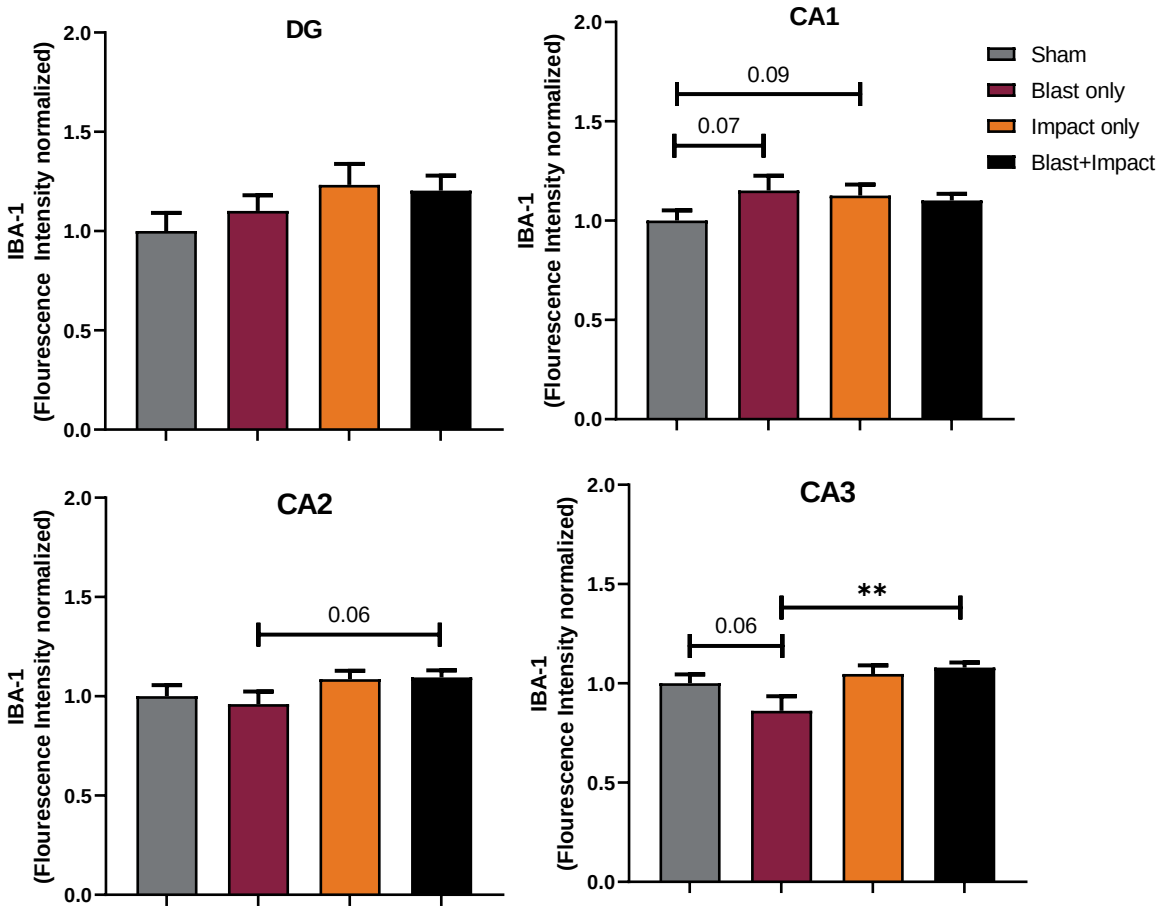

Figure 66. Blast+impact injury led to sub-region-specific changes in IBA-1 expression. A significant increase in fluorescent intensity was observed in the CA3 of the blast+impact group compared to the blast-only group. A trending decrease in fluorescent intensity was found in the blast-only group compared to shams. Trending differences were observed in the CA1 and CA2 sub-regions across injury groups, but the differences were not found to be significant. **p<0.01. Data represented as Mean ± SEM.

6.3.1.0 Changes in microglia morphology were prevalent in the hippocampus

Morphological analysis of microglia indicated a significant change in both branch/length and branch points/cell in the hippocampus. Within the DG sub-region, changes in branch length/cell were found ($F(3, 32) = 3.358$, $p=0.03$), with a significant decrease in branch length/cell observed in the DG of the blast-only group compared to shams ($p=0.01$), and the blast-only group compared to the blast+impact group ($p=0.006$). A trending increase in branch points/cell was found in the DG of the impact-only group compared to shams ($p=0.09$) (Fig. 67).

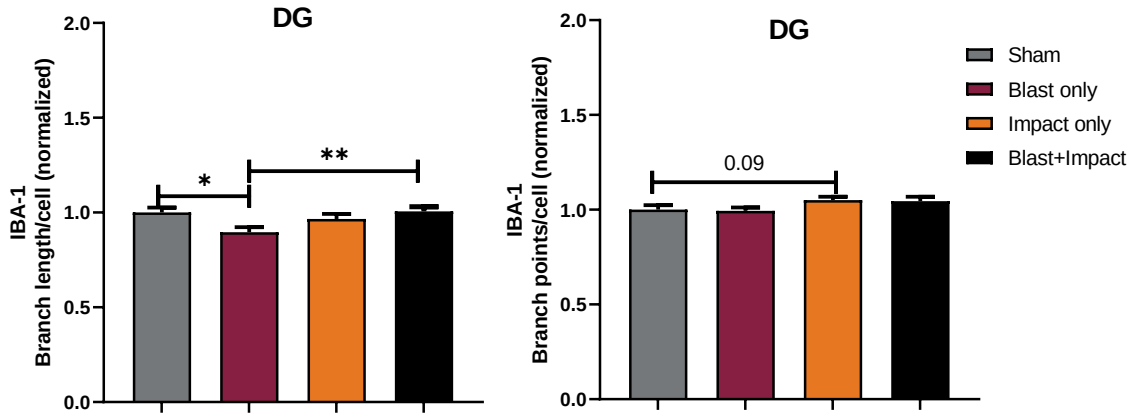

Figure 67. Blast exposure led to changes in microglia morphology within the DG. A significant decrease in branch length/cell was observed in the blast-only group compared to shams and the blast+impact groups. A trending increase in branch points/cell was found in the impact-only group compared to the sham group. *p<0.05, **p<0.01. Data represented as Mean ± SEM.

In the CA1 sub-region, a significant decrease in branch length/cell was found in the blast+impact group compared to shams (p=0.04) and the blast-only group compared to shams (p=0.04). No significant differences were observed in the impact-only group compared to shams. Branch points/cell indicated a significant decrease in the blast+impact group compared to their sham counterparts (p=0.04), and this significant decrease was also observed in the blast+impact group compared to the impact-only group (Fig. 68-69).

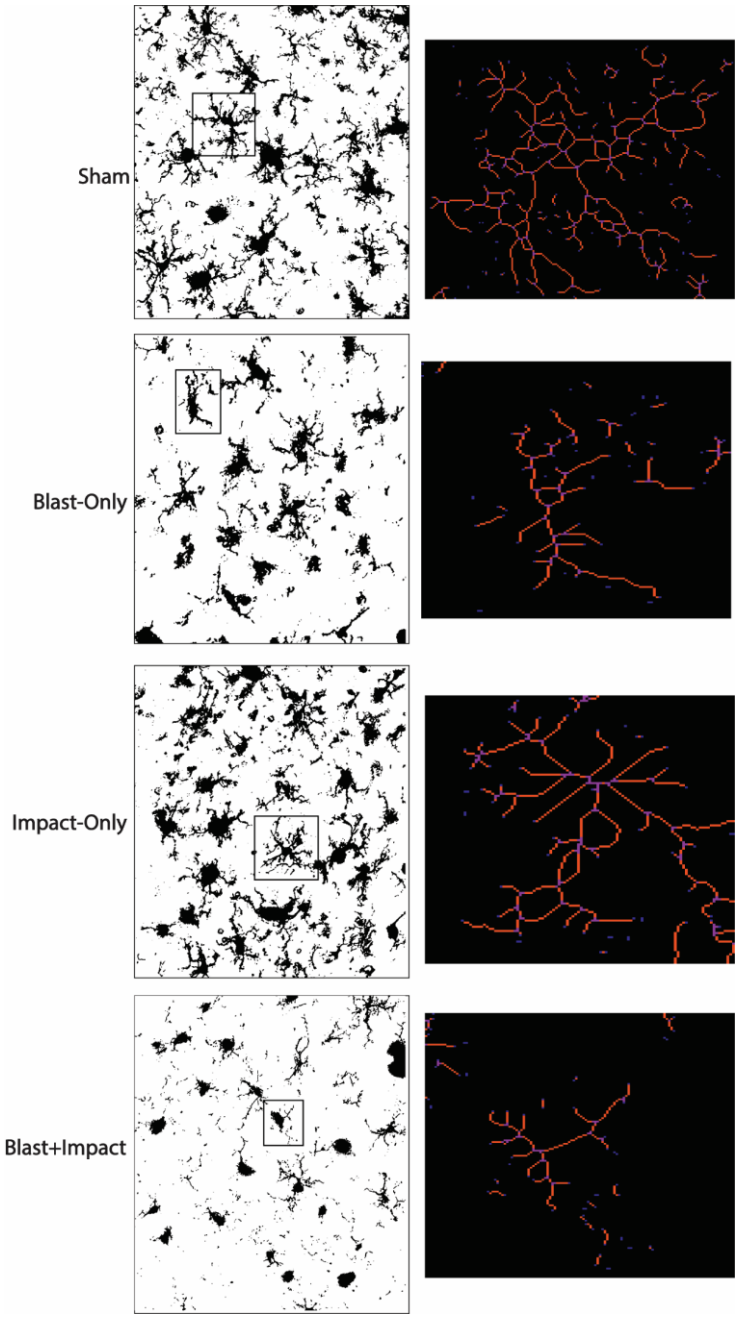

Figure 68. Morphological changes in microglia were present within the CA1 sub-region of the hippocampus in the blast-only and blast+impact groups. Representative images depict decreased branch-length in blast-only and blast+impact groups, with limited branching observed in blast+impact animals.

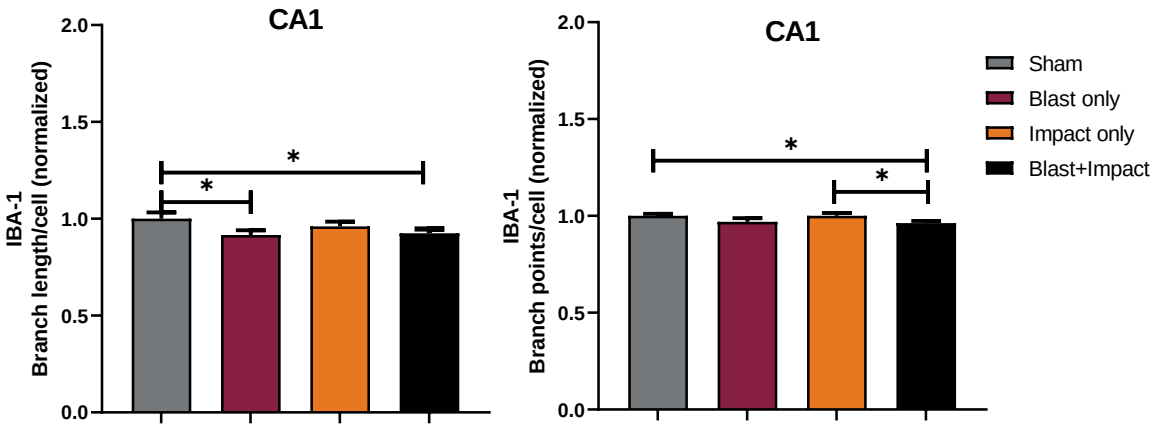

Figure 69. Notable phenotypic changes in microglia were observed in the CA1 following injury. A significant decrease in branch length/cell was observed in the blast-only group compared to shams and the blast+impact group compared to shams. A significant decrease in branch points/cell was observed in the blast+impact group compared to shams, as well as compared to the impact-only group.*$p<0.05$. Data represented as Mean ± SEM.

Furthermore, in the CA2, a significant decrease in branch length/cell was found in the blast+impact group compared to shams ($p=0.01$), the blast-only group compared to shams ($p=0.03$), as well as the impact-only group compared to shams ($p=0.01$). A significant decrease in branch points/cell was also observed in the impact-only group compared to shams within the CA2 ($p=0.03$), with this decrease trending in the blast+impact group compared to shams ($p=0.09$) (Fig. 70).

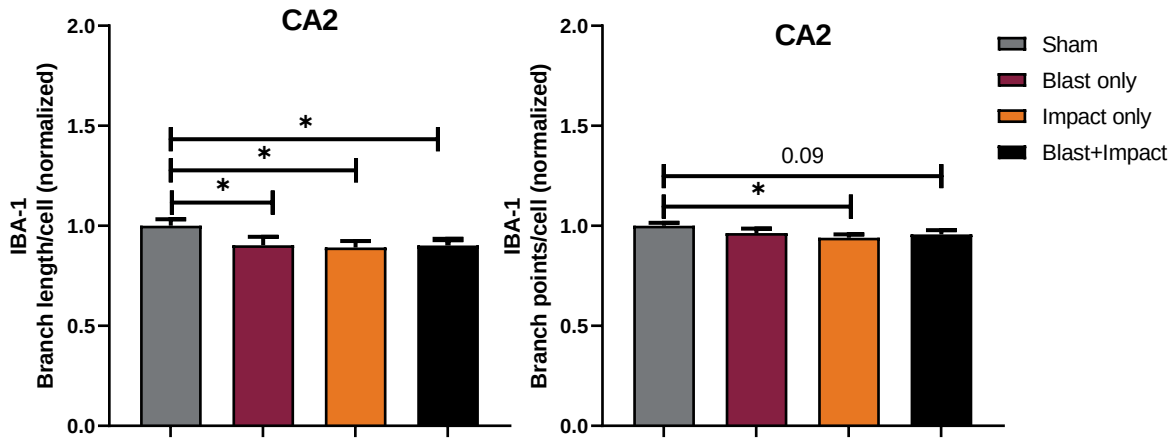

Figure 70. Unique phenotypic changes in microglia were observed in the CA2 following injury. A significant decrease in branch length/cell was observed blast+impact group, blast-only group, and impact-only group compared to shams. A significant decrease in branch points/cell was observed in the impact-only group compared to shams, with this decrease found to be trending in the blast+impact group when compared to the sham group. *p<0.05. Data represented as Mean ± SEM.

Finally, skeleton analysis indicated no significant differences in branch length/cell or branch points/cell between any of the groups in the CA3 sub-region of the hippocampus (Fig. 71).

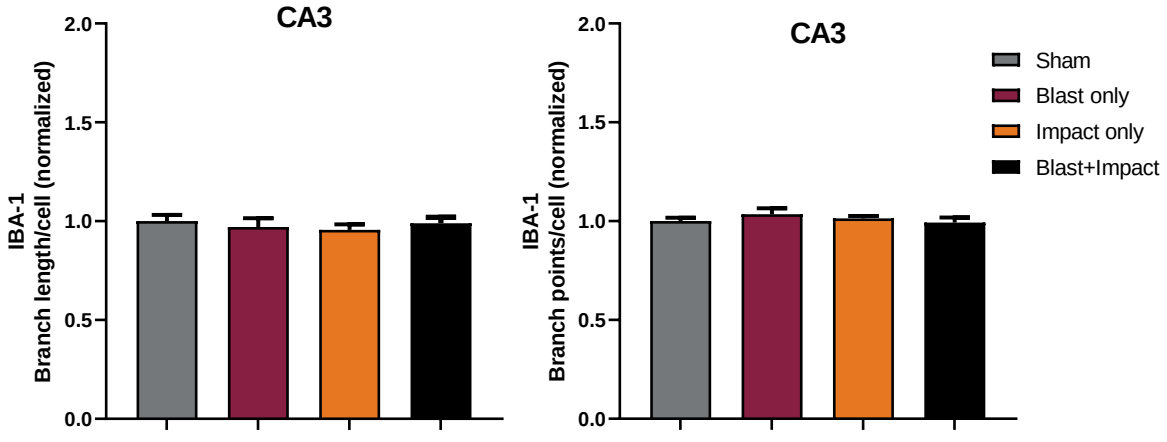

Figure 71. No changes in microglia morphology were observed in the CA3. Data represented as Mean ± SEM.

6.4 Discussion

Mild forms of bTBI are prevalent among military personnel and Veterans following high combat situations, with reports of this injury altering mental status, with no "outwardly" signs of injury such as loss of consciousness. Because of this, many personnel return to combat, which increases their susceptibility to repeated bTBIs. Growing concerns of exposure to multiple low-level blasts during military training also contribute to concussive deficits, with reports of repeated blast exposure leading to chronic issues such as memory deficits, anxiety, and increased risk-taking behaviors. Once returning home, Veterans are at a greater risk of subsequent concussions, which may be associated with an increased risk of disinhibition.[343] The "blast plus" complex, which refers to the frequent head injury where exposure to blast proceeds other traumas such as impact or penetrating injuries, has been speculated within military populations. Still, there is a lack of evidence-based research that confirms that exposure to a blast event predisposes the brain to neuropathological deficits that influence subsequent TBI outcomes. In the current study, we aimed to characterize the "blast plus impact" condition to identify whether there is increased susceptibility to pathological changes associated with microglia dynamics within the brain following repeated blast exposure. Animals were subjected to three repetitive blast events with an inter-blast interval of one hour each, and then two weeks later were subjected to a closed-head controlled cortical impact. Through pathological assessments, microglia activation was observed within the somatosensory and motor cortices, as well as the hippocampus following blast+impact injury. We have previously established the pathological differences within a repeated mild bTBI model (Chapter 3) and concussion (Chapter 4). Microglial activation was observed in both models, with morphological analysis indicating that the onset of activated microglia phenotypes varies within the SC, MC, and hippocampus across each injury modality.

To our knowledge, a study by Aravind et al. is the only other study to test whether blast injury predisposes the brain to increased neurological deficits in a rodent model of blast plus TBI.[348] The research design of the combined blast plus impact injury of their study involved animals being exposed to a single blast insult with a craniotomy performed immediately afterward to prepare for FPI, an impact injury that was produced 24 hours later. While their research design did not examine microglial responses following this complex injury, they found increased neurodegeneration at both acute and chronic time points in the hippocampus of their blast plus blunt TBI group, suggesting that the blast injury predisposed the brain to increased deficits

following a subsequent TBI. In the current study, microglia become activated which could be in response to neuronal dysfunction present within the brain of blast+impact animals. Moreover, increases in area/cell of microglia were found in the blast+impact and impact only group compared to shams in the MC and SC, with these same increases observed in all sub-regions of the hippocampus in the blast+impact, impact only, and blast only groups. Results in the comparative study showed vast increases in neurological deficits in the blast+impact compared to blast- and impact-only injuries, whereas results from the present study showed incremental changes between injury groups, making it difficult to predict whether the blast predisposed the brain to increased deficits. While the results from our study differed, there were vast differences in the experimental design that could have influenced variations in results. The lack of the previous study investigating microglia responses, as they are essential in neuropathology following TBI, emphasizes the novelty of the present study, as the investigation of microglia-mediated responses following blast plus impact has yet to be accomplished.

One unique feature of this study was identifying the morphological changes in the blast+impact injury group compared to shams, blast-only, and impact-only groups. In Chapter 3, animals subjected to repeated blast exposure showed subacute changes in microglia morphology within the hippocampus. Changes in microglial morphology (↓area/cell, ↑ branch length/cell, and ↑ endpoint/cell) in the hippocampus resembled dystrophic phenotypes often associated with activated microglia, with no significant changes observed in the MC. In Chapter 4, acute changes in microglia morphology resembled microglia that are associated with stressed/primed microglia (↑ branch length/cell, ↑ branch points/cell) in the MC, and microglia with increased branch points/cell were found within the hippocampus, yet no significant changes were observed within the SC. In the present study, decreases in branch length/cell were found within the SC of the blast+impact group, suggesting that diverse morphologies in the SC of the blast+impact group are contributed by pathological changes associated with both injury modalities. Moreover, increases in branch length/cell were found in the MC of all injury groups compared to shams, showing that microglia changes may be more dependent on time in this region rather than an "injury frequency" effect. Significant increases in area/cell and decreases in branch length/cell within the SC and MC of the blast+impact and impact-only group, may indicate that microglia are starting to develop a more amoeboid-like morphology, which is characterized by a swelling soma and retraction of processes. As this is only seen within the blast+impact and impact-only groups in the SC and MC,

this may indicate that impact injury and time may be what is driving this specific microglia phenotype in "blast plus" injuries.

Numerous studies have identified that the hippocampus is vulnerable to blast injury, with the high-speed compression of the blast wave leading to shear stress between fluid and tissue interfaces. More specifically, brain tissue at interfaces with fluid, such as those that border cerebrospinal-fluid-filled ventricles or blood-filled sinuses, such as the hippocampus, are thought to be particularly susceptible to primary blast injury.[72,219] Additionally, blast research has indicated significant changes in microglia activity within the hippocampus that have persisted past seven days.[219,350] Because of this, blast injury could increase vulnerability to secondary injury responses within the hippocampus in a blast+impact model. In the hippocampus, area/cell of microglia was increased within the hippocampus in blast+impact, blast-only, and impact-only groups compared to shams, with this increase found to be greater within the blast+impact group compared to blast- and impact-only groups. These results may contribute to the hypothesis that repeated blast exposure may cause susceptibility to additional TBIs, with the hippocampus a major region at play when characterizing blast plus injuries. Additionally, increases in IBA-1 expression (area fraction and fluorescent intensity) were found in blast+impact animals in the CA3 sub-region compared to the blast-only group. This may be linked to differences in intrinsic and extrinsic factors influencing microglial activation between blast and impact injuries. While blast exposure may have contributed to changes in IBA-1 expression, the addition of impact injury may have caused an upregulation in IBA-1 that is seen in the blast+impact group compared to the blast-only group.

As mentioned previously, quantification of microglia morphology in previous chapters indicated subacute phenotypes in repeat bTBI animals that resemble dystrophic microglia in the hippocampus. In contrast, a unique phenotype of microglia (↑ branch points/cell) that is associated with anti-inflammatory properties, and increases in β-integrin, are found within the hippocampus of impact animals at acute stages of injury. Morphological analysis of microglia within the present study indicated dynamic changes that take place within the hippocampus, with blast+impact animals resembling morphologies similar to the impact-only group within the DG, while microglia seem to take on a more amoeboid morphology (↑ area/cell, ↓ branch length/cell, ↓ branch points/cell) in both the blast-only and blast+impact groups in the CA1 and CA2 sub-regions. A study by Hernandez et al. found that mild blast forces have induced biochemical changes within neurons seven days following bTBI, driving pro-inflammation.[68] As described in section 2.5,

microglia that become more amoeboid-like have been associated with pro-inflammatory, phagocytic phenotypes, responding to cellular debris such as dying cells and fragmented dendrites. This may explain why amoeboid-like morphologies are present following this injury. Dynamic responses in the hippocampus of the blast+impact group that resembles changes within the blast-only group may also suggest that while injury frequency may affect microglia responses, the type of TBI and the secondary injury mechanisms accompanying that injury is heterogeneous across regions. It is complicated to claim that repeated blast exposure predisposes the brain to increased pathological changes in blast+impact TBI.

Future studies will need to explore blast+impact injuries further by characterizing microglia pathology at different time points, such as varying the time between injuries. For example, future studies can expose the animals to blast injury, and then 24 hours later, animals are subjected to cCCI. Furthermore, having the study carried out further, such as looking at more chronic microglia outcomes following blast plus impact, may provide more insights into this complex injury. Advancing characterization of the autonomous response of microglia, such as genomics and proteomics of isolated microglia following blast+impact, blast-only, and impact-only TBI, may also lead to understanding the underlying molecular changes that vary between injury modalities that may dominate in specific regions within the blast+impact TBI model. Additionally, identifying the spatiotemporal response of processes such as apoptosis, oxidative stress, BBB permeability, and neurodegeneration should be investigated.

As clinical reports have indicated cognitive and behavioral deficits such as memory loss, anxiety, depression, and risk-taking behaviors in Veterans who return home, behavioral assessments such as open field thigmotaxis, novel object recognition, and the three-chamber test, to name a few,[206,232,351,352] would be critical in the robust analysis of outcomes that blast+impact TBI may have. Overall, this is the first study to explore a blast+impact model that includes repeated blast exposure, which is resembled in military training and combat, accompanied by a closed head cCCI, a subsequent TBI that could occur when Veterans return home. This study aids in generating relevant preclinical knowledge that can lead to developing strategies to improve and mitigate TBI outcomes that plague the Veteran community.

Chapter 7: PEGylated Polyester Nanoparticles Alleviate Microglia Pathology Following Impact-Induced Neurotrauma

This data is a result of collaboration with Dr. Erin Lavik's lab at University of Maryland, Baltimore County. The nanoparticles and treatments were synthesized and developed by Dr. Nuzhat Maisha and other collaborators within the Lavik Lab.

7.1. Introduction

Microglia are at the forefront of the secondary injury response following TBI, having both a neuroprotective and neurotoxic role that can persist for days and even weeks following injury. As TBI is a leading cause of mortality and disability worldwide, it is essential to assess strategies that can aid in mediating microglial activation, thus improving TBI outcomes.

To date, no treatment strategies for TBI have made it past phase 3 clinical trials, and few have focused on targeting and analyzing the mechanistic changes of microglia in response to treatment.[353–356] Hemostatic nanoparticles are one treatment that may be effective in mediating microglial activation. Hemostatic nanoparticles (HNPs) were initially created to stop bleeding following polytrauma, and PLGA-PEG synthesized hemostatic nanoparticles have even been used to treat blast TBI *in vivo*.[232,357,358] While these steps have been influential in pioneering the research of therapeutic strategies for blast TBI, it is vital to continue exploring microglia-specific changes, especially as functional properties of activated microglia may differ in TBI caused by impact versus blast. When investigating strategies that can aid in mitigating TBI pathology, it is crucial to continue to characterize therapeutic strategies for their translation to clinical settings. For example, Poly (lactic acid)-b-poly(ethylene glycol) (PLA-PEG) specific HNPs have proven advantageous because PLA-PEG properties include higher glass transition temperatures and core stability, making it possible to store in extreme temperatures.[359] This modified nanoparticle structure allows for survival in varying environments aiding in long-term storage (-80^{o}C) and swift availability in the field, while remaining safe to use ($\leq$ 50^{o}C).

The functional properties of HNPs include conjugation with a specific peptide (GRGDS) that binds with activated platelets via the glycoprotein IIb/IIIa receptor, promoting coagulation, and decreasing clot formation time following trauma.[358] For example, consequences of TBI can be injury to the vasculature such as hemorrhage and BBB dysfunction. Changes in vascularization can lead to the recruitment of platelets that can aggregate on vascular walls, leading to platelet plug formation. Platelet plug formation can then induce microthrombus and if unregulated, microvascular dysfunction.[360] Research shows that molecules such as CD40L are released from platelets, activating the MAP-K and NF-κB pathways.[361,362] Platelets also secrete inflammatory signals such as RANTES, recruiting macrophages and neutrophils, increasing inflammatory cascades that microglia are essentially involved in (Fig. 72).[363] As HNPs aid in increasing clot

formation through interactions of platelets involved in these inflammatory responses, this may play a role in microglia activation following TBI.

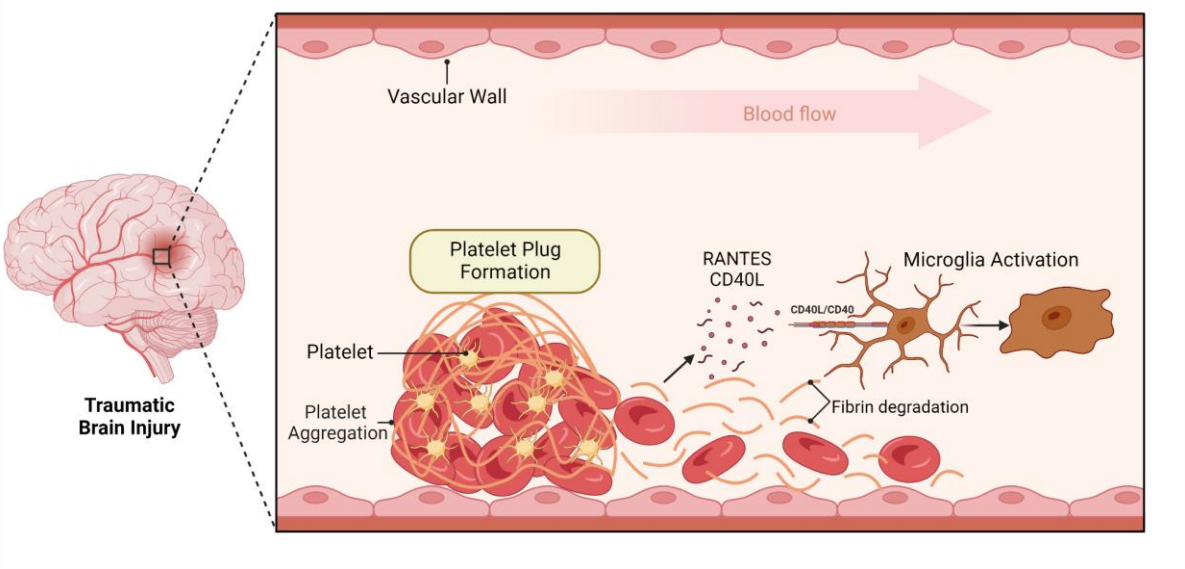

Figure 72. Platelet plug formation can induce microglia activation following TBI. Following injury, changes to the vasculature can cause the recruitment of platelets through the BBB, forming what is known as a platelet plug. Platelets can then release molecules that binds to receptors on microglia, signaling pathways that influence inflammatory responses within microglia. Created with BioRender.com.

As glial-driven pathology in the brain is linked to sequelae such as anxiety, depression, vestibulomotor deficits, and cognitive impairments, understanding if HNPs can alleviate microglia-induced inflammatory responses may assist in creating personalized treatments for patients suffering from a TBI. Furthermore, the use of HNPs has not been explored in a closed-head CCI model, which increases the innovation of the study. Also, as previously described, microglia dynamics may differ across injury modalities, so it is imperative to investigate whether HNPs can mediate microglial activation in this model.

Studies have indicated that BBB disruption following impact trauma can lead to platelet plug formation, even in mild TBI; thus, we explored whether HNPs affect inflammatory cascades, mitigating microglia pathology following TBI. It is hypothesized that intravenous administration of HNPs will reduce subacute microglia activation by restoring levels of microglia to pre-injury levels.

7.2. Methods

HNPs were designed, synthesized and characterized by Dr. Erin Lavik's lab. The procedures outlined below are adapted from their publication, Maisha et al. 2022.[364]

7.2.1 Nanoparticle Synthesis

The ring-opening polymerization procedure was used to create block copolymers of Poly (lactic acid)-b-Poly(ethylene glycol) (PLA-PEG) with either 3400 or 5000Da PEG. Co-isomers Poly(L-lactic acid)-b-poly(ethylene glycol) (PLLA-b-PEG5000) and Poly(D-lactic acid)-b-poly(ethylene glycol) (PDLA-b-PEG3400) were used to create the nanoparticles using nanoprecipitation. The weight ratio for the polymers was 3:1, with the control and hemostatic nanoparticles made using 90 mg of PLLA-b-PEG5000 and 30 mg of PDLA-b-PEG3400. The phosphate-buffered saline was doubled in volume, and the polymer was dissolved in the organic phase, Tetrahydrofuran (THF), at a concentration of 20 mg/ml and stir-hardened to produce the nanoparticles. Excess THF was removed by exposing it to air after 3 hours of stir hardening, and poloxamer was added as the stabilizer. After being separated by centrifugation at 4000xg for 10 minutes at 4°C, the nanoparticles were resuspended in phosphate-buffered saline. Dynamic light scattering was used to characterize the particles to calculate their hydrodynamic diameter and zeta potential for nanoparticles in diluted potassium chloride solution (10mM). The degree of PEGylation was also assessed using 1H-NMR.

7.2.2 A Coupling Reaction Generates Targeted HNPs

GRGDS, the target peptide, was coupled to the block copolymer PLLA-b-PEG5000 using NHS/EDC conjugation. Moreover, the NHS/EDC based conjugation uses the carboxyl end of the bi-functional PEG and results in coupling with the amine end of the peptide GRGDS. First, 4mL of DCM was used to dissolve 300g of the PLA-b-PEG block copolymer. To create an amine-reactive NHS-ester, 12 mg NHS and 10 mg EDC was dissolved in DMSO. After 60 minutes of reaction time, any extra DCM was removed by exposing it to air. The polymer was dissolved in methanol, precipitated, and collected by centrifugation at 4000 rpm for 5 minutes. It was then lyophilized the next day. In 3mL of DCM, the lyophilized intermediate product was dissolved, and then 8mg of the peptide was dissolved in 1.5 mL of DSMO and added to the mixture. After 24

hours of reaction time, the excess DCM was removed by air exposure, and the polymer was precipitated in methanol. Centrifugation at 4000 rpm for 5 minutes was used to collect the precipitated PLLA-b-PEG-GRGS, which was then lyophilized. The PLA-PEG-GRGDS system's hemostatic ability is decreased by inhibiting the glycoprotein IIb/IIIa receptor, which in turn inhibits the GRGDS peptide's ability to connect with the glycoprotein IIb/IIIa receptor on active platelets. Due to this, there are two types of nanoparticles in this study: control nanoparticles made of PLA-PEG and hemostatic nanoparticles made of PLA-PEG with GRGDS attached.

7.2.3 OPA Assay to Measure Peptide Density

An o-phthalaldehyde (OPA) assay, which produces fluorescence when free amines are present, was used to validate the presence of the peptide in the nanoparticles. Then, 20uL of DMSO-dissolved nanoparticles were combined with 200uL of OPA reagent and thoroughly blended. Using an excitation wavelength of 340 nm and an emission wavelength of 455 nm, the fluorescence was measured after 15 minutes of incubation in the dark. Once characterized, nanoparticles were transported to Virginia Tech on dry ice, and stored at -80C until further use.

7.2.4 Animal Procedures and Experimental Design

The Virginia Tech Institutional Animal Care and Use Committee approved the experimental protocols described herein. Male Sprague Dawley rats (~300 g, Envigo, Dublin, VA, USA) were acclimated for several days (12 h light/dark cycle) with food and water provided *ab libitum.* Animals were subjected to a cCCI, with the impactor (tip diameter: 5 mm) creating a force at a velocity of 6 m/s, at a depth of 3 mm, and a dwell time of 1.5 ms (Impact One, Leica Biosystems, Buffalo Grove, IL). Animals were then placed on a heating pad at 37ºC, monitored, and righting time was recorded. Sham animals went through all the same procedures except for the impact. Once animals righted, they were briefly placed under anesthesia again and were then randomly assigned to one of three treatments groups with both cCCI (n=6) and sham (n=6) within each group: Saline, control nanoparticles (CNPs), and hemostatic nanoparticles (HNPs). Nanoparticles were then thawed to room temperature (no heat treatment used to thaw), and vortexed five times for five seconds. Once the nanoparticle solution was uniform, with no aggregation of nanoparticles visible, animals were administered 500 uL of either HNPs or CNPs (20 mg/mL).

7.2.5 Tissue Processing and Analysis

Seven days following injury, animals were euthanized; brains were collected and then stained for IBA-1 as previously described in Section 3.2.2. The ipsilateral and contralateral sides of the SC were regions of interest in identifying microglia activation (-3.00 mm posterior from Bregma). Tissue sections were then imaged and analyzed as described in Section 3.2.3, with the parameters mean area/cell, area fraction, count per area, and fluorescent intensity used to understand overall changes in microglia activity in response to nanoparticle administration.

7.2.6 Statistical Analysis

All statistical analyses were performed in GraphPad Prism Version 9 (GraphPad Software, La Jolla, CA). The Kolmogorov-Smirnov test, in association with the Shapiro-Wilk test, was performed to test for normal distribution and equal variance of the data. If the data passed the two assumptions, a one-way ANOVA and post hoc tests were performed where appropriate for the shams, contralateral side, and ipsilateral sides of the cCCI group for each treatment cohort. Data that did not pass normality or equal variance assumptions were assessed using a one-way Kruskal Wallis test and/or Welch's Test. Data were considered statistically significant with $p<0.05$ and trending at $p<0.1$. All histology data were normalized to respective shams, and data are represented as the mean ± standard error of the mean, or SEM.

7.3 Results

7.3.1 Results of Nanoparticle Characterization

Each batch of nanoparticles was characterized by the Lavik lab for size and peptide content before shipping for this study. Detailed values for HNP and CNP batches are displayed in Table 5.

Table 5. Nanoparticle characterization for the cCCI study. Table of properties for both the PLA-PEG control nanoparticles and PLA-PEG-GRGDS hemostatic nanoparticles.

Group	Diameter (nm)	Peptide Content (%)
Control nanoparticles	325.8 ± 8.3	
Hemostatic nanoparticles	317.1 ± 25.7	10.07

7.3.2 Animal Recovery and Righting Reflex

Following cCCI, no apparent signs of injury were discernable, though animals subjected to cCCI showed significant delays in righting compared to the sham group (Fig. 73). Over the seven days, no significant differences in weight in the cCCI group compared to shams were detected.

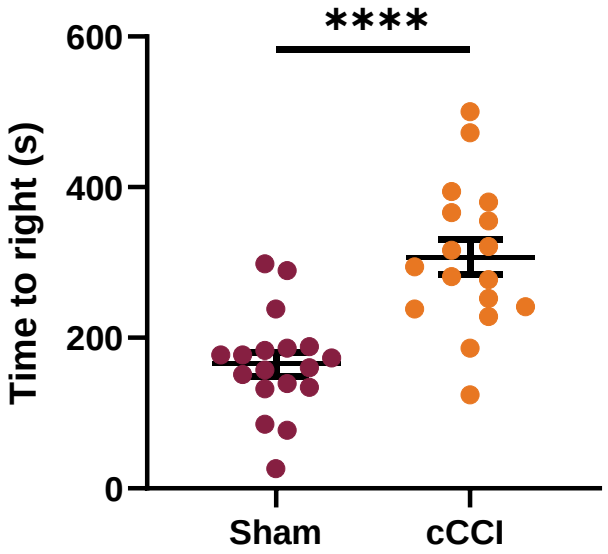

Figure 73. Delays in righting were detected in cCCI animals. A significant increase in righting time was observed in the cCCI animals compared to shams immediately following the impact. ****p<0.0001. Data represented as Mean ± SEM.

7.3.3 Nanoparticle administration restored the size of microglia in the SC of cCCI animals to pre-injury levels

A Brown-Forsythe ANOVA test indicated significant changes area/cell in the injured and sham animals within the vehicle-only (saline) group. Furthermore, a significant decrease in area/cell was observed in the contralateral side of the SC compared to the sham group (p=0.02), with this significant decrease also found in the ipsilateral side of the SC compared to shams (p=0.003). Within the CNP and HNP groups, no significant changes in area/cell were found between either side of the SC and their respective shams (Fig. 74).

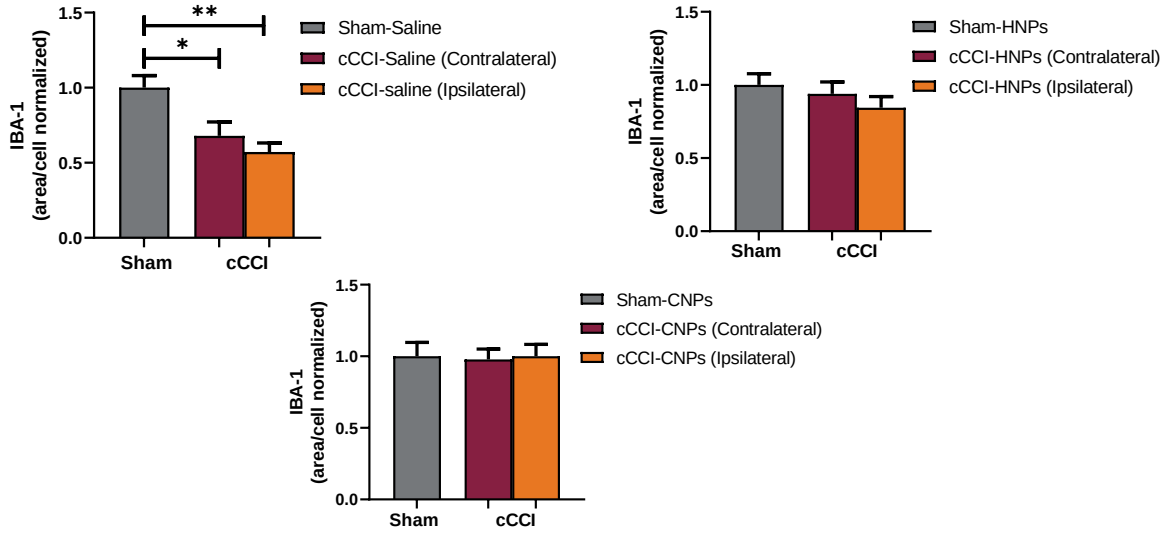

Figure 74. Changes in microglial size were prevalent in the SC of the saline-treated animals following cCCI. A significant decrease in area/cell was found in the saline group, with the ipsilateral and contralateral sides of the SC different than the SC in shams. No significant differences in the size of microglia were observed in the CNPs or HNPs groups. **p<0.01, ****p<0.001. Data represented as Mean ± SEM.

7.3.4 Nanoparticles improved microglia activation in cCCI animals seven days following injury

A one-way ANOVA indicated significant changes in area fraction in the vehicle-only group following injury ($F(2, 13) = 13.39$, $p=0.007$). More specifically, a significant decrease in area fraction was observed in the ipsilateral side of the SC compared to the SC of the sham group (p=0.0004) and the contralateral side compared to the sham group (p=0.0012). No significant

changes in area fraction were found when comparing cCCI animals to shams within the CNP or the HNP treatment groups (Fig. 75).

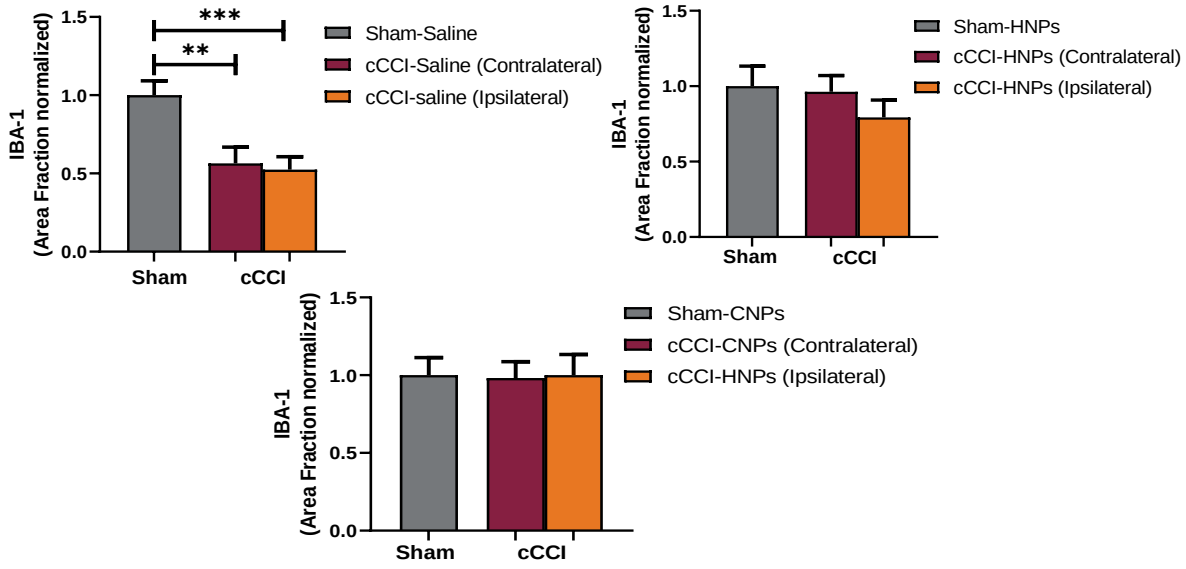

Figure 75. IBA-1 levels in cCCI animals resemble those of shams following nanoparticle administration. In the vehicle-only group, a significant decrease in area fraction was observed in the ipsilateral and contralateral sides of the SC in the cCCI animals compared to shams. No significant changes were observed between cCCI animals and shams within the CNP or HNP groups. **p<0.01, ***p<0.001. Data represented as Mean ± SEM.

7.3.5 Decreases in the number of microglia were observed in the vehicle-only cCCI group

Changes in count per area were observed in the SC of the cCCI animals of the saline group compared to shams ($F(2, 12) = 3.763$, $p=0.05$), with post hoc tests indicating a significant decrease in count per area in the contralateral side of the SC in the cCCI group compared to the shams ($p=0.01$). A decrease was observed in the ipsilateral side compared to sham animals, but this decrease was insignificant. Moreover, no significant differences in count per area were found in the cCCI animals compared to shams in the CNP or HNP groups (Fig. 76-77).

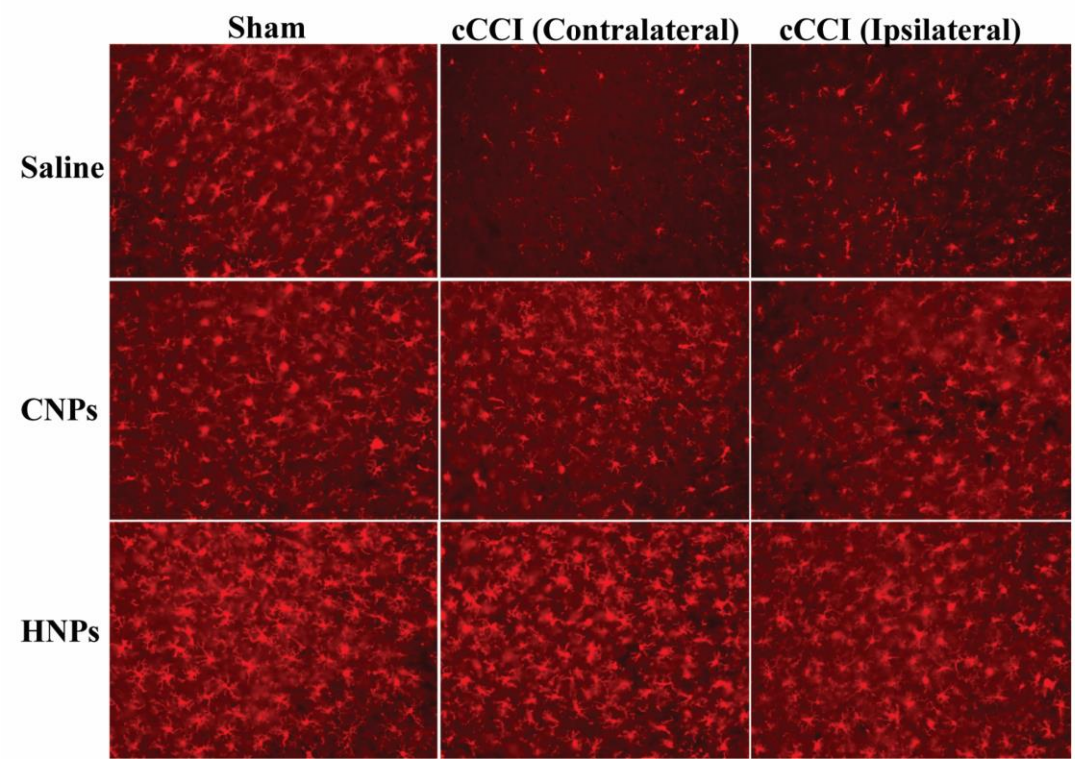

Figure 76. Nanoparticle administration may restore microglia to pre-injury levels. Images taken at 20x magnification indicate that vehicle-only injured animals had a decrease in the amount of microglia compared to shams, whereas cCCI animals treated with either CNPs or HNPs showed no notable changes in the amount of microglia within the cortex**.**

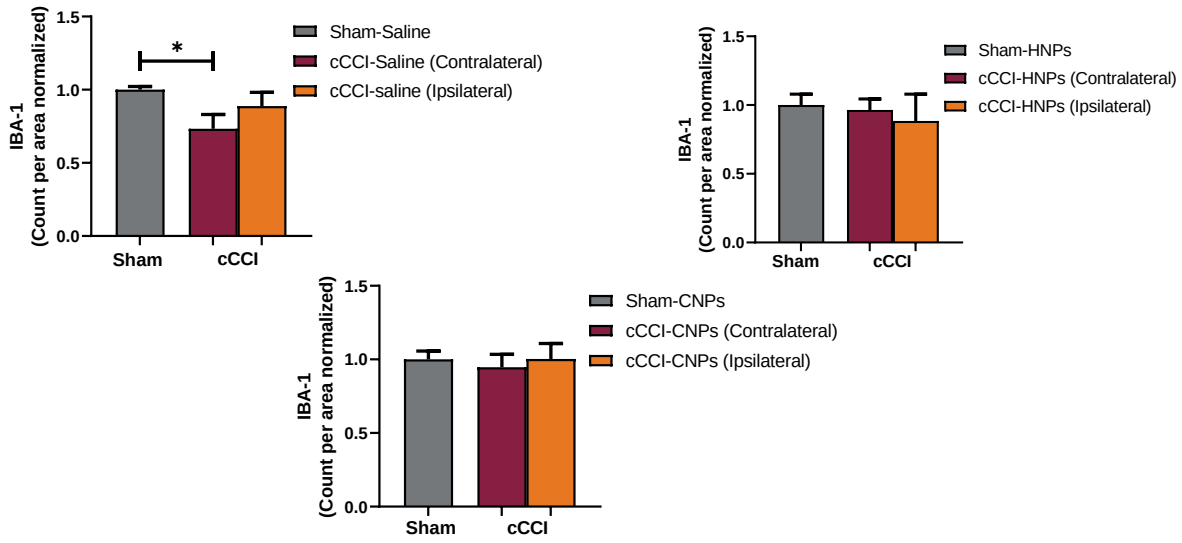

Figure 77. Nanoparticles restored microglia levels to baseline. Within the saline-treated group, a significant decrease in count per area was observed in the contralateral side of the SC compared to the SC in shams. No significant differences in count per area were found in the SC of cCCI animals compared to shams within the CNP- or HNP-treated groups. *p<0.05. Data represented as Mean ± SEM.

7.3.6 IBA-1 levels were restored following nanoparticle treatment seven days following injury

Within the saline-treated group, a Brown-Forsythe ANOVA test indicated significant changes in fluorescent intensity of IBA-1, with the ipsilateral and contralateral sides of the SC showing significant decreases when compared to the SC of the sham group (p=0.01 and p=0.05 respectively). Fluorescent intensity was not significantly different in the SC of the cCCI animals treated with CNPs or HNPs compared to their respective shams (Fig. 78).

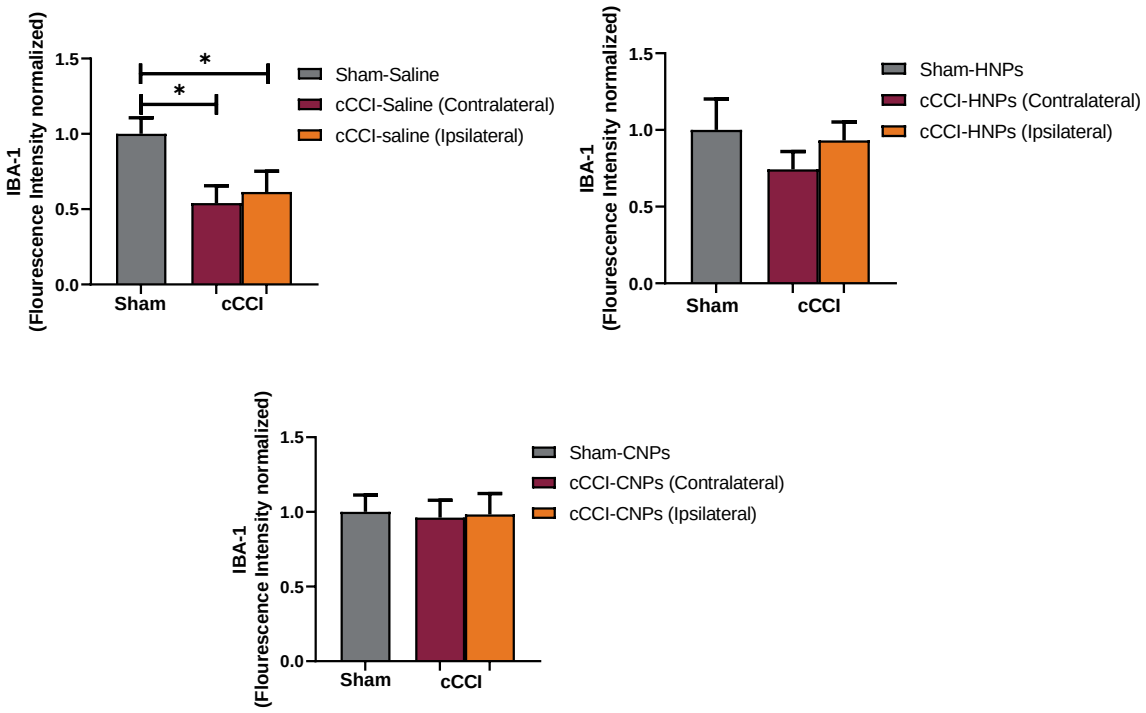

Figure 78. Decreased IBA-1 expression was found in the vehicle-only group. A significant decrease in fluorescent intensity of IBA-1 was observed in both the ipsilateral and contralateral sides of the SC in cCCI animals of the saline group compared to their respective shams. These significant differences were not seen within the CNPs, or HNPs treated groups. *p<0.05. Data represented as Mean ± SEM.

7.4 Discussion

The nanoparticles within this study engineered by the Lavik group were PEGylated polyester nanoparticles, with HNPs functionalized with a GRGDS peptide. While these nanoparticles have been shown to mitigate internal bleeding through their hemostatic properties, studies have indicated their contribution in mitigating neuropathology following TBI.[232,359] Microglia alterations following TBI are shown to occur and have a unique role in TBI pathologies, with microglia being an early-responder to the pathological processes following injury. They exhibit distinct polarization states in response to microenvironmental cues, and microglial polarization states are accompanied by phenotypic changes that may lead to increases in pro- and/or anti-inflammatory cytokines, an increase in the secretion of ROS, or phagocytic properties leading to synaptic pruning, and/or removal of cell debris.[326,328,334,336] While studies have explored

treatment options to mitigate microglia-induced pathologies,[365–367] there are still clinical gaps in how treatments contribute to mechanistic changes within microglia, restoring them to pre-injury levels. Moreover, an extensive comprehension of microglia dynamics following a closed-head rodent model of impact trauma using PEGylated polyester nanoparticles has yet to be considered.

In the present study, microglia-induced activation was decreased following cCCI with the administration of nanoparticles, whether they were conjugated with a functionalized GRGDS peptide (HNPs) or with the peptide properties inhibited (CNPs). More specifically, a significant decrease in the amount and size of IBA-1+ microglia was observed within the SC of the vehicle-only group of cCCI animals compared to their sham counterparts. In contrast, no significant differences in the size of microglia or the amount within the SC were observed in the contralateral or ipsilateral side in cCCI animals treated with either CNPs or HNPs compared to their respective shams. These changes in microglia profiles were also observed as levels of IBA-1 (area fraction and fluorescence intensity) in the SC of the cCCI animals within both the CNP and HNP groups were restored to sham levels. Changes in IBA-1 expression back to baseline levels were not observed within the saline-only group, where significant decreases in area fraction and fluorescent intensity were detected in the SC of the cCCI animals. As the reduction in microglia activation was present following both CNP and HNP administration, this may suggest that the therapeutic role of GRGDS may not be the only factor in restoring microglia levels. Maisha et al. explored the surface properties of the same PEGylated polyester nanoparticles *in vitro* by understanding the crosstalk between nanoparticles and immune responses. By incubating the nanoparticles in whole blood, followed by a cytokine assay, nanoparticles were found to impact inflammation by significantly reducing levels of IL-16. IL-16 is an immunomodulatory cytokine that induces lymphocyte migration and the expression of pro-inflammatory cytokines IL-1β, IL-6, and TNF-α.[368–370] Upregulation of IL-16 has been found in experimental models of TBI as early as 24 hours,[371] and may persist sub-acutely following TBI. IL-16, also considered a DAMP, are recognized by surface receptors on microglia, inducing their activation, further amplifying the pro-inflammatory responses.[372] While the study by Maisha et al. utilized *in vitro* methods, this can still be translated and explored in pre-clinical studies, to speculate on what may be influencing microglia dynamics. More specifically, CNPs and HNPs could reduce IL-16 levels that initially influenced secondary injury cascades triggered by cCCI, which may aid in restoring microglia to a healthy state. Macrophage migration inhibitory factor (MIF), another pro-inflammatory cytokine

was also significantly reduced by both the HNPs and CNPs following the *in vitro* study, increasing evidence of the role that the nanoparticles have in modulating the immune response. Enhanced expression of MIF, which is produced by cells such as macrophages, microglia, astrocytes, and neurons, are known to contribute to persistent activation of glial cells, and neuroinflammation, well within the chronic stages.[373] MIF is also known to upregulate the expression of TLR-4, which is plays a role in driving in microglia activation, especially the pro-inflammatory response.[374,375] Thus, nanoparticles reducing the levels of MIF may contribute to IBA-1 expression and IBA-1+ microglia resembling sham levels following injury.

DAMPs such as IL-16 and MIF are also found to represent the passive release of danger signaling in response to stress and/or cell death due to traumatic injury.[376,377] In the untreated cCCI group (saline-only), decreases in cell size were observed, and this could be due to decreases in the cell soma size, which could be linked to morphological changes in microglia. These changes may be associated with a stressed/primed phenotype that responds to stress signals such as oxidative stress or genotoxic DNA damage, or a rod-like phenotype that aligns end-to-end along damaged axons. With studies suggesting that CNPs and HNPs reduce this immunomodulatory cytokine, this may explain why area/cell was not significantly different in the cCCI animals in both nanoparticle groups compared to their respective shams. The PEGylated polyester nanoparticles could re-establish homeostasis, by limiting signals that promote non-autonomous microglia polarization, returning microglia to a healthy state.

Furthermore, a study by Hubbard et al. indicated a decrease in IBA-1 expression seven days following bTBI in animals that were not treated with nanoparticles. They hypothesized that this decrease in IBA-1 expression could also be linked to microglia morphology through the retraction of processes.[232] While there are differences in the injury paradigm (blast versus impact), the present study also indicated similar differences in levels of IBA-1 that could be linked to morphological changes. Future studies that link changes in microglia morphology to their diverse activation states, or the lack thereof following nanoparticle administration are warranted. This will allow for the understanding of how these polyester nanoparticles impart mechanistic changes that affect the microglia-mediated immune responses to continue.

The PLA-PEG property of the nanoparticles having a more considerable impact on microglia activation rather than the hemostatic properties may also be related to time-dependent inflammatory cascades. Research indicates transient platelet profiles in the brain, with the

upregulation of platelets present 24 hours following a mild TBI.[378] In contrast, previous research also revealed that platelets may lose their function up to seven days within the rodent brain,[379] meaning that thrombosis induced by platelets' may be less prominent in influencing microglia activation at seven days post cCCI. This may provide insight as to why HNPs themselves are not the key drivers in restoring homeostasis, contributing to the fact that at subacute time points, other characteristics of PLA-PEG nanoparticles have a more significant impact on reducing microglia activation than GRGDS peptide conjugation.

The work presented within has successfully begun to characterize the use of PEGylated nanoparticles to restore microglia's homeostatic functions *in vivo*. Nanoparticle administration indicated microglia activation returning to sham levels one week following injury, by restoring the number of microglia and IBA-1 expression to sham levels. These results suggest that PEGylated polyester nanoparticles improve neurological recovery by influencing microglia contributions to neuropathology. This study highlights the advantages of using these nanoparticles to treat TBIs, though more studies are needed to assess the benefits of PLA-PEG nanoparticles after injury. Future directions need to quantify microglia morphology within the SC to provide a comprehensive analysis of morphological changes or the lack thereof following nanoparticle administration. Identifying morphological changes in microglia may also aid in understanding if specific phenotypes are associated with decreases in IBA-1 expression in the untreated injury group.

Cytokine profiles following injury and nanoparticle treatment would be valuable to determine further, the contribution of microglia to the recovery process. Many approaches can be used to explore this aspect of the study such as ELISA assays or Luminex platforms. More specifically, identifying whether upregulation of IL-16 and MIF are observed following cCCI, or if it is attenuated following nanoparticle administration will support the theory that decreases in cytokine profiles are key drivers in restoring microglia to their healthy state. Another outstanding question is whether time-dependent inflammatory responses that influence microglial activation are the reason why hemostatic properties of nanoparticles were less prominent. Studies that explore the interaction of microglia activation and platelet plug formation at acute time points such as 4 and 24 hours may provide insight into whether the presence of platelets induce microglia polarization, and whether hemostatic properties of the polyester nanoparticles play a role in the early injury response of cCCI.

Finally, microglia responses are also heterogeneous across brain regions, with diverse phenotypes spread throughout different areas. Because of this, analyzing microglia responses in other brain regions, such as the hippocampus, MC, and the thalamus, to name a few, is essential in providing a robust analysis of the role of PLA-PEG nanoparticles in mediating microglial activation. Overall, the results of this study are promising in identifying life-saving treatments for traumatic brain injury.

Chapter 8: Summary

8.1 Conclusions

Microglia play a substantial role in the pathology that develops following TBI. Preclinical models demonstrate that microglia become activated, presenting diverse phenotypes associated with functions that drive secondary injury responses like neuroinflammation. There is a critical need to understand the underlying mechanisms within microglia that mediate secondary injury, as their phenotypic changes can have both protective and deleterious effects that can persist within the chronic stages of injury. If left unrestrained, microglia dysfunction can lead to irreversible consequences such as neurodegeneration. *In vivo* models are a great way to delineate characteristics of activated microglial phenotypes while also considering the underlying molecular drivers that influence secondary injury cascades. Furthermore, building a comprehensive knowledge base of microglia dynamics following TBI will also facilitate design of therapeutic interventions that target the cellular and molecular drivers of microglia dysfunction.

The overall objective of these studies was to elucidate microglia dynamics following both blast- and impact-induced neurotrauma while also assessing the role of hemostatic nanoparticles in mitigating microglia-mediated pathology. Each of the following specific aims were addressed in this work:

8.1.1 Specific Aim 1

Chapter 3 detailed the work conducted to accomplish Specific Aim 1, sub-aim 1a. This work described how repeated blast exposure triggered transient changes in microglia phenotypes that also displayed regional heterogeneity. Acute changes in microglia indicated a distinct morphology in the motor cortex that may be associated with a pro-inflammatory function, aligning with damaged neuronal synapses and axons. Changes in microglia following repeated blast exposure were most notable at seven days, with dramatic decreases in IBA-1 expression and morphology similar to microglia who display dystrophic phenotypes. This phenotype is typically displayed in anti-inflammatory microglia, which are fragmented, losing physiological function, and ultimately degenerating. Histological analysis of NLRP3 following repeated blast exposure indicated trending decreases in NLRP3 expression, which may be linked to the observed microglial phenotype.

In Chapter 4, acute and subacute microglia changes were observed following cCCI, with results exhibiting microglia activation in both the contralateral and ipsilateral side of the somatosensory and motor cortices, along with hippocampus. Moreover, transient changes in microglia indicated proliferation in microglia cells and IBA-1 expression three days following cCCI, whereas a decrease in microglia cells and IBA-1 expression were observed in the cortex and hippocampus up to one week following injury. Moreover, acute morphological changes in microglia were associated with pro-inflammatory phenotypes within the cortex, whereas anti-inflammatory phenotypes were observed in the cortex and hippocampus at one week. Microglia within the hippocampus of animals subjected to a cCCI displayed a unique morphology, with associated phenotypic and functional changes that are not thoroughly reported in research. Subacute changes in NLRP3 levels indicated significant decreases in the cortex and hippocampus of cCCI animals, which may be related to the specific microglia phenotypes predominant within the cortex and hippocampus after injury. Characterizing a cCCI rodent model also contributed to the evidence that regardless of the TBI model being CCI, which is typically classified as a focal injury; the closed-head aspect of this injury model showed that the injury is more diffuse than others report, with microglia alterations found in both the ipsilateral and contralateral sides of the brain.

8.1.2 Specific Aim 2

Chapter 5 describes work that accomplishes Specific Aim 2, which sought to identify microglia-specific gene patterns contributing to inflammatory responses following TBI. This work first established and optimized the ability to use cell-sorting techniques to isolate cortical microglia from the adult rodent brain following TBI, producing a high enrichment of pure microglia. This innovative approach allows cell-specific responses to be identified following tissue-level injury. An association between NLRP3 inflammasome activation in microglia, and increased production of IL-1β, as well as other polarization states that are present within the cortex following blast exposure and cCCI were confirmed through qPCR. Repeated blast exposure indicated elevated genetic expression of COX2 within microglia at three days, whereas CD206 was increased in cortical microglia at seven days. Following cCCI, increases in the genetic expression of NLRP3, with a trending increase in IL-1β were found in cortical microglia. Moreover, increases in gene expression of COX2 and CD206 were also observed in the acute stages of injury. At the seven day

time point, similar genetic patterns were observed, with NLRP3, IL-1β, COX2, and CD206 upregulated in cortical microglia following cCCI. Altogether, results from this chapter suggest that microglia alterations may be time-dependent, with distinct, contrasting molecular changes in bTBI versus impact TBI. This work demonstrates the importance of developing personalized treatments to combat microglia-mediated inflammation, as their phenotypes may be injury-dependent.

8.1.3 Specific Aim 3

Chapter 6 elucidated the work addressed in sub-aim 3a of Specific Aim 3. The work established a "blast plus" injury model, exploring microglia alterations following complex injuries that include both repeated blast exposure and a cCCI. The model itself is novel and recapitulates a Veteran-relate clinical condition that had not been previously modeled. The results provided a unique response as compared to the impact or blast alone injury models. Rather than increases or decreases in microglia proliferation in the cortex and/or hippocampus as seen in previous chapters, morphological changes were the main indicator of activation. Unlike morphologies observed in the cortex and hippocampus of bTBI and cCCI animals in Chapters 3 and 4, animals subjected to blast+impact injury showed a different type of morphology, with microglia adopting an amoeboid phenotype. Additionally, repeated blast exposure predisposing the brain to increases in microglia activation seems to be region-specific, with substantial changes in microglia activation found within the hippocampus of the blast+impact group compared to the blast- or impact-only group. In contrast, similar changes in microglia activation were exhibited in the blast+impact and impact-only groups in the SC, and similarities in microglia activation were observed across all groups in the MC. This work assisted in providing the fundamental understanding of microglia function in the injured brain in a “blast plus” complex injury, displaying the crucial need to explore this type of repeated TBI further.

Chapter 7 summarized the hypothesis of sub-aim 3b, exploring how PEGylated polyester nanoparticles influenced subacute microglia responses to impact trauma. Both hemostatic and control PLA-PEG nanoparticles appeared to attenuate microglia activation following cCCI by restoring microglia levels. More specifically, subacute microglia activation in the SC following cCCI, as seen in Chapter 4, was displayed through decreases in microglia cells and changes in IBA-1 expression. In contrast, in the present study, no significant changes in microglia populations or IBA-1 expression were observed in animals treated with nanoparticles compared to the vehicle-

only group. As both CNP and HNP administration seemed to restore microglia to sham levels, this indicated that the polymeric structure of the nanoparticles, which has previously been shown to reduce inflammatory signals that may activate microglia, has a more significant effect on attenuating microglial responses than the hemostatic properties of the nanoparticles, as initially hypothesized.

8.2 Limitations

The work within each Specific Aim was accompanied by experimental limitations, which may affect the results, and should be considered:

1. **Studies described were limited to *in vivo* approaches in a rodent model.**
   The rodent brain is notably smaller, lacking distinctive patterns that are present in the human brain, such as gyri and sulci. These structures contribute to differences in the cellular make-up and complex network of neurons within the brain, which may cause a difference in microglia phenotypes that are exhibited in the rodent brain.[380,381] Moreover, variations in skull differences between the human skull and rat skull could influence the transmission of blast waves to the brain and the mechanical insult from cCCI. Despite these limitations, studies continue to indicate that rodent models of blast and impact trauma elicit neuropathology associated with TBI's clinical outcomes. Thus, to confirm the small animal results, a larger animal model with a brain more representative of the human brain anatomy, such as mini-pig or non-human primate TBI models, should be considered to further advance the field.

2. **These studies did not evaluate sex as a biological variable.**
   The use of males exclusively in the work may not be fully representative of microglia activation in TBI. Blast and impact neurotrauma affect both males and females in military and civilian populations. Studies have demonstrated that sex differences influence microglia phenotypes and can play a distinct role in microglia-mediated inflammatory responses.[382,383] As such, it is essential for future studies to explore cellular and molecular changes following blast, impact, and blast+impact models to begin to evaluate microglia

responses in both female and male subjects to contribute to generating more personalized treatment options.

3. **IBA-1 is expressed in both microglia and peripheral macrophages.**

   We chose to use the marker IBA-1 to acquire histological results on microglia through image processing of fluorescent staining. It is known that IBA-1 has an affinity for both microglia and peripheral macrophages, yet it is widely used for investigating microglia activation following TBI.[201,220,338,384,385] Because of this, macrophage contributions could also affect temporal and spatial IBA-1 levels. Quantifying microglia morphology and particle size exclusion in the image processing step aids in distinguishing between the two cell types, but optimizing microglia-specific markers (TMEM-119, P2RY12, TREM-2 and CXC3R1) for histological analysis is warranted.

4. **mRNA expression does not fully represent glial-specific responses following TBI.**

   As mentioned in Chapter 5, microglia-specific molecular patterns were only measured through mRNA expression. Protein expression was not measured. This is primarily due to the low yield of protein extracted from isolated microglia, which complicated protein quantification using Western Blotting techniques. While mRNA expression values are helpful in identifying molecular drivers that influence microglia activation, this is only one step in the transcription pathway, and protein expression will be more indicative of molecular alterations as proteins actively contribute to the cell-type-specific function. Protein levels of NLRP3 from histological data were the first step in drawing correlations between mRNA and protein expression in this study, but quantification of microglia-specific protein expression will provide necessary contributions to understanding molecular changes that drive activation. Continued optimization of MACS technique to increase the yield of microglia to combat complexities in protein abundance is needed to address this limitation.

5. **Only one injection and time point for injection of nanoparticles were tested following injury.**

Nanoparticles were administered immediately following injury as a proof of concept for this injury model. While studies using nanoparticles designed and produced from the Lavik lab have indicated the efficacy of administering treatment immediately following trauma, immediate injection is not always feasible right after the injury occurs. Studies determining the maximum time allowable for optimal treatment, as well as the efficacy of multiple dosing need to be considered.

8.3 Future Directions

The extensive results of this work identified multiple phenotypes of microglia involved in their activation, driving inflammation following blast, impact, and blast+impact TBI. As this research aims to generate relevant data to advance diagnostic and therapeutic tools for those affected by TBI, it is crucial to explore further the outstanding research questions that still exist. The following areas of research are of particular interest for future studies:

1. **Expand regions of interest to determine connectivity and injury severity.**

   In Chapter 4, histological analysis showed significant decreases in protein levels of NLRP3 seven days following injury, whereas genetic expression of NLRP3 was significantly decreased in isolated cortical microglia at this same time point. While direct correlations or comparisons might be challenging to make, one potential reason why opposite effects in NLRP3 levels are seen could be that one specific area of the cortex was explored through histological analysis, whereas mRNA results encompass microglia from the whole cortex, which may increase the chance of diverse microglia phenotypes to be present. Future IHC studies exploring areas such as the pre-frontal, retrosplenial, parietal, and visual cortices should be explored to determine if NLRP3 levels are still decreased. Thus, exploring multiple regions within the cerebral cortex that are both rostral and caudal to -3.00 mm posterior from bregma (current regions of interest) will enhance the understanding and contribution of NLRP3 activation

2. **Further characterize microglia responses following blast+impact injury.**

Our pilot study of the blast+impact model showed promise in understanding microglia phenotypes following this clinically relevant, yet complex injury. More studies are needed to characterize whether repeated blast exposure increases the chance of neurological deficits following a subsequent impact TBI. Furthermore, our model depicts a delayed impact following blast exposure. Active military personnel and Veterans could sustain "blast plus" injury within minutes through the primary blast injury exposure and a secondary blast injury, which involves exposure to the blast wave and displacement due to the force of the wave, accelerating the body leading to head impact. Thus, varying the timing between blast and impact TBI can further explore how this repeated injury influences mechanistic changes of microglia. Expanding to include the exploration of microglia-specific genetic patterns through MACS may provide insight into molecular changes in microglia that may differ from blast- or impact-only TBIs.

3. **Associating microglia-specific phenotypes to sequelae such as depression, anxiety, and memory impairment following TBI.**

   Dickerson et al. 2020 determined that vestibulomotor deficits following blast-induced neurotrauma are linked to glial activation. Dickerson et al. 2021 determined that anxiety- and depressive-like behaviors are also associated with glial-driven pathologies. Additional studies exploring injury-induced pathologies following TBI have found that neuropathology may contribute to behavioral deficits.[86,386–388] Taking steps to further quantify microglia morphology and determining microglia-specific genetic patterns can aid in understanding whether amoeboid, stressed/primed, rod-like, or dystrophic microglia drive these clinical outcomes; and the role that NLRP3 activation may play in driving specific behavioral responses. This is crucial in monitoring acute and chronic injury progression, contributing to therapeutic interventions that can reduce behavioral and cognitive impairments.

4. **Continue to validate the efficacy of PEGylated polyester nanoparticles to restore microglia to baseline and its use as a vehicle for drugs that can treat pro-inflammatory responses following injury.**

Chapter 7 demonstrated the potential ability of nanoparticles to treat microglia pathology following cCCI. Studies by Hubbard et al. utilized hemostatic nanoparticles; specifically nanoparticles encapsulated with dexamethasone, and demonstrated the treatment capabilities in mitigating bTBI pathology. Pending work is currently exploring multiple drug candidates encapsulated in nanoparticles to attenuate microglia-mediated pathologies following TBI. This continued research will be essential in identifying novel techniques to improve the quality of life for patients who suffer from a TBI.

8.4 Author's Contributions to the Field

Year	**Title**	**Journal**
2020	Glial Activation in the Thalamus Contributes to Vestibulomotor Deficits Following Blast-Induced Neurotrauma*	Frontiers in Neurology
2021	Chronic Anxiety- and Depression-Like Behaviors are Associated with Glial-Driven Pathology Following Repeated Blast Induced Neurotrauma*	Frontiers in Behavioral Neuroscience
2022	Age-Relevant in vitro models may lead to improved translational research for traumatic brain injury	Current Opinion in Biomedical Engineering
2022	Osteopathy in the cranial field as a method to enhance brain injury recovery: A preliminary study	Neurotrauma Reports (in review)
2023	Characterizing glial dysfunction in a clinically relevant model of impact-induced neurotrauma	*In preparation*
2023	Influences of microglia-specific genetic patterns on activation states following traumatic brain injury	*In preparation*
2023	Dystrophic and amoeboid microglia are the predominant phenotypes in a model of Blast plus Impact Traumatic Brain Injury	*In preparation*

*Represents first author publications cited in this work, with full citations located in the reference section.

References

1. Giner J, Mesa Galán L, Yus Teruel S, Guallar Espallargas MC, Pérez López C, Isla Guerrero A, Roda Frade J. Traumatic brain injury in the new millennium: new population and new management. Neurologia (Barcelona, Spain). 2022;37(5):383–389. doi:10.1016/j.nrleng.2019.03.024

2. Adugna DG, Aragie H, Kibret AA, Belay DG. Therapeutic Application of Stem Cells in the Repair of Traumatic Brain Injury. Stem Cells and Cloning: Advances and Applications. 2022;15:53–61. doi:10.2147/SCCAA.S369577

3. Alarie C, Gagnon IJ, Quilico E, Swaine B. Characteristics and outcomes of physical activity interventions for individuals with mild traumatic brain injury: a scoping review protocol. BMJ open. 2019;9(6):e027240. doi:10.1136/bmjopen-2018-027240

4. Leo P, McCrea M. Epidemiology. In: Laskowitz D, Grant G, editors. Translational Research in Traumatic Brain Injury. Boca Raton (FL): CRC Press/Taylor and Francis Group; 2016. (Frontiers in Neuroscience). http://www.ncbi.nlm.nih.gov/books/NBK326730/

5. Collins SM, O'Connell CJ, Reeder EL, Norman SV, Lungani K, Gopalan P, Gudelsky GA, Robson MJ. Altered Serotonin 2A (5-HT2A) Receptor Signaling Underlies Mild TBI-Elicited Deficits in Social Dominance. Frontiers in Pharmacology. 2022;13. doi:10.3389/fphar.2022.930346

6. Laskowski RA, Creed JA, Raghupathi R. Pathophysiology of Mild TBI: Implications for Altered Signaling Pathways. In: Kobeissy FH, editor. Brain Neurotrauma: Molecular, Neuropsychological, and Rehabilitation Aspects. Boca Raton (FL): CRC Press/Taylor & Francis; 2015. (Frontiers in Neuroengineering). http://www.ncbi.nlm.nih.gov/books/NBK299203/

7. Langlois LD, Selvaraj P, Simmons SC, Gouty S, Zhang Y, Nugent FS. Repetitive mild traumatic brain injury induces persistent alterations in spontaneous synaptic activity of hippocampal CA1 pyramidal neurons. IBRO neuroscience reports. 2022;12:157–162. doi:10.1016/j.ibneur.2022.02.002

8. Almeida-Suhett CP, Prager EM, Pidoplichko V, Figueiredo TH, Marini AM, Li Z, Eiden LE, Braga MFM. GABAergic interneuronal loss and reduced inhibitory synaptic transmission in the hippocampal CA1 region after mild traumatic brain injury. Experimental Neurology. 2015;273:11–23. doi:10.1016/j.expneurol.2015.07.028

9. Badea A, Kamnaksh A, Anderson RJ, Calabrese E, Long JB, Agoston DV. Repeated mild blast exposure in young adult rats results in dynamic and persistent microstructural changes in the brain. NeuroImage : Clinical. 2018;18:60–73. doi:10.1016/j.nicl.2018.01.007

10. Dickstein DL, De Gasperi R, Gama Sosa MA, Perez-Garcia G, Short JA, Sosa H, Perez GM, Tschiffely AE, Dams-O'Connor K, Pullman MY, et al. Brain and blood biomarkers of tauopathy and neuronal injury in humans and rats with neurobehavioral syndromes following blast exposure. Molecular Psychiatry. 2021;26(10):5940–5954. doi:10.1038/s41380-020-0674-z

11. Graham R, Rivara FP, Ford MA, Spicer CM, Youth C on S-RC in, Board on Children Y, Medicine I of, Council NR. Consequences of Repetitive Head Impacts and Multiple Concussions. National Academies Press (US); 2014. https://www.ncbi.nlm.nih.gov/books/NBK185336/

12. Juan SMA, Daglas M, Adlard PA. Tau Pathology, Metal Dyshomeostasis and Repetitive Mild Traumatic Brain Injury: An Unexplored Link Paving the Way for Neurodegeneration. Journal of Neurotrauma. 2022;39(13–14):902–922. doi:10.1089/neu.2021.0241

13. O'Brien WT, Pham L, Symons GF, Monif M, Shultz SR, McDonald SJ. The NLRP3 inflammasome in traumatic brain injury: potential as a biomarker and therapeutic target. Journal of Neuroinflammation. 2020;17(1):104. doi:10.1186/s12974-020-01778-5

14. Lindquist LK, Love HC, Elbogen EB. Traumatic Brain Injury in Iraq and Afghanistan Veterans: New Results from a National Random Sample Study. The Journal of neuropsychiatry and clinical neurosciences. 2017;29(3):254–259. doi:10.1176/appi.neuropsych.16050100

15. Faul M, Coronado V. Epidemiology of traumatic brain injury. Handbook of Clinical Neurology. 2015;127:3–13. doi:10.1016/B978-0-444-52892-6.00001-5

16. Bryden DW, Tilghman JI, Hinds SR. Blast-Related Traumatic Brain Injury: Current Concepts and Research Considerations. Journal of Experimental Neuroscience. 2019;13. doi:10.1177/1179069519872213

17. Nguyen R, Fiest KM, McChesney J, Kwon C-S, Jette N, Frolkis AD, Atta C, Mah S, Dhaliwal H, Reid A, et al. The International Incidence of Traumatic Brain Injury: A Systematic Review and Meta-Analysis. The Canadian Journal of Neurological Sciences. Le Journal Canadien Des Sciences Neurologiques. 2016;43(6):774–785. doi:10.1017/cjn.2016.290

18. Roozenbeek B, Maas AIR, Menon DK. Changing patterns in the epidemiology of traumatic brain injury. Nature Reviews. Neurology. 2013;9(4):231–236. doi:10.1038/nrneurol.2013.22

19. Jassam YN, Izzy S, Whalen M, McGavern DB, El Khoury J. Neuroimmunology of Traumatic Brain Injury: Time for a Paradigm Shift. Neuron. 2017;95(6):1246–1265. doi:10.1016/j.neuron.2017.07.010

20. Blennow K, Brody DL, Kochanek PM, Levin H, McKee A, Ribbers GM, Yaffe K, Zetterberg H. Traumatic brain injuries. Nature Reviews Disease Primers. 2016;2(1):1–19. doi:10.1038/nrdp.2016.84

21. Georges A, Booker JG. Traumatic Brain Injury. In: StatPearls. Treasure Island (FL): StatPearls Publishing; 2019. http://www.ncbi.nlm.nih.gov/books/NBK459300/

22. Elder GA, Mitsis EM, Ahlers ST, Cristian A. Blast-induced Mild Traumatic Brain Injury. Psychiatric Clinics of North America. 2010;33(4):757–781. (Traumatic Brain Injury: Defining Best Practice). doi:10.1016/j.psc.2010.08.001

23. Ma X, Aravind A, Pfister BJ, Chandra N, Haorah J. Animal Models of Traumatic Brain Injury and Assessment of Injury Severity. Molecular Neurobiology. 2019;56(8):5332–5345. doi:10.1007/s12035-018-1454-5

24. Spruiell Eldridge SL, Teetsel JFK, Torres RA, Ulrich CH, Shah VV, Singh D, Zamora MJ, Zamora S, Sater AK. A Focal Impact Model of Traumatic Brain Injury in Xenopus Tadpoles Reveals Behavioral Alterations, Neuroinflammation, and an Astroglial Response. International Journal of Molecular Sciences. 2022;23(14):7578. doi:10.3390/ijms23147578

25. Muccigrosso MM, Ford J, Benner B, Moussa D, Burnsides C, Fenn AM, Popovich PG, Lifshitz J, Walker FR, Eiferman DS, et al. Cognitive Deficits Develop 1 month after Diffuse Brain Injury and are Exaggerated by Microglia-Associated Reactivity to Peripheral Immune Challenge. Brain, behavior, and immunity. 2016;54:95–109. doi:10.1016/j.bbi.2016.01.009

26. Meaney DF, Morrison B, Dale Bass C. The Mechanics of Traumatic Brain Injury: A Review of What We Know and What We Need to Know for Reducing Its Societal Burden. Journal of Biomechanical Engineering. 2014;136(2):0210081–02100814. doi:10.1115/1.4026364

27. Andriessen TMJC, Jacobs B, Vos PE. Clinical characteristics and pathophysiological mechanisms of focal and diffuse traumatic brain injury. Journal of Cellular and Molecular Medicine. 2010;14(10):2381–2392. doi:10.1111/j.1582-4934.2010.01164.x

28. McKee AC, Daneshvar DH. The neuropathology of traumatic brain injury. Handbook of clinical neurology. 2015;127:45–66. doi:10.1016/B978-0-444-52892-6.00004-0

29. Neidecker J, Sethi NK, Taylor R, Monsell R, Muzzi D, Spizler B, Lovelace L, Ayoub E, Weinstein R, Estwanik J, et al. Concussion management in combat sports: consensus statement from the Association of Ringside Physicians. British Journal of Sports Medicine. 2019;53(6):328–333. doi:10.1136/bjsports-2017-098799

30. Harmon KG, Drezner JA, Gammons M, Guskiewicz KM, Halstead M, Herring SA, Kutcher JS, Pana A, Putukian M, Roberts WO. American Medical Society for Sports Medicine position statement: concussion in sport. British Journal of Sports Medicine. 2013;47(1):15–26. doi:10.1136/bjsports-2012-091941

31. DuPrey KM, Char AS, Loose SR, Suffredini MV, Walpole K, Cronholm PF. Effect of Sleep-Related Symptoms on Recovery From a Sport-Related Concussion. Orthopaedic Journal of Sports Medicine. 2022;10(7). doi:10.1177/23259671221105256

32. Kostyun RO, Milewski MD, Hafeez I. Sleep disturbance and neurocognitive function during the recovery from a sport-related concussion in adolescents. The American Journal of Sports Medicine. 2015;43(3):633–640. doi:10.1177/0363546514560727

33. Tanczos RL, Shimada SD. Brain injury severity due to direct head contact from near-side motor vehicle collisions. Traffic Injury Prevention. 2021;22:S56–S61. doi:10.1080/15389588.2021.1983177

34. Kuperman P, Granovsky Y, Fadel S, Bosak N, Buxbaum C, Hadad R, Sprecher E, Bahouth H, Ben Lulu H, Yarnitsky D, et al. Head- and neck-related symptoms post-motor vehicle collision (MVC): Separate entities or two-sides of the same coin? Injury. 2021;52(5):1227–1233. doi:10.1016/j.injury.2021.03.003

35. Craig A, Tran Y, Guest R, Gopinath B, Jagnoor J, Bryant RA, Collie A, Tate R, Kenardy J, Middleton JW, et al. Psychological impact of injuries sustained in motor vehicle crashes: systematic review and meta-analysis. BMJ open. 2016;6(9). doi:10.1136/bmjopen-2016-011993

36. West SW, Shill IJ, Sutter B, George J, Ainsworth N, Wiley JP, Patricios J, Emery CA. Caught on camera: a video assessment of suspected concussion and other injury events in women's rugby union. Journal of Science and Medicine in Sport. 2022 Jul 14:S1440-2440(22)00208–0. doi:10.1016/j.jsams.2022.07.008

37. El Sayed T, Mota A, Fraternali F, Ortiz M. Biomechanics of traumatic brain injury. Computer Methods in Applied Mechanics and Engineering. 2008;197(51):4692–4701. doi:10.1016/j.cma.2008.06.006

38. Bandak FA, Ling G, Bandak A, De Lanerolle NC. Injury biomechanics, neuropathology, and simplified physics of explosive blast and impact mild traumatic brain injury. Handbook of Clinical Neurology. 2015;127:89–104. doi:10.1016/B978-0-444-52892-6.00006-4

39. Shi L, Han Y, Huang H, Davidsson J, Thomson R. Evaluation of injury thresholds for predicting severe head injuries in vulnerable road users resulting from ground impact via detailed accident reconstructions. Biomechanics and Modeling in Mechanobiology. 2020;19(5):1845–1863. doi:10.1007/s10237-020-01312-9

40. Scorza KA, Raleigh MF, O'Connor FG. Current concepts in concussion: evaluation and management. American Family Physician. 2012;85(2):123–132.

41. Scorza KA, Cole W. Current Concepts in Concussion: Initial Evaluation and Management. American Family Physician. 2019;99(7):426–434.

42. Bodnar CN, Roberts KN, Higgins EK, Bachstetter AD. A Systematic Review of Closed Head Injury Models of Mild Traumatic Brain Injury in Mice and Rats. Journal of Neurotrauma. 2019;36(11):1683–1706. doi:10.1089/neu.2018.6127

43. Eakin K, Rowe RK, Lifshitz J. Modeling Fluid Percussion Injury: Relevance to Human Traumatic Brain Injury. In: Kobeissy FH, editor. Brain Neurotrauma: Molecular, Neuropsychological, and Rehabilitation Aspects. Boca Raton (FL): CRC Press/Taylor & Francis; 2015. (Frontiers in Neuroengineering). http://www.ncbi.nlm.nih.gov/books/NBK299213/

44. Lafrenaye AD, Todani M, Walker SA, Povlishock JT. Microglia processes associate with diffusely injured axons following mild traumatic brain injury in the micro pig. Journal of Neuroinflammation. 2015;12(1):186. doi:10.1186/s12974-015-0405-6

45. Cernak I, Vink R, Zapple DN, Cruz MI, Ahmed F, Chang T, Fricke ST, Faden AI. The pathobiology of moderate diffuse traumatic brain injury as identified using a new experimental

model of injury in rats. Neurobiology of Disease. 2004;17(1):29–43. doi:10.1016/j.nbd.2004.05.011

46. Shah EJ, Gurdziel K, Ruden DM. Mammalian Models of Traumatic Brain Injury and a Place for Drosophila in TBI Research. Frontiers in Neuroscience. 2019;13. doi:10.3389/fnins.2019.00409

47. Lyeth BG. Historical Review of the Fluid-Percussion TBI Model. Frontiers in Neurology. 2016;7. doi:10.3389/fneur.2016.00217

48. Panikashvili D, Simeonidou C, Ben-Shabat S, Hanus L, Breuer A, Mechoulam R, Shohami E. An endogenous cannabinoid (2-AG) is neuroprotective after brain injury. Nature. 2001;413(6855):527–531. doi:10.1038/35097089

49. Chen Y, Constantini S, Trembovler V, Weinstock M, Shohami E. An experimental model of closed head injury in mice: pathophysiology, histopathology, and cognitive deficits. Journal of Neurotrauma. 1996;13(10):557–568. doi:10.1089/neu.1996.13.557

50. Shapira Y, Shohami E. Experimental studies on brain oedema after blunt head injury: experimental approaches from animal experimentation to actual or possible clinical application. European Journal of Anaesthesiology. 1993;10(3):155–173.

51. Albert-Weißenberger C, Várrallyay C, Raslan F, Kleinschnitz C, Sirén A-L. An experimental protocol for mimicking pathomechanisms of traumatic brain injury in mice. Experimental & Translational Stroke Medicine. 2012;4(1):1. doi:10.1186/2040-7378-4-1

52. Albert-Weissenberger C, Sirén A-L. Experimental traumatic brain injury. Experimental & Translational Stroke Medicine. 2010;2:16. doi:10.1186/2040-7378-2-16

53. Osier N, Dixon CE. The Controlled Cortical Impact Model of Experimental Brain Trauma: Overview, Research Applications, and Protocol. Methods in molecular biology (Clifton, N.J.). 2016;1462:177–192. doi:10.1007/978-1-4939-3816-2_11

54. Xiong Y, Zhang Y, Mahmood A, Chopp M. Investigational agents for treatment of traumatic brain injury. Expert opinion on investigational drugs. 2015;24(6):743–760. doi:10.1517/13543784.2015.1021919

55. Svirsky SE, Ranellone NS, Parry M, Holets E, Henchir J, Li Y, Carlson SW, Edward Dixon C. All-trans Retinoic Acid has Limited Therapeutic Effects on Cognition and Hippocampal Protein Expression After Controlled Cortical Impact. Neuroscience. 2022 Jul 22:S0306-4522(22)00389-X. doi:10.1016/j.neuroscience.2022.07.021

56. Yang L-Y, Greig NH, Huang Y-N, Hsieh T-H, Tweedie D, Yu Q-S, Hoffer BJ, Luo Y, Kao Y-C, Wang J-Y. Post-traumatic administration of the p53 inactivator pifithrin-α oxygen analogue reduces hippocampal neuronal loss and improves cognitive deficits after experimental traumatic brain injury. Neurobiology of disease. 2016;96:216–226. doi:10.1016/j.nbd.2016.08.012

57. Threlkeld SW, Cestero EM, Marshall J, Szmydynger-Chodobska J, Chodobski A. Deficits in Acoustic Startle Reactivity and Auditory Temporal Processing after Traumatic Brain Injury. Neurotrauma Reports. 2022;3(1):207–216. doi:10.1089/neur.2021.0077

58. Woertgen C, Rothoerl RD, Wiesmann M, Missler U, Brawanski A. Glial and neuronal serum markers after controlled cortical impact injury in the rat. Acta Neurochirurgica. Supplement. 2002;81:205–207. doi:10.1007/978-3-7091-6738-0_53

59. Sandhir R, Onyszchuk G, Berman NEJ. Exacerbated glial response in the aged mouse hippocampus following controlled cortical impact injury. Experimental Neurology. 2008;213(2):372–380. doi:10.1016/j.expneurol.2008.06.013

60. Susarla BTS, Villapol S, Yi J-H, Geller HM, Symes AJ. Temporal Patterns of Cortical Proliferation of Glial Cell Populations after Traumatic Brain Injury in Mice. ASN Neuro. 2014;6(3). doi:10.1042/AN20130034

61. Gao X, Wang X, Xiong W, Chen J. In vivo reprogramming reactive glia into iPSCs to produce new neurons in the cortex following traumatic brain injury. Scientific Reports. 2016;6(1):22490. doi:10.1038/srep22490

62. Prins M, Dutta R, Baselmans B, Brevé JJP, Bol JGJM, Deckard SA, van der Valk P, Amor S, Trapp BD, de Vries HE, et al. Discrepancy in CCL2 and CCR2 expression in white versus grey matter hippocampal lesions of Multiple Sclerosis patients. Acta Neuropathologica Communications. 2014;2(1):98. doi:10.1186/s40478-014-0098-6

63. Sauerbeck AD, Fanizzi C, Kim JH, Gangolli M, Bayly PV, Wellington CL, Brody DL, Kummer TT. modCHIMERA: a novel murine closed-head model of moderate traumatic brain injury. Scientific Reports. 2018;8:7677. doi:10.1038/s41598-018-25737-6

64. Jamnia N, Urban JH, Stutzmann GE, Chiren SG, Reisenbigler E, Marr R, Peterson DA, Kozlowski DA. A Clinically Relevant Closed-Head Model of Single and Repeat Concussive Injury in the Adult Rat Using a Controlled Cortical Impact Device. Journal of Neurotrauma. 2017;34(7):1351–1363. doi:10.1089/neu.2016.4517

65. Bolton Hall AN, Joseph B, Brelsfoard JM, Saatman KE. Repeated Closed Head Injury in Mice Results in Sustained Motor and Memory Deficits and Chronic Cellular Changes. PLOS ONE. 2016;11(7):e0159442. doi:10.1371/journal.pone.0159442

66. Hylin MJ, Orsi SA, Rozas NS, Hill JL, Zhao J, Redell JB, Moore AN, Dash PK. Repeated mild closed head injury impairs short-term visuospatial memory and complex learning. Journal of Neurotrauma. 2013;30(9):716–726. doi:10.1089/neu.2012.2717

67. Kochen W, Craven K, Barkey R, Flinn J, Cerri D. Assessing a Novel Adaptation to CCI Devices to Model Human Mild Traumatic Brain Injury. NeuroSports. 2021;1(2).

68. Hernandez A, Tan C, Plattner F, Logsdon AF, Pozo K, Yousuf MA, Singh T, Turner RC, Lucke-Wold BP, Huber JD, et al. Exposure to mild blast forces induces neuropathological effects,

neurophysiological deficits and biochemical changes. Molecular Brain. 2018;11(1). doi:10.1186/s13041-018-0408-1

69. Wolf SJ, Bebarta VS, Bonnett CJ, Pons PT, Cantrill SV. Blast injuries. The Lancet. 2009;374(9687):405–415. doi:10.1016/S0140-6736(09)60257-9

70. Yamamoto S, DeWitt DS, Prough DS. Impact & Blast Traumatic Brain Injury: Implications for Therapy. Molecules : A Journal of Synthetic Chemistry and Natural Product Chemistry. 2018;23(2):245. doi:10.3390/molecules23020245

71. Cernak I. Understanding blast-induced neurotrauma: how far have we come? Concussion. 2017;2(3). doi:10.2217/cnc-2017-0006

72. Fievisohn E, Bailey Z, Guettler A, VandeVord P. Primary Blast Brain Injury Mechanisms: Current Knowledge, Limitations, and Future Directions. Journal of Biomechanical Engineering. 2018;140(2). doi:10.1115/1.4038710

73. Przekwas A, Garimella HT, Tan XG, Chen ZJ, Miao Y, Harrand V, Kraft RH, Gupta RK. Biomechanics of Blast TBI With Time-Resolved Consecutive Primary, Secondary, and Tertiary Loads. Military Medicine. 2019;184:195–205. doi:10.1093/milmed/usy344

74. Cernak I. Blast Injuries and Blast-Induced Neurotrauma: Overview of Pathophysiology and Experimental Knowledge Models and Findings. In: Kobeissy FH, editor. Brain Neurotrauma: Molecular, Neuropsychological, and Rehabilitation Aspects. Boca Raton (FL): CRC Press/Taylor & Francis; 2015. (Frontiers in Neuroengineering). http://www.ncbi.nlm.nih.gov/books/NBK299193/

75. Tasissa AF, Hautefeuille M, Fitek JH, Radovitzky RA. On the formation of Friedlander waves in a compressed-gas-driven shock tube. Proceedings. Mathematical, Physical, and Engineering Sciences / The Royal Society. 2016;472(2186). doi:10.1098/rspa.2015.0611

76. Nelson NW, Davenport ND, Sponheim SR, Anderson CR. Blast-Related Mild Traumatic Brain Injury: Neuropsychological Evaluation and Findings. In: Kobeissy FH, editor. Brain Neurotrauma: Molecular, Neuropsychological, and Rehabilitation Aspects. Boca Raton (FL): CRC Press/Taylor & Francis; 2015. (Frontiers in Neuroengineering).

77. Clemedson CJ. Blast injury. Physiological Reviews. 1956;36(3):336–354. doi:10.1152/physrev.1956.36.3.336

78. Gupta RK, Przekwas A. Mathematical Models of Blast-Induced TBI: Current Status, Challenges, and Prospects. Frontiers in Neurology. 2013;4:59. doi:10.3389/fneur.2013.00059

79. Courtney A, Courtney M. The Complexity of Biomechanics Causing Primary Blast-Induced Traumatic Brain Injury: A Review of Potential Mechanisms. Frontiers in Neurology. 2015;6. doi:10.3389/fneur.2015.00221

80. Sosa MAG, De Gasperi R, Paulino AJ, Pricop PE, Shaughness MC, Maudlin-Jeronimo E, Hall AA, Janssen WGM, Yuk FJ, Dorr NP, et al. Blast overpressure induces shear-related injuries in

the brain of rats exposed to a mild traumatic brain injury. Acta Neuropathologica Communications. 2013;1(1):51. doi:10.1186/2051-5960-1-51

81. Chafi MS, Karami G, Ziejewski M. Biomechanical Assessment of Brain Dynamic Responses Due to Blast Pressure Waves. Annals of Biomedical Engineering. 2010;38(2):490–504. doi:10.1007/s10439-009-9813-z

82. Chavko M, Watanabe T, Adeeb S, Lankasky J, Ahlers ST, McCarron RM. Relationship between orientation to a blast and pressure wave propagation inside the rat brain. Journal of Neuroscience Methods. 2011;195(1):61–66. doi:10.1016/j.jneumeth.2010.11.019

83. Blast-Related Mild Traumatic Brain Injury - Brain Neurotrauma - NCBI Bookshelf. https://www.ncbi.nlm.nih.gov/books/NBK299235/

84. Aravind A, Ravula AR, Chandra N, Pfister BJ. Behavioral Deficits in Animal Models of Blast Traumatic Brain Injury. Frontiers in Neurology. 2020;11. doi:doi.org/10.3389/fneur.2020.00990

85. Sundaramurthy A, Alai A, Ganpule S, Holmberg A, Plougonven E, Chandra N. Blast-induced biomechanical loading of the rat: an experimental and anatomically accurate computational blast injury model. Journal of Neurotrauma. 2012;29(13):2352–2364. doi:10.1089/neu.2012.2413

86. Awwad HO, Gonzalez LP, Tompkins P, Lerner M, Brackett DJ, Awasthi V, Standifer KM. Blast Overpressure Waves Induce Transient Anxiety and Regional Changes in Cerebral Glucose Metabolism and Delayed Hyperarousal in Rats. Frontiers in Neurology. 2015;6:132. doi:10.3389/fneur.2015.00132

87. Zuckerman A, Ram O, Ifergane G, Matar MA, Sagi R, Ostfeld I, Hoffman JR, Kaplan Z, Sadot O, Cohen H. Controlled Low-Pressure Blast-Wave Exposure Causes Distinct Behavioral and Morphological Responses Modelling Mild Traumatic Brain Injury, Post-Traumatic Stress Disorder, and Comorbid Mild Traumatic Brain Injury-Post-Traumatic Stress Disorder. Journal of Neurotrauma. 2017;34(1):145–164. doi:10.1089/neu.2015.4310

88. Sajja VSS, Hubbard W, VandeVord P. Subacute Oxidative Stress and Glial Reactivity in the Amygdala are Associated with Increased Anxiety Following Blast Neurotrauma. Shock. 2015;44:71–78. doi:10.1097/SHK.0000000000000311

89. VandeVord PJ, Leonardi ADC, Ritzel D. Bridging the Gap of Standardized Animals Models for Blast Neurotrauma: Methodology for Appropriate Experimental Testing. In: Kobeissy FH, Dixon CE, Hayes RL, Mondello S, editors. Injury Models of the Central Nervous System: Methods and Protocols. Vol. 1462. New York, NY: Springer; 2016. p. 101–118. (Methods in Molecular Biology). doi:10.1007/978-1-4939-3816-2_7

90. Rafaels K, Bass CR, Salzar RS, Panzer MB, Woods W, Feldman S, Cummings T, Capehart B. Survival risk assessment for primary blast exposures to the head. Journal of Neurotrauma. 2011;28(11):2319–2329. doi:10.1089/neu.2009.1207

91. Blast Effects in Warfare. Radiology. 1943;40(6):608–609. doi:10.1148/40.6.608

92. Chen Y, Constantini S. Caveats for Using Shock Tube in Blast-Induced Traumatic Brain Injury Research. Frontiers in Neurology. 2013;4. doi:10.3389/fneur.2013.00117

93. Ning Y-L, Zhou Y-G. Shock tubes and blast injury modeling. Chinese Journal of Traumatology. 2015;18(4):187–193. doi:10.1016/j.cjtee.2015.04.005

94. Petersen EL, Hanson RK, Division T, Petersen E, Tube HS, Petersen EL, Hanson RK. Nonideal Effects behind Reflected Shock Waves in a High Pressure Shock Tube. Shock Waves. 2001;10:405–420. doi:10.1007/PL00004051

95. Ben-Dor G. Shock Wave Reflection Phenomena. 2nd ed. Springer; 2007. (Shock Wave and High Pressure Phenomena). doi:10.1007/978-3-540-71382-1

96. Goldstein LE, Fisher AM, Tagge CA, Zhang X-L, Velisek L, Sullivan JA, Upreti C, Kracht JM, Ericsson M, Wojnarowicz MW, et al. Chronic traumatic encephalopathy in blast-exposed military veterans and a blast neurotrauma mouse model. Science Translational Medicine. 2012;4(134). doi:10.1126/scitranslmed.3003716

97. Garman RH, Jenkins LW, Switzer RC, Bauman RA, Tong LC, Swauger PV, Parks SA, Ritzel DV, Dixon CE, Clark RSB, et al. Blast exposure in rats with body shielding is characterized primarily by diffuse axonal injury. Journal of Neurotrauma. 2011;28(6):947–959. doi:10.1089/neu.2010.1540

98. Arun P, Wilder DM, Eken O, Urioste R, Batuure A, Sajja S, Van Albert S, Wang Y, Gist ID, Long JB. Long-Term Effects of Blast Exposure: A Functional Study in Rats Using an Advanced Blast Simulator. Journal of Neurotrauma. 2019;37(4):647–655. doi:10.1089/neu.2019.6591

99. Kawoos U, Gu M, Lankasky J, McCarron RM, Chavko M. Effects of Exposure to Blast Overpressure on Intracranial Pressure and Blood-Brain Barrier Permeability in a Rat Model. PLOS ONE. 2016;11(12):e0167510. doi:10.1371/journal.pone.0167510

100. Kim S, Han SC, Gallan AJ, Hayes JP. Neurometabolic indicators of mitochondrial dysfunction in repetitive mild traumatic brain injury. Concussion (London, England). 2017;2(3). doi:10.2217/cnc-2017-0013

101. Hill RL, Singh IN, Wang JA, Hall ED. Time courses of post-injury mitochondrial oxidative damage and respiratory dysfunction and neuronal cytoskeletal degradation in a rat model of focal traumatic brain injury. Neurochemistry International. 2017;111:45–56. doi:10.1016/j.neuint.2017.03.015

102. Cho HJ, Sajja VSSS, VandeVord PJ, Lee YW. Blast induces oxidative stress, inflammation, neuronal loss and subsequent short-term memory impairment in rats. Neuroscience. 2013;253:9–20. doi:10.1016/j.neuroscience.2013.08.037

103. Cash A, Theus MH. Mechanisms of Blood–Brain Barrier Dysfunction in Traumatic Brain Injury. International Journal of Molecular Sciences. 2020;21(9):3344. doi:10.3390/ijms21093344

104. Shetty AK, Mishra V, Kodali M, Hattiangady B. Blood brain barrier dysfunction and delayed neurological deficits in mild traumatic brain injury induced by blast shock waves. Frontiers in Cellular Neuroscience. 2014;8. doi:10.3389/fncel.2014.00232

105. Rusiecki J, Levin LI, Wang L, Byrne C, Krishnamurthy J, Chen L, Galdzicki Z, French LM. Blast traumatic brain injury and serum inflammatory cytokines: a repeated measures case-control study among U.S. military service members. Journal of Neuroinflammation. 2020;17. doi:10.1186/s12974-019-1624-z

106. Alawieh A, Langley EF, Weber S, Adkins D, Tomlinson S. Identifying the Role of Complement in Triggering Neuroinflammation after Traumatic Brain Injury. The Journal of Neuroscience: The Official Journal of the Society for Neuroscience. 2018;38(10):2519–2532. doi:10.1523/JNEUROSCI.2197-17.2018

107. Hiskens MI, Schneiders AG, Vella RK, Fenning AS. Repetitive mild traumatic brain injury affects inflammation and excitotoxic mRNA expression at acute and chronic time-points. PLOS ONE. 2021;16(5). doi:10.1371/journal.pone.0251315

108. Heyburn L, Abutarboush R, Goodrich S, Urioste R, Batuure A, Statz J, Wilder D, Ahlers ST, Long JB, Sajja VSSS. Repeated Low-Level Blast Overpressure Leads to Endovascular Disruption and Alterations in TDP-43 and Piezo2 in a Rat Model of Blast TBI. Frontiers in Neurology. 2019;10. doi:10.3389/fncel.2021.636707

109. Säljö A, Svensson B, Mayorga M, Hamberger A, Bolouri H. Low-Level Blasts Raise Intracranial Pressure and Impair Cognitive Function in Rats. Journal of Neurotrauma. 2009;26(8):1345–1352. doi:10.1089/neu.2008.0856

110. Donat CK, Scott G, Gentleman SM, Sastre M. Microglial Activation in Traumatic Brain Injury. Frontiers in Aging Neuroscience. 2017;9. doi:10.3389/fneur.2018.00964

111. Karve IP, Taylor JM, Crack PJ. The contribution of astrocytes and microglia to traumatic brain injury. British Journal of Pharmacology. 2016;173(4):692–702. doi:10.1111/bph.13125

112. Lotocki G, de Rivero Vaccari J, Alonso O, Sanchez Molano J, Nixon R, Dietrich WD, Bramlett HM. Oligodendrocyte Vulnerability Following Traumatic Brain Injury in Rats: Effect of Moderate Hypothermia. Therapeutic Hypothermia and Temperature Management. 2011;1(1):43–51. doi:10.1089/ther.2010.0011

113. Huntemer-Silveira A, Patil N, Brickner MA, Parr AM. Strategies for Oligodendrocyte and Myelin Repair in Traumatic CNS Injury. Frontiers in Cellular Neuroscience. 2021;14.

114. Davalos D, Grutzendler J, Yang G, Kim JV, Zuo Y, Jung S, Littman DR, Dustin ML, Gan W-B. ATP mediates rapid microglial response to local brain injury in vivo. Nature Neuroscience. 2005;8(6):752–758. doi:10.1038/nn1472

115. Sajja VSSS, Hlavac N, VandeVord PJ. Role of Glia in Memory Deficits Following Traumatic Brain Injury: Biomarkers of Glia Dysfunction. Frontiers in Integrative Neuroscience. 2016;10.

116. Johnson VE, Stewart W, Arena JD, Smith DH. Traumatic Brain Injury as a Trigger of Neurodegeneration. Advances in Neurobiology. 2017;15:383–400. doi:10.1007/978-3-319-57193-5_15

117. Simon DW, McGeachy M, Bayır H, Clark RSB, Loane DJ, Kochanek PM. Neuroinflammation in the Evolution of Secondary Injury, Repair, and Chronic Neurodegeneration after Traumatic Brain Injury. Nature reviews. Neurology. 2017;13(3):171–191. doi:10.1038/nrneurol.2017.13

118. Ritzel RM, Li Y, He J, Khan N, Doran SJ, Faden AI, Wu J. Sustained neuronal and microglial alterations are associated with diverse neurobehavioral dysfunction long after experimental brain injury. Neurobiology of Disease. 2020;136:104713. doi:10.1016/j.nbd.2019.104713

119. Magnuson J, Leonessa F, Ling GSF. Neuropathology of Explosive Blast Traumatic Brain Injury. Current Neurology and Neuroscience Reports. 2012;12(5):570–579. doi:10.1007/s11910-012-0303-6

120. Hernadez-Ontiveros D, Tajiri N, Acosta S, Giunta B, Tan J, Borlongan C. Microglia Activation as a Biomarker for Traumatic Brain Injury. Frontiers in Neurology. 2013;4. doi:10.3389/fneur.2013.00030

121. Lenz KM, Nelson LH. Microglia and Beyond: Innate Immune Cells As Regulators of Brain Development and Behavioral Function. Frontiers in Immunology. 2018;9. doi:doi.org/10.3389/fimmu.2018.00698

122. Salter MW, Stevens B. Microglia emerge as central players in brain disease. Nature Medicine. 2017;23(9):1018–1027. doi:10.1038/nm.4397

123. Benmamar-Badel A, Owens T, Wlodarczyk A. Protective Microglial Subset in Development, Aging, and Disease: Lessons From Transcriptomic Studies. Frontiers in Immunology. 2020;11:430. doi:10.3389/fimmu.2020.00430

124. Michell-Robinson MA, Touil H, Healy LM, Owen DR, Durafourt BA, Bar-Or A, Antel JP, Moore CS. Roles of microglia in brain development, tissue maintenance and repair. Brain. 2015;138(5):1138–1159. doi:10.1093/brain/awv066

125. Harry GJ, Kraft AD. Microglia in the developing brain: a potential target with lifetime effects. Neurotoxicology. 2012;33(2):191–206. doi:10.1016/j.neuro.2012.01.012

126. Goldmann T, Blank T, Prinz M. Fine-tuning of type I IFN-signaling in microglia — implications for homeostasis, CNS autoimmunity and interferonopathies. Current Opinion in Neurobiology. 2016;36:38–42. doi:10.1016/j.conb.2015.09.003

127. Fujita Y, Yamashita T. Neuroprotective function of microglia in the developing brain. Neuronal Signaling. 2021;5(1). doi:10.1042/NS20200024

128. Kaur C, Rathnasamy G, Ling E-A. Biology of Microglia in the Developing Brain. Journal of Neuropathology & Experimental Neurology. 2017;76(9):736–753. doi:10.1093/jnen/nlx056

129. Santos EN, Fields RD. Regulation of myelination by microglia. Science Advances. 2021;7(50). doi:10.1126/sciadv.abk1131

130. Okajima T, Tsuruta F. Microglial dynamics during brain development. Neural Regeneration Research. 2018;13(2):222–223. doi:10.4103/1673-5374.226386

131. Streit WJ. Microglial Cells. Oxford Academic. 2012 Dec 1:86–97. doi:10.1093/med/9780199794591.003.0008

132. Loane DJ, Kumar A. Microglia in the TBI brain: The good, the bad, and the dysregulated. Experimental Neurology. 2016;275:316–327. (Traumatic Brain Injury). doi:10.1016/j.expneurol.2015.08.018

133. Augusto-Oliveira M, Arrifano GP, Lopes-Araújo A, Santos-Sacramento L, Takeda PY, Anthony DC, Malva JO, Crespo-Lopez ME. What Do Microglia Really Do in Healthy Adult Brain? Cells. 2019;8(10):1293. doi:10.3390/cells8101293

134. Quagliato LA, Nardi AE. The role of convergent ion channel pathways in microglial phenotypes: a systematic review of the implications for neurological and psychiatric disorders. Translational Psychiatry. 2018;8(1):1–11. doi:10.1038/s41398-018-0318-0

135. Nimmerjahn A. Two-photon imaging of microglia in the mouse cortex in vivo. Cold Spring Harbor Protocols. 2012;2012(5). doi:10.1101/pdb.prot069294

136. Tremblay M-È, Stevens B, Sierra A, Wake H, Bessis A, Nimmerjahn A. The Role of Microglia in the Healthy Brain. The Journal of Neuroscience. 2011;31(45):16064–16069. doi:10.1523/JNEUROSCI.4158-11.2011

137. Menassa DA, Gomez-Nicola D. Microglial Dynamics During Human Brain Development. Frontiers in Immunology. 2018;9. doi:10.3389/fimmu.2018.01014

138. Takagi S, Furube E, Nakano Y, Morita M, Miyata S. Microglia are continuously activated in the circumventricular organs of mouse brain. Journal of Neuroimmunology. 2019;331:74–86. doi:10.1016/j.jneuroim.2017.10.008

139. Acosta SA, Tajiri N, Shinozuka K, Ishikawa H, Grimmig B, Diamond D, Sanberg PR, Bickford PC, Kaneko Y, Borlongan CV. Long-Term Upregulation of Inflammation and Suppression of Cell Proliferation in the Brain of Adult Rats Exposed to Traumatic Brain Injury Using the Controlled Cortical Impact Model. PLOS ONE. 2013;8(1). doi:10.1371/journal.pone.0053376

140. Kumar A, Alvarez-Croda D-M, Stoica BA, Faden AI, Loane DJ. Microglial/Macrophage Polarization Dynamics following Traumatic Brain Injury. Journal of Neurotrauma. 2016;33(19):1732–1750. doi:10.1089/neu.2015.4268

141. Dheen ST, Kaur C, Ling E-A. Microglial activation and its implications in the brain diseases. Current Medicinal Chemistry. 2007;14(11):1189–1197.

142. Hsieh CL, Kim CC, Ryba BE, Niemi EC, Bando JK, Locksley RM, Liu J, Nakamura MC, Seaman WE. Traumatic brain injury induces macrophage subsets in the brain. European journal of immunology. 2013;43(8):2010–2022. doi:10.1002/eji.201243084

143. Schafer DP, Lehrman EK, Kautzman AG, Koyama R, Mardinly AR, Yamasaki R, Ransohoff RM, Greenberg ME, Barres BA, Stevens B. Microglia Sculpt Postnatal Neural Circuits in an Activity and Complement-Dependent Manner. Neuron. 2012;74(4):691–705. doi:10.1016/j.neuron.2012.03.026

144. Fernández-Arjona M del M, Grondona JM, Granados-Durán P, Fernández-Llebrez P, López-Ávalos MD. Microglia Morphological Categorization in a Rat Model of Neuroinflammation by Hierarchical Cluster and Principal Components Analysis. Frontiers in Cellular Neuroscience. 2017;11. doi:doi.org/10.3389/fncel.2017.00235

145. Cao T, Thomas TC, Ziebell JM, Pauly JR, Lifshitz J. Morphological and Genetic Activation of Microglia After Diffuse Traumatic Brain Injury in the Rat. Neuroscience. 2012;225:65–75. doi:10.1016/j.neuroscience.2012.08.058

146. Morrison HW, Filosa JA. A quantitative spatiotemporal analysis of microglia morphology during ischemic stroke and reperfusion. Journal of Neuroinflammation. 2013;10:4. doi:10.1186/1742-2094-10-4

147. Davis BM, Salinas-Navarro M, Cordeiro MF, Moons L, De Groef L. Characterizing microglia activation: a spatial statistics approach to maximize information extraction. Scientific Reports. 2017;7(1):1576. doi:10.1038/s41598-017-01747-8

148. Tam WY, Ma CHE. Bipolar/rod-shaped microglia are proliferating microglia with distinct M1/M2 phenotypes. Scientific Reports. 2014;4:7279. doi:10.1038/srep07279

149. Dickerson M, Guilhaume-Corrêa F, Strickler J, VandeVord PJ. Age-relevant in vitro models may lead to improved translational research for traumatic brain injury. Current Opinion in Biomedical Engineering. 2022;22:100391. doi:10.1016/j.cobme.2022.100391

150. Cullen DK, Harris JP, Browne KD, Wolf JA, Duda JE, Meaney DF, Margulies SS, Smith DH. A Porcine Model of Traumatic Brain Injury via Head Rotational Acceleration. In: Kobeissy FH, Dixon CE, Hayes RL, Mondello S, editors. Injury Models of the Central Nervous System: Methods and Protocols. New York, NY: Springer; 2016. p. 289–324. (Methods in Molecular Biology). doi:10.1007/978-1-4939-3816-2_17

151. Ziebell JM, Taylor SE, Cao T, Harrison JL, Lifshitz J. Rod microglia: elongation, alignment, and coupling to form trains across the somatosensory cortex after experimental diffuse brain injury. Journal of Neuroinflammation. 2012;9(1):247. doi:10.1186/1742-2094-9-247

152. Das M, Mohapatra S, Mohapatra SS. New perspectives on central and peripheral immune responses to acute traumatic brain injury. Journal of Neuroinflammation. 2012;9(1):236. doi:10.1186/1742-2094-9-236

153. Wofford K, Loane D, Cullen Dk. Acute drivers of neuroinflammation in traumatic brain injury. Neural Regeneration Research. 2019;14(9):1481. doi:10.4103/1673-5374.255958

154. Schilling S, Chausse B, Dikmen HO, Almouhanna F, Hollnagel J-O, Lewen A, Kann O. TLR2- and TLR3-activated microglia induce different levels of neuronal network dysfunction in a context-dependent manner. Brain, Behavior, and Immunity. 2021;96:80–91. doi:10.1016/j.bbi.2021.05.013

155. Ifuku M, Hinkelmann L, Kuhrt LD, Efe IE, Kumbol V, Buonfiglioli A, Krüger C, Jordan P, Fulde M, Noda M, et al. Activation of Toll-like receptor 5 in microglia modulates their function and triggers neuronal injury. Acta Neuropathologica Communications. 2020;8(1):159. doi:10.1186/s40478-020-01031-3

156. Gülke E, Gelderblom M, Magnus T. Danger signals in stroke and their role on microglia activation after ischemia. Therapeutic Advances in Neurological Disorders. 2018;11:1756286418774254. doi:10.1177/1756286418774254

157. Balu R. Inflammation and Immune System Activation After Traumatic Brain Injury. Current Neurology and Neuroscience Reports. 2014;14(10):484. doi:10.1007/s11910-014-0484-2

158. Neal JW, Gasque P. How Does the Brain Limit the Severity of Inflammation and Tissue Injury During Bacterial Meningitis? Journal of Neuropathology & Experimental Neurology. 2013;72(5):370–385. doi:10.1097/NEN.0b013e3182909f2f

159. Roh JS, Sohn DH. Damage-Associated Molecular Patterns in Inflammatory Diseases. Immune Network. 2018;18(4):e27. doi:10.4110/in.2018.18.e27

160. Relja B, Land WG. Damage-associated molecular patterns in trauma. European Journal of Trauma and Emergency Surgery. 2020;46(4):751–775. doi:10.1007/s00068-019-01235-w

161. Vénéreau E, Ceriotti C, Bianchi ME. DAMPs from Cell Death to New Life. Frontiers in Immunology. 2015;6. doi:10.3389/fimmu.2015.00422

162. Murao A, Aziz M, Wang H, Brenner M, Wang P. Release mechanisms of major DAMPs. Apoptosis. 2021;26(3):152–162. doi:10.1007/s10495-021-01663-3

163. Moro N, Ghavim SS, Sutton RL. Massive efflux of adenosine triphosphate into the extracellular space immediately after experimental traumatic brain injury. Experimental and Therapeutic Medicine. 2021;21(6):575. doi:10.3892/etm.2021.10007

164. Hiskens MI, Schneiders AG, Vella RK, Fenning AS. Repetitive mild traumatic brain injury affects inflammation and excitotoxic mRNA expression at acute and chronic time-points. PLoS ONE. 2021;16(5):e0251315. doi:10.1371/journal.pone.0251315

165. Elder GA, Gama Sosa MA, De Gasperi R, Stone JR, Dickstein DL, Haghighi F, Hof PR, Ahlers ST. Vascular and Inflammatory Factors in the Pathophysiology of Blast-Induced Brain Injury. Frontiers in Neurology. 2015;6. doi:10.3389/fneur.2015.00048

166. Vinh To X, Mohamed AZ, Cumming P, Nasrallah FA. Subacute cytokine changes after a traumatic brain injury predict chronic brain microstructural alterations on advanced diffusion imaging in the male rat. Brain, Behavior, and Immunity. 2022;102:137–150. doi:10.1016/j.bbi.2022.02.017

167. Tweedie D, Karnati HK, Mullins R, Pick CG, Hoffer BJ, Goetzl EJ, Kapogiannis D, Greig NH. Time-dependent cytokine and chemokine changes in mouse cerebral cortex following a mild traumatic brain injury Harvey BK, Taniguchi T, Borlongan C, editors. eLife. 2020;9. doi:10.7554/eLife.55827

168. Guo H, Callaway JB, Ting JP-Y. Inflammasomes: mechanism of action, role in disease, and therapeutics. Nature Medicine. 2015;21(7):677–687. doi:10.1038/nm.3893

169. Broz P, Dixit VM. Inflammasomes: mechanism of assembly, regulation and signalling. Nature Reviews. Immunology. 2016;16(7):407–420. doi:10.1038/nri.2016.58

170. Shao B-Z, Xu Z-Q, Han B-Z, Su D-F, Liu C. NLRP3 inflammasome and its inhibitors: a review. Frontiers in Pharmacology. 2015;6. doi:10.3389/fphar.2015.00262

171. Yang Y, Wang H, Kouadir M, Song H, Shi F. Recent advances in the mechanisms of NLRP3 inflammasome activation and its inhibitors. Cell Death & Disease. 2019;10(2). doi:10.1038/s41419-019-1413-8

172. Kelley N, Jeltema D, Duan Y, He Y. The NLRP3 Inflammasome: An Overview of Mechanisms of Activation and Regulation. International Journal of Molecular Sciences. 2019;20(13). doi:10.3390/ijms20133328

173. Groslambert M, Py BF. Spotlight on the NLRP3 inflammasome pathway. Journal of Inflammation Research. 2018;11:359–374. doi:10.2147/JIR.S141220

174. Muñoz-Planillo R, Kuffa P, Martínez-Colón G, Smith BL, Rajendiran TM, Núñez G. K^+ efflux is the common trigger of NLRP3 inflammasome activation by bacterial toxins and particulate matter. Immunity. 2013;38(6):1142–1153. doi:10.1016/j.immuni.2013.05.016

175. Lei J, Gao G, Jiang J. Acute Traumatic Brain Injury: Is Current Management Evidence Based? An Empirical Analysis of Systematic Reviews. Journal of Neurotrauma. 2012;30(7):529–537. doi:10.1089/neu.2012.2548

176. Fann JR, Hart T, Schomer KG. Treatment for Depression after Traumatic Brain Injury: A Systematic Review. Journal of Neurotrauma. 2009;26(12):2383–2402. doi:10.1089/neu.2009.1091

177. Fann JR, Bombardier CH, Vannoy S, Dyer J, Ludman E, Dikmen S, Marshall K, Barber J, Temkin N. Telephone and In-Person Cognitive Behavioral Therapy for Major Depression after Traumatic Brain Injury: A Randomized Controlled Trial. Journal of Neurotrauma. 2015;32(1):45–57. doi:10.1089/neu.2014.3423

178. Dietch JR, Furst AJ. Perspective: Cognitive Behavioral Therapy for Insomnia Is a Promising Intervention for Mild Traumatic Brain Injury. Frontiers in Neurology. 2020;11:530273. doi:10.3389/fneur.2020.530273

179. Daneman R, Prat A. The Blood–Brain Barrier. Cold Spring Harbor Perspectives in Biology. 2015;7(1). doi:10.1101/cshperspect.a020412

180. Abbott NJ, Rönnbäck L, Hansson E. Astrocyte–endothelial interactions at the blood–brain barrier. Nature Reviews Neuroscience. 2006;7(1):41–53. doi:10.1038/nrn1824

181. Upadhyay RK. Drug Delivery Systems, CNS Protection, and the Blood Brain Barrier. BioMed Research International. 2014;2014. doi:10.1155/2014/869269

182. Bell RD, Ehlers MD. Breaching the Blood-Brain Barrier for Drug Delivery. Neuron. 2014;81(1):1–3. doi:10.1016/j.neuron.2013.12.023

183. Dong X. Current Strategies for Brain Drug Delivery. Theranostics. 2018;8(6):1481–1493. doi:10.7150/thno.21254

184. Bony BA, Kievit FM. A Role for Nanoparticles in Treating Traumatic Brain Injury. Pharmaceutics. 2019;11(9):473. doi:10.3390/pharmaceutics11090473

185. Bharadwaj VN, Nguyen DT, Kodibagkar VD, Stabenfeldt SE. Nanoparticle-Based Therapeutics for Brain Injury. Advanced Healthcare Materials. 2018;7(1). doi:10.1002/adhm.201700668

186. Teleanu DM, Chircov C, Grumezescu AM, Volceanov A, Teleanu RI. Blood-Brain Delivery Methods Using Nanotechnology. Pharmaceutics. 2018;10(4):269. doi:10.3390/pharmaceutics10040269

187. Bailey ZS, Nilson E, Bates JA, Oyalowo A, Hockey KS, Sajja VSSS, Thorpe C, Rogers H, Dunn B, Frey AS, et al. Cerium Oxide Nanoparticles Improve Outcome After In Vitro and In Vivo Mild Traumatic Brain Injury. Journal of Neurotrauma. 37(12):1452–1462. doi:10.1089/neu.2016.4644

188. Li Q, Tang G, Xue S, He X, Miao P, Li Y, Wang J, Xiong L, Wang Y, Zhang C, et al. Silica-coated superparamagnetic iron oxide nanoparticles targeting of EPCs in ischemic brain injury. Biomaterials. 2013;34(21):4982–4992. doi:10.1016/j.biomaterials.2013.03.030

189. Choi CHJ, Alabi CA, Webster P, Davis ME. Mechanism of active targeting in solid tumors with transferrin-containing gold nanoparticles. Proceedings of the National Academy of Sciences of the United States of America. 2010;107(3):1235–1240. doi:10.1073/pnas.0914140107

190. Bharadwaj VN, Rowe RK, Harrison J, Wu C, Anderson TR, Lifshitz J, Adelson PD, Kodibagkar VD, Stabenfeldt SE. Blood–brainbarrier disruption dictates nanoparticle accumulation following experimental brain injury. Nanomedicine: Nanotechnology, Biology and Medicine. 2018;14(7):2155–2166. doi:10.1016/j.nano.2018.06.004

191. Ali A, Zafar H, Zia M, ul Haq I, Phull AR, Ali JS, Hussain A. Synthesis, characterization, applications, and challenges of iron oxide nanoparticles. Nanotechnology, Science and Applications. 2016;9:49–67. doi:10.2147/NSA.S99986

192. Maisha N, Naik N, Okesola M, Coombs T, Zilberberg R, Pandala N, Lavik E. Engineering PEGylated Polyester Nanoparticles to Reduce Complement-Mediated Infusion Reaction. Bioconjugate Chemistry. 2021;32(10):2154–2166. doi:10.1021/acs.bioconjchem.1c00339

193. Salmaso S, Caliceti P. Stealth Properties to Improve Therapeutic Efficacy of Drug Nanocarriers. Journal of Drug Delivery. 2013. doi:10.1155/2013/374252

194. Onyeje C, Lavik E. Highlighting the usage of polymeric nanoparticles for the treatment of traumatic brain injury: A review study. Neurochemistry International. 2021;147:105048. doi:10.1016/j.neuint.2021.105048

195. Cruz LJ, Stammes MA, Que I, van Beek ER, Knol-Blankevoort VT, Snoeks TJA, Chan A, Kaijzel EL, Löwik CWGM. Effect of PLGA NP size on efficiency to target traumatic brain injury. Journal of Controlled Release: Official Journal of the Controlled Release Society. 2016;223:31–41. doi:10.1016/j.jconrel.2015.12.029

196. Carroll RT, Bhatia D, Geldenhuys W, Bhatia R, Miladore N, Bishayee A, Sutariya V. Brain-targeted delivery of Tempol-loaded nanoparticles for neurological disorders. Journal of Drug Targeting. 2010;18(9):665–674. doi:10.3109/10611861003639796

197. Tahara K, Miyazaki Y, Kawashima Y, Kreuter J, Yamamoto H. Brain targeting with surface-modified poly(D,L-lactic-co-glycolic acid) nanoparticles delivered via carotid artery administration. European Journal of Pharmaceutics and Biopharmaceutics: Official Journal of Arbeitsgemeinschaft Fur Pharmazeutische Verfahrenstechnik e.V. 2011;77(1):84–88. doi:10.1016/j.ejpb.2010.11.002

198. Khalin I, Alyautdin R, Wong TW, Gnanou J, Kocherga G, Kreuter J. Brain-derived neurotrophic factor delivered to the brain using poly (lactide-co-glycolide) nanoparticles improves neurological and cognitive outcome in mice with traumatic brain injury. Drug Delivery. 2016;23(9):3520–3528. doi:10.1080/10717544.2016.1199609

199. Anand KS, Dhikav V. Hippocampus in health and disease: An overview. Annals of Indian Academy of Neurology. 2012;15(4):239–246. doi:10.4103/0972-2327.104323

200. Caplan HW, Cardenas F, Gudenkauf F, Zelnick P, Xue H, Cox CS, Bedi SS. Spatiotemporal Distribution of Microglia After Traumatic Brain Injury in Male Mice. ASN Neuro. 2020;12. doi:10.1177/1759091420911770

201. Madathil SK, Wilfred BS, Urankar SE, Yang W, Leung LY, Gilsdorf JS, Shear DA. Early Microglial Activation Following Closed-Head Concussive Injury Is Dominated by Pro-Inflammatory M-1 Type. Frontiers in Neurology. 2018;9. doi:10.3389/fneur.2018.00964

202. Carmichael ST, Chesselet M-F. Synchronous Neuronal Activity Is a Signal for Axonal Sprouting after Cortical Lesions in the Adult. Journal of Neuroscience. 2002;22(14):6062–6070. doi:10.1523/JNEUROSCI.22-14-06062.2002

203. Uesaka N, Ruthazer ES, Yamamoto N. The Role of Neural Activity in Cortical Axon Branching: The Neuroscientist. 12(2):102–106. doi:10.1177/1073858405281673

204. Nudo R. Recovery after brain injury: mechanisms and principles. Frontiers in Human Neuroscience. 2013;7. doi:10.3389/fnhum.2013.00887

205. Donat CK, Scott G, Gentleman SM, Sastre M. Microglial Activation in Traumatic Brain Injury. Frontiers in Aging Neuroscience.;9. https://www.ncbi.nlm.nih.gov/pmc/articles/PMC5487478/. doi:10.3389/fnagi.2017.00208

206. Dickerson MR, Murphy SF, Urban MJ, White Z, VandeVord PJ. Chronic Anxiety- and Depression-Like Behaviors Are Associated With Glial-Driven Pathology Following Repeated Blast Induced Neurotrauma. Frontiers in Behavioral Neuroscience. 2021;15.

207. Merkel S, Andrews A, Lutton E, Razmpour R, Cannella L, Ramirez S. Dexamethasone Attenuates the Enhanced Rewarding Effects of Cocaine Following Experimental Traumatic Brain Injury. Cell Transplantation. 2017;26:1178–1192. doi:10.1177/0963689717714341

208. Nasser M, Ballout N, Mantash S, Bejjani F, Najdi F, Ramadan N, Soueid J, Zibara K, Kobeissy F. Transplantation of Embryonic Neural Stem Cells and Differentiated Cells in a Controlled Cortical Impact (CCI) Model of Adult Mouse Somatosensory Cortex. Front. Neurol. 2018. doi:10.3389/fneur.2018.00895

209. Radomski K, Zhou Q, Yi K, Doughty M. Cortical contusion injury disrupts olfactory bulb neurogenesis in adult mice. BMC neuroscience. 2013;14:142. doi:10.1186/1471-2202-14-142

210. Phipps H, Mondello S, Wilson A, Dittmer T, Rohde NN, Schroeder PJ, Nichols J, McGirt C, Hoffman J, Tanksley K, et al. Characteristics and Impact of U.S. Military Blast-Related Mild Traumatic Brain Injury: A Systematic Review. Frontiers in Neurology. 2020;11:559318. doi:10.3389/fneur.2020.559318

211. Brundage JF, Taubman SB, Hunt DJ, Clark LL. Whither the “signature wounds of the war” after the war: estimates of incidence rates and proportions of TBI and PTSD diagnoses attributable to background risk, enhanced ascertainment, and active war zone service, active component, U.S. Armed Forces, 2003-2014. MSMR. 2015;22(2):2–11.

212. Vanderploeg RD, Belanger HG, Horner RD, Spehar AM, Powell-Cope G, Luther SL, Scott SG. Health outcomes associated with military deployment: mild traumatic brain injury, blast, trauma, and combat associations in the Florida National Guard. Archives of Physical Medicine and Rehabilitation. 2012;93(11):1887–1895. doi:10.1016/j.apmr.2012.05.024

213. Carr W, Polejaeva E, Grome A, Crandall B, LaValle C, Eonta SE, Young LA. Relation of repeated low-level blast exposure with symptomology similar to concussion. The Journal of Head Trauma Rehabilitation. 2015;30(1):47–55. doi:10.1097/HTR.0000000000000064

214. Kubli LR, Pinto RL, Burrows HL, Littlefield PD, Brungart DS. The Effects of Repeated Low-Level Blast Exposure on Hearing in Marines. Noise & Health. 2017;19(90):227–238. doi:10.4103/nah.NAH_58_16

215. Nakashima A MASc, Vartanian O PhD, Rhind SG PhD, King K MSc, Tenn C PhD, Jetly CR MD. Repeated Occupational Exposure to Low-level Blast in the Canadian Armed Forces: Effects on Hearing, Balance, and Ataxia. Military Medicine. 2022;187(1–2):e201–e208. doi:10.1093/milmed/usaa439

216. Bachiller S, Jiménez-Ferrer I, Paulus A, Yang Y, Swanberg M, Deierborg T, Boza-Serrano A. Microglia in Neurological Diseases: A Road Map to Brain-Disease Dependent-Inflammatory Response. Frontiers in Cellular Neuroscience. 2018;12. doi:doi.org/10.3389/fncel.2018.00488

217. Ito D, Tanaka K, Suzuki S, Dembo T, Fukuuchi Y. Enhanced Expression of Iba1, Ionized Calcium-Binding Adapter Molecule 1, After Transient Focal Cerebral Ischemia In Rat Brain. Stroke. 2001;32(5):1208–1215. doi:10.1161/01.STR.32.5.1208

218. Mikkelsen HB, Huizinga JD, Larsen JO, Kirkeby S. Ionized calcium-binding adaptor molecule 1 positive macrophages and HO-1 up-regulation in intestinal muscularis resident macrophages. Anatomical Record (Hoboken, N.j. : 2007). 2017;300(6):1114–1122. doi:10.1002/ar.23517

219. Dickerson MR, Bailey ZS, Murphy SF, Urban MJ, VandeVord PJ. Glial Activation in the Thalamus Contributes to Vestibulomotor Deficits Following Blast-Induced Neurotrauma. Frontiers in Neurology. 2020;11:618. doi:10.3389/fneur.2020.00618

220. Lafrenaye AD, Mondello S, Wang KK, Yang Z, Povlishock JT, Gorse K, Walker S, Hayes RL, Kochanek PM. Circulating GFAP and Iba-1 levels are associated with pathophysiological sequelae in the thalamus in a pig model of mild TBI. Scientific Reports. 2020;10(1):13369. doi:10.1038/s41598-020-70266-w

221. He W, Long T, Pan Q, Zhang S, Zhang Y, Zhang D, Qin G, Chen L, Zhou J. Microglial NLRP3 inflammasome activation mediates IL-1β release and contributes to central sensitization in a recurrent nitroglycerin-induced migraine model. Journal of Neuroinflammation. 2019;16(1):78. doi:10.1186/s12974-019-1459-7

222. Hanslik KL, Ulland TK. The Role of Microglia and the Nlrp3 Inflammasome in Alzheimer's Disease. Frontiers in Neurology. 2020;11. doi:10.3389/fneur.2020.570711

223. Young K, Morrison H. Quantifying Microglia Morphology from Photomicrographs of Immunohistochemistry Prepared Tissue Using ImageJ. Journal of Visualized Experiments : JoVE. 2018;(136):57648. doi:10.3791/57648

224. Higgins DM, Kerns RD, Brandt CA, Haskell SG, Bathulapalli H, Gilliam W, Goulet JL. Persistent pain and comorbidity among Operation Enduring Freedom/Operation Iraqi Freedom/operation New Dawn veterans. Pain Medicine (Malden, Mass.). 2014;15(5):782–790. doi:10.1111/pme.12388

225. Jaramillo CA, Eapen BC, McGeary CA, McGeary DD, Robinson J, Amuan M, Pugh MJ. A cohort study examining headaches among veterans of Iraq and Afghanistan wars: Associations with traumatic brain injury, PTSD, and depression. Headache. 2016;56(3):528–539. doi:10.1111/head.12726

226. Simmons M, Engel C, Hoch E, Orr P, Anderson B, Azhar G. Neurological Effects of Repeated Exposure to Military Occupational Levels of Blast: A Review of Scientific Literature. RAND Corporation; 2020. doi:10.7249/RR2350

227. Au NPB, Ma CHE. Recent Advances in the Study of Bipolar/Rod-Shaped Microglia and their Roles in Neurodegeneration. Frontiers in Aging Neuroscience. 2017;9. doi:10.3389/fnagi.2017.00128

228. Rao Y, Liang Y-X, Peng B. A revisit of rod microglia in preclinical studies. Neural Regeneration Research. 2017;12(1):56–57. doi:10.4103/1673-5374.195276

229. Holloway OG, Canty AJ, King AE, Ziebell JM. Rod microglia and their role in neurological diseases. Seminars in Cell & Developmental Biology. 2019;94:96–103. (SI: Calcium signalling). doi:10.1016/j.semcdb.2019.02.005

230. Taylor SE, Morganti-Kossmann C, Lifshitz J, Ziebell JM. Rod Microglia: A Morphological Definition. PLOS ONE. 2014;9(5). doi:10.1371/journal.pone.0097096

231. Huber BR, Meabon JS, Hoffer ZS, Zhang J, Hoekstra JG, Pagulayan KF, McMillan PJ, Mayer CL, Banks WA, Kraemer BC, et al. Blast Exposure Causes Dynamic Microglial/Macrophage Responses and Microdomains of Brain Microvessel Dysfunction. Neuroscience. 2016;319:206–220. doi:10.1016/j.neuroscience.2016.01.022

232. Hubbard WB, Lashof-Sullivan M, Greenberg S, Norris C, Eck J, Lavik E, VandeVord P. Hemostatic nanoparticles increase survival, mitigate neuropathology and alleviate anxiety in a rodent blast trauma model. Scientific Reports. 2018;8(1). doi:10.1038/s41598-018-28848-2

233. Sajja VSSS, Ereifej ES, VandeVord PJ. Hippocampal vulnerability and subacute response following varied blast magnitudes. Neuroscience Letters. 2014;570:33–37. doi:10.1016/j.neulet.2014.03.072

234. Bachstetter AD, Van Eldik LJ, Schmitt FA, Neltner JH, Ighodaro ET, Webster SJ, Patel E, Abner EL, Kryscio RJ, Nelson PT. Disease-related microglia heterogeneity in the hippocampus of Alzheimer's disease, dementia with Lewy bodies, and hippocampal sclerosis of aging. Acta Neuropathologica Communications. 2015;3(1):32. doi:10.1186/s40478-015-0209-z

235. Streit WJ, Xue Q-S, Tischer J, Bechmann I. Microglial pathology. Acta Neuropathologica Communications. 2014;2(1):142. doi:10.1186/s40478-014-0142-6

236. Shahidehpour RK, Higdon RE, Crawford NG, Neltner JH, Ighodaro ET, Patel E, Price D, Nelson PT, Bachstetter AD. Dystrophic microglia are associated with neurodegenerative disease and not healthy aging in the human brain. Neurobiology of Aging. 2021;99:19–27. doi:10.1016/j.neurobiolaging.2020.12.003

237. Streit WJ, Braak H, Xue Q-S, Bechmann I. Dystrophic (senescent) rather than activated microglial cells are associated with tau pathology and likely precede neurodegeneration in Alzheimer's disease. Acta Neuropathologica. 2009;118(4):475–485. doi:10.1007/s00401-009-0556-6

238. Streit WJ, Khoshbouei H, Bechmann I. Dystrophic microglia in late-onset Alzheimer's disease. Glia. 2020;68(4):845–854. doi:10.1002/glia.23782

239. Streit WJ, Sammons NW, Kuhns AJ, Sparks DL. Dystrophic microglia in the aging human brain. Glia. 2004;45(2):208–212. doi:10.1002/glia.10319

240. Candlish M, Hefendehl JK. Microglia Phenotypes Converge in Aging and Neurodegenerative Disease. Frontiers in Neurology. 2021;12. doi:10.3389/fneur.2021.660720

241. Royo NC, Conte V, Saatman KE, Shimizu S, Belfield CM, Soltesz KM, Davis JE, Fujimoto ST, McIntosh TK. Hippocampal vulnerability following traumatic brain injury: a potential role for neurotrophin-4/5 in pyramidal cell neuroprotection. The European Journal of Neuroscience. 2006;23(5):1089–1102. doi:10.1111/j.1460-9568.2006.04642.x

242. Atkins CM. Decoding Hippocampal Signaling Deficits after Traumatic Brain Injury. Translational stroke research. 2011;2(4):546–555. doi:10.1007/s12975-011-0123-z

243. Zhang B-L, Chen X, Tan T, Yang Z, Carlos D, Jiang R-C, Zhang J-N. Traumatic brain injury impairs synaptic plasticity in hippocampus in rats. Chinese Medical Journal. 2011;124(5):740–745.

244. Yamamoto H, Matsumura R, Takaoki H, Katsurabayashi S, Hirano-Iwata A, Niwano M. Unidirectional signal propagation in primary neurons micropatterned at a single-cell resolution. Applied Physics Letters. 2016;109(4):043703. doi:10.1063/1.4959836

245. Kesner R. Neurobiological foundations of an attribute model of memory. Comparative Cognition & Behavior Reviews. 2013;8:29–59. doi:10.3819/ccbr.2013.80003

246. le Feber J, Postma W, de Weerd E, Weusthof M, Rutten WLC. Barbed channels enhance unidirectional connectivity between neuronal networks cultured on multi electrode arrays. Frontiers in Neuroscience. 2015;9. doi:10.3389/fnins.2015.00412

247. Dudek SM, Alexander GM, Farris S. Rediscovering area CA2: unique properties and functions. Nature reviews. Neuroscience. 2016;17(2):89–102. doi:10.1038/nrn.2015.22

248. Buch S, Chen Y, Jella P, Ge Y, Haacke EM. Vascular mapping of the human hippocampus using Ferumoxytol-enhanced MRI. NeuroImage. 2022;250:118957. doi:10.1016/j.neuroimage.2022.118957

249. Angelova PR, Kasymov V, Christie I, Sheikhbahaei S, Turovsky E, Marina N, Korsak A, Zwicker J, Teschemacher AG, Ackland GL, et al. Functional Oxygen Sensitivity of Astrocytes. The Journal of Neuroscience. 2015;35(29):10460–10473. doi:10.1523/JNEUROSCI.0045-15.2015

250. Grabert K, Michoel T, Karavolos MH, Clohisey S, Baillie JK, Stevens MP, Freeman TC, Summers KM, McColl BW. Microglial brain region-dependent diversity and selective regional sensitivities to ageing. Nature neuroscience. 2016;19(3):504–516. doi:10.1038/nn.4222

251. Pan J, Ma N, Yu B, Zhang W, Wan J. Transcriptomic profiling of microglia and astrocytes throughout aging. Journal of Neuroinflammation. 2020;17:97. doi:10.1186/s12974-020-01774-9

252. Olah M, Menon V, Habib N, Taga MF, Ma Y, Yung CJ, Cimpean M, Khairallah A, Coronas-Samano G, Sankowski R, et al. Single cell RNA sequencing of human microglia uncovers a subset associated with Alzheimer's disease. Nature Communications. 2020;11(1):6129. doi:10.1038/s41467-020-19737-2

253. Américo-Da-Silva L, Aguilera J, Quinteros-Waltemath O, Sánchez-Aguilera P, Russell J, Cadagan C, Meneses-Valdés R, Sánchez G, Estrada M, Jorquera G, et al. Activation of the NLRP3 Inflammasome Increases the IL-1β Level and Decreases GLUT4 Translocation in Skeletal Muscle during Insulin Resistance. International Journal of Molecular Sciences. 2021;22(19):10212. doi:10.3390/ijms221910212

254. Grebe A, Hoss F, Latz E. NLRP3 Inflammasome and the IL-1 Pathway in Atherosclerosis. Circulation Research. 2018;122(12):1722–1740. doi:10.1161/CIRCRESAHA.118.311362

255. Vijayaraj SL, Feltham R, Rashidi M, Frank D, Liu Z, Simpson DS, Ebert G, Vince A, Herold MJ, Kueh A, et al. The inflammasome-activated cytokine IL-1β is targeted for ubiquitylation and proteasomal degradation to limit its inflammatory potential. 2021:2021.03.15.435390. doi:10.1101/2021.03.15.435390

256. Marchetti C, Swartzwelter B, Gamboni F, Neff CP, Richter K, Azam T, Carta S, Tengesdal I, Nemkov T, D'Alessandro A, et al. OLT1177, a β-sulfonyl nitrile compound, safe in humans, inhibits the NLRP3 inflammasome and reverses the metabolic cost of inflammation. Proceedings of the National Academy of Sciences. 2018;115(7):E1530–E1539. doi:10.1073/pnas.1716095115

257. Meaney DF, Smith DH. Biomechanics of Concussion. Clinics in sports medicine. 2011;30(1):19–vii. doi:10.1016/j.csm.2010.08.009

258. Fakharian E, Banaee S, Momeny HY and M. Head Injury Mechanisms. IntechOpen; 2018. doi:10.5772/intechopen.75454

259. Bayly PV, Cohen TS, Leister EP, Ajo D, Leuthardt E, Genin GM. Deformation of the human brain induced by mild acceleration. Journal of neurotrauma. 2005;22(8):845–856. doi:10.1089/neu.2005.22.845

260. Stemper BD, Shah AS, Pintar FA, McCrea M, Kurpad SN, Glavaski-Joksimovic A, Olsen C, Budde MD. Head Rotational Acceleration Characteristics Influence Behavioral and Diffusion Tensor Imaging Outcomes Following Concussion. Annals of biomedical engineering. 2015;43(5):1071–1088. doi:10.1007/s10439-014-1171-9

261. Post A. Rotational Acceleration, Brain Tissue Strain, and the Relationship to Concussion. Journal of Biomechanical Engineering. 2014;137. doi:10.1115/1.4028983

262. Ferry B, DeCastro A. Concussion. In: StatPearls. Treasure Island (FL): StatPearls Publishing; 2022. http://www.ncbi.nlm.nih.gov/books/NBK537017/

263. Tator CH. Concussions and their consequences: current diagnosis, management and prevention. CMAJ : Canadian Medical Association Journal. 2013;185(11):975–979. doi:10.1503/cmaj.120039

264. Bolouri H, Zetterberg H. Animal Models for Concussion: Molecular and Cognitive Assessments—Relevance to Sport and Military Concussions. In: Kobeissy FH, editor. Brain Neurotrauma: Molecular, Neuropsychological, and Rehabilitation Aspects. Boca Raton (FL): CRC Press/Taylor & Francis; 2015. (Frontiers in Neuroengineering).

265. Silverberg ND, Lange RT, Millis SR, Rose A, Hopp G, Leach S, Iverson GL. Post-concussion symptom reporting after multiple mild traumatic brain injuries. Journal of Neurotrauma. 2013;30(16):1398–1404. doi:10.1089/neu.2012.2827

266. Wilk JE, Herrell RK, Wynn GH, Riviere LA, Hoge CW. Mild traumatic brain injury (concussion), posttraumatic stress disorder, and depression in U.S. soldiers involved in combat deployments: association with postdeployment symptoms. Psychosomatic Medicine. 2012;74(3):249–257. doi:10.1097/PSY.0b013e318244c604

267. Stone ME, Safadjou S, Farber B, Velazco N, Man J, Reddy SH, Todor R, Teperman S. Utility of the Military Acute Concussion Evaluation as a screening tool for mild traumatic brain injury in a civilian trauma population. The Journal of Trauma and Acute Care Surgery. 2015;79(1):147–151. doi:10.1097/TA.0000000000000679

268. Fish AM, Vanni J, Mohammed FN, Fedonni D, Metzger KB, Shoop J, Master CL, Arbogast KB, McDonald CC. Comparison of Anxiety and Depression Symptoms in Concussed and Nonconcussed Adolescents. Sports Health. 2022 Aug 2:19417381221113840. doi:10.1177/19417381221113840

269. Kraemer Y, Mäki K, Marinkovic I, Nybo T, Isokuortti H, Huovinen A, Korvenoja A, Melkas S, Harno H. Post-traumatic headache after mild traumatic brain injury in a one-year follow up study - risk factors and return to work. The Journal of Headache and Pain. 2022;23(1):27. doi:10.1186/s10194-022-01398-9

270. Terpstra AR, Louie DR, Iverson GL, Yeates KO, Picon E, Leddy JJ, Silverberg ND. Psychological Contributions to Symptom Provocation Testing After Concussion. The Journal of Head Trauma Rehabilitation. 2022 Jun 9. doi:10.1097/HTR.0000000000000796

271. Prins ML, Alexander D, Giza CC, Hovda DA. Repeated Mild Traumatic Brain Injury: Mechanisms of Cerebral Vulnerability. Journal of Neurotrauma. 2013;30(1):30–38. doi:10.1089/neu.2012.2399

272. McNamara EH, Grillakis AA, Tucker LB, McCabe JT. The closed-head impact model of engineered rotational acceleration (CHIMERA) as an application for traumatic brain injury pre-clinical research: A status report. Experimental Neurology. 2020;333:113409. doi:10.1016/j.expneurol.2020.113409

273. Shitaka Y, Tran HT, Bennett RE, Sanchez L, Levy MA, Dikranian K, Brody DL. Repetitive Closed-Skull Traumatic Brain Injury in Mice Causes Persistent Multifocal Axonal Injury and Microglial Reactivity. Journal of neuropathology and experimental neurology. 2011;70(7):551–567. doi:10.1097/NEN.0b013e31821f891f

274. Lier J, Ondruschka B, Bechmann I, Dreßler J. Fast microglial activation after severe traumatic brain injuries. International Journal of Legal Medicine. 2020;134(6):2187–2193. doi:10.1007/s00414-020-02308-x

275. Ryu J, Stone P, Lee S, Payne B, Gorse K, Lafrenaye A. Buprenorphine alters microglia and astrocytes acutely following diffuse traumatic brain injury. Scientific Reports. 2021;11:8620. doi:10.1038/s41598-021-88030-z

276. Prins ML, Hales A, Reger M, Giza CC, Hovda DA. Repeat Traumatic Brain Injury in the Juvenile Rat Is Associated with Increased Axonal Injury and Cognitive Impairments. Developmental Neuroscience. 2011;32(5–6):510–518. doi:10.1159/000316800

277. Izzy S, Liu Q, Fang Z, Lule S, Wu L, Chung JY, Sarro-Schwartz A, Brown-Whalen A, Perner C, Hickman SE, et al. Time-Dependent Changes in Microglia Transcriptional Networks Following Traumatic Brain Injury. Frontiers in Cellular Neuroscience. 2019;13. doi:10.3389/fncel.2019.00307

278. Tessier M, Garcia MS, Goubert E, Tian L, Molinari F, Blasco E, Laurin J, Guillemot F, Hübner C, Pellegrino C, et al. Bumetanide increases microglia-interneuron contact following traumatic brain injury. 2022:2022.06.03.494659. doi:10.1101/2022.06.03.494659

279. Theus M, Brickler T, Meza A, Coutermarsh-Ott S, Hazy A, Gris D, Allen I. Loss of NLRX1 Exacerbates Neural Tissue Damage and NF-κB Signaling following Brain Injury. The Journal of Immunology. 2017;199:ji1700251. doi:10.4049/jimmunol.1700251

280. Young GB. Diaschisis. In: Aminoff MJ, Daroff RB, editors. Encyclopedia of the Neurological Sciences (Second Edition). Oxford: Academic Press; 2014. p. 995. doi:10.1016/B978-0-12-385157-4.00325-0

281. Wiley CA, Bissel SJ, Lesniak A, Dixon CE, Franks J, Beer Stolz D, Sun M, Wang G, Switzer R, Kochanek PM, et al. Ultrastructure of Diaschisis Lesions after Traumatic Brain Injury. Journal of Neurotrauma. 2016;33(20):1866–1882. doi:10.1089/neu.2015.4272

282. Le Prieult F, Thal SC, Engelhard K, Imbrosci B, Mittmann T. Acute Cortical Transhemispheric Diaschisis after Unilateral Traumatic Brain Injury. Journal of Neurotrauma. 2017;34(5):1097–1110. doi:10.1089/neu.2016.4575

283. McGrath AG, Briand LA. A potential role for microglia in stress- and drug-induced plasticity in the nucleus accumbens: A mechanism for stress-induced vulnerability to substance use disorder. Neuroscience and biobehavioral reviews. 2019;107:360–369. doi:10.1016/j.neubiorev.2019.09.007

284. Frank MG, Fonken LK, Watkins LR, Maier SF. Microglia: neuroimmune-sensors of stress. Seminars in cell & developmental biology. 2019;94:176–185. doi:10.1016/j.semcdb.2019.01.001

285. DiBona VL, Zhu W, Shah MK, Rafalia A, Ben Cheikh H, Crockett DP, Zhang H. Loss of Par1b/MARK2 primes microglia during brain development and enhances their sensitivity to injury. Journal of Neuroinflammation. 2019;16(1):11. doi:10.1186/s12974-018-1390-3

286. Witcher KG, Bray CE, Dziabis JE, McKim DB, Benner BN, Rowe RK, Kokiko-Cochran ON, Popovich PG, Lifshitz J, Eiferman DS, et al. Traumatic brain injury-induced neuronal damage in the somatosensory cortex causes formation of rod-shaped microglia that promote astrogliosis and persistent neuroinflammation. Glia. 2018;66(12):2719–2736. doi:10.1002/glia.23523

287. Hinwood M, Tynan RJ, Charnley JL, Beynon SB, Day TA, Walker FR. Chronic Stress Induced Remodeling of the Prefrontal Cortex: Structural Re-Organization of Microglia and the Inhibitory Effect of Minocycline. Cerebral Cortex. 2013;23(8):1784–1797. doi:10.1093/cercor/bhs151

288. Wu X, Reddy DS. Integrins as Receptor Targets for Neurological Disorders. Pharmacology & therapeutics. 2012;134(1):68–81. doi:10.1016/j.pharmthera.2011.12.008

289. Kim C, Cho E-D, Kim H-K, You S, Lee H-J, Hwang D, Lee S-J. β1-integrin-dependent migration of microglia in response to neuron-released α-synuclein. Experimental & Molecular Medicine. 2014;46(4):e91. doi:10.1038/emm.2014.6

290. Burré J. The Synaptic Function of α-Synuclein. Journal of Parkinson's Disease. 2015;5(4):699–713. doi:10.3233/JPD-150642

291. Bellani S, Sousa VL, Ronzitti G, Valtorta F, Meldolesi J, Chieregatti E. The regulation of synaptic function by α-synuclein. Communicative & Integrative Biology. 2010;3(2):106–109. doi:10.4161/cib.3.2.10964

292. Luna E, Decker SC, Riddle DM, Caputo A, Zhang B, Cole T, Caswell C, Xie SX, Lee VMY, Luk KC. Differential α-synuclein expression contributes to selective vulnerability of hippocampal neuron subpopulations to fibril-induced toxicity. Acta neuropathologica. 2018;135(6):855–875. doi:10.1007/s00401-018-1829-8

293. Grady MS, Charleston JS, Maris D, Witgen BM, Lifshitz J. Neuronal and glial cell number in the hippocampus after experimental traumatic brain injury: analysis by stereological estimation. Journal of Neurotrauma. 2003;20(10):929–941. doi:10.1089/089771503770195786

294. Hicks RR, Smith DH, Lowenstein DH, Saint Marie R, McIntosh TK. Mild experimental brain injury in the rat induces cognitive deficits associated with regional neuronal loss in the hippocampus. Journal of Neurotrauma. 1993;10(4):405–414. doi:10.1089/neu.1993.10.405

295. Baldwin SA, Gibson T, Callihan CT, Sullivan PG, Palmer E, Scheff SW. Neuronal cell loss in the CA3 subfield of the hippocampus following cortical contusion utilizing the optical disector method for cell counting. Journal of Neurotrauma. 1997;14(6):385–398. doi:10.1089/neu.1997.14.385

296. Lier J, Streit WJ, Bechmann I. Beyond Activation: Characterizing Microglial Functional Phenotypes. Cells. 2021;10(9):2236. doi:10.3390/cells10092236

297. Fehily B, Fitzgerald M. Repeated Mild Traumatic Brain Injury. Cell Transplantation. 2017;26(7):1131–1155. doi:10.1177/0963689717714092

298. Timmerman R, Burm SM, Bajramovic JJ. An Overview of in vitro Methods to Study Microglia. Frontiers in Cellular Neuroscience. 2018;12:242. doi:10.3389/fncel.2018.00242

299. Luan W, Li M, Wu C, Shen X, Sun Z. Proteomic dissimilarities of primary microglia and BV2 cells under stimuli. European Journal of Neuroscience. 2022;55(7):1709–1723. doi:10.1111/ejn.15637

300. He Y, Taylor N, Yao X, Bhattacharya A. Mouse primary microglia respond differently to LPS and poly(I:C) in vitro. Scientific Reports. 2021;11(1):10447. doi:10.1038/s41598-021-89777-1

301. Yao Y, Fu K-Y, Yao Y, Fu K-Y. Serum-deprivation leads to activation-like changes in primary microglia and BV-2 cells but not astrocytes. Biomedical Reports. 2020;13(5):1–1. doi:10.3892/br.2020.1358

302. Lam D, Lively S, Schlichter LC. Responses of rat and mouse primary microglia to pro- and anti-inflammatory stimuli: molecular profiles, K+ channels and migration. Journal of Neuroinflammation. 2017;14(1):166. doi:10.1186/s12974-017-0941-3

303. Bennett ML, Bennett FC, Liddelow SA, Ajami B, Zamanian JL, Fernhoff NB, Mulinyawe SB, Bohlen CJ, Adil A, Tucker A, et al. New tools for studying microglia in the mouse and human CNS. Proceedings of the National Academy of Sciences. 2016;113(12):E1738–E1746. doi:10.1073/pnas.1525528113

304. Holt LM, Stoyanof ST, Olsen ML. Magnetic Cell Sorting for In Vivo and In Vitro Astrocyte, Neuron, and Microglia Analysis. Current Protocols in Neuroscience. 2019;88(1):e71. doi:10.1002/cpns.71

305. Holt LM, Olsen ML. Novel Applications of Magnetic Cell Sorting to Analyze Cell-Type Specific Gene and Protein Expression in the Central Nervous System. PLoS ONE. 2016;11(2). doi:10.1371/journal.pone.0150290

306. Lynch MA. Neuroinflammatory changes negatively impact on LTP: A focus on IL-1β. Brain Research. 2015;1621:197–204. (Brain and Memory: Old Arguments and New Perspectives). doi:10.1016/j.brainres.2014.08.040

307. Lynch MA. The Multifaceted Profile of Activated Microglia. Molecular Neurobiology. 2009;40(2):139–156. doi:10.1007/s12035-009-8077-9

308. Mizoue LS, Sullivan SK, King DS, Kledal TN, Schwartz TW, Bacon KB, Handel TM. Molecular Determinants of Receptor Binding and Signaling by the CX3C Chemokine Fractalkine. Journal of Biological Chemistry. 2001;276(36):33906–33914. doi:10.1074/jbc.M101348200

309. Xia Q, Hu Q, Wang H, Yang H, Gao F, Ren H, Chen D, Fu C, Zheng L, Zhen X, et al. Induction of COX-2-PGE2 synthesis by activation of the MAPK/ERK pathway contributes to neuronal death triggered by TDP-43-depleted microglia. Cell Death & Disease. 2015;6(3):e1702–e1702. doi:10.1038/cddis.2015.69

310. Umekawa T, Osman AM, Han W, Ikeda T, Blomgren K. Resident microglia, rather than blood-derived macrophages, contribute to the earlier and more pronounced inflammatory reaction in the immature compared with the adult hippocampus after hypoxia-ischemia. Glia. 2015;63(12):2220–2230. doi:10.1002/glia.22887

311. Morimoto M, Nakano T, Egashira S, Irie K, Matsuyama K, Wada M, Nakamura Y, Shigemori Y, Ishikura H, Yamashita Y, et al. Haptoglobin Regulates Macrophage/Microglia-Induced Inflammation and Prevents Ischemic Brain Damage Via Binding to HMGB1. Journal of the American Heart Association. 2022;11(6):e024424. doi:10.1161/JAHA.121.024424

312. Tyagi A, Kamal MA, Poddar NK. Integrated Pathways of COX-2 and mTOR: Roles in Cell Sensing and Alzheimer's Disease. Frontiers in Neuroscience. 2020;14. doi:10.3389/fnins.2020.00693

313. Tanaka S, Ohgidani M, Hata N, Inamine S, Sagata N, Shirouzu N, Mukae N, Suzuki SO, Hamasaki H, Hatae R, et al. CD206 Expression in Induced Microglia-Like Cells From Peripheral Blood as a Surrogate Biomarker for the Specific Immune Microenvironment of Neurosurgical Diseases Including Glioma. Frontiers in Immunology. 2021;12:670131. doi:10.3389/fimmu.2021.670131

314. Yuan T-F, Liang Y-X, Peng B, Lin B, So K-F. Local proliferation is the main source of rod microglia after optic nerve transection. Scientific Reports. 2015;5(1):10788. doi:10.1038/srep10788

315. Timmerman R, Burm SM, Bajramovic JJ. An Overview of in vitro Methods to Study Microglia. Frontiers in Cellular Neuroscience. 2018;12. https://www.ncbi.nlm.nih.gov/pmc/articles/PMC6087748/. doi:10.3389/fncel.2018.00242

316. Cuní-López C, Stewart R, Quek H, White AR. Recent Advances in Microglia Modelling to Address Translational Outcomes in Neurodegenerative Diseases. Cells. 2022;11(10):1662. doi:10.3390/cells11101662

317. Carson MJ, Crane J, Xie AX. Modeling CNS microglia: the quest to identify predictive models. Drug discovery today. Disease models. 2008;5(1):19–25. doi:10.1016/j.ddmod.2008.07.006

318. Stansley B, Post J, Hensley K. A comparative review of cell culture systems for the study of microglial biology in Alzheimer's disease. Journal of Neuroinflammation. 2012;9:115. doi:10.1186/1742-2094-9-115

319. Nikolakopoulou P, Rauti R, Voulgaris D, Shlomy I, Maoz BM, Herland A. Recent progress in translational engineered in vitro models of the central nervous system. Brain. 2020;143(11):3181–3213. doi:10.1093/brain/awaa268

320. Johann S, Heitzer M, Kanagaratnam M, Goswami A, Rizo T, Weis J, Troost D, Beyer C. NLRP3 inflammasome is expressed by astrocytes in the SOD1 mouse model of ALS and in human sporadic ALS patients. Glia. 2015;63(12):2260–2273. doi:10.1002/glia.22891

321. Lin H-B, Wei G-S, Li F-X, Guo W-J, Hong P, Weng Y-Q, Zhang Q-Q, Xu S-Y, Liang W-B, You Z-J, et al. Macrophage–NLRP3 Inflammasome Activation Exacerbates Cardiac Dysfunction after Ischemic Stroke in a Mouse Model of Diabetes. Neuroscience Bulletin. 2020;36(9):1035–1045. doi:10.1007/s12264-020-00544-0

322. López DE, Ballaz SJ. The Role of Brain Cyclooxygenase-2 (Cox-2) Beyond Neuroinflammation: Neuronal Homeostasis in Memory and Anxiety. Molecular Neurobiology. 2020;57(12):5167–5176. doi:10.1007/s12035-020-02087-x

323. Ohgidani M, Kato TA, Haraguchi Y, Matsushima T, Mizoguchi Y, Murakawa-Hirachi T, Sagata N, Monji A, Kanba S. Microglial CD206 Gene Has Potential as a State Marker of Bipolar Disorder. Frontiers in Immunology. 2017;7:676. doi:10.3389/fimmu.2016.00676

324. Bazan NG. COX-2 as a multifunctional neuronal modulator. Nature Medicine. 2001;7(4):414–415. doi:10.1038/86477

325. Freeman L, Guo H, David CN, Brickey WJ, Jha S, Ting JP-Y. NLR members NLRC4 and NLRP3 mediate sterile inflammasome activation in microglia and astrocytes. Journal of Experimental Medicine. 2017;214(5):1351–1370. doi:10.1084/jem.20150237

326. Shao F, Wang X, Wu H, Wu Q, Zhang J. Microglia and Neuroinflammation: Crucial Pathological Mechanisms in Traumatic Brain Injury-Induced Neurodegeneration. Frontiers in Aging Neuroscience. 2022;14. doi:10.3389/fnagi.2022.825086

327. Cai L, Gong Q, Qi L, Xu T, Suo Q, Li X, Wang W, Jing Y, Yang D, Xu Z, et al. ACT001 attenuates microglia-mediated neuroinflammation after traumatic brain injury via inhibiting AKT/NFκB/NLRP3 pathway. Cell Communication and Signaling : CCS. 2022;20:56. doi:10.1186/s12964-022-00862-y

328. Cornell J, Salinas S, Huang H-Y, Zhou M. Microglia regulation of synaptic plasticity and learning and memory. Neural Regeneration Research. 2021;17(4):705–716. doi:10.4103/1673-5374.322423

329. Augusto-Oliveira M, Arrifano GP, Delage CI, Tremblay M-È, Crespo-Lopez ME, Verkhratsky A. Plasticity of microglia. Biological Reviews. 2022;97(1):217–250. doi:10.1111/brv.12797

330. Shojo H, Borlongan C, Mabuchi T. Genetic and Histological Alterations Reveal Key Role of Prostaglandin Synthase and Cyclooxygenase 1 and 2 in Traumatic Brain Injury–Induced Neuroinflammation in the Cerebral Cortex of Rats Exposed to Moderate Fluid Percussion Injury. Cell Transplantation. 2017;26:1301–1313. doi:10.1177/0963689717715169

331. Chhor V, Le Charpentier T, Lebon S, Oré M-V, Celador IL, Josserand J, Degos V, Jacotot E, Hagberg H, Sävman K, et al. Characterization of phenotype markers and neuronotoxic potential

of polarised primary microglia in vitro. Brain, Behavior, and Immunity. 2013;32:70–85. doi:10.1016/j.bbi.2013.02.005

332. Fenn AM, Henry CJ, Huang Y, Dugan A, Godbout JP. Lipopolysaccharide-induced interleukin (IL)-4 receptor-α expression and corresponding sensitivity to the M2 promoting effects of IL-4 are impaired in microglia of aged mice. Brain, Behavior, and Immunity. 2012;26(5):766–777. (Aging, Brain, Behavior, and Immunity). doi:10.1016/j.bbi.2011.10.003

333. Kane MJ, Angoa-Pérez M, Francescutti DM, Sykes CE, Briggs DI, Leung LY, VandeVord PJ, Kuhn DM. Altered gene expression in cultured microglia in response to simulated blast overpressure: possible role of pulse duration. Neuroscience Letters. 2012;522(1):47–51. doi:10.1016/j.neulet.2012.06.012

334. Greenhalgh AD, David S. Differences in the phagocytic response of microglia and peripheral macrophages after spinal cord injury and its effects on cell death. The Journal of Neuroscience: The Official Journal of the Society for Neuroscience. 2014;34(18):6316–6322. doi:10.1523/JNEUROSCI.4912-13.2014

335. Sabirzhanov B, Stoica BA, Zhao Z, Loane DJ, Wu J, Dorsey SG, Faden AI. miR-711 upregulation induces neuronal cell death after traumatic brain injury. Cell Death and Differentiation. 2016;23(4):654–668. doi:10.1038/cdd.2015.132

336. Krukowski K, Nolan A, Becker M, Picard K, Vernoux N, Frias ES, Feng X, Tremblay M-E, Rosi S. Novel microglia-mediated mechanisms underlying synaptic loss and cognitive impairment after traumatic brain injury. Brain, Behavior, and Immunity. 2021;98:122–135. doi:10.1016/j.bbi.2021.08.210

337. Ritzel RM, Li Y, Lei Z, Carter J, He J, Choi HMC, Khan N, Li H, Allen S, Lipinski MM, et al. Functional and transcriptional profiling of microglial activation during the chronic phase of TBI identifies an age-related driver of poor outcome in old mice. GeroScience. 2022;44(3):1407–1440. doi:10.1007/s11357-022-00562-y

338. Morganti JM, Riparip L-K, Rosi S. Call Off the Dog(ma): M1/M2 Polarization Is Concurrent following Traumatic Brain Injury. PLOS ONE. 2016;11(1). doi:10.1371/journal.pone.0148001

339. Ordek G, Asan AS, Cetinkaya E, Skotak M, Kakulavarapu VR, Chandra N, Sahin M. Electrophysiological Correlates of Blast-Wave Induced Cerebellar Injury. Scientific Reports. 2018;8(1):13633. doi:10.1038/s41598-018-31728-4

340. Holiday KA, Clark AL, Merritt VC, Nakhla MZ, Sorg S, Delano-Wood L, Schiehser DM. Response inhibition in Veterans with a history of mild traumatic brain injury: The role of self-reported complaints in objective performance. Journal of Clinical and Experimental Neuropsychology. 2020;42(6):556–568. doi:10.1080/13803395.2020.1776847

341. Schindler AG, Meabon JS, Pagulayan KF, Hendrickson RC, Meeker KD, Cline M, Li G, Sikkema C, Wilkinson CW, Perl DP, et al. Blast–related disinhibition and risk seeking in mice and combat Veterans: Potential role for dysfunctional phasic dopamine release. Neurobiology of Disease. 2017;106:23–34. doi:10.1016/j.nbd.2017.06.004

342. Vest BM, Brady LA, Brimmer MJ, Homish GG. Variations in Risk and Motivations for Substance Use over the Course of Military Service. Substance Use & Misuse. 2021;56(4):559–566. doi:10.1080/10826084.2021.1887257

343. Olson-Madden JH, Brenner LA, Corrigan JD, Emrick CD, Britton PC. Substance Use and Mild Traumatic Brain Injury Risk Reduction and Prevention: A Novel Model for Treatment. Rehabilitation Research and Practice. 2012;2012. doi:10.1155/2012/174579

344. James LM, Strom TQ, Leskela J. Risk-Taking Behaviors and Impulsivity Among Veterans With and Without PTSD and Mild TBI. Military Medicine. 2014;179(4):357–363. doi:10.7205/MILMED-D-13-00241

345. PK Bernstein J, Milberg WP, McGlinchey RE, Fortier CB. Associations between Post-Traumatic stress disorder symptoms and automobile driving behaviors: A review of the literature. Accident Analysis & Prevention. 2022;170. doi:10.1016/j.aap.2022.106648

346. Theadom A, Parmar P, Jones K, Barker-Collo S, Starkey NJ, McPherson KM, Ameratunga S, Feigin VL, BIONIC Research Group. Frequency and impact of recurrent traumatic brain injury in a population-based sample. Journal of Neurotrauma. 2015;32(10):674–681. doi:10.1089/neu.2014.3579

347. MacDonald CL, Johnson AM, Nelson EC, Werner NJ, Fang R, Flaherty SF, Brody DL. Functional Status after Blast-Plus-Impact Complex Concussive Traumatic Brain Injury in Evacuated United States Military Personnel. Journal of Neurotrauma. 2014;31(10):889–898. doi:10.1089/neu.2013.3173

348. Aravind A, Kosty J, Chandra N, Pfister BJ. Blast exposure predisposes the brain to increased neurological deficits in a model of blast plus blunt traumatic brain injury. Experimental Neurology. 2020;332. doi:10.1016/j.expneurol.2020.113378

349. Yamamoto S, DeWitt DS, Prough DS. Impact & Blast Traumatic Brain Injury: Implications for Therapy. Molecules (Basel, Switzerland). 2018;23(2). doi:10.3390/molecules23020245

350. Arun P, Rossetti F, Wilder DM, Sajja S, Van Albert SA, Wang Y, Gist ID, Long JB. Blast Exposure Leads to Accelerated Cellular Senescence in the Rat Brain. Frontiers in Neurology. 2020;11:438. doi:10.3389/fneur.2020.00438

351. Wu R, Jiang X, Wu X, Pang J, Tang Y, Ren Z, Yang F, Yang S, Wei W. Interspecific differences in sociability, social novelty preference, anxiety- and depression-like behaviors between Brandt's voles and C57BL/6J mice. Behavioural Processes. 2022;197. doi:10.1016/j.beproc.2022.104624

352. Bailey ZS, Grinter MB, VandeVord PJ. Astrocyte Reactivity Following Blast Exposure Involves Aberrant Histone Acetylation. Frontiers in Molecular Neuroscience. 2016;9. doi:10.3389/fnmol.2016.00064

353. Stein DG. Embracing failure: What the Phase III progesterone studies can teach about TBI clinical trials. Brain Injury. 2015;29(11):1259–1272. doi:10.3109/02699052.2015.1065344

354. Howard RB, Sayeed I, Stein DG. Suboptimal Dosing Parameters as Possible Factors in the Negative Phase III Clinical Trials of Progesterone for Traumatic Brain Injury. Journal of Neurotrauma. 2017;34(11):1915–1918. doi:10.1089/neu.2015.4179

355. Mohamadpour M, Whitney K, Bergold PJ. The Importance of Therapeutic Time Window in the Treatment of Traumatic Brain Injury. Frontiers in Neuroscience. 2019;13. doi:10.3389/fnins.2019.00007

356. Rabinowitz AR, Watanabe TK. Pharmacotherapy for Treatment of Cognitive and Neuropsychiatric Symptoms After mTBI. The Journal of head trauma rehabilitation. 2020;35(1):76–83. doi:10.1097/HTR.0000000000000537

357. Hubbard WB, Lashof-Sullivan MM, Lavik EB, VandeVord PJ. Steroid-Loaded Hemostatic Nanoparticles Combat Lung Injury after Blast Trauma. ACS macro letters. 2015;4(4):387–391. doi:10.1021/acsmacrolett.5b00061

358. Lashof-Sullivan MM, Shoffstall E, Atkins KT, Keane N, Bir C, VandeVord P, Lavik EB. Intravenously administered nanoparticles increase survival following blast trauma. Proceedings of the National Academy of Sciences of the United States of America. 2014;111(28):10293–10298. doi:10.1073/pnas.1406979111

359. Lashof-Sullivan M, Holland M, Groynom R, Campbell D, Shoffstall A, Lavik E. Hemostatic Nanoparticles Improve Survival Following Blunt Trauma Even after 1 Week Incubation at 50 °C. ACS biomaterials science & engineering. 2016;2(3):385–392. doi:10.1021/acsbiomaterials.5b00493

360. Brailoiu E, Barlow CL, Ramirez SH, Abood ME, Brailoiu GC. Effects of Platelet-Activating Factor on brain microvascular endothelial cells. Neuroscience. 2018;377:105–113. doi:10.1016/j.neuroscience.2018.02.039

361. Kojok K, Akoum SE, Mohsen M, Mourad W, Merhi Y. CD40L Priming of Platelets via NF-κB Activation is CD40- and TAK1-Dependent. Journal of the American Heart Association: Cardiovascular and Cerebrovascular Disease. 2018;7(23). doi:10.1161/JAHA.118.009636

362. Aoui C, Prigent A, Sut C, Tariket S, Hamzeh-Cognasse H, Pozzetto B, Richard Y, Cognasse F, Laradi S, Garraud O. The Signaling Role of CD40 Ligand in Platelet Biology and in Platelet Component Transfusion. International Journal of Molecular Sciences. 2014;15(12):22342–22364. doi:10.3390/ijms151222342

363. Machlus KR, Johnson KE, Kulenthirarajan R, Forward JA, Tippy MD, Soussou TS, El-Husayni SH, Wu SK, Wang S, Watnick RS, et al. CCL5 derived from platelets increases megakaryocyte proplatelet formation. Blood. 2016;127(7):921–926. doi:10.1182/blood-2015-05-644583

364. Maisha N, Kulkarni C, Pandala N, Zilberberg R, Schaub L, Neidert L, Glaser J, Cannon J, Janeja V, Lavik EB. PEGylated Polyester Nanoparticles Trigger Adverse Events in a Large Animal Model of Trauma and in Naïve Animals: Understanding Cytokine and Cellular Correlations with These Events. ACS nano. 2022;16(7):10566–10580. doi:10.1021/acsnano.2c01993

365. Gray E, Ginty M, Kemp K, Scolding N, Wilkins A. The PPAR-gamma agonist pioglitazone protects cortical neurons from inflammatory mediators via improvement in peroxisomal function. Journal of Neuroinflammation. 2012;9(1):63. doi:10.1186/1742-2094-9-63

366. Bu W, Ren H, Deng Y, Del Mar N, Guley NM, Moore BM, Honig MG, Reiner A. Mild Traumatic Brain Injury Produces Neuron Loss That Can Be Rescued by Modulating Microglial Activation Using a CB2 Receptor Inverse Agonist. Frontiers in Neuroscience. 2016;10:449. doi:10.3389/fnins.2016.00449

367. Katsumoto A, Miranda AS, Butovsky O, Teixeira AL, Ransohoff RM, Lamb BT. Laquinimod attenuates inflammation by modulating macrophage functions in traumatic brain injury mouse model. Journal of Neuroinflammation. 2018;15:26. doi:10.1186/s12974-018-1075-y

368. Parada NA, Cruikshank WW, Danis HL, Ryan TC, Center DM. IL-16- and other CD4 ligand-induced migration is dependent upon protein kinase C. Cellular Immunology. 1996;168(1):100–106. doi:10.1006/cimm.1996.0054

369. Wilson K, Zhang Y, Kornfeld H, Center D, Cruikshank W. Interleukin-16. In: Henry HL, Norman AW, editors. Encyclopedia of Hormones. New York: Academic Press; 2003. p. 484–493. doi:10.1016/B0-12-341103-3/00161-3

370. Mathy NL, Scheuer W, Lanzendörfer M, Honold K, Ambrosius D, Norley S, Kurth R. Interleukin-16 stimulates the expression and production of pro-inflammatory cytokines by human monocytes. Immunology. 2000;100(1):63–69. doi:10.1046/j.1365-2567.2000.00997.x

371. Zhang Z, Fauser U, Schluesener HJ. Early attenuation of lesional interleukin-16 up-regulation by dexamethasone and FTY720 in experimental traumatic brain injury. Neuropathology and Applied Neurobiology. 2008;34(3):330–339. doi:10.1111/j.1365-2990.2007.00893.x

372. Rider P, Voronov E, Dinarello CA, Apte RN, Cohen I. Alarmins: Feel the Stress. The Journal of Immunology. 2017;198(4):1395–1402. doi:10.4049/jimmunol.1601342

373. Nasiri E, Sankowski R, Dietrich H, Oikonomidi A, Huerta PT, Popp J, Al-Abed Y, Bacher M. Key role of MIF-related neuroinflammation in neurodegeneration and cognitive impairment in Alzheimer's disease. Molecular Medicine (Cambridge, Mass.). 2020;26(1):34. doi:10.1186/s10020-020-00163-5

374. Zhang S, Zhao J, Zhang Y, Zhang Y, Cai F, Wang L, Song W. Upregulation of MIF as a defense mechanism and a biomarker of Alzheimer's disease. Alzheimer's Research & Therapy. 2019;11(1):54. doi:10.1186/s13195-019-0508-x

375. Alibashe-Ahmed M, Roger T, Serre-Beinier V, Berishvili E, Reith W, Bosco D, Berney T. Macrophage migration inhibitory factor regulates TLR4 expression and modulates TCR/CD3-mediated activation in CD4+ T lymphocytes. Scientific Reports. 2019;9(1):9380. doi:10.1038/s41598-019-45260-6

376. Land WG. Endogenous DAMPs, Category I: Constitutively Expressed, Native Molecules (Cat. I DAMPs). Damage-Associated Molecular Patterns in Human Diseases. 2018:219–268. doi:10.1007/978-3-319-78655-1_12

377. Amarante-Mendes GP, Adjemian S, Branco LM, Zanetti LC, Weinlich R, Bortoluci KR. Pattern Recognition Receptors and the Host Cell Death Molecular Machinery. Frontiers in Immunology. 2018;9. doi:10.3389/fimmu.2018.02379

378. Hubbard WB, Banerjee M, Vekaria H, Prakhya KS, Joshi S, Wang QJ, Saatman KE, Whiteheart SW, Sullivan PG. Differential Leukocyte and Platelet Profiles in Distinct Models of Traumatic Brain Injury. Cells. 2021;10(3):500. doi:10.3390/cells10030500

379. Kniewallner KM, Foidl BM, Humpel C. Platelets isolated from an Alzheimer mouse damage healthy cortical vessels and cause inflammation in an organotypic ex vivo brain slice model. Scientific Reports. 2018;8:15483. doi:10.1038/s41598-018-33768-2

380. Liu T, Wen W, Zhu W, Kochan NA, Trollor JN, Reppermund S, Jin JS, Luo S, Brodaty H, Sachdev PS. The relationship between cortical sulcal variability and cognitive performance in the elderly. NeuroImage. 2011;56(3):865–873. doi:10.1016/j.neuroimage.2011.03.015

381. Mortazavi F, Romano SE, Rosene DL, Rockland KS. A Survey of White Matter Neurons at the Gyral Crowns and Sulcal Depths in the Rhesus Monkey. Frontiers in Neuroanatomy. 2017;11. doi:10.3389/fnana.2017.00069

382. Lynch MA. Exploring Sex-Related Differences in Microglia May Be a Game-Changer in Precision Medicine. Frontiers in Aging Neuroscience. 2022;14. doi:10.3389/fnagi.2022.868448

383. Villa A, Gelosa P, Castiglioni L, Cimino M, Rizzi N, Pepe G, Lolli F, Marcello E, Sironi L, Vegeto E, et al. Sex-Specific Features of Microglia from Adult Mice. Cell Reports. 2018;23(12):3501–3511. doi:10.1016/j.celrep.2018.05.048

384. Velayudhan PS, Schwab N, Hazrati L-N, Wheeler AL. Temporal patterns of microglial activation in white matter following experimental mild traumatic brain injury: a systematic literature review. Acta Neuropathologica Communications. 2021;9:197. doi:10.1186/s40478-021-01297-1

385. Turtzo LC, Lescher J, Janes L, Dean DD, Budde MD, Frank JA. Macrophagic and microglial responses after focal traumatic brain injury in the female rat. Journal of Neuroinflammation. 2014;11:82. doi:10.1186/1742-2094-11-82

386. Blaze J, Choi I, Wang Z, Umali M, Mendelev N, Tschiffely AE, Ahlers ST, Elder GA, Ge Y, Haghighi F. Blast-Related Mild TBI Alters Anxiety-Like Behavior and Transcriptional Signatures in the Rat Amygdala. Frontiers in Behavioral Neuroscience. 2020;14:160. doi:10.3389/fnbeh.2020.00160

387. Pallanti S, Borgheresi A, Pampaloni I, Giovannelli F, Bernardi S, Cantisani A, Zaccara G, Cincotta M. Motor cortex excitability correlates with novelty seeking in social anxiety: a

transcranial magnetic stimulation investigation. Journal of Neurology. 2010;257(8):1362–1368. doi:10.1007/s00415-010-5533-4

388. Rosenthal M, Christensen BK, Ross TP. Depression following traumatic brain injury. Archives of Physical Medicine and Rehabilitation. 1998;79(1):90–103. doi:10.1016/s0003-9993(98)90215-5

Appendix A. Citations of Copyrighted Works

Figure 1 – [Fair Use]

Osier N, Dixon CE. The Controlled Cortical Impact Model of Experimental Brain Trauma: Overview, Research Applications, and Protocol. Methods in molecular biology (Clifton, N.J.). 2016;1462:177–192. doi:10.1007/978-1-4939-3816-2_11 (Fair Use Determination Attached)

Figure 2 - [Fair Use]

Cernak I. Blast Injuries and Blast-Induced Neurotrauma: Overview of Pathophysiology and Experimental Knowledge Models and Findings. In: Kobeissy FH, editor. Brain Neurotrauma: Molecular, Neuropsychological, and Rehabilitation Aspects. Boca Raton (FL): CRC Press/Taylor & Francis; 2015. (Frontiers in Neuroengineering). http://www.ncbi.nlm.nih.gov/books/NBK299193/ (Fair Use Determination Attached)

Figure 3 - [Fair Use]

Cernak I. Blast Injuries and Blast-Induced Neurotrauma: Overview of Pathophysiology and Experimental Knowledge Models and Findings. In: Kobeissy FH, editor. Brain Neurotrauma: Molecular, Neuropsychological, and Rehabilitation Aspects. Boca Raton (FL): CRC Press/Taylor & Francis; 2015. (Frontiers in Neuroengineering). http://www.ncbi.nlm.nih.gov/books/NBK299193/ (Fair Use Determination Attached)

Figure 4 - [Fair Use]

Chen Y, Constantini S. Caveats for Using Shock Tube in Blast-Induced Traumatic Brain Injury Research. Frontiers in Neurology. 2013;4. doi:10.3389/fneur.2013.00117 (Fair Use Determination Attached)

Figure 6- Creative Common License Attached (BioRender.com)

Figure 8- Creative Common License Attached (BioRender.com)

Figure 9- Creative Common License Attached (BioRender.com)

Figure 26- Creative Common License Attached (BioRender.com)

Figure 56 – Creative Common License Attached (BioRender.com)